Ontwikkeling van een techno-economisch energiemodel voor CO_2-arme bedrijventerreinen

Development of a Techno-Economic Energy Model for Low Carbon Business Parks

Jonas Timmerman

Promotoren: prof. dr. ir. G. Van Eetvelde, prof. dr. ir. L. Vandevelde
Proefschrift ingediend tot het behalen van de graad van
Doctor in de Ingenieurswetenschappen

Vakgroep Civiele Techniek
Voorzitter: prof. dr. ir. P. Troch

Vakgroep Elektrische Energie, Systemen en Automatisering
Voorzitter: prof. dr. ir. J. Melkebeek

Faculteit Ingenieurswetenschappen en Architectuur
Academiejaar 2015 - 2016

UNIVERSITEIT
GENT

ISBN 978-90-8578-869-0
NUR 961
Wettelijk depot: D/2015/10.500/112

Examencommissie

prof. dr. ir.	Greet Van Eetvelde (promotor)	Universiteit Gent
prof. dr. ir.	Lieven Vandevelde (promotor)	Universiteit Gent
prof. dr.	François Maréchal	École Polytechnique Fédérale de Lausanne
prof. dr.	Simon Harvey	Chalmers University of Technology
prof. dr. ir.	Michel De Paepe	Universiteit Gent
	Pieter Lodewijks	VITO
prof. dr. ir.	Jan Desmet (secretaris)	Universiteit Gent
prof. dr. ir.	Luc Taerwe (voorzitter)	Universiteit Gent

Universiteit Gent
Faculteit Ingenieurswetenschappen en Architectuur
Vakgroep Civiele Techniek
Vakgroep Elektrische Energie, Systemen en Automatisering

Preface

From a young age, I have been concerned about environmental issues worldwide. For example, I remember being extremely worried about the hole in the ozone layer at the age of six. In the youth movement, my interest in the nature surrounding us was only strengthened. After my engineering studies and some first work experience, I went on an eight month journey through Central America. It was a breathtakingly beautiful adventure: climbing volcanoes, swimming in azure blue lakes, discovering ancient Maya ruins in dense jungles, and relaxing on white sandy islands in the middle of a vast tropical aquarium. However, quickly it became clear that much of this natural beauty is threatened by our increasingly expanding civilization. In Nicaragua, a twin volcano, Ometepe, rises up from the second largest sweet water lake in Latin-America. This scenery possesses an indescribable serenity and tranquillity. In 2015, the Chinese HKND Group started the construction of a Nicaraguan version of the Panama canal, cutting right through the pristine lake. It only takes common sense to see that the construction and exploitation of this canal will destroy the ecosystems in this area and beyond. On the beaches of Costa Rica's famous coastal natural reserves, the flood line is littered with plastic particles. In the natural reserve Monteverde, the park guides worry about the future of the cloud forest. Due to climate change, stronger winds push passing clouds to higher altitudes and as a result, the forest is drying out. These are just a few concrete examples of the sustainability problems we are facing today.

Authorities from global to regional level play a key role in enforcing stringent regulations to control the environmental and social impact of large projects. Moreover, a strong engagement towards environmental and social sustainability should be embedded in every hierarchical level of an organisation or company. Engineers should not shift environmental and social responsibility to the higher level, but be critical themselves. From this mind-set, I started my PhD in the field of sustainable energy use.

I took the first step into energy engineering in 2010, when I was working for Solar Without Borders, founded by Bert Bernolet. I planned and installed photovoltaic solar installations for schools, clinics and orphanages in Togo and Benin. To facilitate the design, I developed a spreadsheet model, which was the original inspiration for this thesis. In Belgium, we organised the first festival driven by a completely autonomous solar installation (Fiesta Solar). A smaller project was "Bar Solar", a mobile bamboo bar equipped with solar panels. A year later, I personally experienced the effect of a the derailed Flemish solar power subsidy scheme, which forced sponsors to reduce their financial support. Bert continued straightforward, innovating and extending his organisation. At the moment, solar kiosks have been installed in more than 150 villages, creating a local economy and introducing renewable energy in West-Africa.

During my search for a new challenge, I encountered Power-Link, an energy knowledge platform of Ghent University located at the technology park Greenbridge in Ostend. Professor Greet Van Eetvelde employed me as a researcher at Power-Link, but two months later she offered me the opportunity to start a PhD research on the European ACE project (Answers to the Carbon Economy, June 2011 – September 2014). My main task was to compose a manual for the development of low carbon business parks. This lead to an extensive document describing the context of low carbon business parks and the various energy measures that can be taken, illustrated with case studies carried out by the project partners.

Following my engineering instinct, I started studying how an energy system on business park scale could be mathematically modelled. Such a model would help to understand the interaction between the different technologies in the system, and the effect of different energy measures on the system's economic, energetic and environmental performances.

Via the Climate Team of Ghent, I came into contact with Ulrich Leopold and Laurent Drouet of the Henri Tudor institute in Luxemburg. They were developing a tool to integrate energy as a layer in urban planning, based on the energy model ETEM. During a one week scientific visit at Henri Tudor, I was introduced to the world of energy system optimisation. Subsequently, a review on energy models brought me into contact with David Connolly, who composed an extensive overview of energy models. He invited me to the PhD course '*Advanced Energy System Analysis on the EnergyPLAN model*' given by professor Henrik Lund and Poul Østergaard in Aalborg University, Denmark. In this research phase, I also contacted VITO, since they use the energy model TIMES as a tool for national and regional climate and energy policy analysis. After following the PhD course '*Modelling, optimisation, design and analysis of integrated energy systems*' given by professor François Maréchal at EPFL in Lausanne, I realised that aforementioned models do not include a thermodynamic representation of thermal energy flows. At the PRES13' conference in Rhodes, I presented the results of my energy model review, including a pathway towards a model suited for energy system optimisation at business park scale. During this conference, I attended Maike Hennen's presentation about a novel energy system synthesis approach, based on the work of Philip Voll. Eventually, this lead to an intensive scientific cooperation at RWTH Aachen University for a total duration of six weeks. I started from an embryonic model, developed during the course 'Optimisation techniques' at Ghent University. Maike Hennen translated this model into the GAMS programming environment and assisted me to stepwise develop a comprehensive energy system optimisation model in GAMS myself. When the ACE project was finalised, VITO was interested to support my research for an additional eight months. A one week scientific visit to VITO inspired me to integrate energy storage into the model. Subsequently, during a two week cooperation at EPFL, I focussed on design methods for heat exchanger networks in industrial energy systems. This resulted in inspiring discussions with fellow researchers Alberto Mian and Stéphane Bungener, and with professor François Maréchal. By the end of the 4-year PhD-period, the model had grown into adolescence. Since the research still had to be put into the form of a dissertation, I continued my research on a voluntary basis. Finally, at the end of 2015, I arrived at the finish, tired, but satisfied about my work.

The realisation of this work would not have been possible without the support of many people: Professor Greet Van Eetvelde, many thanks for giving me the initial opportunity to embark on this PhD journey, and believing in the aim and quality of my research. Professor Lieven Vandevelde, thank you for your kind but critical remarks and for the careful review of my writings. I also would like to thank the members of the examination committee for their expert advice.

The ACE crew enabled a smooth cooperation in a friendly atmosphere and greatly contributed to promote the concept of low carbon business parks. The moments before and after the congresses and events were very enjoyable. I would like to thank Björn, Mieke, Indra, Barbara, Nathalie, Marianne, Eveline, Véronique, Ian, Pranesh, Chrissie, Sara, Jane, Kevin, John, Peggy, and any person involved in ACE which I may have forgotten. Christof, it was a pleasure to be your 'PhD partner in crime' during the ACE project and the energy monitoring campaigns in Poperinge and Ghent.

Special thanks to Laurent and Ulrich for introducing me to the ETEM model. I really enjoyed the picanha restaurants in Esch-sur-Alzette. David, Poul and professor Henrik Lund, the EneryPLAN course really inspired me to dedicate the past years to energy modelling. Pieter, Luc and Yoko, thank you for believing in my research and the warm welcome at VITO. Maike, your help was of vital importance, since your GAMS programming skills triggered a major breakthrough in my research. I also would like to thank Matthias Lampe and professor André Bardow for reviewing my second paper in the Energy journal. It was a pleasure to work in Aachen and I immediately felt connected to the Technical Thermodynamics team. Björn, Jan, Dinah, Niklas, Arne, Sarah, Leonard, André and Rico, thanks for the nice after-work drinks and darts games. Lausanne, an extraordinary city with breath-taking views on the Alps and the Jura mountains. It's technical university resembles a labyrinth of Jenga-blocks covered with roof gardens. Stéphane and Alberto guided me through this labyrinth. Alberto, two words: "Ponce-Ortega!". Stéphane, thanks for connecting me to a lot of interesting people and taking me to the right apéro's and parties. Lindsay your home-made caramel bars are unparalleled.

Having fantastic colleagues is a key ingredient for being successful in your work. The original composition of our penthouse office crew (Jan, Karel, Tom and Koen) was a recipe for hilarious and sometimes absurd humour. Especially when Karel's funny remarks reached the "over-the-top" level. Jan, you infected me with your "out-of-the box-thinking" mentality and your positivism. Tom, you provided a pretty comprehensive work from which I could start, introducing me to the frontrunners of sustainability. Koen, thanks for unleashing your Photoshop-skills on our personal pictures, they are still decorating the wall. The next crew occupying the office were Joke and Samuel, aka 'Amule'. I thought the days of absurd humour would be over, but luckily I was wrong. Karel, Samuel and me invented the infamous game of 'office tennis', which was an efficient method to blow off some steam. Due to the thin wall, we were practically forming one team with the colleagues in the adjacent office: Barbara, Karel, Els, and Thomas, thanks for the research advice, the psychological support and the practical help on various topics, especially during the last year. The coffee break was always a refreshing moment. In the last phase of my research, also Suzanne, Nicolas, Hwa-Chyi and Yan Wang joined the troops. I wish you all a lot of persistence and confidence in your future research. Furthermore, I would like to thank all AMRP colleagues from the floor below who frequently helped me with their advice (professor Luuk Boelens, Kobe, Giustino, Enrica, and Els).

Thanks to my friends and family for supporting me throughout the process. Special thanks to the members of DriveUpDevice - the greatest band that ever walked the face of the Earth - for the fresh breeze, or rather tornado, in days of intellectual burden. Mom and dad, thank you for your unconditional support during my PhD. I could rely on you when difficult decisions had to be made and you helped me to see things in the right perspective. Soetkin, thank you from the bottom of my heart. You were able to deal with my over-occupied brain. Especially during the last year, when I was at the office until late in the evening and in the weekends, leaving little time for each other. Nevertheless, you stood by me during the down moments. I am so glad that we made it this far and I hope we will continue far beyond.

Ghent, December 2015
Jonas Timmerman

Table of contents

Samenvatting

Om de destabilisering van het klimaat tegen te gaan moet de wereldwijde uitstoot van broeikasgassen onmiddellijk worden verlaagd en tegen het eind van deze eeuw zelfs tot nul worden herleid. Op Europees niveau zijn duidelijke streefdoelen uitgezet voor de reductie van broeikasgasemissies en primair energiegebruik en voor de integratie van hernieuwbare energie. De uitstoot van koolstofdioxide (CO_2) door verbranding van fossiele brandstoffen in de industrie- en de energiesector vormt een belangrijk deel van de broeikasgasemissies. Daarom is een overgang naar CO_2-arme energiesystemen op industrieparken en bedrijventerreinen noodzakelijk. Op CO_2-arme bedrijventerreinen worden energie-gerelateerde CO_2-emissies geminimaliseerd door verbeterde energie efficiëntie, warmte-uitwisseling in en tussen bedrijven, maximale benutting van lokale hernieuwbare energie, en energieopslag, gecombineerd in een collectief energiesysteem. Bovendien worden bedrijven met complementaire energieprofielen geclusterd om energiesynergiën te kunnen exploiteren.

Door hun holistische aanpak bieden techno-economische energiemodellen een hulpmiddel voor het ontwerp van CO_2-arme energiesystemen. Dergelijke modellen brengen de complexe interacties in rekening tussen de componenten van het energiesysteem en laten toe om de prestaties van het systeem op het vlak van energie, economie en milieu optimaal op elkaar af te stemmen. In dit werk worden bestaande classificaties van energiemodellen gescand op geschikte modeleigenschappen. Op basis daarvan worden een beperkt aantal modellen geselecteerd en beschreven. Daarna wordt een praktische categorisatie voorgesteld bestaande uit energiesysteem evolutie, optimalisatie, simulatie, accounting en integratie modellen, terwijl de belangrijkste modeleigenschappen vergeleken worden. Vervolgens worden verschillende eigenschappen geïdentificeerd die essentieel zijn voor het modelleren van energiesystemen op schaal van een bedrijventerrein:

Ten eerste kunnen a priori beslissingen omtrent de configuratie van het energiesysteem vermeden worden door gebruik te maken van optimalisatie in een superstructuur. Een wiskundig algoritme berekent dan automatisch de beste configuratie in een referentiesysteem dat alle mogelijke configuraties bevat. Ten tweede moet de geanalyseerde tijdshorizon met voldoende detail gemodelleerd worden om belangrijke karakteristieken en pieken in variërende energievraag, energieprijzen, en werking van energietechnologieën weer te kunnen geven. Een derde vereiste is dat energietechnologieën nauwkeurig voorgesteld worden op het niveau van één enkele installatie. Daarom moeten de werking in deellast en de effecten van schaalvoordelen op de investeringskost worden inbegrepen. Bovendien moet het energiemodel configuraties met meerdere installaties per technologie in het energiesysteem kunnen analyseren. Verder vereenvoudigt een generieke formulering van technologiemodellen het toevoegen van nieuwe technologietypes. Ten vierde moet warmte-uitwisseling tussen thermische processen thermodynamisch gemodelleerd kunnen worden en moet het volledige potentieel ervan worden benut. Om de resterende thermische energievraag te vervullen moeten energietechnologieën optimaal geïntegreerd worden. De thermodynamisch modellering vereist een voorstelling van alle thermische stromen op basis van warmte-temperatuur profielen. Bovendien is het essentieel om beperkingen in directe warmte-uitwisseling tussen thermische processen in rekening te brengen. Als laatste punt moet energieopslag gemodelleerd kunnen worden om integratie van oncontroleerbare hernieuwbare energietechnologieën te bevorderen en om ongelijktijdigheid tussen koude- en warmtevraag te overbruggen.

Op basis van deze essentiële eigenschappen is in dit werk een techno-economisch optimalisatiemodel (*Syn-E-Sys*) ontwikkeld dat is afgestemd op het ontwerp van CO_2-arme energiesystemen op de schaal van een bedrijventerrein. Het model bevat twee opeenvolgende fases. In de eerste fase wordt warmte-uitwisseling in het energiesysteem gemaximaliseerd, terwijl energieconversie- en energieopslagtechnologieën optimaal worden geïntegreerd en ontworpen om de resterende energievraag in te vullen tegen minimale totale kosten op jaarbasis. Naast een CO_2-emissieplafond worden vastgelegde variaties in thermische en elektrische energievraag en -aanbod in rekening gebracht. Tegelijkertijd worden warmtenetwerken optimaal ingezet om warmte te transporteren tussen geïsoleerde delen van het systeem. In de tweede fase genereert het model automatisch een optimaal warmte-uitwisselingsnetwerk dat alle nodige warmte-uitwisselingen mogelijk maakt.

Syn-E-Sys is gebaseerd op een *multi-period* energie-integratiemodel waarin rechtstreekse warmte-uitwisseling tussen bepaalde delen van het energiesysteem kan worden beperkt. Dit model is gecombineerd met een generiek technologiemodel en met een model voor energieopslag. Het technologiemodel simuleert werking in deellast en houdt rekening met de effecten van schaalvoordelen op de investeringskost. Door de generieke formulering kunnen uiteenlopende technologieën voor thermische en elektrische energieconversie gemodelleerd worden. Bovendien vormt het model een bouwsteen voor meer complexe technologieën. Het model voor elektrische of thermische energieopslag brengt de effecten van energieverlies op het laadniveau in rekening, zonder dat het aantal te analyseren tijdsstappen hoeft te worden uitgebreid. De hiervoor benodigde tijdsequentie is ingevoerd door het jaar op te delen in een reeks tijdschijven, die gelinkt zijn aan een hiërarchische tijdsstructuur. Daarnaast is een meer complex model voor opslag van voelbare warmte uitgewerkt, dat is opgebouwd uit onderling verbonden virtuele tanks. Om ook het aantal installaties per technologie te kunnen optimaliseren is een procedure ingebouwd die de superstructuur van het energiemodel stapsgewijs uitbreidt. Om de keuze van geschikte temperatuurniveaus voor warmtenetwerken te leiden, berekent het energiemodel a priori een enveloppe voor warmteoverdracht. Wanneer de thermische stromen van de warmtenetwerken omsloten zijn door deze enveloppe, is de extra thermische energiebehoefte, die te wijten zou zijn aan de restricties in rechtstreekse warmte-uitwisseling tussen geïsoleerde delen van het energiesysteem, volledig vermeden. Het warmte-uitwisselingsnetwerk uit de tweede fase wordt automatisch gegenereerd met behulp van een *multi-period* superstructuur die opgebouwd is uit verschillende stages.

Tijdens de ontwikkeling van het energiemodel zijn twee problemen ontdekt die inherent zijn aan de formulering van de warmtecascade. Een eerste probleem is dat warmtenetwerken een zelfvoorzienende energie-lus kunnen vormen, wanneer hun thermische stromen niet volledig binnen de enveloppe vallen. Dit fenomeen wordt in onderhavig werk omschreven als fantoomwarmte. Een tweede probleem bestaat erin dat de formulering van de warmtecascade niet verhindert dat een warmte-opslagreservoir zijn warmte afgeeft aan een technologie die warmte weg koelt.

Om de specifieke eigenschappen van *Syn-E-Sys* en de holistische aanpak voor de synthese van CO_2-arme energiesystemen te demonstreren, worden een generieke case study en een case study uit de literatuur uitgewerkt. De generieke case study analyseert het optimale ontwerp van een energiesysteem waarbij hernieuwbare energie en energieopslag worden geïntegreerd, terwijl de CO_2-uitstoot onder een vooraf bepaald plafond moet blijven. Om de evolutie van het energieopslagniveau te kunnen volgen is tijdsequentie toegevoegd door het jaar op te splitsen in

tijdschijven, gelinkt aan een tijdsstructuur opgebouwd uit seizoenen, dag-types en dag-segmenten. Uit de resultaten valt af te leiden dat de energievraag gedekt wordt door een complexe interactie tussen energieopwekking, energieopslag en energie-import en –export, terwijl het opgelegd emissieplafond gerespecteerd wordt. Bovendien zijn de capaciteit en het op- en ontlaadpatroon van de energieopslaginstallaties geoptimaliseerd. Het benodigde optimale warmte-uitwisselingsnetwerk is automatisch gegenereerd. De tweede case study optimaliseert de warmte-uitwisseling in een droogproces uit de papierindustrie. Warmtenetwerken worden optimaal geïntegreerd met behulp van de warmteoverdracht-enveloppe. Op die manier wordt de extra thermische energiebehoefte, gerelateerd aan restricties in warmte-uitwisseling tussen twee geïsoleerde delen van het proces, volledig vermeden. Een vereenvoudigde versie van het originele probleem is gemodelleerd in *Syn-E-Sys* en de verkregen resultaten zijn in overeenstemming met de literatuur. Vervolgens wordt het probleem uitgebreid om de integratie van warmtenetwerken ook in een *multi-period* situatie te demonstreren. Er kan besloten worden dat *Syn-E-Sys* het optimale ontwerp van CO_2-arme energiesystemen op bedrijventerreinschaal faciliteert, rekening houdend met de complexe tijdsafhankelijke interacties tussen thermische en elektrische energievraag, energieconversie en energieopslag, terwijl het potentieel voor warmte-uitwisseling ten volle wordt benut.

Summary

To mitigate climate destabilisation, global emissions of human-induced greenhouse gases urgently need to be reduced, to be nearly zeroed at the end of the century. Clear targets are set at European level for the reduction of greenhouse gas emissions and primary energy consumption and for the integration of renewable energy. Carbon dioxide emissions from fossil fuel combustion in the industry and energy sectors account for a major share of greenhouse gas emissions. Hence, a low carbon shift in industrial and business park energy systems is called for. Low carbon business parks minimise energy-related carbon dioxide emissions by enhanced energy efficiency, heat recovery in and between companies, maximal exploitation of local renewable energy production, and energy storage, combined in a collective energy system. Moreover, companies with complementary energy profiles are clustered to exploit energy synergies.

The design of low carbon energy systems is facilitated using the holistic approach of techno-economic energy models. These models take into account the complex interactions between the components of an energy system and assist in determining an optimal trade-off between energetic, economic and environmental performances. In this work, existing energy model classifications are scanned for adequate model characteristics and accordingly, a confined number of energy models are selected and described. Subsequently, a practical categorisation is proposed, existing of energy system evolution, optimisation, simulation, accounting and integration models, while key model features are compared. Next, essential features for modelling energy systems at business park scale are identified:

As a first key feature, a superstructure-based optimisation approach avoids the need for a priori decisions on the system's configuration, since a mathematical algorithm automatically identifies the optimal configuration in a superstructure that embeds all feasible configurations. Secondly, the representation of time needs to incorporate sufficient temporal detail to capture important characteristics and peaks in time-varying energy demands, energy prices and operation conditions of energy conversion technologies. Thirdly, energy technologies need to be accurately represented at equipment unit level by incorporating part-load operation and investment cost subject to economy of scale in the model formulation. In addition, the benefits of installing multiple units per technology must be considered. A generic model formulation of technology models facilitates the introduction of new technology types. As a fourth important feature, the potential of thermodynamically feasible heat exchange between thermal processes needs to be exploited, while optimally integrating energy technologies to fulfil remaining thermal demands. For this purpose, thermal streams need to be represented by heat –temperature profiles. Moreover, restrictions to direct heat exchange between process streams need to be taken into account. Finally, the possibility for energy storage needs to be included to enhance the integration of non-dispatchable renewable energy technologies and to bridge any asynchrony between cooling and heating demands.

Starting from these essential features, a techno-economic optimisation model (*Syn-E-Sys*), is developed customised for the design of low carbon energy systems on business park scale. The model comprises two sequential stages. In the first stage, heat recovery within the system is maximised, while energy supply and energy storage technologies are optimally integrated and designed to fulfil remaining energy requirements at minimum total annualised costs. Predefined variations in thermal and electrical energy demand and supply are taken into account, next to a

carbon emission cap. At the same time, heat networks can be deployed to transfer heat between separate parts of the system. In the second stage, the model generates an optimal multi-period heat exchanger network enabling all required heat exchanges.

Syn-E-Sys builds upon a multi-period energy integration model that can deal with restrictions in heat exchange. It is combined with a generic technology model, that features part-load operation as well as investment cost subject to economy of scale, and a generic energy storage model. The technology model can be manipulated to represent various thermal or electrical energy conversion technology units, and serves as a building block to model more complex technologies. The storage model covers electrical as well as thermal energy storage, taking into account the effect of hourly energy losses on the storage level, without increasing the number of time steps to be analysed. For this purpose, time sequence is introduced by dividing the year into a set of time slices and assigning them to a hierarchical time structure. In addition, a more complex model for storage of sensible heat is integrated, consisting of a stack of interconnected virtual tanks. To enable the optimisation of the number of units per technology in the energy system configuration, an automated superstructure expansion procedure is incorporated. Heat transfer unit envelope curves are calculated to facilitate the choice of appropriate temperature levels for heat networks. Heat networks that are embedded within this envelope, completely avoid the increase in energy requirements that would result from the heat exchange restrictions between separated parts of the energy system. Finally, the heat exchanger network is automatically generated using a multi-period stage-wise superstructure.

Two problems inherent to the heat cascade formulation are encountered during model development. As a first issue, heat networks can form self-sustaining energy loops if their hot and cold streams are not completely embedded within the envelope. This phenomenon is referred to in this work as phantom heat. As a second issue, the heat cascade formulation does not prevent that a thermal storage releases its heat to a cooling technology.

To demonstrate the specific features of *Syn-E-Sys* and its holistic approach towards the synthesis of low carbon energy systems, the model is applied to a generic case study and to a case study from literature. The generic case study is set up to demonstrate the design of an energy system including non-dispatchable renewable energy and energy storage, subject to a carbon emission cap. For this purpose, the year is subdivided into a set of empirically defined time slices that are connected to a hierarchical time structure composed of seasons, daytypes and intra-daily time segments. The results obtained by *Syn-E-Sys* show a complex interaction between energy supply, energy storage and energy import/export to fulfil energy demands, while keeping carbon emissions below the predefined cap. The model enables optimisation of the intra-annual charge pattern and the capacity of thermal and electrical storage. Moreover, an optimal heat exchanger network is automatically generated. In the second case study, heat recovery is optimised for a drying process in the paper industry. To avoid the energy penalty due to heat exchange restrictions between two separated process parts, heat transfer units need to be optimally integrated. Firstly, a simplified version of the original problem is set up in *Syn-E-Sys* and the obtained results correspond well to literature. Subsequently, the original problem is extended to demonstrate the optimal integration of heat transfer units in a multi-period situation. In conclusion, *Syn-E-Sys* facilitates optimal design of low carbon energy systems on business park scale, taking into account the complex time-varying interactions between thermal and electrical energy demand, supply and storage, while the potential for heat recovery is fully exploited.

General introduction

To mitigate global warming, anthropogenic greenhouse gas emissions urgently need to be curbed. The major share of these emissions exists of carbon dioxide (CO_2), caused by combustion of fossil fuels and by industrial processes. On European level, more than a quarter of CO_2 emissions related to fossil fuel combustion can be allocated to the energy use of the industry sector. As a consequence, a low carbon energy shift in the industry sector is called for.

Low carbon business parks provide an answer to this need by applying a set of low carbon energy measures. The implementation of these measures into the park's energy system can be facilitated and their effect can be enhanced by exploiting energy synergies between companies (energy clustering). It is of key importance that the integration of energy measures into the energy system is optimised on system level to maximise the overall cost-effectiveness of the related investments in energy infrastructure.

However, evaluating and optimising the effect of a set of energy measures on the economic, energetic and environmental performance of a business park scale energy system can be cumbersome. Energy demands, renewable energy sources and energy prices are subject to variations in time, which results in complex interactions between the system's components. Consequently, there is a clear need for a mathematical modelling tool to facilitate investment decision-making for energy systems on low carbon business parks.

An appropriate model needs to integrate a set of essential features, identified in this work. The review conducted in this work shows that a large number of techno-economic energy models have been developed during the last decades, each serving particular purposes. The studied models each establish a number of essential features. However, there is a need to develop a holistic model that integrates all essential features at once.

Therefore, the main focus of this work is to develop a holistic energy model customised to optimise the design of a low carbon energy system on business park scale. The proposed model, called *Syn-E-Sys* integrates all essential features by modifying, extending, merging and aligning existing model formulations, supplemented with new approaches and insights. Performance and features of the model are illustrated with two small-scale case studies that allow for verification and interpretation of the results. Future perspectives for further development and application of *Syn-E-Sys* on a full scale business park case study are discussed.

Reading guide

In this thesis, a mathematical model is developed to facilitate the design of low carbon energy systems on business park scale. The proposed model comprises two sequential stages. In the first stage, heat recovery within the system is maximised, while energy conversion and energy storage units are optimally integrated and designed to fulfil remaining energy requirements at minimum total annualised costs. Predefined variations in thermal and electrical energy demand and supply are taken into account, next to a carbon emission cap. At the same time, heat networks can be deployed to transfer heat between separate parts of the system. In the second stage, the model generates an optimal multi-period heat exchanger network enabling all required heat exchanges.

The manuscript consists of three subsequent parts, in line with the stepwise development of the conducted research.

In Part 1, the context for low carbon business parks is mapped out. Firstly, the European climate and energy policy is introduced, while focussing on policy measures applicable to the industry and the energy sector. Subsequently, the concept of low carbon business parks is explained and illustrated with a number of examples. Low carbon energy measures are identified starting from a generic representation of a business park energy system. Finally, the idea of energy clustering to enable the exploitation and realisation of energy synergies within and with the energy system is explained.

Part 2 addresses the need for a holistic mathematical model to facilitate the design of low carbon energy systems at business park scale. Based on a confined review of energy models, a pragmatic model categorisation is proposed containing Energy System (ES) evolution, optimisation, simulation, accounting and integration models. The key features of these models are compared and discussed. Subsequently, essential features for the modelling of energy systems on business park scale are identified, which compose the framework for the model developed in Part 3.

In Part 3, a holistic techno-economic optimisation model is developed, called *Syn-E-Sys*, customised for business park scale energy systems. Firstly, the concept of superstructure-based energy system optimisation is introduced. Next, methods for energy integration and the corresponding mathematical models are reviewed. Based thereon, a two-staged method is derived, which forms the backbone of *Syn-E-Sys*. Subsequently, the model formulation is built up by stepwise integration of all essential features identified in Part 2. For this purpose, a number of existing models are merged and aligned. Finally, the performance and features of *Syn-E-Sys* are demonstrated by two case studies. Future perspectives for further development and application of the model on a full scale business park case study are discussed.

Part 1

Context for low carbon business parks

1. Introduction

To mitigate the effects of global warming, greenhouse gas emissions need to be reduced substantially, to be nearly zeroed at the end of this century [1]. Ambitious climate and energy policies from global to local level are prerequisite to achieve this vital goal. Carbon dioxide emissions from fossil fuel combustion and industrial processes account for the major share of global greenhouse gas emissions [1]. On European level, more than a quarter of these carbon emissions are related to energy consumption within the industry sector [2]. As a consequence, a transition towards low carbon energy systems is required. For this purpose, low carbon business parks aim at significant reductions of energy-related carbon emissions by exploiting energy synergies between companies.

Chapter 2 provides an introduction to European climate and energy policy. In chapter 3, the concept of low carbon business parks is explained and illustrated with worldwide examples. Low carbon energy measures are discussed from an organisational perspective and identified starting from a generic representation of a business park energy system. Chapter 4 focusses on the exploitation of energy synergies, also referred to as energy clustering. Major parts in Part 1 are adopted from the "Low carbon business park manual", which was one of the outcomes of the project "Answers to the Carbon Economy" (ACE). For more information on the project and its results, reference is made to Timmerman *et al.* [3].

2. Climate and energy policy

This chapter provides a brief introduction to climate change. Next, carbon emissions in the energy and industry sector are focussed on. An overview is given of European climate and energy policy and policy measures taken in the industry and energy sector.

2.1. Climate change

During the last decades, anthropogenic greenhouse gas (GHG) emissions have drastically increased, in line with industrialisation and population growth. The natural balance between greenhouse gas sources and sinks is disturbed, resulting in increasing GHG concentrations in the atmosphere. This leads to a gradually intensifying greenhouse effect, which causes the Earth's climate to change. Symptoms are: increase of global mean surface temperature (global warming), melting of polar ice and glaciers, sea level rise, extreme weather events, such as droughts heat waves and flooding, acidification of the oceans, etc. These phenomena result in severe societal, economic and environmental damage [4].

The main anthropogenic GHGs are carbon dioxide (CO_2), methane (CH_4), nitrous oxide (N_2O), hydrofluorocarbons (HFCs), perfluorocarbons (PFCs), and sulphur hexafluoride (SF_6). Since CO_2 is the largest contributor to global warming in absolute terms, GHG emissions and atmospheric GHG concentrations are expressed in CO_2-equivalents (CO_2-eq) [1]. The CO_2-equivalent concentration of a mixture of GHGs in the atmosphere corresponds to the concentration of CO_2 that would cause the same radiative forcing (net heat flux absorbed by the Earth system). In addition, the radiative forcing related to aerosols and albedo change can be incorporated. The CO_2-equivalent of an amount of GHG

emission corresponds to the amount of CO_2 that would cause the same radiative forcing over a given time horizon [1].

To mitigate climate change, global climate policy aims at keeping global warming below 2 °C compared to pre-industrial times. For this purpose, the CO_2-equivalent GHG concentration (including aerosols and albedo change) must be stabilised below 450 ppm CO_2-eq in 2100. To achieve this goal, global annual CO_2-equivalent GHG emissions should be decreased by 2050 with 40 to 70% compared to 2010 and be zeroed by 2100 [1]. In 2012 the CO_2-equivalent GHG concentration already surpassed a value of 435 ppm CO_2-eq [5], as shown in Fig. 1. At the moment, the atmospheric concentration of CO_2 only has nearly reached 400 ppm and is increasing at a rate of about 2.1 ppm a year. However, if other GHGs are added (excluding aerosols and albedo change), a CO_2-equivalent concentration of about 478 ppm CO_2-eq is obtained [6]. Global climate policy and action now and in the coming few decades will be decisive for the severity of climate change.

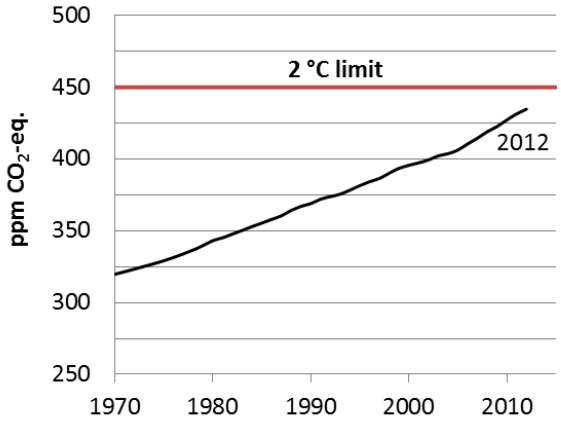

Fig. 1: Total CO_2-equivalent GHG concentration up to 2012 and 2°C limit (including aerosols and albedo change) [5]

2.2. Carbon emissions in the industry sector

In 2010, 65% of global, total annual GHG emissions (expressed in CO_2-eq) were related to CO_2 from fossil fuel combustion and industrial processes [1]. In this work, the focus is on reducing CO_2 emissions (carbon emissions) from fossil fuel combustion related to energy consumption in the industry sector. These emissions can be allocated to energy generation within the sector itself (direct emissions), and to heat and electricity imported from the energy sector (indirect emissions). In Europe, direct CO_2 emissions in the industry sector account for about 15% of total energy-related CO_2 emissions, and this share increases to about 28% when indirect emissions are added. (Table 1). The data for direct emissions in Table 1 cover emissions from coke inputs into blast furnaces, which alternatively could be classified as emissions from industrial processes (non-energy use).

To calculate carbon emissions related to electricity import, carbon intensities are used, expressing the average emissions of electricity production in g CO_2/kWh$_e$. These factors (Table 1, last column) depend on the type of fuels and the efficiencies of technologies employed for electricity generation in the energy sector.

CO_2-emissions (Mt/y)	Total	Manufacturing industries and construction*				Carbon intensity g CO_2/kWh_e
		Direct		*Direct and indirect*		
EU27 (2010) [7]	3659,5	546,9	→14,9%	1005,9	→27,5%	347
EU28 (2012) [2]	3504.9	527.3	→15.0%	981.0	→28.0%	-

**excluding unallocated autoproducers*

Table 1: CO_2-emissions from energy generation by fossil fuel combustion in the industry sector (incl. emissions from coke inputs into blast furnaces), and carbon intensity of electricity generation [2, 7]

In Fig. 2, the direct CO_2-emissions from fossil fuel combustion for energy use in the EU's industry sector are allocated to the main industry sub-sectors. Emissions from industrial processes (non-energy use) are not included. The iron and steel, non-metallic minerals and chemical and petrochemical sectors are the largest CO_2-emitters, followed by the sector food and tobacco and the paper, pulp and printing sector.

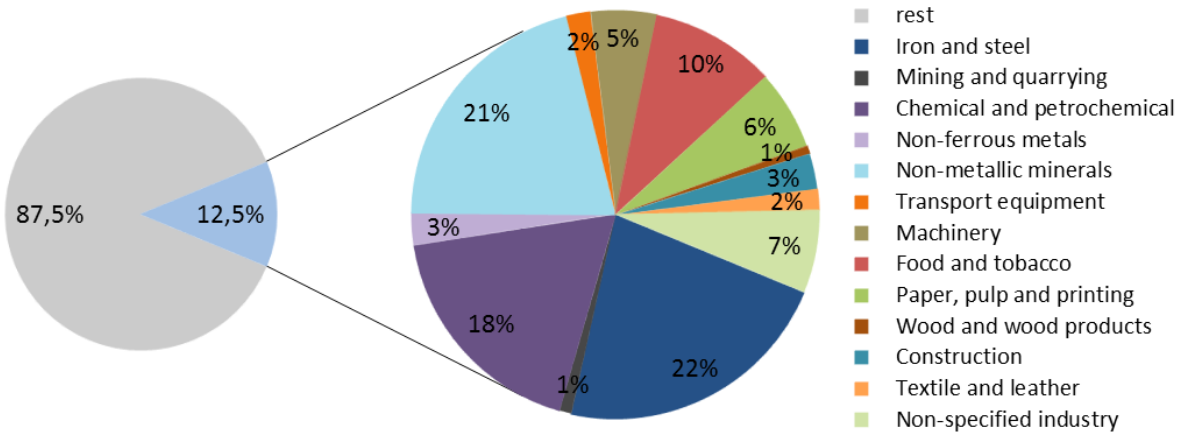

Fig. 2: Direct CO_2 emissions from fossil fuel combustion for energy use in the industry sector and sub-sectors for EU27 in 2010, based on data retrieved from IEA

2.3. European climate and energy policy

At a global level, the EU has committed to achieve the Kyoto Protocol targets. In addition, it has set out and initiated a transition pathway towards a low carbon economy, in which the key elements are: the Climate and Energy Package (2020), the Framework 2030 and the Roadmap 2050 (Fig. 3). The Climate and Energy Package includes directives, which have to be transposed, together with other climate and energy related directives, into National Application Plans. These need to be put into practice by national authorities through concrete national policy measures (Fig. 4). Furthermore, the Climate & Energy package is part of the overarching Europe 2020 strategy.

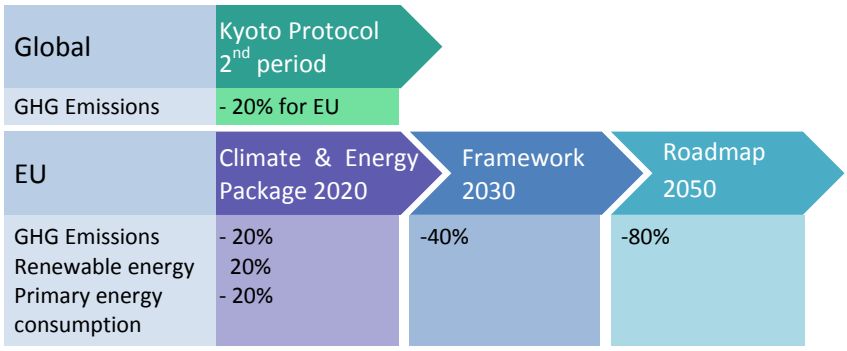

Fig. 3: Climate and energy policy [8]

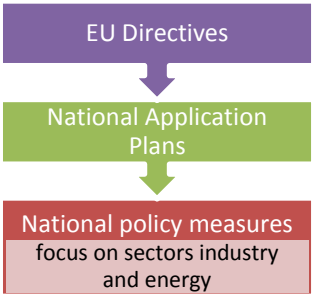

Fig. 4: Policy implementation [8]

2.3.1. Kyoto Protocol

The Kyoto Protocol is the only legally binding treaty on global scale to reduce greenhouse gas emissions. It was adopted in 1997 and entered into force early 2005. The protocol's GHG basket includes the gasses mentioned in Section 2.1 and from 2013 on also nitrogen trifluoride (NF_3). Reduction targets are set on total GHG emissions expressed in CO_2-equivalents. In the first commitment period from 2008 to 2012, the participating developed countries needed to reduce annual GHG emissions over the entire period with an average of 5% below 1990 levels. However, in 2002, the 15 EU member states at that time raised their collective reduction target to 8% below 1990 levels, which has been translated into national targets under the burden sharing agreement (BSA). In the second commitment period, from 2013 to 2020, the 28 EU member states and Iceland commit to keep joint annual emissions at an average of 20% below 1990 levels over the whole period. To achieve Kyoto targets, countries are in the first place expected to take internal policy measures to lower emissions or to enhance carbon sinks. In addition, emission credits can be traded among developed countries or earned by financing emission reducing projects in either developed or developing countries. For EU countries this is regulated by the Emissions Trading System.

2.3.2. Europe 2020

In the overarching Europe 2020 strategy, the EU puts smart, sustainable and inclusive growth as its main priorities (Fig. 5).

Fig. 5: Europe 2020 strategy [8]

These priorities are concretised into five key targets, covering employment, R&D, education, climate and energy, and social inclusion and poverty reduction. Subsequently, these overall objectives have been translated to the national level. Seven flagship initiatives provide a framework to achieve those

goals. Climate and energy goals are bundled in the Climate and Energy Package and are referred to as the 20/20/20 targets. The implementation of the Europe 2020 strategy will improve security of energy supply and increase competitiveness of industry. Additionally, the European Commission aims at increasing industry's share of GDP to 20% by 2020, to establish a solid industrial base.

2.3.3. Climate and Energy Package

The European Union has set three major objectives towards 2020, also referred to as the 20/20/20 targets: reduction of annual greenhouse gas emissions with 20% beneath 1990 levels, increase of the share of renewable energy in final energy consumption to 20%, and reduction of annual primary energy consumption with 20% compared to Business As Usual (BAU) projections for 2020. Emission reduction may even be lifted to 30% if other major economies raise efforts. The first two targets are elaborated and disaggregated to the national level in the Climate and Energy package, launched in 2009. It establishes a legal framework through EU directives, imposing end results to member states that have to be included in national legislations and policies.

20% emission reduction

For practical reasons, the emission target has been reformulated as a 14% decrease of emissions in comparison to 2005. Efforts are divided among two complementary emission accounting schemes, being the Emissions Trading System (ETS) and the Effort Sharing Decision (ESD). Under the ETS, a collective emission reduction of 21% has to be achieved, while under the ESD, national targets are set, resulting in an overall emission reduction of 10% against 2005 levels.

Emissions Trading System (ETS): The Emissions Trading System is a policy tool to gradually decrease overall European GHG emissions. It covers CO_2 emissions from power stations, energy-intensive industrial plants and commercial airlines, N_2O emissions from the production of certain acids and emissions of PFCs from the aluminium industry. The ETS was established in 2003 under the Emissions Trading Directive (ETD), which has been revised in 2009. In 2013, it covered about 45% of total emissions. Each year, the companies included in the system are obliged to submit one emission allowance per ton of CO_2-equivalent emitted. For every missing credit a fine must be paid. Reduction of overall emissions is achieved by gradually decreasing the total amount of allowances available in the system. Depending on the sector, part of the available allowances is granted for free, according to harmonised EU-wide rules, that reward best practice in low-emission production. To fully cover their emissions, companies can buy additional credits at auction from other companies or from approved emission-saving projects around the world. Excess allowances, on the other hand, can be sold at auction or saved to be used at a later time. In conclusion, the ETS was meant to put a price on emissions and to create an incentive for companies to invest in technologies that reduce emissions. Unfortunately, the ETS is currently facing a short-term problem, because the economic crisis created an excess of emission allowances, that has lowered the carbon price.

Effort Sharing Decision (ESD): The Effort Sharing Decision establishes emission reduction goals for most of the sectors not included in the ETS, such as transport (except aviation), buildings, agriculture, waste and the non-ETS part of energy and industry. By 2020, total emissions under ESD have to decrease with 10% compared to 2005 levels. This has been translated into national reduction targets, ranging from -20% to +20%. The emission increases against 2005 levels for the least wealthy states nevertheless imply a reduction when compared with projected business as usual emissions. To

achieve these targets, countries or regions can employ flexibility mechanisms and acquire additional emission credits.

Carbon Capture and Storage Directive (CCSD): Additionally to reduction of carbon emissions, CO_2 from industrial sites and power plants can be captured and stored in underground geological formations where it does not contribute to global warming. The Carbon Capture and Storage Directive (CCSD) establishes a legal framework to ensure the environmentally safe implementation of CCS technologies.

20% renewable energy

The Renewable Energy Directive (RED) provides a legislative framework to promote the use of energy from renewable sources and the shift to cleaner forms of transportation. It translates the collective EU target of a 20% renewable energy share in final energy consumption into binding national targets, ranging from 10% to 49%. Moreover, each member state has to achieve a 10% renewable energy share in final energy consumption of the transport sector by 2020. In this context, biofuels and bio liquids are only taken into account if they are qualified as "sustainable". To put this in practice, national renewable energy action plans (NREAPs) for renewable energy and procedures for the use of biofuels are defined.

20% reduction primary energy consumption

By 2020, the EU aims to reduce its annual primary energy consumption with 20% compared to projections. However, the energy efficiency target is not directly addressed in the Climate and Energy package, but through the Energy Efficiency Directive (EED). The EED establishes a legal framework for the implementation of energy efficiency policies and measures proposed in the Energy Efficiency Plan (EEP). These measures cover every stage of the energy chain from generation to final consumption. Especially the sectors energy, industry, buildings and transport hold great energy saving potentials. The public sector is expected to take the lead and is obliged to energetically renovate each year 3% of government building floor surface from 2014 on. Measures include promotion of combined heat and power generation in the energy and industry sector, district heating and cooling, smart grids, energy monitoring and audits for small and medium-sized enterprises, energy management systems, smart metering for buildings, labelling of energy performance of buildings and appliances, eco-design of products, etc. EU member states are required to compose national energy efficiency action plans (NEEAPs), describing national strategies and measures to achieve individual indicative energy efficiency targets for 2020. Those national plans will have to be reviewed and improved every three year.

2.3.4. Energy Performance of Buildings Directive

The Energy Performance of Buildings Directive (EPBD) creates a legal framework to promote reduction of energy consumption in the building sector, that currently accounts for 40 % of total EU energy consumption. Under this directive, EU states must establish minimum requirements for and certification of energy performance for existing and new buildings, next to a regular inspection of boilers and air-conditioning systems, introduce low carbon technologies for heating and cooling and electricity generation. By 2021 all new buildings should be nearly zero energy buildings (NZEBs). Each member state has to develop an NZEB national plan.

2.3.5. Framework 2030

The EU is currently developing a green paper for a 2030 framework for EU climate change and energy policies, based on lessons learned from the 2020 framework and taking into account the pathways set out in the Roadmap 2050.

2.3.6. Roadmap 2050

The EU "roadmap towards a competitive low carbon economy" defines a cost-effective pathway to reduce greenhouse gas emissions by 80 to 95% in 2050 against 1990 levels, with intermediary steps of 40% in 2030 and 60% in 2040. Efforts are divided between different economic sectors, according to their technological and economic potential to reduce emissions (Fig. 6).

The power sector has the highest potential and could almost totally eliminate greenhouse gas emissions by 2050 by fully employing renewable and low carbon technologies. This requires a strong decline of the ETS emission cap for the power sector and investment into smart grids. Part of transport and heating could shift from fossil fuel combustion to electricity, while heavy transport and aviation could shift to biofuels. In the transport sector, emission reductions of 60% could be achieved by improving efficiencies of traditional engines and fuels, followed by a shift towards hybrid and electric engines, and by better exploitation of transportation networks.

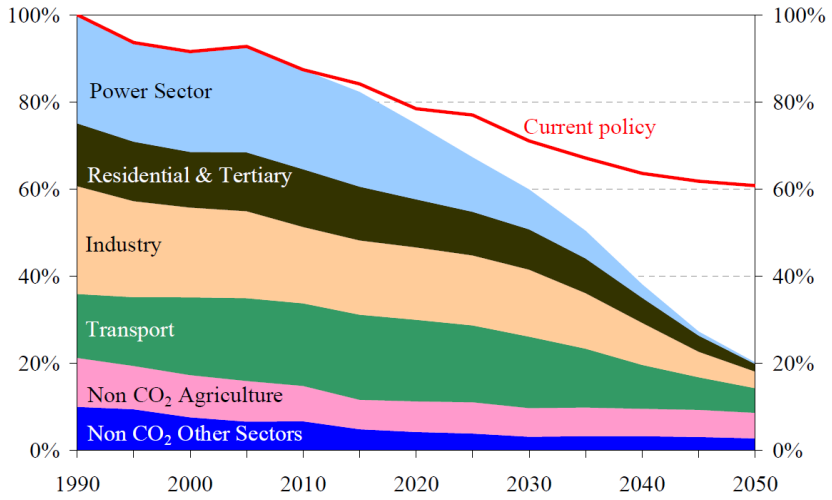

Fig. 6: Roadmap towards a competitive low carbon economy, sectoral perspectives [8]

Emissions from the residential and tertiary sector can be cut by about 90%, by improving the energy performance of existing buildings, introducing low carbon technologies for individual electricity production and space heating, and promoting district heating. Moreover, nearly zero energy buildings will become the new build standard from 2021 on. Energy intensive industries could lower their emissions by about 80%, using cleaner and more efficient processes and carbon capture and storage technologies. Agricultural emissions need to be cut by more efficient farming practices and conversion of animal waste to biogas. Eventually, the low-carbon roadmap would lead to a 30% reduction of energy consumption versus 2005 levels by 2050. A desired pathway specifically for the energy sector is elaborated in the Energy Roadmap 2050 (Fig. 6).

2.3.7. Industrial Emissions Directive

The Industrial Emissions Directive (IED) aims at reducing pollution of industrial sources across the EU, especially emissions of greenhouse gasses and acidifying substances, wastewater and waste. A higher material and energy efficiency is pursued. Therefore, environmental permits are linked to a positive evaluation of the complete environmental performance of a company and the application of Best Available Techniques (BAT), which are described in the BAT reference documents (BREFs).

2.3.8. Regulation F-gas emissions

The F-gas Regulation aims to curb fluorinated gas emissions on EU-level from industrial processes and from cooling installations and heat pumps. Measures include monitoring, labelling, restrictions to the use of certain products and containing F-gases, certification of staff, limit access to F-gas containing products, prescribe alternatives, etc. This regulation is incorporated in the national legislations.

2.3.9. Horizon 2020 instruments

The flagship 'Innovation Union' (2014-2020) under the Europe 2020 strategy aims at securing Europe's competiveness and is financially implemented through the Horizon 2020 program. Horizon 2020 basically needs to close the gap between research and the market. As a result, PPPs (Public Private Partnership), ETPs (European Technology Platforms) and Joint Technology Initiatives (JTIs) are established, that set out industrial research and innovation roadmaps and priorities.

SPIRE (Sustainable Process Industry through Resource and Energy Efficiency) is a public private partnership between the European Commission and the European process industry, including the sectors cement, ceramics, chemicals, engineering, minerals and ores, non-ferrous metals, steel and water. The partnership supports and enables the development of technologies and solutions needed to reach sustainability for European industry in terms of competitiveness, ecology and employment. SPIRE has set two targets for 2030, in line with the European climate and energy strategy. Firstly, a reduction in fossil energy intensity of 30% against current levels (2008-2011) is targeted. Secondly, a reduction of 20% in non-renewable, primary raw material intensity compared to current levels is aimed at. A roadmap towards these goals has been composed, identifying measures to be taken regarding energy and material resources. These measures include optimisation of energy systems, energy recovery, renewable energy and combined heat and power production, process optimisation, innovative energy-saving processes, recycling, renewable raw materials, process intensification, industrial symbiosis, enhanced sharing of knowledge and best practices, broadening of societal involvement, etc.

2.3.10. Policy challenges

Kyoto: Despite all efforts, the Kyoto Protocol is not sufficient to cut global greenhouse gas emissions, as no binding targets are imposed to major emerging economies in the developing world (e.g. China, India, Brazil, Indonesia), the United States of America have never ratified it and Canada has withdrawn its support. In the second Kyoto period, only the EU and a small number of other countries are participating, covering a minor share of global emissions (13,4% in 2010). In 2013, global carbon dioxide emissions stood at about 60% above 1990 levels. Therefore, a new global legal

framework with overall binding emission reduction targets needs to be established. This has been the subject of the subsequent international climate conferences, that are organised every year by the United Nations Framework Convention on Climate Change (UNFCCC). Eventually, the 2015 climate conference in Paris should result in a new global treaty, taking effect from 2020 on. Despite the alarming conclusions of the IPCC [4] on human-induced climate change, little progress was made in the Warsaw Climate Change Conference in November 2013, and major environmental and social organisations left the conference table. Keeping global temperature rise beneath the 2°C threshold seems to become virtually impossible.

EU-ETS: The EU-ETS faces several short-term problems. In 2013, the carbon price collapsed to about 5 €/ton CO_2-equivalents, due to an excess of emission allowances on the market. There are two reasons for this **surplus** of emission credits. Energy intensive, fossil fuel based industries claim that European climate policy endangers their market position in comparison to regions outside Europe with less stringent climate legislation, forcing them to shut down their plants or to delocalise their production activity. This so-called carbon leakage would have negative effects on local economy. Emissions would decrease in Europe, but proportionally increase in the rest of the world. Therefore, a number of national governments have chosen to grant free emission allowances to ETS-companies and installations prone to carbon leakage, or to compensate the costs for emission credits charged through electricity prices. This approach clearly favours extending the operational lifetime of older less efficient technologies. To achieve emission reduction targets, countries and companies can achieve extra emission credits by carbon offset projects. Due to weak regulations, some offset projects are questionable or even perverse [9].

2.3.11. Overview of European climate and energy policy

The climate and energy policy overview below is based on information from the EC [8].

Year	Policy	EU targets	National targets	National Plans
2012	***Kyoto Protocol*** 2008-2012 ***BSA***	**average Em. -8%** EU-15	EU-15: average Em. -28% to +27%; rest EU: -5% to -8% vs. different base years	
2020	***Kyoto protocol*** 2013-2020	**average Em. -20%** EU, Croatia, Iceland	average Em. -20%	
	Climate & energy package			
		Em. -20% (-30%)		
	***ETD* (ETS)**	Em. -21% vs. 2005		
	***ESD* (non-ETS)**	Em. -10% vs. 2005	Em. -20% to +20% vs. 2005	
	RED	**20% RE** (transport: 10%)	10% to 49% RE	***NREAP***
	EED	**PEC -20%**	Indicative targets	***NEEAP***
	CCSD			
	EPBD		new-build: NZEB by 2021	***NZEB NP***
2030	***2030 Framework***	Em. -40%		
2040	***Roadmap 2050***	Em. -60%		
2050		Em. -80-95%		
IED, F-gas Regulation, PPPs, ETPs				

Em. annual greenhouse gas emissions in CO_2 equivalents, reduction compared to 1990 levels, unless other base year specified in table
PEC annual primary energy consumption, reduction compared to projected levels for 2020
RE renewable energy share in final energy consumption

2.4. National and regional energy policy measures for industry

National targets on GHG emissions, renewable energy and energy efficiency, imposed by the EU through the Climate and Energy Package, have to be implemented in national and regional policies and legislations. Member states are obliged to submit national action plans to the European Commission, extensively describing the policy measures they will take, according to the Renewable Energy Directive (RED), the Energy Efficiency Directive (EED) and the Energy Performance of Buildings Directive (EPBD). National and regional policies are in turn put into practice through a series of policy measures. Measures in the industrial and energy sector can be subdivided according to their approach: regulation, financial support, funds and loans, voluntary agreements and information dissemination. Building regulations follow the EPBD, and environmental permit regulations for industrial processes and energy production installations are based on the EID or the former IPPCD. F-gas emissions from industrial processes and equipment are controlled by an EU-wide regulation. Financial support mechanisms include income tax deduction, (proportional) investment support, (fixed) energy premiums, energy production or carbon saving certificates, subsidies for studies, audits and R&D, subsidies for energy monitoring systems, subsidies for business parks development. Information dissemination is done through consultancy, awareness raising campaigns, training programmes and informative websites. An extensive overview and comparison of national or regional policy measures in different countries is provided in Timmerman *et al.* [3].

3. Low Carbon Business Parks

In this chapter, sustainability concepts for business parks are defined. Subsequently, low carbon energy measures are indicated on a generic scheme of a business park energy system, following the Trias Energetica strategy [10]. Four levels are identified at which these measures can be taken. Finally, some examples of low carbon business parks worldwide are described.

3.1. Sustainability concepts for business parks

A number of different approaches towards sustainability on business parks can be distinguished [3, 11, 12]. Sustainable industrial parks focus on inter-firm cooperation in all aspects, while eco-industrial parks specifically aim at exploiting synergies in the supply chains of energy, materials and water (industrial symbiosis). Green industry parks, on the other hand, are a collection of individually sustainable companies. Low carbon business parks combine elements of both eco-industrial and green industrial parks (Fig. 7), with a specific focus on energy.

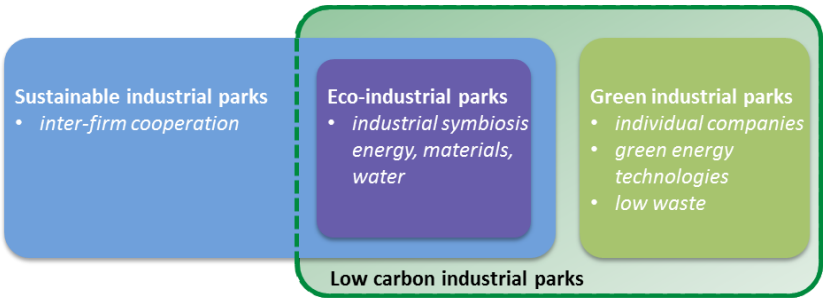

Fig. 7: business park sustainability approaches

3.1.1. Sustainable industrial parks

Sustainable industrial parks aim at exploiting the technologic, economic, ecologic, social and spatial advantages that originate from local inter-firm cooperation in the field of facility and utility management, infrastructure and industrial processes [13]. More specifically, inter-firm cooperation may include collective organisation of energy and resource supply, waste water treatment, transport and green space maintenance, the collective use of equipment and facilities, the exchange of material or energy streams between companies or with the surrounding region, etc. A complete integration of this concept requires measures and actions in every phase of the park development and can be facilitated by installing a multidisciplinary business park management. Voluntary inter-firm cooperation requires immediate benefits on the short term, a better competitiveness on the medium term and a sustainable relation with all stakeholders on the long term.

3.1.2. Eco-industrial parks

On eco-industrial parks, the individual companies specifically exploit synergies in supply chains of water, material and energy in order to enhance economic performance, while reducing environmental impact [12]. In this concept, also referred to as industrial symbiosis, waste products of one company serve as resource for another, and heat is cascaded and exchanged between companies. To enhance the potential of synergies, companies with complementary water, material or energy profiles must be clustered. Furthermore, eco-industrial parks must be integrated into the industrial metabolism of the region.

A well-known example of industrial symbiosis is the eco-industrial park of Kalundborg in Denmark. At the moment, 27 symbiotic relations in terms of energy, water and materials are created and exploited between nine public and private enterprises, and the system is still expanding (Fig. 8).

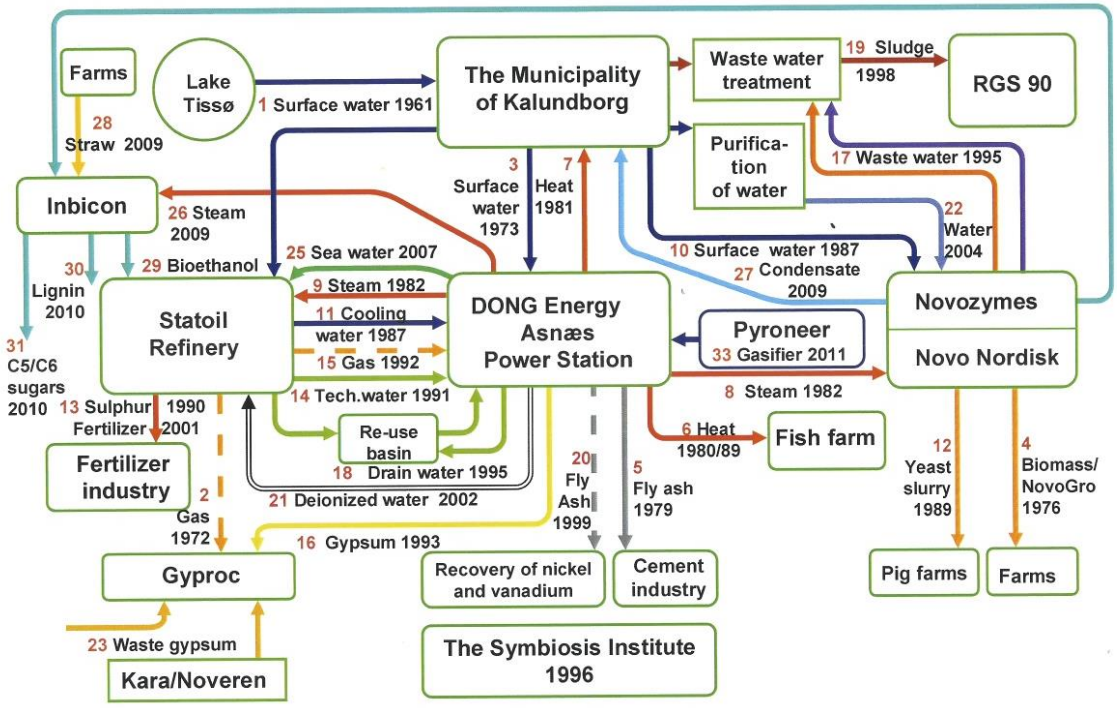

Fig. 8: Kalundborg eco-industrial park [14]

The eco-industrial park in Kymenlaakso, Finland, exploits various symbiotic relations between the Kymi pulp and paper plant, a power plant, three chemical plants, a regional energy supplier and a municipal waste water treatment plant. The pulp and paper plant partly generates its own energy by combusting the waste product (black liquor) from pulp production. Remaining steam, electricity and heat demands are purchased from the power plant, while excess heat and electricity production is sold to the chemical factories. The power plant receives bark, wood chips, fibre suspension and milled peat from the pulp and paper plant to be used as fuel and sells electricity and heat to the regional energy supplier, which sells electricity to the municipal waste water treatment plant [15].

3.1.3. Green industry parks

Green industry parks consist of a collection of companies that employ clean and renewable energy technologies and processes in order to reduce emissions and minimise waste, without specifically searching for and exploiting synergies [12].

3.1.4. Low carbon business parks

Low carbon business parks cover green industry parks as well as eco-industrial parks. The application of renewable energy and clean processes and products is combined with the exploration and exploitation of synergies in energy, material and water supply chains, in order to drastically lower greenhouse gas emissions, while creating economic benefits. In this work, low carbon business parks are analysed from an energy perspective.

Advantages of low carbon business parks are manifold. Synergies between company supply chains reduce the need for energy resources, raw materials and fresh water, while waste can be recycled, energetically valorised or even totally eliminated when resource loops are closed. This results in a significant reduction of operational and production costs. Clean and efficient processes and equipment, and renewable energy production or purchase decrease emissions of greenhouse gasses and other polluting substances. Consequently, present or future environmental penalties and taxes can be avoided. In addition, local renewable production lowers dependence on fluctuating fossil energy prices and is beneficial for local employment and enhances local anchorage. It also puts the control of energy supply in the hands of companies, business park managers or local energy service companies. Excess in local renewable energy can be sold, thus creating an extra export product. Next, companies located on low carbon business parks show social and environmental commitment and can use this to attract more customers. Finally, success stories such as Kalundborg prove that innovation between and in companies is triggered and companies are positively challenged.

3.2. Low carbon energy measures

The Trias Energetica strategy, proposed by Lysen [10] provides a general three step approach to reduce carbon emissions related to energy consumption: step 1: reduce energy demand, step 2: maximise renewable energy production, step 3: fulfil remaining energy demands by efficient use of fossil fuels. To customise this priority sequence of energy measures to low carbon energy management on business parks, sub-steps have been proposed by Maes et al. [11] (Fig. 9). In step 1, first the demands for energy services need to be reduced. In a following sub-step, the efficiencies of the equipment supplying these energy services need to be upgraded. A third sub-step comprises recovery of residual heat by heat exchange and the energy valorisation of waste (waste as fuel). Step 3 can be extended with carbon capture, utilisation and storage. Nonetheless fossil-based energy must be avoided as much as possible.

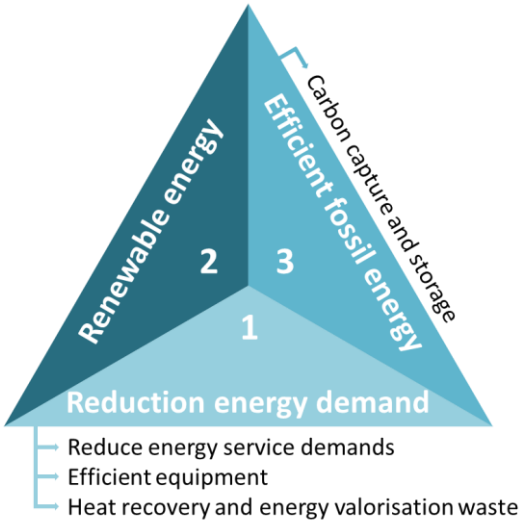

Fig. 9: stepwise approach towards low carbon energy use

3.2.1. … from organisational perspective

Low carbon energy measures, corresponding to the (sub-)steps of the Trias Energetica strategy, can be taken on 4 different organisational levels: individual business, business cluster, business park and district level (Fig. 10, Table 2).

- Energy measures on individual business level comprise: improvement of the energy performance of buildings and processes, waste heat recovery and heat exchange between processes or energy services, individual production or purchase of energy based on cogeneration or renewable resources, and use of waste products as fuel for energy generation.

- On business cluster level, facilities or activities of different companies requiring the same energy services may be bundled in shared buildings. Waste heat can be exchanged between two companies through direct heat links, and waste of one company can be energetically valorised in another one. Production or purchase of energy based on cogeneration or renewable sources can be jointly organised.

- At business park level, a park-wide energy system, including collective energy production, an energy network and a collective energy management system can be implemented. To facilitate the exploitation of energy synergies within this energy system, the park layout can be structured in such a way that companies with complementary energy profiles are clustered

- Extending the scope to district level, business parks can be connected to the district heating network and exchange heat with the district. Furthermore, the business park can exploit nearby renewable energy sources, or use waste from the district as a fuel for energy generation.

Fig. 10: Oragnisational levels of low carbon energy measures: individual business, business cluster, business park, district (Image: business park Sappenleen in Poperinge, Belgium)

Level	*Energy demand reduction and energy efficiency*	*Heat exchange and energy valorisation of waste*	*Renewable energy and cogeneration*
Individual business	improved energy performance of buildings and processes	(direct) heat exchange between processes/energy services, waste as fuel	individual production or purchase
Business cluster	bundling company activities with the same energy services in shared buildings	heat exchange between companies via direct heat links, waste from another company as fuel	joint production or purchase
Business park	collective energy management system	heat exchange between companies via heat network	collective energy production or purchase
District		heat exchange between business park and district via district heating network, waste from district as fuel	exploitation of (renewable) energy sources in district

Table 2: Low carbon energy measures per level

3.2.2. … from energy system perspective

An intuitive generic superstructure of a business park energy system is presented in Fig. 13: Energy sources are transformed by energy conversion technologies into forms (heat and electricity) suitable for energy services. These conversion technologies can be directly linked to individual companies or first be connected to a local energy network with energy storage facilities, supplying a number of companies. The local network, as well as individual companies, can exchange energy with the regional electric grid or with a district heating network.

By implementing a series of energy measures (indicated by the numbers in Fig. 13), the energy system's overall efficiency can be improved and its carbon emissions reduced:

1. Following the Trias Energetica strategy, energy measures must focus in the first place on reducing the demand for energy services related to building use and to production processes at business level. These measures include installing efficient devices, optimising equipment operation, applying sufficient insulation, choosing efficient processes and low carbon product design.
2. Secondly, heat can be recovered at business level, by exchanging heat between process units, processes and energy services for building use.
3. Next, local energy networks and storage enable exchange of residual heat and excess electricity production between companies and allow to set up a collective energy production system to fulfil a collective energy demand profile.
4. Furthermore, zero-carbon energy can by generated from renewable energy sources.
5. Moreover, by employing efficient energy conversion technologies, energy losses during conversion are reduced.
6. By matching energy services and energy production in terms of energy quality (temperature profile), the destruction of energy quality is minimised.

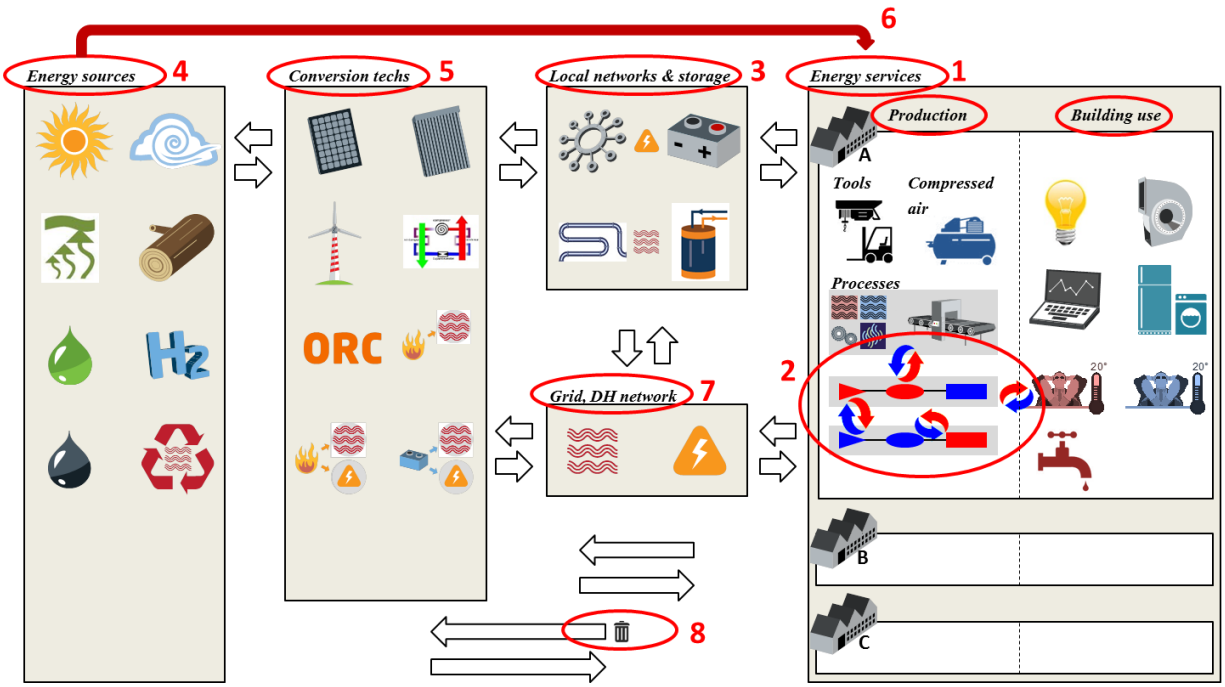

Fig. 11: Indicative energy system superstructure and indication of technological energy measures

7. Any difference between local energy production and consumption, that cannot be compensated by charging or discharging of storage facilities, is levelled out by exporting excess energy to or importing energy from the public electrical distribution network and the district heating network. The corresponding indirect carbon emissions can be reduced by purchasing heat and electricity from renewable resources.
8. Finally, waste produced in industrial processes can be recycled in the system as 'renewable' energy source.

These measures on system level involve all organisational levels: business, cluster, business park and district level. A more elaborate description of these technological measures can be found in [3]

3.3. Worldwide examples

Worldwide, a number of newly developed business parks are integrating sustainability and low carbon concepts, such as Ecofactorij and Hessenpoort in the Netherlands, Evolis in Belgium and TaigaNova and Innovista in Canada.

Ecofactorij is a recently developed business park destined for large scale production and distribution companies in Apeldoorn, that promotes sustainability and carbon neutrality as the primary objective. A park management organisation has been established and is located in a low energy building, equipped with a wood pellet stove, thermal salt panels for internal climate regulation and solar cells. The park also has its own private electricity grid to which five wind turbines will be connected, and a number of companies are equipped with individual cold heat storage systems.

On business park Hessenpoort in Zwolle a number of companies have installed individual cold heat storage systems and solar cells, and the possibilities for adapting an existing biomass fermentation plant for collective energy production have been investigated. In Kortrijk, Belgium, the intermunicipal organisation Leiedal is developing a new business park, Evolis, which has its own park management. Four wind turbines have been installed and space is reserved for a future biomass-driven combined heat and power (CHP) unit.

Taiga Nova, in Fort McMurray, and Innovista, in Hinton, are conceived as eco-industrial parks for light to medium industry. Sustainability principles are incorporated into the park's spatial design and into a set of mandatory and optional development guidelines for companies. These guidelines relate to energy consumption, production and efficiency, exchange of waste and residual heat, infrastructure, mobility and green spaces. Candidate businesses are evaluated by the number of sustainability measures they are willing to implement. However, the integration of sustainability principles is not confined to business park scale and also larger scale initiatives arise.

The Climate Initiative Rotterdam aims at a reducing carbon emissions within its territory with 50% by 2025, compared to 1990. Meanwhile, the petrochemical industry cluster needs to shift to alternative raw materials and fuels. In London, the entire Green Enterprise District is dedicated to the creation of jobs in the low carbon economy, by attracting businesses in low carbon products, services and technologies, waste valorisation and renewable energy.

4. Energy clustering

This chapter introduces energy clustering and discusses its application, organisation, and feasibility. Energy clustering refers to the exploitation of synergies between different components of a business park energy system. In other words, it establishes industrial symbiosis in terms of energy. Various physical and non-physical forms of energy clustering can be distinguished. Profitable energy clustering projects can be outsourced to energy service companies, allowing companies to focus on their core activity. Opportunities for energy clustering on a business park can be enhanced by attracting companies with complementary energy profiles. In addition, energy synergies between business park and surrounding district can be exploited by connecting the business park energy system to the district heating network. Smart microgrids assist in exploiting synergies by controlling the balance between local electricity consumption, production, storage, and import/export.

4.1. Industrial ecology concepts

Industrial ecology is a multidisciplinary approach in which the energy, water and resource streams running through industrial systems, such as industrial parks, are mapped and analysed. Its aim is to detect profitable synergies between companies that enhance sustainable use of resources and reduce environmental impacts. Emphasis is put on shifting from open to closed loop systems, in which residual (waste) streams are reintegrated into the system [15, 16]. The implementation of such synergies is referred to as industrial symbiosis, which is also the main objective of eco-industrial parks [12, 17]. An example is the eco-industrial complex in Kalundburg, Denmark

Energy clustering on industrial parks refers to all forms of inter-firm cooperation that exploit synergies within the park's energy system (Table 3). In other words, energy clustering can be considered as industrial symbiosis in terms of energy. It provides an effective strategy to simultaneously reduce environmental emissions and costs. Physical realisations of energy clustering are collective energy production, local energy distribution networks, exchange of heat between companies and exchange of resources. Besides physical energy clustering, also services (related to energy) can be clustered, such as the purchase and sale of energy, energy monitoring and management, and maintenance of utilities [11]. When looking at energy clustering from a business perspective, financial profit is the stimulus, while reducing environmental impacts is the advantage. As an example, without industrial symbiosis, CO_2-emissions from the Kymi Eco-industrial Park in Finland, would be 40 to 75% higher [15]. In addition, energy clustering can be extended beyond the business park boundaries, to include synergies with the surrounding region.

Energy clustering = Exploitation of energy synergies

Physical clustering:	***Energy service clustering:***
• Collective energy production	• Collective energy purchase/sale
• Local energy networks	• Collective procurement energy monitoring/management system
• Exchange of heat	
• Exchange of resources	• Collective maintenance

Table 3: Industrial ecology: the energy perspective

4.2. Physical energy clustering

4.2.1. Collective energy production

Collective energy production refers to energy generation on or near the business park with the aim of fulfilling the aggregate energy demand of a group of companies or of the entire business park. The installations are either jointly owned by a number of companies or by a third party (energy service company). As a first advantage of collective compared to individual energy production, the aggregate energy demand profile is more stable than the individual profiles, and peaks are flattened. This reduces the required maximum capacity and thus the overall costs of installations. Another advantage is that investment and operation and maintenance costs are reduced by economy of scale effects. Moreover, larger installations exhibit higher efficiencies than smaller ones, leading to lower operation or fuel costs and related emissions. For the same capacity, a collective installation may have a smaller spatial footprint than a number of individual ones. Low carbon energy production technologies that are too expensive on smaller scale, may become economically viable at larger scales. Large investments, such as geothermal installations, may not be financially feasible for one company, but may become feasible for a cluster of companies. Smaller companies and even parties located outside the business park are able to participate in collective energy production. Since collective energy production is managed by a collective corporation or a third party, the organisational burden is taken away from individual businesses. Such corporations contractually guarantee security of supply. As an alternative to large installations, a collective energy system can also be conceived as an array of smaller units.

4.2.2. Local energy networks

Local energy networks are essential to distribute energy from collective energy production installations to the individual companies. Alternatively, such networks can be used to connect individual energy production installations so that (temporary) excess capacity of one company can be made available for and sold to other companies.

4.2.3. Exchange of heat

Waste heat from industrial processes and excess heat from energy production installations can be exchanged between different companies via direct heat links or via heat networks (steam or water). However, economically feasible opportunities for energy integration at company level should be focussed on first. Total Site Analysis [18, 19] provides a practical tool to detect possibilities for energy integration at cluster or business park level, taking into account the existing heat network infrastructure. The method calculates the theoretical potential of heat exchange between companies or processes via one or more heat transfer networks.

The chemical cluster of Stenungsund in Sweden exists of five large chemical companies that strongly exploit symbiotic relations in terms of resources and energy [20]. At the heart of the cluster, a steam cracker produces olefins and fuels from saturated hydrocarbons. The olefins serve as feedstock for the other processes in the cluster, while the fuels are combusted for heat generation (see Fig. 12). Heat recovery is optimised on plant level, using individual heat networks (steam, hot oil). A Total Site Analysis has been carried out to calculate the energy savings that could be achieved by connecting

(integrating) the existing steam systems of the individual plants. It was found that the use of fuel for heat generation could theoretically be avoided, provided that a hot water loop is integrated.

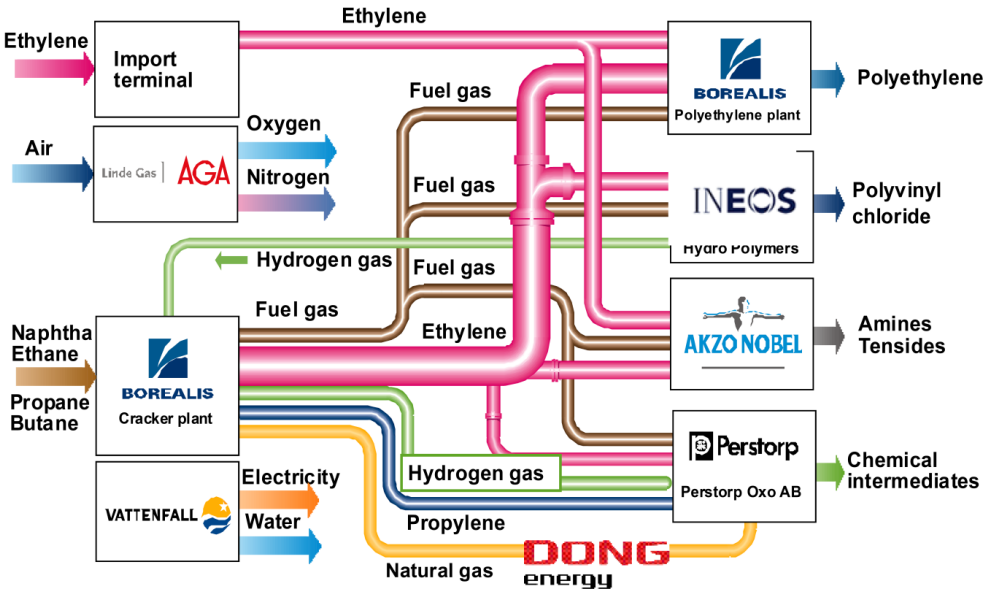

Fig. 12: Chemical cluster at Stenungsund, Sweden [20]

4.2.4. Exchange of resources

Next to heat, also resources, such as waste, biomass, biofuels or hydrogen, can be exchanged between companies and used as a fuel. This also requires direct connections or networks. As an example, biological residues from food industry, manure, or sludge from sewers can be converted to biogas by fermentation in waste treatment plants. This biogas could be used in a CHP installation of a nearby company. Also wood chips from wood manufacturing industry or pruning waste could be used as fuel in a CHP.

4.3. Clustering of services related to energy

Joint purchase or sale of energy (electricity, fuel, heat), collective procurement of energy monitoring and energy management systems, joint maintenance of utilities, etc., can generate significant cost reductions. It strengthens the negotiating position with regard to the possible suppliers of these services. Service clustering can be facilitated by the park management or by the local business association. When companies jointly purchase electricity from an electricity supplier, the aggregate demand is more stable and shows less peaks than their individual demands. In this way, taxes related to peak demands can be decreased. Demand response could even actively avoid peaks by shifting demands in time (load shifting) or by capping them (peak shaving). Alternatively, part of the demand could be temporarily supplied from a local energy generator. Demand response is illustrated in the Dutch Agrogas project, where the gas consumption of different greenhouse companies is controlled by a manager [21].

4.4. Complementary energy profiles

Company energy profiles are called complementary if they show opportunities for energy clustering. More specifically, energy functions within different companies can be complementary in nature and/or time profile. For example, waste heat originating from cooling in warehouses (refrigerators) or datacentres could be used for space heating of adjacent buildings in colder seasons. When space heating is not required e.g. in warmer seasons, it can be stored in the ground or released to the environment. As another example, the heat that needs to be evacuated from greenhouses in summer could be stored in the ground (Borehole Energy Storage) to be used in colder seasons for low temperature space heating of adjacent buildings. Time profiles of both electricity and heat demand in offices and homes could also be complementary. As a consequence, the combined demand profile is more continuous than the separate profiles, which is advantageous for a collective CHP for example.

Complementarity of energy services can be enhanced by energy storage. For example, in greenhouse companies without assimilation lighting, demands for CO_2 fertilisation and space heating do not coincide in time. CO_2 fertilisation is needed during daytime to promote crop growth and space heating is required mostly during night-time [22]. Both demands can be generated by a CHP. However, the CHP needs to operate during daytime, as CO_2 is provided instantaneously to the crops, while excess electricity can be sold to the grid during daytime peak demands. By storing the heat produced during daytime as hot water, and using it for space heating at night, complementarity of energy services is enhanced. For greenhouses with assimilation lighting, however, CHP operation will be tuned to the lighting schedule.

4.5. Energy Service Companies

Energy clustering projects on business park scale can be outsourced to an energy service company (ESCO). An ESCO provides energy services, implements energy efficiency measures, or performs energy audits in a final customer's facility or premises [23]. ESCO projects can include design, construction, operation and maintenance of energy production installations (CHP, wind, solar) and installations or equipment to deliver energy services (space heating, space cooling, lighting,…), next to energy auditing, monitoring or management. As the organisation and coordination of energy projects is transferred to the ESCO, customers (businesses) can stay focussed on their core activities.

The ESCO finances or arranges financing for energy projects and their remuneration is partly or entirely linked to the energy produced or the energy savings achieved. The customer gradually repays, corresponding to the energy cost savings created by the project. ESCOs could use their expertise to identify energy synergies to implement the project in the most cost-effective way and install accurate energy monitoring. ESCOs focussing on business park scale could exploit synergies between companies (=energy clustering) to supply energy services to their customers in the most efficient way. In order to promote the introduction of ESCOs on low carbon business parks, they need to be incentivised towards carbon neutrality. Financing of projects can be done by the ESCO, the final customer, a third party, or a combination thereof. An international market study of ESCOs has been performed by Marino et al. [23]. Note that ESCOs can assist in energy production as well as energy efficiency projects, at company, company cluster or business park scale.

Public ESCOs focus on public buildings, while private ones also operate in the industrial, commercial, housing sectors, etc. Internationally, also large energy suppliers, are starting to offer ESCO services and therefore try to exploit local energy synergies. The working of private ESCOs is based on Energy Performance Contracts (EPCs), in which payment is based on a contractually agreed energy performance criterion that is verified and monitored during the full term of the contract.

4.6. District and local heat networks

Within a business park, heat can be exchanged between companies by means of direct heat links or through a local heat network. In addition, excess heat from the business park could be injected into the regional district heating network. Hence, it can be used for space heating in the nearby city centre, hospital or sport complex, for heating a public swimming pool, or for heating greenhouses. Vice versa, the business park heat network can be connected to an external heat supplier, such as a waste incinerator or a power plant. Connecting the local heat network to the district heating network provides extra security of heat supply and demand.

Traditional district heating networks have a top-down structure, in which heat is centrally generated and distributed to the individual consumers. Similar to electricity networks, a shift towards smart thermal networks will support the integration of decentralised and renewable heat producers. A strategy could be to start local thermal networks and eventually connect them to form a regional heat network. District heating may in a first phase be provided by CHP and waste heat, to be supplemented or replaced in a later phase by renewable heat sources. Heat losses and costs related to heating networks are proportional with the network length. For a heat network with a supply temperature of 100°C, the heat losses could amount 1 to 1.5 °C/km. Therefore, demand and supply of heat must be geographically clustered. District heating networks entail high investment costs and long payback times, and therefore long term supply and demand contracts are demanded. Because of the long lifetimes of such networks, short payback times are not considered reasonable. Flexibility and robustness are of paramount importance so that those networks can be easily adapted to changing energy demands and emerging opportunities, while guaranteeing security of supply and demand. Robustness can be achieved by installing backup installations and storage facilities. A comprehensive district heating manual is composed by Frederiksen and Werner [24].

4.7. Smart microgrids

The traditional electricity grid has a strong hierarchic top-down architecture. Electricity is produced centrally and subsequently transported through the transmission network to the local distribution grids that deliver it to the consumers. However, this one-way structure is inappropriate for large-scale integration of decentralised electricity production. Therefore, a new bottom-up bidirectional approach better suited for the integration of prosumers (energy consumers that also produce energy) is required. Smart microgrids with intelligent control are able to balance local energy consumption with local energy production and storage, while exporting the electricity excess to or importing the deficit from the public electrical distribution network. Microgrids can provide ancillary services and benefits for both the electrical distribution network operator and microgrid participants [25]. Unlike heat networks, electricity networks exhibit limited energy losses. Business parks offer a good geographical scope for the implementation of smart microgrids. The concept of virtual power

plants even allows to extend the concept of microgrids beyond the geographical boundaries of business parks [26, 27].

4.8. Feasibility of energy clustering projects

The feasibility of energy cluster projects is subject to technical, spatial, economical, legal and social constraints [28]. First of all, the theoretical potential of renewable resources is narrowed to the technical potential by the available conversion technologies and spatial planning restrictions. Moreover, different technologies can influence, hinder or exclude each other. Economic viability expressed in return on investment, payback period or net present value has to be guaranteed for the investing parties. So different scenarios have to be selected and compared, further limiting the potential. This economic potential has to be checked with legal aspects, such as permits for installations, networks and connections to regional grids, legal structure and business model. The parties involved need to be committed to achieve a successful energy clustering project.

For investments at company level concerning energy efficiency in buildings or optimisation and integration of processes, companies expect short payback periods (< 2 max 3 year) and high IRRs. In this way profitable investments on slightly longer term are missed. In addition, net present value (NPV), discounted payback period or internal rate of return (IRR) are more accurate investment performance indicators. These remarks are also valid for energy clustering projects involving different companies.

In collective energy production or heat exchange projects, quality, security and continuity of supply is of key importance and is a contractual obligation, which puts extra stress on the individual companies involved. ESCOs can offer a solution, as they take over these responsibilities and provide backup installations, so that energy synergies are facilitated. Unfortunately, energy clustering projects are sometimes obstructed by inadequate legislation.

A joint business park management can play a key role in facilitating energy clustering by attracting businesses with complementary energy profiles in the issuance phase, assisting companies to identify possibilities for inter-firm energy cooperation and eliminate barriers for the realisation of these energy synergies. Also, the park developer can reserve space in the spatial design for collective energy production, networks or direct connections between businesses. If feasible, the developer could also start up a collective energy production corporation, or act as an ESCO. For an extensive discussion on the role of business park management, reference is made to Maes *et al.* [29].

5. Summary and conclusions

To mitigate climate change, European climate and energy policy aims at reducing greenhouse gas emissions, while increasing the share of renewable energy production and enhancing energy efficiency. The major share of greenhouse gas emissions consists of carbon dioxide (CO_2) caused by fossil fuel combustion for energy generation. A significant share of these emissions can be allocated to energy use in the industry sector. Therefore, a low carbon energy shift in the industry sector is required. To promote this transition, a series of policy measures and instruments are in effect, which have been described in detail.

On low carbon business parks, the required transition is realised by combining the application of renewable energy and clean processes and products with the exploration and exploitation of energy synergies within the energy system. More specifically, energy-related CO_2 emissions are reduced by implementing a set of low carbon energy measures in the business park's energy system. The priority of these measures follows the Trias Energetica strategy, in which reduction of energy service demands is the primary focus, next to renewable energy generation and efficient conversion of fossil fuels. From an organisational point of view, measures can be taken on individual business, business cluster, business park and district level. The implementation of energy measures can be facilitated and their effect can be enhanced by exploiting energy synergies between companies (energy clustering). Different forms of energy clustering, their organisation and feasibility have been described.

Energy service demands related to building use and production processes, the availability of renewable energy (solar and wind), and the prices of purchased energy are subject to variations over time. This complicates the evaluation of the cost-effectiveness of low carbon energy measures. However, investment decision making can be facilitated by mathematical modelling. Therefore, the search for an appropriate modelling tool will be the main target of Part 2 of this work.

Part 2

Towards low carbon business park energy systems: Review and classification of techno-economic energy models

1. Introduction

Fossil fuel based energy generation in the manufacturing industry and the sector's consumption of externally produced electricity and heat, are responsible for about 28% of total energy-related CO_2-emissions on European level [2]. Therefore, a low carbon shift in the energy system of industrial parks must be initiated. Low carbon business parks envision a collective energy system that employs energy efficient technologies, maximises the integration of local renewable energy sources using energy storage and enables heat exchange between companies [29]. Techno-economic energy models provide a holistic approach towards the configuration and operation of such systems, and facilitate the optimal trade-off between energetic, economic and environmental performances. To our knowledge, there is no techno-economic, bottom-up energy model available that has been custom tailored for industrial parks and therefore, the development of such a model by adapting an existing model or by developing a new one is of high priority.

Starting from the viewpoint of low carbon business park energy systems, this work attempts to unravel the plethora of energy models, proposes a pragmatic model categorisation and identifies key model features. Chapter 2 describes the configuration of a business park energy system and its components and assesses the need for a holistic modelling approach. In Chapter 3, several existing classifications of techno-economic energy models are screened for appropriate model features and based thereon a new classification is proposed. Its model categories are presented and exemplified throughout Sections 3.1 to 3.6. Chapter 4 provides a clear comparison between these model types per key characteristic. Chapter 5 focusses on the use of generic sub-models to represent technologies in an energy system's superstructure. In Chapter 6, essential features for modelling business park energy systems are distilled. Based on these features, the studied models are evaluated in Chapter 7 and conclusions are drawn. Part 2 is based on a previously published journal paper [30].

2. Business park energy system modelling

2.1. Business park energy system

An intuitive general superstructure for business park energy systems is presented in Fig. 13: Energy sources are transformed by energy conversion technologies into forms (heat and electricity) suitable for energy service demands. These conversion technologies can be directly linked to individual companies or first be connected to a local energy network with storage facilities, supplying a number of companies. The local network, as well as individual companies, can exchange energy with the regional electric grid or district heating network.

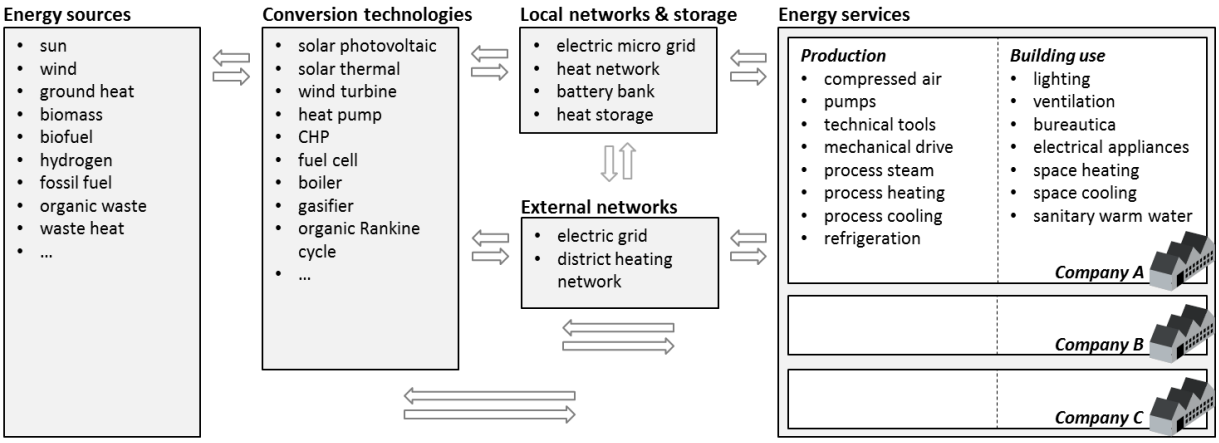

Fig. 13: Energy system superstructure

2.2. Energy consumption profile

The overall energy consumption profile of the business park consists of the composition of the energy profiles of the individual companies. A company's annual energy consumption profile is fully known when the annual consumption of each energy carrier (electricity, heat, fuels) is allocated to the different energy services within the company (see Fig. 14). Energy services are related either to the usage and occupancy of the buildings or to the industrial production itself. Intra-annual detail is achieved by assigning time profiles to each energy service or on a more aggregate level, to the consumption of each energy carrier (e.g. as a yearly distribution of hourly values or by disaggregating parameter values on intra-annual time slice level). Intra-annual variations of non-controllable renewable energy production technologies, depend on climatic conditions. Energy service time profiles may depend on both climatic conditions and company or process operating schedules. The thermodynamic signature of a company's energy consumption profile is obtained by assigning temperature levels to all thermal demands.

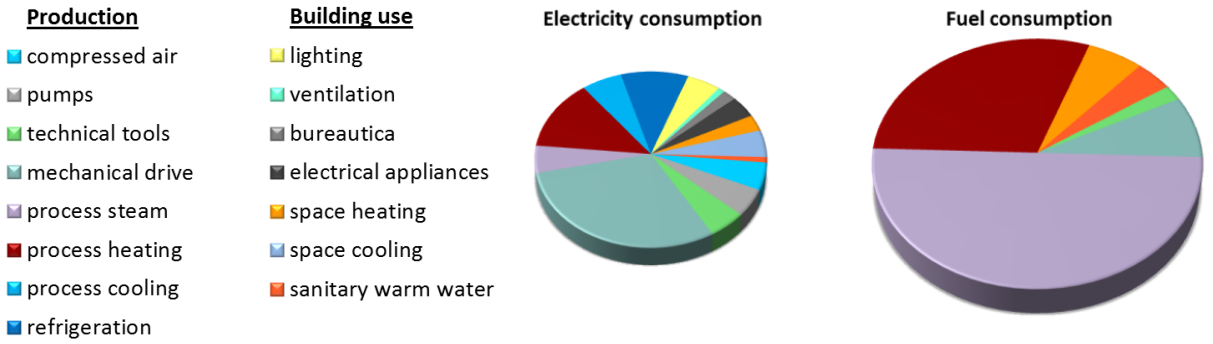

Fig. 14: Allocation of annual consumption energy carriers to energy service on company level

2.3. Targets for system design

The design of an energy system exists in finding a configuration of energy production technologies that satisfies demands, while attaining one or more, possibly conflicting targets. Depending on the target and on the external conditions under which it has to be achieved, the optimal system

configuration will alter. A variety of targets can be envisioned, taking the form of minimisation, maximisation, limitation or minimum thresholds. Examples of variables that could be subjected to limitation or minimisation are: total energy volume exchanged with external networks, import costs or total discounted system costs, total carbon emissions, thermodynamic quality loss, fossil fuel consumption, etc. Maximisation or minimum thresholds could be targeted for profits on individual generator or system level, the share of renewable energy production or consumption, etc. Moreover, the system designer has to take into account the techno-economic and environmental characteristics of all system components, the intra-annual variations (time profiles) of uncontrollable renewable energy technologies and energy service demands, the dispatch strategies of energy generators, as well as the temperature levels of heat producing technologies and thermal demands. For this complex task the holistic approach provided by techno-economic energy models is essential.

2.4. Energy system modelling

A techno-economic energy model is a mathematical representation of an energy system, describing its configuration and the technologic and economic characteristics of its components. Interactions between the components vary over time, as they depend on time profiles of non-controllable renewable energy, generator dispatch strategies, and intra-annual variations or operating schedules of energy services. Techno-economic energy models can be applied to calculate the optimal configuration and operation of an energy system in terms of energy efficiency, costs or environmental impacts, and to analyse past or to predict future behaviour of a system. The different types of techno-economic energy models and their features are the subject of Sections 3.1 to 3.6.

3. Classification and selection of energy models

During the last decades a variety of techno-economic energy models has been developed, each serving particular purposes. Van Beeck proposed a classification scheme, in the process of identifying suitable models for local energy planning in developing countries, differentiating energy models according to characteristics in ten dimensions [31]. Also Nakata adopted the same categorisation [32]. Connolly et al. [33], however, established a more concise classification of energy tools by means of a survey sent out to tool developers, and presented it as a guide to identify a suitable tool for analysing the integration of renewable energy technologies. This classification distinguishes seven tool types, including simulation, scenario, equilibrium, top-down, bottom-up, operation optimisation and investment optimisation tools. The distinction between bottom-up and top-down approaches in energy models has been discussed by Grubb et al. [34] and Van Beeck [31]. Throughout literature, model, tool, modelling framework and model generator are used interchangeably. However, in a strict sense, an energy model is a simplified representation of a specific energy system, whereas a tool, modelling framework or model generator refers to the computer programme enabling the creation of various models.

From van Beeck's classification, appropriate features for modelling an industrial park's energy system are identified. Firstly, the search for an optimal future energy system, requires a scenario analysis or backcasting perspective. Secondly, an integrated approach, focusing simultaneously on technical configuration, environmental impact and comparison of different options, is called for. As a local energy system does not influence overall economy, and due to the need for flexible manipulation of

the model, exogenous parameter specification is required. Also, energy supply and demand should be disaggregated, with a high level of technological detail, in order to differentiate between technologies, requiring a bottom-up approach. Furthermore, partial equilibrium, simulation and optimisation, as well as spread sheet methods are applicable. Translated to Connolly's classification, the model needs to follow a bottom-up approach, that can be applied for either simulation or scenario analysis and needs to enable optimisation of technology investment and/or operation. Taking into account these considerations, a preliminary selection of freely available models is made from Connolly's and Nakata's review, supplemented with additional models. Subsequently, a practical categorisation of energy system (ES) models is proposed, distinguishing types according to primary focus, namely ES evolution, optimisation, simulation, accounting and integration models, which are described in the following sections.

3.1. Energy system evolution models

Energy system evolution models analyse the long term evolution of an energy system, driven by techno-economic optimisation, from international down to municipal level. Numerous modelling frameworks carry this label, such as MARKAL [35], TIMES [36], ETEM [37], and OSeMOSYS [38]. These models can be used for exploring the least-cost investment paths under different scenarios that reflect alternative future visions and policies, or for developing policies to achieve a desired future (backcasting). In this context, future visions include assumptions about increase in energy demand, availability and costs of energy resources, technology efficiency and innovation, whereas energy-environmental policies decide on taxes, subsidies, exclusion of technologies, etc.

The time horizon consists of a number of periods, containing an equal or varying number of years, that are subdivided into time slices to capture intra-annual variations. Parameters and variables are disaggregated and specified accordingly, but values do not vary beyond time slice level. Time slices are defined either on an equal, or on descending hierarchic levels, such as season, weekday/weekend, day/night up to diurnal divisions. Starting from the base year, the model endogenously develops the configuration and regulates the operation of the energy system over the entire time horizon, in order to satisfy energy service demands at minimum costs, while complying with technologic, economic and environmental limits.

Therefore, an optimisation algorithm is employed, that in every time slice computes the values of the decision variables for which an objective function is minimised, subject to a number of constraints. Decision variables are the choices to be made by the model, being investments in and operation levels of technologies and import/export of commodities. The objective function represents total discounted costs to be minimised or, equivalently, net total surplus to be maximised. Indeed, for models that take into account demand price-elasticity and assume competitive markets for all commodities, supply-demand equilibrium corresponds to maximisation of net total surplus. When demands are inelastic, however, equilibrium translates into minimisation of total discounted costs [36]. These are obtained by accumulating the net present values of all costs related to technologies (investment, dismantling, operation and maintenance (O&M), salvage), and commodities (import, export, delivery, taxes), over all time segments. Either a global or technology-specific discount rates can be applied. Optimisation constraints are given by mathematical formulations that discount and accumulate costs, model the operation of technologies, keep track of capacity extension, describe

commodity balances and impose bounds to decision variables. Commodity balances ensure that the supply of a specific commodity is equal to or greater than the demand for it. Bounds can be used to introduce a minimum share of renewables, phase out existing technologies, impose a gradually decreasing carbon emission cap, etc. The optimisation assumes perfect foresight implicating full inter-temporal knowledge of future policy and economic developments over the entire planning horizon. In case objective function and equations are linear, linear programming techniques can be used, but when discrete technology sizes matter, mixed integer linear programming is required. MARKAL and TIMES are conceptualised with the General Algebraic Modelling System (GAMS) [39], whereas ETEM and OSeMOSYS are composed with the GNU Linear Programming Kit (GLPK) [40]

The overall superstructure of the energy model, also referred to as the Reference Energy System (RES), consists of a number of 'processes' that are interlinked by in- and outflows of commodities. Processes represent existing or future technologies for extraction, production, conversion, storage or use of various energy forms, whereas commodities represent energy carriers, energy services, materials or emissions. Various technologic, environmental and economic characteristics specify the behaviour of these components. Some models (ETEM, OSeMOSYS) use a single generic sub-model for all technologies, while other models (MARKAL, TIMES) utilise one generic sub-model per technology subset. Furthermore, the base year RES configuration is calibrated to a well-documented historic year, while subsequent future configurations are determined by the model. In most ES evolution models, energy service demands are allocated to economic sectors, such as the residential, public, service, transport and industry sector. Some models (ETEM, OSeMOSYS) can only handle price-inelastic demands which, as a consequence, have to be specified for each scenario. Other models however (MARKAL, TIMES), do take into account price-elasticity. In this case, the demand in the reference scenario has to be fully specified, while in alternate scenarios, it is calculated endogenously, without intervention, starting from user-defined elasticities.

3.1.1. MARKAL

The MARKAL model generator has been developed by the International Energy Agency under the auspices of the Energy Technology Systems Analysis Program (IEA-ETSAP), in order to facilitate exploration of possible energy futures [35]. It has been widely applied for energy system modelling on global to community level. As an example, the MARKAL framework has been employed to replicate the UK energy system [41]. This model was later extended with flexible time slice definition to better capture peaks in electricity demand and renewable energy sources [42]. Turning to municipal level, a MARKAL instance has been set up to study the integration of renewable energy in the residential, commercial and service sectors of an Italian town [43].

3.1.2. TIMES

TIMES has been developed by IEA-ETSAP as a successor of the MARKAL framework and includes enhanced features [36]. In contrast to MARKAL, where only electricity and low-temperature heat can be disaggregated into a fixed number of rigid time slices, TIMES allows to disaggregate any commodity into any number of user-defined time slices (flexible time slicing). Moreover, input data are specified independently from the definition of time periods, which allows to easily modify the time horizon. Time-dependent data are allocated to years and the model matches these data to the periods, intra- or extrapolating where necessary. Also, processes can be vintaged, meaning that

properties may be dependent of installation date of new capacity and age of a technology. Furthermore, the storage feature has been elaborated, as TIMES allows commodities to be stored in one time slice and discharged in another, whereas MARKAL only supports night-to-day-storage. STEM-E is an single-region instance of the TIMES framework covering the entire Swiss electricity system and the interconnection with neighbouring countries [44, 45]. Its aim was to analyse the long-term development of the national electricity system and to explore TIMES' suitability as an electricity dispatch model. Also for the Belgian energy system the TIMES framework has been employed, in order to identify and explore pathways towards a 100% renewable energy [46]. On community level, TIMES has been applied to evaluate local energy policies for the town of Pesaro [47].

3.1.3. OSeMOSYS

OSeMOSYS is an open and compact modelling framework, developed by a coalition of organisations including SEI, the International Atomic Energy Agency (IAEA), the UK Energy Research Center, and the Royal Technical University (KTH) in Sweden [38]. In contrast to the other ES evolution models, the time horizon consists of a series of single-year, instead of multi-year, periods. The programming code has been further elaborated and modified in order to incorporate key elements inherent to smart grids, such as prioritising of demands, demand shifting and storage [48]. Economic optimisation of the mix between these elements has been exemplified for a local urban energy system. These model enhancements required time slice division to be automatically converted into a series of sequential time segments. This has been solved by labelling consecutive time segments by season, day-type and time of day in which they occur. Data specified at time slice level are then converted to time segment level and vice versa by means of conversion factors. Next to standard demand, which has to be satisfied at every moment, also flexible demand types are introduced, which can be shifted over a certain timespan within one day or partly remain unmet. The amount of unmet demand, or the time over which a quantity of demand is shifted, correspond to costs, which are integrated in the objective function. Storage levels are tracked throughout the year by accumulating net charges over preceding consecutive time intervals. In order to keep the storage level between minimum and maximum limits, new storage capacity can be invested in.

3.1.4. ETEM

ETEM is derived from the MARKAL/TIMES framework and is tailored for urban energy systems by the ORDECSYS company. It has been elaborated for the canton of Geneva in Switzerland [37]. Recently, it has been integrated in the Luxembourg Energy–Air Quality model (LEAQ) at CRP Henri Tudor [49].

3.2. Energy system optimisation models

Energy system optimisation models follow a similar methodology as ES evolution models to calculate the least cost configuration and operation, but the time horizon is limited to a single representative year or time span, subdivided into time slices. All technology investments are made at the start and the optimised system configuration does not change over time. Optimal configurations corresponding to multiple scenarios can be compared in terms of techno-economic and environmental performance. Analogue to ES evolution models, a generic technology description is employed.

3.2.1. Energy modelling framework by Voll et al.

At Aachen University, Germany, Voll et al. [50] developed a modelling framework for automated superstructure generation and optimisation of distributed energy supply systems, written in GAMS [39]. In order to represent annual variations in energy service demands, the representative year can be subdivided into user-defined time slices. At the relatively small scale of local distributed energy systems, the techno-economic characteristics of individual technology units play an important role. Therefore, part-load efficiency and size-dependent investment costs need to be taken into account. As a consequence, also configurations with multiple redundant units of the same technology need to be included in the solution space. This could be done by incorporating a sufficient number of units of each technology in the Reference Energy System. However, this a priori construction of possibly very large superstructures is circumvented with the automated superstructure-free synthesis and optimisation method developed by Voll et all. [50].

Voll's methodology first employs an algorithm for maximal superstructure generation to create all feasible combinations containing only one unit per technology type. Subsequently this initial superstructure is expanded by one redundant unit per technology and topographic constraints are included. Next, an optimisation algorithm calculates the configuration within the superstructure at hand and the dispatch of technology units in every time slice, that yield the minimum net-present value (or maximum when net present value is negative). Then, in a successive approach, the superstructure is continuously expanded and system configuration and operation are optimised, until the global optimal solution is found. The mathematical implementation of this method is based on a connectivity matrix that interconnects technologies and energy services. Multiple redundant units and topographic constraints are incorporated by matrix manipulations. Technologies are represented in the RES by a generic sub-model, existing of nominal efficiency, one or more part-load efficiency performance curves and an investment cost function. Functions are piecewise linearised and part-load behaviour is assumed to be independent of equipment size. However, to simulate the size-dependent nominal electric and thermal efficiencies for CHP installations, three complementary capacity ranges are incorporated.

3.3. Energy system simulation models

ES simulation models simulate the operation of an energy system within a user-defined configuration that is fixed over time. These models are used to compare alternative system configurations and to evaluate different operation strategies in terms of energetic, economic and environmental performance. Operation is simulated over a one year timespan, divided into chronologic time steps of one hour or less. Accordingly, yearly distributions of renewable energy production and energy demand are modelled either by imported measured hourly data, or by artificially created hourly time series that replicate stochastic character. The models EnergyPLAN and Homer correspond to this label.

3.3.1. EnergyPLAN

EnergyPLAN has been developed since 1999 at Aalborg University, Denmark, to assist in techno-economic analysis of regional and national energy systems. Meanwhile, it has been widely applied in Europe to analyse the integration of renewable energy technologies. A detailed technical model

description can be found in [51], while a guide for the practical use of EnergyPLAN, including the collection of relevant data can be found in [52].

EnergyPLAN is a deterministic input/output model that computes hourly energy balances for district heating and cooling, electricity, hydrogen and natural gas, within a user-defined system layout, subject to a user-selected dispatch strategy. In the technical optimisation strategy, technologies are dispatched to satisfy demand, disregarding cost data, which allows the model to be run without any input of costs. Moreover, fossil fuel consumption is minimised by applying predefined priority sequences in dispatching. Within this strategy, the user can choose to operate heat producing units solely according to heat demand, or to balance both electricity and heat demands by replacing Combined Heat and Power with electric boilers or heat pumps and by using thermal storage. Secondly, in the market optimisation strategy, the operation costs of the system are minimised under the assumption that each production unit operates to maximise its profits. Furthermore, a regulation strategy to reduce electricity production in excess of the transmission line capacity can be activated.

Model results are electricity production or consumption per technology, and electricity import or export, including related costs and revenues, at hourly level. Also hourly heat production and storage per technology are retrieved. From the energy balances, fuel consumption, CO_2 emissions, and fuel, investment and operation costs are derived on an annual basis. The model's Reference Energy System is completely predefined and comprises various types of, conversion and storage technologies, fuels and energy demands, together with all possible interconnections. By specifying the technologic characteristics of these components, a particular system configuration is built up. Technologies are represented in high detail by means of complex sub-models. Energy demands are allocated to energy services and next to standard electricity demand, also three types of flexible electricity demand can be defined.

3.3.2. HOMER

HOMER is developed by the U.S. National Renewable Energy Laboratory (NREL) and is commercially available since 2009 [53]. The model facilitates the design of grid-connected and off-grid small scale energy systems by ranking all possible configurations, according to increasing discounted costs. HOMER simulates a one-year sequence of time steps of user-defined length, ranging from several hours to one minute. Within a user-specified search space, consisting of technology-specific capacity or quantity ranges, the model assembles all possible configurations. Then, for each configuration, energy balances are calculated in every simulation time step, subject to a dispatch strategy. Subsequently, infeasible configurations are omitted and feasible options are ranked by total discounted system costs over the project lifetime. Configurations are only feasible when they comply with the constraints imposed by the user, such as overall emission limits or imposed share of renewables.

When renewable technologies are insufficient to satisfy electric and thermal loads or operating reserve, controllable power sources are operated according to the 'load following' or the 'cycle charging' strategy. Under the load following strategy, when activated, a generator produces no more than required to satisfy the primary load. Consequently, the storage (battery bank) is charged only with excess renewable power. However, under the cycle charging strategy, an activated generator runs as close as possible to full capacity without generating excess electricity, while power in surplus

of the primary load is used to charge the battery bank. Homer calculates the system for both strategies as the least-cost option is not known a priori. Furthermore, load priority rules decide how the produced electricity is allocated to primary load, deferrable load, battery, grid and electrolyser [54].

HOMER's Reference Energy System contains various predefined energy production, conversion and storage technologies, renewable resources, fuels, one thermal demand, and one deferrable and two primary electric demands. A particular system configuration is built up by selecting the components, and specifying their economic, technologic and environmental characteristics. Each technology is modelled in high detail by specific sub-models. For generators, they include nonlinear technology efficiency curves, linear cost curves and operation schedules.

3.4. Energy system accounting models

Energy system accounting models are used to quickly assess the energy requirements, costs, environmental impacts and financial feasibility of a proposed energy system in comparison to a reference case. System configurations in both proposed and reference case are user-defined and remain unchanged over time. Simplified system operation is simulated in a representative year, divided into intra-annual time slices, subject to user-selected dispatch strategies. The Reference Energy System includes a database of various separate technology sub-models. Of the studied models, only RETScreen applies for this model category.

3.4.1. RETScreen

RETSCREEN is a spreadsheet-based energy modelling tool that has been developed by the Canadian Department of Natural Resources to facilitate feasibility and prefeasibility studies for small scale renewable energy systems [55]. The model enables the comparison between a proposed renewable energy project and a conventional base case system in terms of energy efficiency, greenhouse gas emissions, life cycle costs and financial viability. A variety of project types can be analysed, such as the implementation of energy efficiency measures, power, heating or cooling projects or any combination of the latter three. The modelling period stretches over one year, subdivided into monthly time slices. In each time step, RETScreen calculates the energy balances for electricity, heating and cooling, taking into account user-defined operating strategies. Cogeneration units can be operated at full capacity or follow heat or power load, depending on the chosen dispatch strategy [56]. To meet the average monthly and peak loads for heating, cooling or power demands, first base, then intermediate, and finally peak load systems are deployed, while the fraction of total demand met by each system depends on its respective size. Simultaneously, cost analysis is performed and represented in a cumulative cashflow graph over the project life time. Furthermore, emission analysis quantifies the annual greenhouse gas emissions for both base case and proposed case. Finally, a financial analysis is performed, yielding financial indicators that enable the evaluation of the project viability. Dependent on the chosen project type, various technology types are predefined in the model's Reference Energy System. The actual configurations of both base case and proposed case energy systems are exogenously built up by specifying capacities and efficiencies. Moreover, assessment of the potential of renewable energy sources and the composition of space heating and cooling demands are aided by an integrated climate database and user-defined operating schedules.

3.5. Energy system integration models

Energy system integration models facilitate the optimal design of complex thermal energy systems, such as industrial processes, industrial plants and heat networks. They employ Pinch analysis [18] to minimise energy requirements by heat exchange between process streams, and identify the optimal conditions for the integration of appropriate energy conversion technologies. Models that are covered by this category are EINSTEIN and OSMOSE. The methodology followed by energy system integration models comprises different steps, though elaboration differs between the studied models. In a first step, after assembling the process flow model, thermodynamic calculation is performed and for each process stream the required heating or cooling load in function of temperature is computed. Secondly, from the composite curves of these cold and hot streams, the maximum heat recovery, and consequently the minimum external energy requirements, are determined, taking into account a minimum temperature difference for heat transfer. Moreover, starting from the grand composite curve, modifications to process conditions that generate energy savings can be identified. In a third step, appropriate energy conversion technologies are selected and integrated into the heat cascade. This can be done manually by the analyst or by means of an optimisation algorithm that selects utility units from a technology database and optimises their operation levels in such a way that minimum energy requirements are satisfied at minimum annual costs. In a final step, the heat exchanger network, that physically enables the exchange of heat between hot and cold streams of both processes and utilities, is designed and optimised.

3.5.1. EINSTEIN

Einstein combines an energy system integration model with a guide for thermal energy audits [57, 58]. It has been developed in the European Intelligent Energy Europe project Einstein II, to optimise thermal energy supply in companies, tertiary buildings and district heating or cooling networks. The model compares the existing thermal energy supply system with a proposed alternative, which includes an optimised heat exchanger network. Simulation is carried out in hourly time steps over a one-year time horizon. The mathematical equations describing the energy system are solved iteratively, to cope with feedback loops, and dispatch strategies are approximated by a priority sequence. The Reference Energy System includes energy production, distribution and storage technologies and a heat recovery system, as well as the processes or energy services that require thermal energy. Thermal processes are modelled by means of a generic sub-model, in which a circulating fluid and a thermal reservoir are heated by external sources or by internal heat recovery.

The model is organised in different interacting modules that correspond to the steps described earlier in this section. However, the selection of utility units has to be done manually instead of by a cost optimisation algorithm. In a first module, the existing system layout is configured within the RES, by specifying the characteristics of the thermal processes, the heat supply system and the existing heat recovery system. Based thereon, thermodynamic calculation is performed and for each process stream the required heating or cooling load in function of temperature is determined. A second module identifies optimisation measures for processes and equipment, from an extensive database. Subsequent modules make a preliminary optimised design of a heat exchanger network, taking into account the process time schedules, and assist the user in the manual selection and design of appropriate energy supply technologies. In a final module, the existing and the proposed energy system, including the optimised heat exchanger network, are compared in terms of economic and

environmental performance. As economic performance indicators, net present value over the system's lifetime and payback time are used.

3.5.2. OSMOSE

OSMOSE is a software tool, developed by the Industrial Energy Systems Laboratory at the Swiss Federal Institute of Technology Lausanne (EPFL), for analysis and design of complex energy systems [59]. It interconnects several models, that correspond to the stepwise ES integration methodology, and steers computation sequence and data exchange.

A first model assists in assembling the processes and performs thermodynamic calculation. The second model applies Pinch analysis and optimally integrates utility units. Therefore it employs an optimisation algorithm that selects utility units from a technology database and optimises their operation levels in such a way that minimum energy requirements are satisfied at minimum annual costs. In the technology database, energy production technologies are represented by separate complex sub-models. Finally, a third model evaluates the energetic, economic and environmental performance of the energy system. In case multiple performance indicators have to be optimised, a multi-objective optimisation algorithm is activated. When multiple conflicting objectives are involved, such as the minimisation of both annual costs and emissions, a multi-objective optimisation algorithm must be used [60]. Furthermore, when using multiple intra-annual time steps, utility units have to be integrated in every time step, in such a way that annual costs are minimised [61]. In case some process streams are excluded from direct heat exchange, intermediate heat transfer units can be introduced [62]. Up to this moment, OSMOSE does not include the design and optimisation of a heat exchanger network. The methodology used by OSMOSE can be applied for the optimisation of one or more processes in an industrial plant or for the preliminary design of thermal energy networks between industrial processes at industrial sites or clusters [62, 63]. Other applications are the optimisation of the layout and the energy supply system of district energy systems [64], and the design of energy conversion systems in urban areas [65].

3.6. Hybrid models

Hybrid models integrate features of several model types and cannot be put into one category. LEAP combines the long-term approach and time slice division of ES evolution models with the accounting calculations of ES accounting models and the operation simulation of ES simulation models. In addition, it can be inter-linked with an ES evolution model.

3.6.1. LEAP

The energy modelling framework LEAP has been developed at the Stockholm Environment Institute (SEI), USA, to facilitate long-term energy-environment policy analysis from urban to national level [66]. Alternative scenarios, reflecting different future policies or visions can be easily constructed and compared. The model is able to encompass all sectors of an economy from resource extraction and transformation to energy consumption.

LEAP's time horizon consists of an unlimited series of subsequent years, which can be split into time slices. Due to this intra-annual subdivision, yearly shapes can be constructed to reflect the variation

of various variables, such as the maximum availability of technologies. Variations in electricity demand can be introduced by allocating a yearly load shape to the entire electricity generation sector, or alternatively, by allocating energy or power load shapes to individual electric demand devices. Consequently, the electricity generation dispatch can be analysed and controlled on intra-annual level. However, also other energy demands than electricity could be time sliced. Scenarios created within LEAP correspond to different energy-environment policies or economic, technologic and demographic development assumptions over the time horizon, that influence energy demand and supply. The model compares these scenarios in terms of primary energy consumption, (social) costs and emissions. Prior to scenario analysis, the model is calibrated to a base year.

LEAP's Reference Energy System is organised in a hierarchical tree structure with separate branches for energy demand, energy transformation and energy resources. The energy transformation branch is subdivided into energy subsector modules that contain processes representing individual or average technologies or technology groups. Each process converts feedstock fuels and auxiliary fuels into the output fuels of the module to which it belongs. Branches, modules, processes and fuels are incorporated in the RES with generic sub-models that can be easily customised by the user. A specific system configuration is set up by adding components to the RES and specifying their characteristics. At technology level, input fuels, capacity, capacity factor, efficiency, availability, investment and O&M costs, emission factors, etc. are specified by the user.

In the same LEAP analysis, different methodologies can be combined. On the demand side, bottom-up, end-use accounting as well as top-down macroeconomic techniques, can be applied to project future energy demands. On the supply side, either standard simulation or optimisation methods can be employed to calculate the capacity expansion and dispatch of technologies in the energy transformation sector, needed to meet energy demands in every time slice. In both strategies, exogenous capacity can be specified by the user to represent existing capacity as well as planned capacity additions or retirements over the time horizon. In standard simulation mode, the model calculates the investments in extra capacity that are needed, in addition to the exogenous capacity level, to maintain a minimum planning reserve margin in each year. Endogenous capacity is added in discrete sizes and following a technology order specified by the user. In optimisation mode, on the other hand, the model calculates the least-cost capacity expansion pathway and dispatch of energy production technologies in each time slice, taking into account the exogenous capacity. Least-cost in this context refers to the minimisation of total discounted costs. The optimisation is performed by OSeMOSYS (Subsection 3.1.3), an ES evolution model that has been integrated in the LEAP framework. In standard simulation mode, the dispatch of energy generation technologies is subject to user-selected dispatch strategies. Some strategies dispatch technologies to meet both the power requirements specified by a cumulative annual load curve and the overall annual energy requirements on a module, following a merit order or the ascending order of running cost. Other strategies force technologies to run at full capacity, to meet a specified fraction of the module's energy requirement, or to operate in proportion to their available capacity in each time slice. Energy demands are inelastic and are defined either directly, or as the multiplication of activity demand and energy intensity of that activity. Costs are calculated within a user-specified costing boundary and include investment and O&M costs related to technologies, fuel import costs and export revenues, and costs of primary resource extraction.

4. Comparison model features

Based on the description of the studied energy models in previous chapter, important model features are identified and compared (see Table 4). In the following sections, these characteristics are discussed in more detail.

4.1. Focus

ES evolution models are used to construct and analyse least cost investment paths towards a desired long-term future, taking into account changing external conditions. ES optimisation models, however, calculate the least-cost configuration for a representative year. ES simulation models are used to compare different configurations and to evaluate different operation strategies. ES accounting models are employed to assess the financial feasibility of proposed configurations, while comparing them with a reference case. ES integration models focus on optimal integration of energy conversion technologies, starting from thermal energy demands that have been minimised by heat exchange.

4.1. Time horizon

ES evolution models cover a time horizon, extending from base year to end year, that consists of a series of multi-year (or single-year) periods. Each period is conceived as a repetition of its representative year, and at this level the energy system data are specified. Annual and periodic costs are discounted and accumulated over the time horizon to yield total discounted costs. Other model types however, analyse techno-economic aspects only in a single representative year or timespan. As a result, they cannot model evolution of parameters and variables over subsequent years. Nevertheless, a simplified financial analysis can be performed over the project lifetime.

4.2. Temporal detail

Seasonal, weekly or daily variations in energy supply and demand patterns can be captured by subdividing the year into time segments. Parameters and variables are disaggregated and specified accordingly, keeping constant values at segment level. Consequently, this intra-annual subdivision should be sufficiently detailed to capture key characteristics and peaks in time profiles [45]. Time slices aggregate time intervals over the year with similar conditions and thus have no inherent chronology, whereas time steps are sequential uniform increments in time. For modelling the behaviour of storage technologies, chronologic time steps are required, although time sequence can also be extracted from time slice definition [48]. ES evolution and ES optimisation models use time slice division, that may be hierarchically organised in seasonal, weekly and diurnal levels. Also ES accounting models use time slices, in order to include e.g. monthly variations. ES simulation models on the other hand, apply hourly time steps and thus exhibit a higher temporal detail. By importing either measured or artificially created annual distributions of hourly values, these models can represent the stochastic character of renewable energy and unpredictable deviations in energy demand. In the case of ES integration models, EINSTEIN simulates hourly time steps, while time slices with OSMOSE are user-defined.

Table 4: Comparison features techno-economic models

Model Type	ES evolution	ES optimisation	ES simulation		ES accounting	ES integration	
Model names	**ETEM, OSeMOSYS, TIMES, MARKAL**	**Voll**	**EnergyPLAN**	**HOMER**	**RETScreen**	**EINSTEIN**	**OSMOSE**
Focus	least-cost investment path	least-cost configuration	configuration & operation analysis	configuration & operation analysis	feasibility study	energy integration	least-cost configuration energy integration
Time horizon	series of single-/multi-year periods	representative year	representative year	representative year	representative year	representative year	representative year
Temporal detail	time slices	time slices	1h time steps	≤1h time steps	monthly time slices	1h time steps	time slices
Methodology	optimisation investment & operation	optimisation configuration & operation	performance calculation specified system dispatch strategy	performance calculation specified system dispatch strategy	performance calculation specified system dispatch strategy	performance calculation specified system dispatch strategy	(multi-obj.) optimisation configuration & operation
Calculation	LP	MILP	sequence of calculation steps	sequence of calculation steps	sequence of calculation steps	sequence of calculation steps	MILP
Programming	GAMS, GLPK	GAMS	Delphi Pascal	Visual C++	Excel, Visual Basic, C#	Python	Matlab
Comparative analysis	scenarios	scenarios	configurations	configurations	configurations	configurations	scenarios
RES configuration	endogenous evolves over time generic technology model extendable	endogenous fixed in time generic technology model extendable	exogenous fixed in time specific technology models not extendable	exogenous endogenous combinations fixed in time specific technology models not extendable	exogenous fixed in time specific technology models not extendable	exogenous fixed in time specific technology models not extendable	endogenous fixed in time specific technology models extendable
Demand	energy services electricity, heat, fuel elastic / inelastic	energy services electricity, heat, fuel inelastic	electricity, heat, fuel allocated to energy services electricity elastic	electricity, heat, overall demand inelastic	space heating & cooling, hot water electricity inelastic	electricity, heat, fuel thermal processes, buildings inelastic	energy services electricity, heat, fuel for process units inelastic
Heat representation	commodity	commodity	commodity	commodity	commodity	heat-temperature	heat-temperature
Application scale	global to municipal	project, site, district	national to municipal	project	project	industrial plant	industrial plant, site, district
User interface	model, data and output files (+GUI)	model, data and output files (+GUI)	GUI	GUI	GUI	GUI	GUIs depending on software programs included

4.3. Methodology

ES evolution models employ an optimisation algorithm to calculate the values of the decision variables that minimise or maximise an objective function, expressing economic performance, subject to a number of constraints. When demands are inelastic, total discounted costs are minimised, whereas with elastic demands, total surplus is maximised. Decision variables are technology investments, technology operation levels and trade of commodities. Constraints are given by the equations governing the system's operation, and by bounds to decision and output variables in every time slice and/or every period. ES optimisation models follow an analogous approach, but all investments are made at the start of the representative year. The ES integration model OSMOSE first calculates minimum energy requirements and subsequently employs an optimisation algorithm to optimise selection and operation levels of energy conversion units, so that annualised costs are minimised, subject to heat and power balances and equations and bounds modelling process and utility units. When multiple conflicting objectives are involved, such as the minimisation of both costs and carbon emissions, a multi-objective optimisation algorithm is required. In contrast, ES simulation and ES accounting models start from user-defined system configurations and dispatch strategies, and calculate the energetic, economic and environmental performance thereof. EINSTEIN performs energy integration, starting from a user-defined system layout and subsequently calculates the system's performance. .

ES simulation models, ES accounting models and EINSTEIN employ analytical methods, in which a sequence of calculations steps is performed, as opposed to optimisation methods. Where necessary, iterations are used to cope with feedback loops. ES evolution models employ linear programming (LP) methods, whereas the ES optimisation model described by Voll uses mixed integer linear programming (MILP) to allow for selection of technology units to be included in the configuration and for piecewise linearisation of investment costs and efficiencies. In a similar way, OSMOSE employs MILP to allow for selection of technologies.

4.4. Comparative analysis

ES evolution models generate the least-cost technology investment path and operation, for a specific scenario. Optimal solutions for alternative scenarios can be compared to the solution for a reference scenario, in terms of energetic, economic and environmental performance. In this context, each scenario corresponds to a separate model set-up, represented by a coherent set of input parameters over the time horizon that define energy service demands, resource potentials, technology characteristics and regulatory or policy constraints. ES optimisation models and OSMOSE compute the least cost system configuration and operation in a specific scenario. Therefore, also these model types allow for comparison of alternative scenarios to a reference scenario. In this case, a scenario is defined by a parameter set describing the conditions in the representative (future) year. Other model types evaluate the performance of user-defined alternative configurations that reflect different choices and conditions in the representative year.

4.5. Reference energy system configuration

The Reference Energy System (RES) or superstructure describes the techno-economic behaviour of all model components (energy resources, -technologies, -carriers and -demands) and the possible interactions between them. A particular configuration is set up by selecting the components to be included and specifying their characteristics. In the case of ES evolution models, the system configuration endogenously evolves over subsequent time periods, starting from the initial configuration and following the computed optimal investment path. ES optimisation models and OSMOSE, compute the optimal configuration once for the representative year or time span and the configuration does not change over time. The other model types are based on user-defined configurations, which also remain unchanged over time. Yet, Homer endogenously creates a finite number of technology combinations within user-defined ranges with discrete steps. ES evolution and ES optimisation models use a single generic sub-model for all technologies (Chapter 5), which makes their superstructure easily extendable. However, some particular models employ one generic sub-model per technology subset. Osmose on the other hand, uses complex sub-models to represent technologies, but nonetheless, new technology sub-models can readily be added. Also ES simulation, ES accounting models and EINSTEIN include a database of specific technology sub-models, but the predefined superstructure cannot be extended by the user.

4.6. Demand side

In ES evolution and ES optimisation models, any type of energy service demand could be defined by the user due to the generic technology sub-model description. For energy system modelling on municipal scale and beyond, these demands are mostly allocated to residential, public, service, transport and industry sectors. For the other model types however, demand types are predefined and include electricity, heat or fuel demands, allocated to energy services, if applicable. Although, with OSMOSE, energy service demands, such as mobility could directly be included. Some ES evolution models can only handle price-inelastic demands, necessarily specified for each scenario. For price-elastic models of this type however, the demand in the reference scenario has to be fully specified, while in alternate scenarios it is calculated endogenously, based on user-defined elasticities. The other model types do not incorporate elasticity, except for EnergyPLAN, that includes price elasticity for electricity demand.

4.7. Heat representation

ES integration models focus on the thermal demand of process streams in function of temperature, while the other model types consider heat as a commodity that can be produced, consumed, exported or imported, without specifying the level of thermodynamic quality (temperature level).

4.8. Application scale

ES evolution models and EnergyPLAN are typically applied to evaluate the effects of different energy policies on the development of an energy system at global to municipal scale. EINSTEIN and OSMOSE

primarily focus on industrial sites, while RETScreen and HOMER are project-oriented. Energy system optimisation models could fall in either category.

4.9. User interface

In an ES evolution model, all mathematical expressions and the definition of sets, parameters and variables are included in the model file and values of sets and parameters are specified in the data file, both text files. The model generator, set up in the GAMS or GLPK environment, transforms these files into a linear programming problem, which is solved by an optimisation algorithm. The solution is provided in an output text file. The compilation of the data file and the analysis of the output file may be facilitated by a graphical user interface (GUI), specifically developed for each model. ES system optimisation models follow a similar approach. ES simulation models, ES accounting models and EINSTEIN have graphical user interfaces with a tab sheet structure, which at the same time handle data input and output. As OSMOSE controls the communication between several software programs, their corresponding user interfaces are used.

5. Generic technology sub-models

ES evolution and ES optimisation models employ a generic mathematical description to represent technologies. This chapter zooms in on the generic technology sub-models used by ETEM, OSeMOSYS and the framework of Voll et al., into further detail (see Fig. 15).

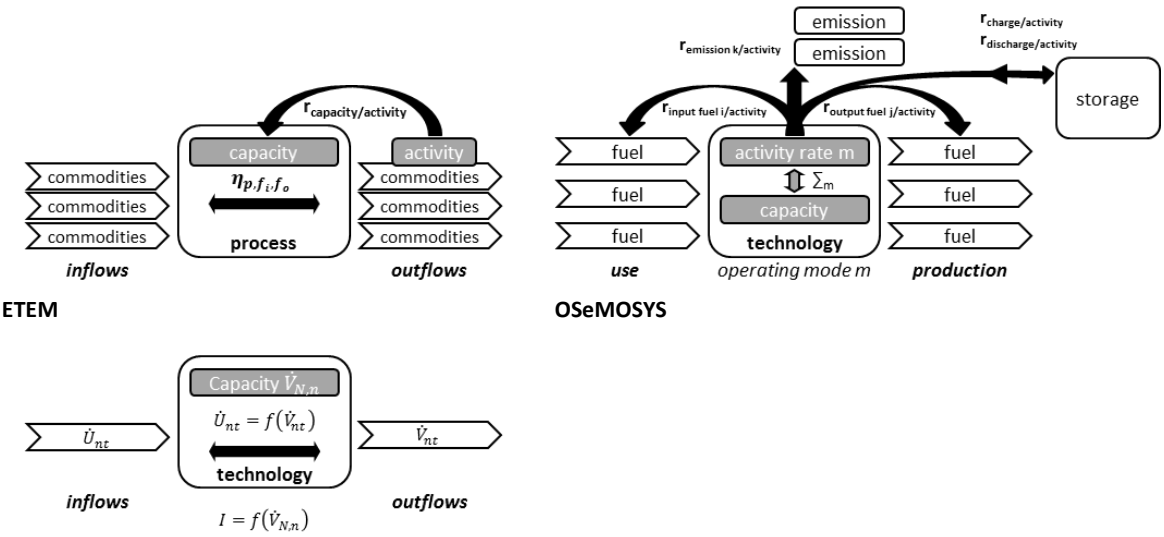

Fig. 15: Generic technology sub-models

In ETEM, a technology is modelled as a process converting ingoing flows to outgoing flows, that each contain one or more commodities, with one of the outflows labelled as the process's activity. In each time slice, the maximal attainable activity level is proportional to the total available capacity of the process. Conversion from a specific inflow to a specific outflow is described by a constant efficiency. Furthermore, in every period, specific investment and fixed and variable O&M costs are constant over the ranges of capacity addition, total installed capacity and activity respectively. Also, specific import, export and delivery costs of commodities are constant at time slice level. Although this

generic technology description is not directly suited for modelling storage, Babonneau et al. [67] introduced intra-day energy storage for electric vehicles and small gas fuel-cells with heat storage. Therefore, these technologies had to be decomposed into a demand and a storage component and extra commodities for storage had to be created.

In OSeMOSYS, all energy conversion technologies, energy imports or resource extractions in the RES are represented by a generic technology sub-model, based on two decision variables: activity rate and capacity. The total activity over all operation modes of a technology is limited by its total available capacity, on both time slice and annual level. The rates of all fuel in- and outputs and emissions are linked to the activity rate by constant ratios. Fuels may comprise energy carriers as well as energy services. Generally, a technology's activity is chosen to represent the use or production of a fuel, so the corresponding fuel-activity ratio equals 1. Furthermore, the technology model can include different operation modes, so that for example different heat/electricity ratios in the operation of a CHP can be simulated. Analogously to ETEM, specific investment, variable operating costs and emission penalties are assumed to be constant. Fuel costs are included as variable operating costs of import or extraction technologies. A technology can charge or discharge a storage facility to which it is connected, in dedicated operation modes, at rates proportional to its activity rate. The model keeps track of the charging level of the storage facility, while keeping it between minimum and maximum boundaries, over a chronologic sequence of time steps, that is automatically derived from time slice formulation [48].

In the framework developed by Voll et al., technologies are represented in the Reference Energy System by a generic sub-model, existing of nominal efficiencies between in- and outflows, one or more part-load efficiency performance curves and an investment cost function. Functions are piecewise linearised and part-load behaviour is assumed to be independent of equipment size. However, to simulate the size-dependent nominal electric and thermal efficiencies for CHP installations, three complementary capacity ranges are incorporated.

In contrast to the Voll et al. framework, present versions of ETEM and OSeMOSYS do not take into account part-load efficiency and economy of scale, due to constant ratios defining technology efficiency and constant specific costs.

6. Essential features for modelling business park energy systems

From the considerations in Chapter 4 and 5, features essential for modelling business park energy systems can be identified. Based thereon, an existing model framework can be modified or a new one can be developed. An optimisation approach is preferred, as it automatically calculates system configuration and operation that achieve one or more predefined targets. To simulate the time-varying interactions between energy service demands, uncontrollable renewable energy sources, local energy storage, controllable energy generators and energy import/export, sufficient temporal detail is required. Furthermore, considering the relatively small scale of business park energy systems, the model must enable the representation of (multiple) separate units per technology, instead of averaged technologies. To correctly model heat flows in energy generation and demand, they must be represented by heat-temperature profiles. These features are discussed more detailed in the following sections.

6.1. Sufficient intra-annual temporal detail

Time slices aggregate time intervals, over the year, that show similar conditions in energy supply and demand (e.g. February weekday evening). As a consequence, time slice division greatly reduces the number of time segments to be analysed, in comparison to the use of sequential time steps. However, these slices should be carefully customised to capture key trends and peaks in energy service demands and renewable resource availability, in order to obtain realistic system operation. The influence of intra-annual detail has been investigated by Kannan and Turton [45]. They concluded that low temporal detail flattens peaks in energy supply and demand, and that consequently the operational constraints to base-load power plants and the need for storage or supply-demand management are underestimated. Especially, taking into account the variation between weekday and weekend appeared to be very important.

6.2. Optimisation

Optimisation-based models that calculate the least-cost configuration and operation of the system avoid the need for configurations proposed by the analyst. In order to facilitate the trade-off between multiple conflicting objectives, such as minimisation of both costs and carbon emissions, multi-objective optimisation methods need to be employed. The GAMS, GLPK or MATLAB programming environments are suited for this purpose. In case the energy system will be built or retrofitted in several stages, or if external conditions are expected to change over a long-term time horizon, the investment path and the gradual development of the system configuration need to be optimised.

6.3. Component-based Reference Energy System

The model framework must cover thermal as well as electrical energy demands that are allocated to energy services. A superstructure description based on generic technology sub-models can easily be extended and enables the introduction of any energy service demand or energy production technology.

6.4. Detail on technology unit level

To accurately replicate the techno-economic characteristics of individual technology units within the energy system, part-load efficiency between operation limits, and size-dependent investment costs must be modelled. Consequently also configurations with multiple redundant units of the same technology belong to the solution space. An automated superstructure generation and optimisation algorithm avoids the a priori definition of the number of redundant units per technology.

6.5. Energy storage and flexible demand

By including storage technologies into the model framework, energy exchange with external networks to balance differences between energy production and demand, can be limited. As time slice division has no inherent chronology, time sequence has to be introduced artificially. Demand-

side management can be modelled by identifying, next to standard demands, also flexible demand types that can be shifted in time or partly remain unmet.

6.6. Thermodynamic quality of heat and heat exchange restrictions

When heat is modelled as a commodity, differences in thermodynamic quality are disregarded. A correct representation of heat flows and heat exchange can only be achieved by including the heat-temperature profiles of heat generators and demands. Energy integration is based on direct heat exchange between all or part of the process streams. However, on mixed business parks, containing a multitude of company types, direct process to process heat exchanges are not always plausible. A more realistic assumption is that heat can only be exchanged between companies through an intermediary heat transfer network, and that companies have already individually performed internal energy integration. This corresponds to the assumptions of Total Site Analysis [19, 68].

7. Summary and conclusions

The design of low carbon business park energy systems requires a holistic techno-economic modelling approach to take into account the complex and time-varying interactions between the system's components. In order to identify appropriate energy models, a confined review has been carried out, while detecting and comparing relevant model features. Based on common properties, a practical new energy model classification has been proposed, existing of ES evolution, optimisation, simulation, accounting and integration models. Essential features for modelling business park scale energy systems have been highlighted: An appropriate model employs (multi-objective) optimisation, uses a generic technology description on equipment level, in a time horizon or representative year with customised time slice division. It automatically generates and successively expands its RES or superstructure, and includes energy storage technologies and flexible energy demands, while heat flows are characterised by temperature-heat profiles. The model should take into account the potential of heat exchange between different companies via heat networks and optimally integrate technologies to fulfil remaining thermal demands.

Based on the comparison of model characteristics between the different categories (Chapter 4) and the identification of essential features for modelling energy systems at business park scale (Chapter 6), the main advantages and shortcomings of each model or model type can be described:

The studied ES simulation and ES accounting models as well as EINSTEIN are not considered flexible enough for modelling business park energy systems, because their predefined superstructure (RES) cannot be extended or modified by the user to include all essential features. Moreover, these models do not calculate the optimal system configuration in terms of a chosen performance criterion, but compute the performance of a user-defined system configuration. In the studied ES simulation and ES accounting models, heat is modelled as a commodity without thermodynamic quality (temperature level) and the model code cannot be modified to include temperature levels. However, the advantage of ES simulation models is that they are able to replicate the actual behaviour of controllable energy generators and storage technologies as their operation is calculated in every hour of the year, taking into account dispatch strategies. Fluctuations in energy demands and

availability of renewable energy sources are also realistically modelled by importing yearly distributions of hourly values.

ES evolution models, ES optimisation models and OSMOSE are more flexible, as their RES can be extended or modified by the analyst. Moreover, they automatically calculate the best system configuration corresponding to a chosen objective. Intra-annual temporal detail is based on the definition of time slices, which do not possess inherent chronology. However, time sequence can be introduced in order to model energy storage, as demonstrated by Welsch *et al.* [48]. In contrast to OSMOSE, the studied ES evolution and ES optimisation models do not represent thermodynamic quality of heat. However, their formulation can be modified and extended in order to represent thermal energy generation and demand by means of temperature-heat curves. In addition, this would allow for calculation of the maximum potential of heat recovery between thermal energy flows and the optimal integration of heat generators to fulfil remaining thermal demands. A major advantage of the ES optimisation model of Voll *et al.* [50]. is that it starts from a generic technology model that features part-load efficiency and that accounts for the economy of scale effects on investment costs. Moreover, configurations with multiple units per technology are also considered in the optimisation. In contrast, the reviewed ES evolution models and OSMOSE only integrate one unit per technology in the system configuration, unless multiple identical technologies are defined in the RES.

Becker *et al.* [62] developed a MILP formulation for energy integration of industrial sites with heat exchange restrictions that has been integrated in OSMOSE. This method models direct heat exchange within and indirect heat exchange between companies via heat transfer networks and calculates the optimal integration and operation of energy conversion technologies, so that operating costs are minimised. Moreover, the selection of optimal heat transfer units is facilitated. The method is only described for one period, but could be extended to a multi-period time horizon.

In conclusion, each of the reviewed models establishes a number of essential features for modelling business park scale energy systems. However, an energy model is needed that integrates all these features at once.

A promising strategy is to combine the model of Voll *et al.* [50] with the formulation for heat integration of Becker *et al.* [62]. The first model employs a generic technology formulation covering detail on technology unit level (part-load operation, economy of scale), and the optimisation procedure considers energy system configurations with multiple units per technology. However, this formulation needs to be extended to represent the thermal energy flows of technologies by means of temperature-heat curves. These thermal streams can be integrated into a multi-period version of the heat integration model of Becker *et al.* [62]. This will allow to maximally exploit the potential for heat recovery within companies and heat exchange between companies via heat networks, while technology units can be optimally integrated and designed to fulfil the remaining energy demands at minimum costs. Furthermore, intra-annual time slice division needs to show sufficient detail to capture key trends and peaks in energy supply and demand. Moreover, time sequence has to be added to enable accurate modelling of storage as proposed by Welsch *et al.* [48]. Starting from this scenario, a model customised for modelling low carbon energy systems on business park scale will be developed in Part 3 of this work.

Part 3

Towards low carbon business park energy systems: Development of a holistic techno-economic optimisation model

1. Introduction

Substantial and sustained reductions of greenhouse gas emissions are required to mitigate global warming [1]. On European level, more than 28% of carbon dioxide emissions from fossil fuel combustion can be allocated to the energy consumption of the manufacturing industry [2]. Therefore, the energy systems of industrial parks and companies urgently need a low carbon shift, by increased energy efficiency, waste heat recovery, integration of renewable energy technologies and energy storage. Since these measures are often in competition with investments in production facilities, their integration in the energy system needs to be optimised to increase cost-effectiveness [50]. For this purpose, techno-economic energy models can be used that provide a mathematical representation of the energy system.

An energy system on business park scale comprises different components (see Part 2, Section 2.1). The energy supply system (utility system) consists of a set of energy conversion technology units (utility units) and is configured to fulfil the thermal and electrical energy demands in the energy system. Energy storage units allow to store excess energy and release it at a later point in time with energy deficit, while heat networks enable heat transfer between separated parts of the system. The heat exchanger network realises heat exchange between the thermal streams in the system.

Techno-economic energy models provide a holistic approach towards the design of energy systems, in which the complex interactions between the technological, economic and environmental aspects of the energy system's components are taken into account (see Part 2). A variety of energy models has been developed in the last decades, each serving particular purposes [30]. In Part 2 of this manuscript, a pragmatic model categorisation is proposed and essential features for an energy system model at business park scale are identified. These features are summarised below.

Firstly, a superstructure-based optimisation approach avoids the need for a priori decisions on the system's configuration, since a mathematical algorithm automatically identifies the optimal configuration in a superstructure that embeds all feasible configurations. Secondly, a multi-period approach providing sufficient temporal detail is required, since energy demands and operation conditions of energy technologies can be subject to variations in time. Thirdly, energy technologies need to be accurately represented at unit level by incorporating part-load operation and investment cost subject to economy of scale in the model formulation. In addition, the benefits of installing multiple units per technology must be considered. A generic formulation of technology submodels facilitates the introduction of new technology types. As a fourth important feature, thermodynamically feasible heat exchange between thermal processes needs to be included, since it may induce substantial overall energy savings. Moreover, restrictions to direct heat exchange between process streams need to be taken into account. Finally, to enhance the integration of non-dispatchable renewable energy technologies and to bridge any asynchrony between cooling and heating demands, energy storage needs to be included.

A number of energy models described in Part 2 of this work incorporate one or more of these essential features. Energy models, such as ETEM [37], TIMES [36] and OSeMOSYS [38] optimise the configuration of the utility system using a superstructure that contains a set of averaged technologies. Voll *et al.* [50] developed a superstructure-based optimisation model using a generic technology formulation proposed by Yokoyama, Hasegawa and Ito [69]. The technology submodel

can be manipulated to represent the different thermal or electrical energy conversion technology units in the utility system and covers part-load operation as well as the effects of economy of scale on investment costs. Moreover, the utility system superstructure is gradually expanded in order to optimise the number of units per technology type. Welsch *et al.* [48] integrated an energy storage model into OSeMOSYS [38] and added time sequence to enable correct calculation of storage levels over the year. Maréchal and Kalitventzeff [70] developed a heat cascade model that simultaneously maximises heat exchange between thermal process streams and optimally integrates the utility system, using a superstructure with elaborated submodels for energy technologies. The same authors elegantly extended their model to multi-period [61]. Becker *et al.* [62] reformulated the heat cascade model to account for predefined restrictions in direct heat exchange between process streams, and integrated heat networks to avoid the increase in energy requirements resulting from these restrictions. Verheyen and Zhang [71] developed a model for optimal multi-period heat exchanger network synthesis, starting from a stage-wise superstructure, while considering one type of hot and one type of cold utility.

The energy models presented in this short review have each established a number of essential features for modelling of low carbon energy systems on business park scale. In this work, a holistic model, called Syn-E-Sys, is developed in GAMS [72] merging and aligning all the essential features at once.

The proposed model comprises two sequential stages. In the first stage, heat recovery within the system is maximised, while utility system and energy storage are optimally integrated and designed to fulfil remaining energy requirements at minimum total annualised costs. Predefined variations in thermal and electrical energy demand and supply are taken into account, next to a carbon emission cap. At the same time, heat networks can be deployed to transfer heat between separate parts of the system. In the second stage, the model generates an optimal multi-period heat exchanger network enabling all required heat exchanges.

The model builds upon a multi-period energy integration model that can deal with restrictions in heat exchange. It is combined with a generic technology model that can be manipulated to represent the various thermal or electrical energy conversion technology units in the utility system. A simple model for thermal and electrical storage is included that allows for correct calculation of storage levels subject to energy loss over time, without increasing the number of time steps to be analysed. In addition, a more elaborated thermal storage model consisting of a stack of virtual tanks is integrated. A method for automated superstructure expansion is incorporated in the solution procedure to enable the optimisation of the number of units per technology in the configuration of the utility system. The heat exchanger network is automatically generated using a multi-period stage-wise heat exchanger network model.

Chapter 2 explains how the synthesis of an energy system can be optimised by applying mathematical optimisation techniques on an overall system superstructure. In Chapter 3, different approaches for energy integration are reviewed and a two-staged method is proposed which forms the backbone of *Syn-E-Sys*.

In Chapter 4, the model is built up by stepwise integration of all essential features, while corresponding submodels are described in detail. Section 4.8 provides an overview of the architecture of the model code. Section 4.2 deals with the representation of time in the model and

the introduction of time sequence. Section 4.3 focusses on the generic formulation used for modelling thermal and electrical technologies at unit level. Section 4.4 starts with an introduction to energy integration, followed by the description of the basic heat cascade model. Subsequently, the heat cascade model with heat exchange restrictions is explained. A problem related to the integration of heat networks in the heat cascade model (called phantom heat) is described and measures to prevent it are explored. Finally, the calculation of envelope curves to identify suitable heat networks is explained and discussed. Section 4.5 introduces the automated procedure for expansion of the utility system superstructure that optimises the number of units per technology. Section 4.6 develops the model for thermal and electrical storage subject to conversion losses and losses over time. Moreover, a more complex model for sensible heat storage is elaborated. Section 4.7 describes the model for optimising the design of the heat exchanger network.

In Chapter 4.8 the model is applied on a literature example and on a generic case study, to demonstrate its possibilities. As a first example, an energy system optimisation problem from literature is reproduced and gradually extended with new features. A second example comprises a generic energy system, especially developed to demonstrate energy storage, carbon emission cap and non-dispatchable energy technologies. Finally, conclusions are drawn in Chapter 6.

2. Energy system synthesis by superstructure-based optimisation

This chapter briefly explains how the synthesis of an energy system can be optimised by applying mathematical optimisation techniques on an overall system superstructure. Section 2.1 focusses on the superstructure of energy system optimisation models and zooms in on the differences between three representative models. Section 2.2 deals with the general formulation of an optimisation problem, while deterministic algorithms to solve it are treated in section 2.3. Finally, section 2.4 derives the equations composing the optimisation problem for a simple example.

2.1. Superstructure of an energy system optimisation model

Optimisation-based energy models [37, 50, 59]start from a predefined superstructure or reference energy system that embeds all feasible system configurations. The superstructure is modelled by a set of mathematical equations describing the behaviour of all its components and all possible interconnections between them. A particular configuration is set up by selecting the components to be included, and by specifying their characteristics. These decisions correspond to the decision variables in the mathematical formulation of the superstructure. Optimisation techniques allow us to find the best performing system configuration according to a certain criterion or objective (see section 2.2). Therefore, a mathematical algorithm is employed that calculates the values of the decision variables for which the objective value is minimised or maximised (see section 2.2). In the optimisation models treated in this work, total system cost is chosen as the objective to be minimised. However, depending on the context in which the system must be optimised, other objectives could be more appropriate, such as carbon emissions, or total fossil fuel consumption. Different criteria for energy system modelling and their impact on the system design are reviewed by Østergaard [73].

The differences between the optimisation-based energy models reviewed in this work can be better understood by exploring the similarities and dissimilarities between their superstructures. As an example, Fig. 16, Fig. 17 and Fig. 18 show the superstructure schemes of respectively the models ETEM[37], the model framework proposed by Voll *et al.* [50], and Osmose [59].

The superstructure of ETEM consists of averaged technologies and of commodities representing energy resources, energy carriers, energy service demands and emissions (see Fig. 16). Technologies and commodities are explicitly linked by allocating commodities to the inflow and outflow of each technology. No binary variables for technology selection are included in the mathematical formulation of the superstructure. The continuous decision variables are technology capacity, commodity consumption or production per technology, and commodity import or export.

The model developed by Voll *et al.* [50] is based on a superstructure consisting of individual technology units and thermal and electrical energy demands (Fig. 17), that are interconnected explicitly by means of a connectivity matrix. In contrast to ETEM, binary variables enable technology selection. Furthermore, technology operation and investment costs are modelled with a set of binary and continuous decision variables, while other continuous decision variables represent resource consumption and electricity import or export.

The superstructure of Osmose comprises technologies that generate thermal and/or electrical energy, a number of thermal energy demands and an overall electrical energy demand (see Fig. 18). The thermal in- or outputs of a technology and the thermal demands are represented by temperature-heat curves. In contrast to the optimisation models described above, technologies and demands in the superstructure cannot be explicitly connected. Instead, they are connected implicitly via the heat cascade or via the electrical energy balance. As a consequence there is no direct control over the exchange of energy between specific components in the superstructure. Another dissimilarity is that thermal energy demands can transfer energy without the intervention of a technology. Similar decision variables as in the model of Voll et al. are used. The superstructure of the *Syn-E-Sys* (see chapter 4) is similar to the superstructure of Osmose.

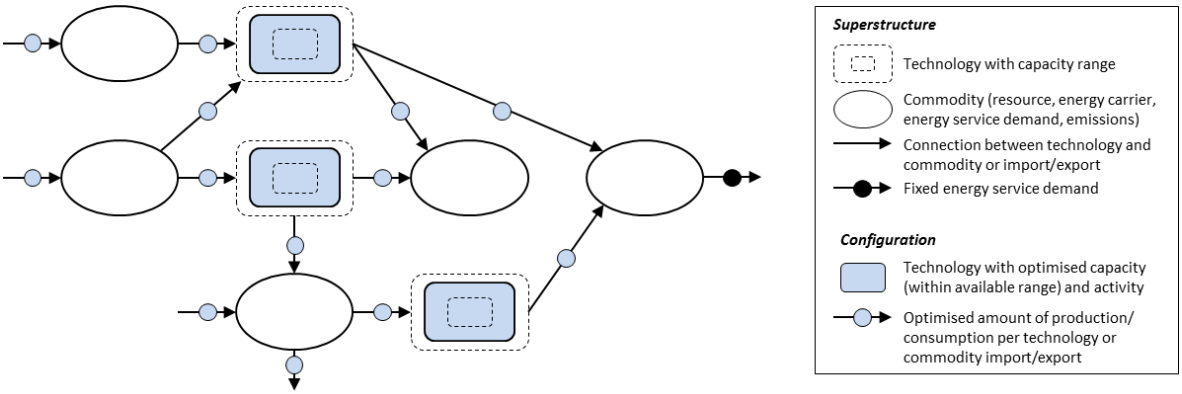

Fig. 16: Superstructure of ETEM and specification of a particular configuration

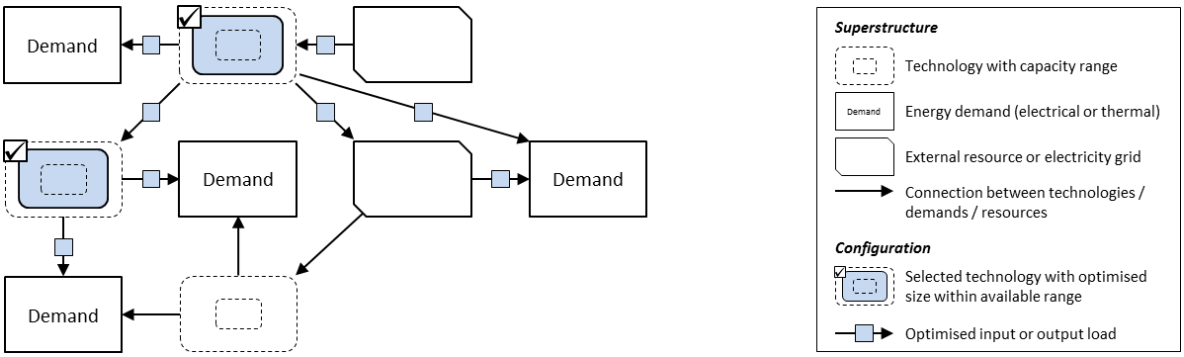

Fig. 17: Superstructure of Voll et al. and specification of a particular configuration

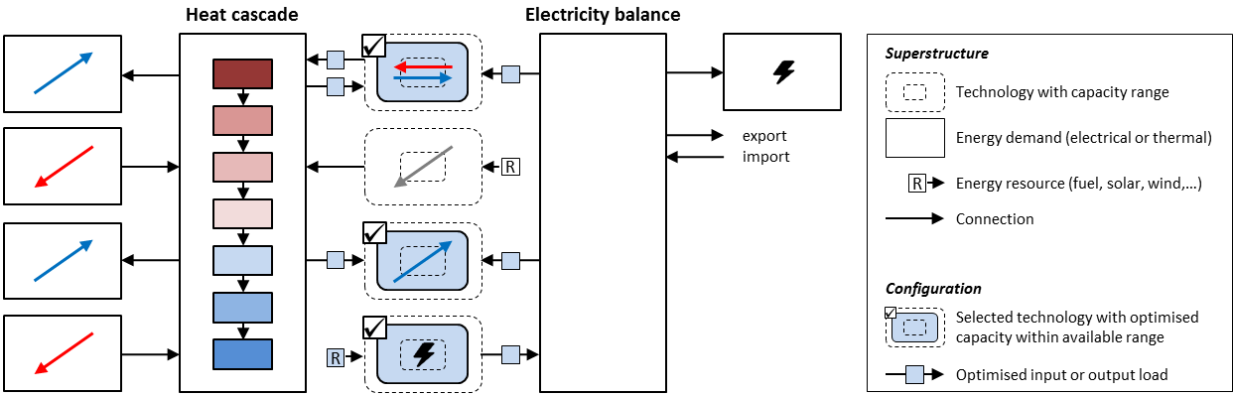

Fig. 18: Superstructure of Osmose as a base for *Syn-E-Sys* and specification of a particular configuration

2.2. General formulation of the optimisation problem

In an optimisation problem, the values of decision variables need to be calculated in order to minimise or maximise the value of an objective function, while complying with a number of constraints. Decision variables represent the problem characteristics to be determined (e.g. technology selection, size and operation in an energy system), while the objective expresses a certain criterion in function of these variables (e.g. total annual system costs), and the constraints represent the relations between them (e.g. behaviour of technologies, energy balances, emission cap). These constraints correspond to the mathematical formulation of the superstructure of an energy system optimisation model.

The general formulation below expresses that the vector of decision variables x needs to be calculated for which the scalar function f reaches a minimum, while complying with the vector functions h and g.

$\min_x f(x)$ objective function

Subject to

$h(x) = 0$ equality constraints

$g(x) \leq 0$ inequality constraints

The feasible region or solution space of the optimisation problem is defined by the equality and inequality constraints expressing the relations between the decision variables. A feasible solution is a set of decision variables that falls within or on the feasible region, and thus complies with all constraints. In case of a minimisation problem, the optimal solution is a feasible solution for which the objective value is minimised.

Depending on the nature of the equations and the decision variables, different types of optimisation problems can be distinguished. In a linear programming problem (LP), objective function and constraints are linear, while this is not the case in a non-linear programming problem (NLP). When next to continuous decision variables, also integer or binary variables are involved, the program is referred to as mixed integer linear (MILP) or mixed integer non-linear (MINLP) programming.

If multiple objectives need to be optimised simultaneously, f is a vector function containing multiple scalar objective functions. Total annualised system costs and annual emissions are an example of two conflicting objectives that are often simultaneously optimised in energy system design.

In general, no solution exists for which all objectives are optimised simultaneously. Therefore, a set of feasible solutions is calculated with the best possible trade-offs between the different objectives, referred to as the Pareto set. The corresponding objective values define the Pareto curve in the objective function space. However, multi-objective optimisation and the different solution methods are not elaborated in this work. For a confined review and links to more extensive literature on multi-objective optimisation, see e.g. [74, 75].

2.3. Deterministic optimisation algorithms

To solve an optimisation program, numerous algorithms are available. As indicated by Voll [75], they can be classified into deterministic algorithms, following predetermined search patterns, and metaheuristic algorithms using randomised search patterns. However, in this work only deterministic algorithms are considered.

In a linear programming problem (LP), the objective function as well as the constraints are linear functions of the decision variables. Consequently, the solution space is a convex polytope and the optimal solution lies on its boundary. Based on this fact, George B. Dantzig developed the simplex algorithm in 1947 to solve linear optimisation problems. This algorithm starts at an arbitrary vertex of the solution space and moves to a next vertex along an edge that shows improvement of the objective value. The search continues until a vertex is found from which no improving edges start, corresponding to the global optimum solution. Before starting the simplex algorithm, the problem is brought to its standard form and inequalities are eliminated by adding slack variables. The CPLEX solver implements the simplex method in the GAMS environment and automatically derives the standard form based on the equations specified by the user.

In a non-linear programming problem (NLP), either the objective function, the constraints or both are non-linear. If the objective function in non-convex, the optimal solution may lie within the feasible region, and if the solution space is non-convex, multiple local optima may exist. Non-linear optimisation algorithms perform search steps in the solution space according to improving directions which depend on the local derivatives of the objective function. In order to achieve converge, these

algorithms require good starting values for the decision variables of the problem. An example of a non-linear solver implemented in GAMS is CONOPT, developed by Drud [76].

Integer or mixed integer linear programming problems (ILP or MILP) can be solved using the branch-and-bound algorithm developed by Land and Doig [77]. The basic principle of this method is explained here for binary decision variables, but is similar for integers. In an initial step, the original problem is relaxed, by turning the binary decision variables into continuous ones constrained between 0 and 1, and solved using the simplex algorithm. Subsequently, the relaxed problem is branched on one of the original binary decision variables for which the optimised value differs from 0 and 1. In a first branch, this variable is fixed to 0, while in a second branch, it is set to 1. Both sub-problems are again solved with simplex and branched on a next relaxed variable that takes a non-binary value. By repeating this procedure, a search tree is systematically built up. However, it is not necessary to solve the problem at each node of the tree. Whenever a solution is obtained in which all relaxed decision variables take binary values, it is saved as the temporarily best solution, until one with a better objective value is found. At each node, where the optimisation returns an objective value worse than that of the temporarily best solution, the branch is cut, because all solutions further down that branch will have worse objective values. A branch is also cut on a node at which no feasible solution is obtained. Finally, the branch-and-bound method yields the solution with the best objective value, and since all sub-problems are linear, global optimality is guaranteed.

Mixed integer non-linear programming problems (MINLP) can be solved by combining the branch-and-bound algorithm with a non-linear optimisation algorithm, but global optimality can only be guaranteed for a convex problem (convex objective function and constraints), with linear discrete variables. To solve MINLP problems in this work, the DICOPT algorithm is employed, developed by Viswanathan and Grossmann [78]. This algorithm decomposes the problem into a series of MILP and NLP sub-problems that can be solved by CPLEX and CONOPT. It can deal with non-convexities, but cannot guarantee global optimality. Global optimisation algorithms have been developed that use methods similar to the branch-and-bound algorithm, but they still suffer from long computation times for real-world problems, as mentioned by Voll [75]. For a broad introduction into optimisation algorithms, reference is made to the book of Vanderbei [79].

2.4. Linear programming formulation for a simple energy system

In this subsection, the mathematical formulation is set up for a linear energy system optimisation problem. Let us consider an example of a simple energy system in which an electricity demand has to be fulfilled at the lowest total annualised costs, taking into account an upper limit to overall carbon emissions ($CO2cap$). The year is divided into two parts (time slices $S1$ and $S2$), each containing a number of hours hrs_S_S, in which the electricity demand takes different constant values. Two technologies $T1$ and $T2$ are available with nominal efficiencies ηnom_{T1} and ηnom_{T2}, specific investment costs cI_{T1} and cI_{T1}, operation costs cO_{T1} and cO_{T2}, and carbon intensities $iCO2_{T1}$ and $iCO2_{T2}$. Electricity can be purchased at a cost $cImp$ and sold at a price $cExp$, while a carbon intensity $iCO2grid$ is allocated to the imported electricity. Investment costs need to be annualised by multiplying with a factor Anf. In order to solve this optimisation problem, a superstructure is composed containing the two technologies and the energy demand, as shown in Fig. 19, which is analogous to Fig. 18.

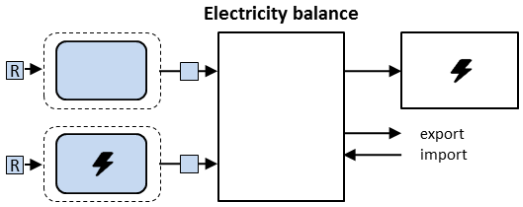

Fig. 19: superstructure of simple energy system

The mathematical formulation of the superstructure consists of a number of linear equations which define the convex solution space of the problem. Decision variables are the installed nominal capacity $\dot{\boldsymbol{E}}\boldsymbol{nom}_T$ of each technology, its input and output load per time slice $\dot{\boldsymbol{E}}\boldsymbol{in}_{T,S}$ and $\dot{\boldsymbol{E}}\boldsymbol{out}_{T,S}$ and electricity import $\boldsymbol{Imp}_S$ and export $\boldsymbol{Exp}_S$ per time slice. Equation A1 describes the conversion from input to output for each technology in each time slice, whereas equation A2 limits the output load of a technology in each time slice to its installed capacity (equation A2). Moreover, equation A3 ensures that the electricity production and import is equal to the electricity demand and export. Equation A4 ensures that the carbon emissions generated by the technologies and related to the electricity import do not surpass the prespecified cap. The objective function to be minimised accumulates annualised technology investment and operation costs and the costs related to electricity import and export.

objective

minimise $\boldsymbol{cost} =$

$$\sum_{T,S} \dot{\boldsymbol{E}}\boldsymbol{in}_{T,S} \cdot hrs\_S_S \cdot cO_T + \sum_{T} \dot{\boldsymbol{E}}\boldsymbol{nom}_T \cdot cI_T.Anf + \sum_{S} \boldsymbol{Imp}_S \cdot hrs\_S_S \cdot cImp - \sum_{S} \boldsymbol{Exp}_S \cdot hrs\_S_S \cdot cExp$$

subject to

A1 $\quad \forall T,S: \dot{\boldsymbol{E}}\boldsymbol{out}_{T,S} = \dot{\boldsymbol{E}}\boldsymbol{in}_{T,S} \cdot \eta nom_T$

A2 $\quad \forall T,S: \dot{\boldsymbol{E}}\boldsymbol{out}_{T,S} \leq \dot{\boldsymbol{E}}\boldsymbol{nom}_T$

A3 $\quad \forall S: \sum_{T} \dot{\boldsymbol{E}}\boldsymbol{out}_{T,S} + \boldsymbol{Imp}_S = dem_S + \boldsymbol{Exp}_S$

A4 $\quad \sum_{T,S} \dot{\boldsymbol{E}}\boldsymbol{in}_{T,S} \cdot hrs\_S_S \cdot iCO2_T + \sum_{S} \boldsymbol{Imp}_S \cdot hrs\_S_S \cdot iCO2grid \leq CO2cap$

$\dot{\boldsymbol{E}}\boldsymbol{nom}_T, \dot{\boldsymbol{E}}\boldsymbol{in}_{T,S}, \dot{\boldsymbol{E}}\boldsymbol{out}_{T,S}, \boldsymbol{Imp}_S, \boldsymbol{Exp}_S \in \mathbb{R}^+, \boldsymbol{cost} \in \mathbb{R}$

Since objective function and constraints are linear and all decision variables are continuous (LP problem), the Simplex algorithm can be used. Before the algorithm is deployed, the problem is written in standard and inequalities (equation A2) are translated into equalities by adding slack variables $\boldsymbol{x}_{T,S}$. Subsequently, the problem is formulated in vector notation as illustrated below for this example, and optimised by the algorithm:

$\min_X C^T \cdot X$ subject to $A \cdot X = B$

Minimise

$$\begin{bmatrix} cI_{T1} \cdot Anf \\ cI_{T2} \cdot Anf \\ hrs\_S_{S1} \cdot cO_{T1} \\ hrs\_S_{S2} \cdot cO_{T1} \\ hrs\_S_{S1} \cdot cO_{T2} \\ hrs\_S_{S2} \cdot cO_{T2} \\ hrs\_S_{S1} \cdot cImp \\ hrs\_S_{S2} \cdot cImp \\ -hrs\_S_{S1} \cdot cExp \\ -hrs\_S_{S2} \cdot cExp \\ 0 \\ 0 \\ 0 \\ 0 \end{bmatrix}^T \cdot \begin{bmatrix} \boldsymbol{\dot{E}nom}_{T1} \\ \boldsymbol{\dot{E}nom}_{T2} \\ \boldsymbol{\dot{E}in}_{T1,S1} \\ \boldsymbol{\dot{E}in}_{T1,S2} \\ \boldsymbol{\dot{E}in}_{T2,S1} \\ \boldsymbol{\dot{E}in}_{T2,S2} \\ \boldsymbol{Imp}_{S1} \\ \boldsymbol{Imp}_{S2} \\ \boldsymbol{Exp}_{S1} \\ \boldsymbol{Exp}_{S2} \\ \boldsymbol{x}_{T1,S1} \\ \boldsymbol{x}_{T1,S2} \\ \boldsymbol{x}_{T2,S1} \\ \boldsymbol{x}_{T2,S2} \end{bmatrix}$$

With $\boldsymbol{\dot{E}nom}_T, \boldsymbol{\dot{E}in}_{T,S}, \boldsymbol{Imp}_S, \boldsymbol{Exp}_S, \boldsymbol{x}_{T,S} \in \mathbb{R}^+$

Subject to

$$\begin{bmatrix} -1 & -1 & 0 & 0 & 0 & 0 & 0 \\ 0 & 0 & -1 & -1 & 0 & 0 & 0 \\ \eta nom_{T1} & 0 & 0 & 0 & \eta nom_{T1} & 0 & \varphi_{T1,S1} \\ 0 & \eta nom_{T1} & 0 & 0 & 0 & \eta nom_{T1} & \varphi_{T1,S2} \\ 0 & 0 & \eta nom_{T2} & 0 & \eta nom_{T2} & 0 & \varphi_{T2,S1} \\ 0 & 0 & 0 & \eta nom_{T2} & 0 & \eta nom_{T2} & \varphi_{T2,S2} \\ 0 & 0 & 0 & 0 & 1 & 0 & \psi_{S1} \\ 0 & 0 & 0 & 0 & 0 & 1 & \psi_{S2} \\ 0 & 0 & 0 & 0 & -1 & 0 & 0 \\ 0 & 0 & 0 & 0 & 0 & -1 & 0 \\ 1 & 0 & 0 & 0 & 0 & 0 & 0 \\ 0 & 1 & 0 & 0 & 0 & 0 & 0 \\ 0 & 0 & 1 & 0 & 0 & 0 & 0 \\ 0 & 0 & 0 & 1 & 0 & 0 & 0 \end{bmatrix}^T \cdot \begin{bmatrix} \boldsymbol{\dot{E}nom}_{T1} \\ \boldsymbol{\dot{E}nom}_{T2} \\ \boldsymbol{\dot{E}in}_{T1,S1} \\ \boldsymbol{\dot{E}in}_{T1,S2} \\ \boldsymbol{\dot{E}in}_{T2,S1} \\ \boldsymbol{\dot{E}in}_{T2,S2} \\ \boldsymbol{Imp}_{S1} \\ \boldsymbol{Imp}_{S2} \\ \boldsymbol{Exp}_{S1} \\ \boldsymbol{Exp}_{S2} \\ \boldsymbol{x}_{T1,S1} \\ \boldsymbol{x}_{T1,S2} \\ \boldsymbol{x}_{T2,S1} \\ \boldsymbol{x}_{T2,S2} \end{bmatrix} = \begin{bmatrix} 0 \\ 0 \\ 0 \\ 0 \\ dem_{S1} \\ dem_{S2} \\ CO2cap \end{bmatrix}$$

With $hrs\_S_S \cdot iCO2_T = \varphi_{T,S}$
$hrs\_S_S \cdot iCO2grid = \psi_S$

3. Two-staged method for energy system synthesis with energy integration

Mathematical programming methods for energy integration can be classified [71, 80-83] according to their approach. In the sequential approach, the problem is decomposed into different sub-problems, while in the simultaneous approach the entire problem is solved in one time. Both approaches are explained in detail in the first two sections of this chapter. In the third section, a two-staged method is proposed, which forms the backbone of *Syn-E-Sys*. Since energy integration is established by a heat exchanger network, the terms energy integration and HEN synthesis are sometimes used interchangeably.

3.1. Sequential approach for energy integration

In the sequential approach, the energy integration problem is decomposed into a number of smaller sub-problems that are solved successively. This reduces the complexity of the problem, but may exclude the optimal solution, since the trade-off between utility costs and heat exchanger costs is not taken into account [71, 80, 84]. Pinch Technology [18] is a widely applied sequential energy integration method that decomposes the problem into three smaller sub-problems, which can be solved using mathematical optimisation models or with manual procedures. An elaborate introduction to Pinch Technology and its key concepts is given in Subsection 4.4.1.

3.1.1. Methodology

Pinch Technology comprises three sequential steps (Fig. 20). In the first step, prior to the design of the actual heat exchanger network, counter-current heat exchange between hot and cold process streams is maximised for a given minimum temperature approach $\Delta Tmin$. Simultaneously, utilities are optimally integrated to fulfil the resulting minimum energy requirements at minimum utility costs. For this purpose, the LP transshipment model of Papoulias and Grossmann [85] or the MILP formulation developed by Maréchal *et al.* [70], also called heat cascade models, can be used. In contrast to the LP model, in which utility costs are directly proportional to the utility flowrates, utilities in the MILP model have a cost component proportional to the flowrate as well as a fixed cost component related to their selection. Consequently, the MILP model optimises continuous flowrate variables as well as binary selection variables. The resulting overall heat cascade indicates the locations of pinch points, at which no residual heat is cascaded down. Heat exchange across these pinches results in an increase of utility cost. Therefore, the problems treated in the next steps can be partitioned into a number of independent subnetworks between consecutive pinch points.

In the second step, all utility heat loads are fixed at their optimal values resulting from the first step. For each subnetwork, the configuration of hot/cold stream matches that features the minimum number of matches is calculated together with the heat loads exchanged at each match. This problem is referred to as the Heat Load Distribution (HLD) and can be solved using the MILP transshipment model of Papoulias *et al.* [85] or the alternative formulation of Maréchal and Kalitventzeff [86]. An actualised description of the latter is given by Pouransari and Maréchal [87]. Note that the solution is not necessarily unique and alternative match configurations can be found by applying integer-cut constraints. In this phase, there is still no information about how connections

between streams and heat exchangers are organised (exchangers in parallel, in series, mixed) nor about heat exchanger areas.

The third step involves the optimal design of the actual heat exchanger network. For each subnetwork, a general HEN superstructure is set up, in which the heat exchangers directly correspond to the hot/cold stream matches and the exchanged heat loads predicted in step 2. The connections in the superstructure enable stream splitting, mixing and bypassing of streams, so that all alternative network configurations (in parallel, in series, mixed) are embedded. Subsequently, the configuration with the lowest heat exchanger investment cost is determined, using the NLP model developed by Floudas, Ciric and Grossmann [88].

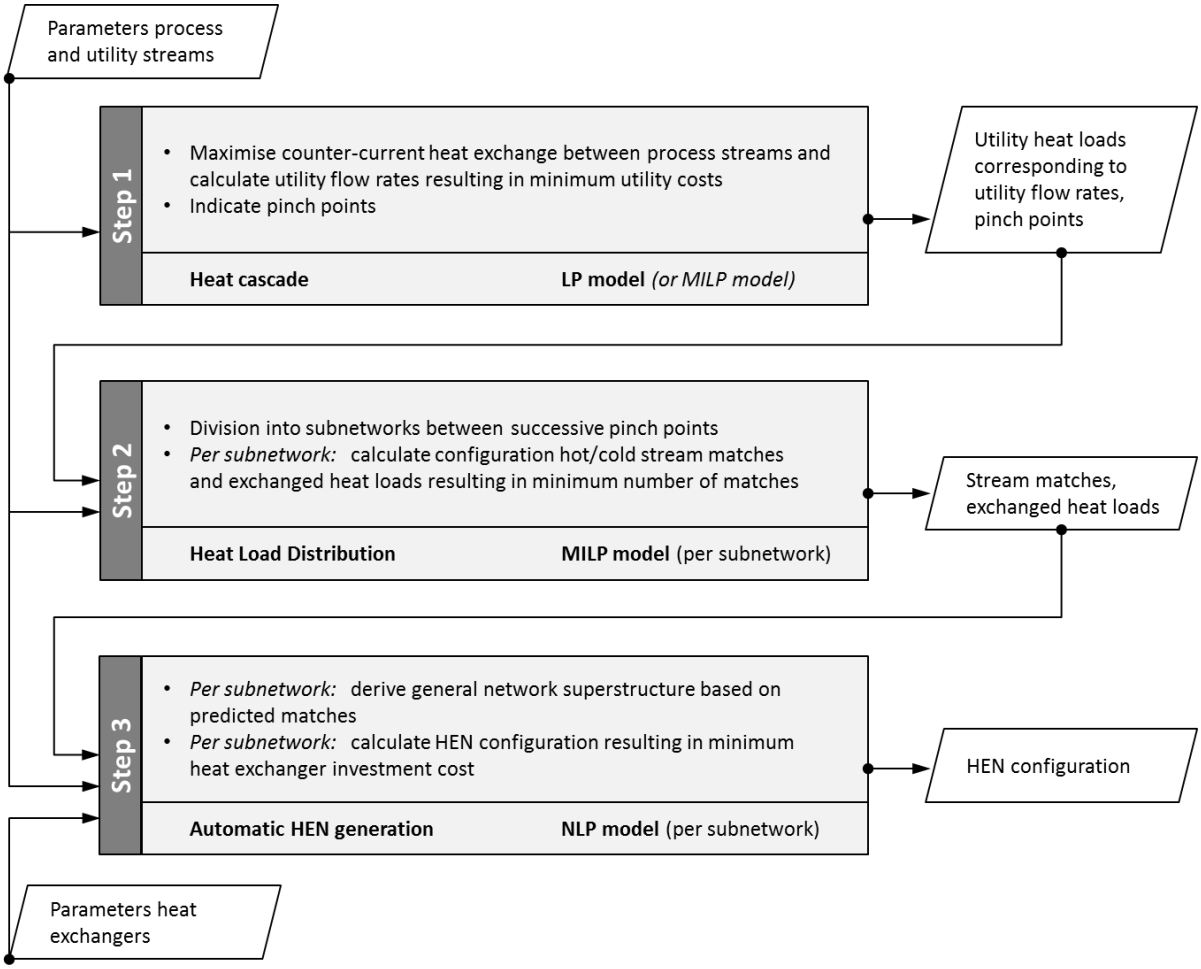

Fig. 20: Steps in sequential energy integration approach

Alternatively to the automated mathematical programming approach of Floudas *et al.* [88], the heat exchanger network can be developed (step 3) with the Pinch Design Method (PDM) proposed by Linnhoff and Hindmarsh [89]. In this method, a sequence of decisions is made by the modeller, based on heuristic and feasibility rules. The PDM does not necessarily lead to networks with the minimum number of heat exchangers or minimum utility costs. However, the number of units can be brought back to the minimum value by deleting heat exchangers and restoring driving forces with the 'loop breaking and path following' technique. The PDM can be applied after step 2 or directly after step 1.

In summary, the sequential approach computes the HEN with minimum investment costs, subject to the minimum utility costs target and the minimum number of matches target. The advantage of this approach is that the decomposition reduces complexity and computation time. Since the minimum utility cost problem (step 1) and the minimum number of unit problem (step 2) are convex, a global optimum can be obtained for these sub-problems. The drawback is that there is no direct trade-off between utility costs and heat exchanger costs. Solutions with a number of heat exchangers higher than the minimum number, but with lower total annualised costs are excluded.

3.1.2. Methodology improvements

During the last decades, various improvements have been proposed to all steps in the sequential method, some of which are briefly described below.

Becker *et al.* [62] modified the heat cascade model (step 1) to take into account restrictions for heat exchange between streams belonging to different parts of an industrial site. Therefore, they split up the energy system into different subsystems that are connected to a central heat transfer system. Streams located in different subsystems can only exchange heat via special heat transfer units in the heat transfer system. A more detailed explanation is provided in subsection 4.4.3.

The solution space of the Heat Load Distribution (HLD) in step 2 increases exponentially with the number of binary decision variables representing all hot/cold stream pairs, and may become difficult to solve for large-scale systems. To tackle this problem, Pouransari and Maréchal [90] recently proposed a method to decompose the original HLD into a number of smaller intermediate HLD problems. After calculating the optimal utility loads in step 1, the process is divided into different process subsystems. Each subsystem is represented by a virtual hot and cold stream, equal to the hot and cold composite curve respectively. In a first stage, the HLD is solved to minimise the number of matches between virtual and utility streams. In the next stages, the subsystems are successively unpacked by switching back from the virtual streams to the real streams, while solving the HLD. The results of each stage are translated into forced and forbidden match constraints for the next stage.

In an earlier publication, Pouransari *et al.* [87] proposed to modify the objective function of the HLD in order to reduce computation time, by multiplying each of the binary decision variables with a weight factor. For each possible hot/cold stream match, the distance between the streams is calculated and the entire list of distances is divided into a number of ranges. Subsequently, priority levels are assigned to these ranges, with the highest priority corresponding to the range of smallest distances. From these priority levels, weight factors are derived for each match.

Floudas and Ciric [91] developed an MINLP model that combines the heat load distribution model of Papoulias *et al.* [85] (step 2) with a generalised match-network hyperstructure derived from the superstructure of Floudas *et al.* [88] (step 3). It simultaneously optimises matches and exchanger heat loads and can lead to a global minimum HEN investment cost.

3.1.3. Multi-period

The methods described in previous subsections [18, 70, 85-91] are suited for energy system synthesis under steady state operating conditions, or in other words for system design according to one single nominal period of operation. However, when stream flow rates or temperatures vary over time, a multi-period energy integration method is required. Process stream flow rates may depend on operating schedules or changes in type of feedstock, while process and utility stream temperatures can be influenced by environmental conditions [61]. It is assumed that the operation parameters are known a priori for every period. A multi-period sequential method delivers a HEN configuration with minimum investment costs and minimum number of exchangers that ensures feasible operation in all periods and that features minimum utility costs in every period [92].

Maréchal *et al.* [61] extended their MILP formulation [70] for calculation of minimum utility costs (step 1) to multi-period. Floudas *et al.* [92] developed multi-period versions of the LP and MILP transshipment models [85] for calculation of respectively minimum utility costs (step 1) and minimum number of matches (step 2). The extension of the LP model is straightforward and consists in solving the model separately for each period. In this way, the optimal utility heat loads that result in minimum utility costs per period are determined. The extension of the Heat Load Distribution (MILP) problem to multiple periods is less trivial, since the variations of stream flow rates and temperatures cause changes in pinch point locations from one period to another. As a consequence, the partitioning of the network problem into subnetworks differs from period to period. To account for this, objective function and constraints are reformulated. A variable representing the maximum number of matches over all periods for each hot/cold stream pair is introduced, and the sum of these variables over all hot/cold stream pairs provides the new objective to be minimised. Note that in a period with more than one subnetwork a hot/cold stream pair may require more than one match to avoid cross-pinch heat exchange. In the multi-period HLD it is assumed that a hot/cold stream match can have heat loads that vary from period to period, which implicates that bypasses need to be available in the real network. By subsequently solving both multi-period problems of Floudas *et al.* [92] (step 1 and 2), a configuration of hot/cold stream matches is obtained that ensures feasible operation in all periods and that features the fewest number of matches and minimum utility costs in every period.

In order to automate the generation of a multi-period HEN configuration with minimum investment costs (step 3), Floudas and Grossmann [93] developed a multi-period version of the single-period NLP model of Floudas *et al.* [88].The multi-period superstructure is set up following a similar procedure. For every hot/cold stream match predicted by the multi-period HLD model [92], a heat exchanger is installed in the superstructure. In each period, the heat load of such an exchanger is then fixed to the predicted heat load of the corresponding match. A heat exchanger is installed with a fixed area, but must be able to handle loads that vary from period to period. Therefore, a bypass around each heat exchanger is required. Additionally, an overall bypass is introduced for each stream. Contrary to the single period model, it is not possible to split the multi-period superstructure into subnetworks, as pinch point locations may vary from period to period. However, starting from the known pinch points locations, the superstructure can be refined by excluding infeasible configurations, with the aid of a handy graph representation. By solving the NLP model based on this superstructure, the multi-period HEN configuration with minimum investment costs is obtained.

3.2. Simultaneous approach for energy integration

In the simultaneous approach, the energy integration problem is solved in one time (Fig. 21). As a consequence, the trade-off between utility costs and heat exchanger costs is taken into account.

3.2.1. Methodology

Simultaneous methods optimise the HEN configuration in a stage-wise superstructure that embeds all feasible HEN configurations. This superstructure leads to a non-convex MINLP model containing a large number of binary and continuous decision variables. To master size and complexity, assumptions need to be made in the superstructure layout, at the expense of excluding feasible system configurations from the solution space. In the simultaneous approach there is no need for a fixed $\Delta Tmin$, since the temperature differences for heat exchange are optimised at the level of each selected heat exchanger [84]. Consequently, pinch points are not predetermined, but are simultaneously optimised and no partitioning into subnetworks needs to be considered [84].

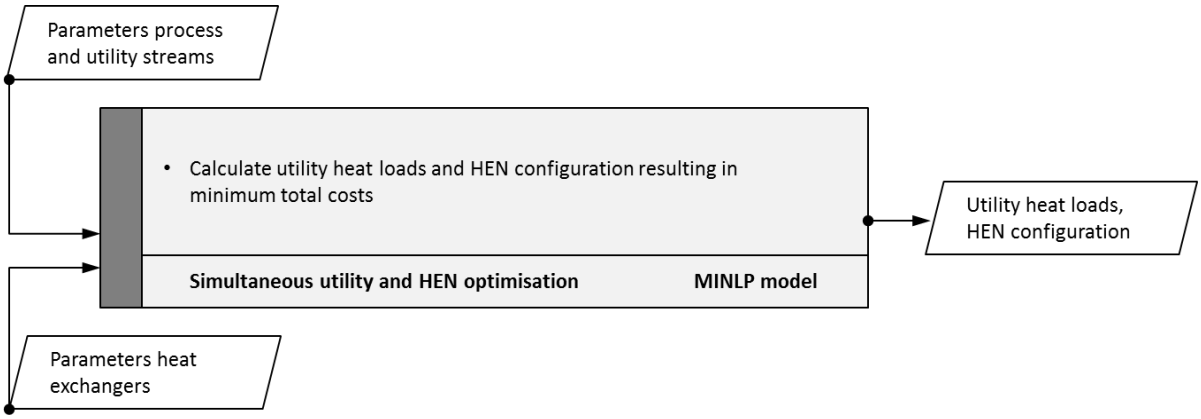

Fig. 21: Scheme for simultaneous HEN synthesis approach

Yee *et al.* [84] proposed a simultaneous synthesis method formulated as an MINLP model based on a stage-wise superstructure (see Fig. 22). This superstructure contains all hot process streams of the system running from left to right, and all cold process streams running from right to left. All streams in the structure are divided into an equal, user-defined number of stages. At every stage, each hot stream is split into a number of branches corresponding to the number of cold streams and analogous for the cold streams. In each stage, heat exchangers connect the hot stream branches with the cold stream branches, in such a way that every hot stream is connected once to every cold stream. Each hot stream is equipped with a cold utility at the right end of the superstructure, while for each cold stream a hot utility is provided at the left side. It must be noted that the model formulation includes only one type of hot and one type of cold utility. Also the heat exchangers between process and utility streams are embedded in the superstructure. At every stage, all branches of a stream are forced to have the same exit temperature (isothermal mixing).

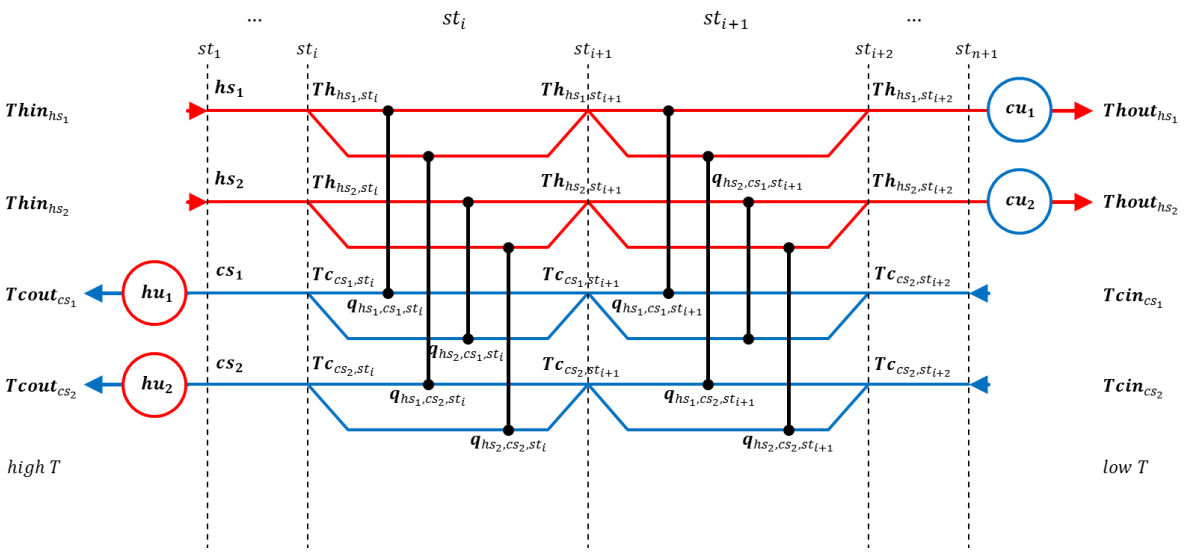

Fig. 22: Multi-stage superstructure hen design [84] (for two hot and two cold steams)

The set of decision variables consists of binaries representing the activation of each heat exchanger in the superstructure, and a set of continuous variables for heat exchanger loads and stage temperatures. The constraints include overall and stage-wise energy balances, assignment of known temperatures, feasibility conditions of stream temperatures, calculation of hot and cold utility loads, constraints related to the existence of a match, and calculation of approach temperatures of each match. The objective function to be minimised expresses the sum of the (annual) utility operation costs and the (annualised) fixed charges and area costs of the heat exchangers. All non-linear mathematical expressions related to the heat exchanger design (Logarithmic Mean Temperature Difference (LMTD), required area and area cost) are embedded in the objective function, which turns it non-linear and non-convex. The constraints however, are linear because of the assumption of isothermal mixing (see subsection 4.7.2). The number of stages related to the best objective value will normally not be higher than the maximum number of hot or cold streams. Due to the composition of the superstructure, a number of feasible HEN configurations are a priori excluded. To partially circumvent this in cases where stream splits occur, Yee *et al.* [84] developed an NLP sub-optimisation problem.

All simultaneous cost-optimal synthesis methods discussed in this work employ the combined penalty function and outer-approximation algorithm developed by Viswanathan *et al.* [78], which is incorporated under the name DICOPT in the General Algebraic Modeling System (GAMS) [72] as the standard MINLP solver.

3.2.2. Multi-period

The methods of Yee *et al.* [84] or Ciric and Floudas [94] are applicable for system design based on one single period. A multi-period simultaneous method delivers a utility and HEN configuration with minimal annualised costs that enables system operation in every period. Aaltola [80] developed a multi-period simultaneous method based on the superstructure and MILNP formulation of Yee *et al.* [84]. He extended the constraints to multiple periods and modified the objective function to account for the weighted utility costs, the average of the heat exchanger area costs over all periods and the fixed charges for the exchangers. The constraints are still linear, while non-linearities are

concentrated in the objective function. To counter the isothermal mixing assumption and the use of average area cost in the objective function, Aaltola [80] proposed an NLP improvement model.

In a first phase of the method, upper bounds for the hot utility loads in each period are calculated by applying the minimum utility cost transshipment model of Papoulias *et al.* [85] in every period. These bounds are used in a multi-period MILP model to determine upper bounds on the minimum number of heat exchangers and on the number of stages. This model is actually derived from Aaltola's MINLP model by modifying the objective function in order to express the number of heat exchangers instead of total costs. Finally, the MINLP model is solved, constrained by previously mentioned bounds. These bounds are gradually increased in order to check for better objective values.

A particular heat exchanger in the superstructure is selected in the final HEN configuration if its heat load differs from zero in at least one period. The required area of a heat exchanger per period is not an explicit decision variable but can be derived from its optimised heat load and the temperature differences at both sides. The actually installed area of a heat exchanger is the maximum of the required areas over all periods. However, the optimisation is performed as if the available heat exchanger area is equal to the required area in every period. To enable this optimal solution in reality, a bypass around each heat exchanger with controllable mass flow needs to be installed. The bypass mass flow has to be set to such a value that the remaining flow through the installed heat exchanger area causes the same heat exchange as in the optimal solution provided by the model. In conclusion, the bypass variables and non-linear heat balances are not included in the optimisation model and can be calculated after optimisation.

Verheyen *et al.* [71] significantly improved the model of Aaltola [80] by switching in the objective function from average heat exchanger area cost to cost of maximum area. Therefore, they added new continuous decision variables representing the installed area of the heat exchangers. Additional constraints demand that the installed area is sufficient to enable the heat exchange in each period. In other words, the installed area must be greater than or equal to the required area in every period. Note that the latter is not an explicit decision variable, but is expressed as a function of exchanger heat load, LMTD and overall heat transfer coefficient. The objective function has been modified to include weighted utility costs, the costs of the maximum area of each heat exchanger over all periods, and the fixed charges for the exchangers. Furthermore, they adapted the NLP improvement model of Aaltola [80].

3.2.3. Multi-utility

All of the simultaneous MINLP methods described before are based on the superstructure of Yee *et al.* [84] and include only one type of hot and one type of cold utility, placed at both ends of the superstructure. This location of utilities builds on the assumption that hot utilities are hotter than the target temperatures of all cold processes and cold utilities are colder than the target temperatures of all hot processes. However, multiple utilities of various temperature ranges may be available in the energy system. Ponce-Ortega *et al.* [81] modified the superstructure of Yee *et al.* [84] in order to enable integration of utilities with arbitrary temperature levels. Therefore, they added heat exchangers between process and utility streams at each stage. As a result a hot process can exchange heat with a cold process or with a cold utility in each stage and analogous for the cold processes. Moreover, at every stage, an optimal choice can be made between multiple utility types through a

disjunctive programming formulation. The model is developed for single period operation. It is able to deal with non-isothermal as well as with isothermal streams, in contrast to the previous models that can only handle non-isothermal streams.

Remarks. It must be noted that the model of Ponce-Ortega *et al.* [81] has some limitations. Firstly, as a result of formulas 20 to 23 in their formulation, a process stream cannot exchange heat with the same non-isothermal utility in two adjacent stages. The reason is that at the border between two stages only one variable is assigned to the temperature difference between the process stream and the utility. The solution is to assign two variables to this temperature difference: one related to the first of two adjacent stages and the other to the next stage. Equations 20 to 23 must be doubled and reformulated accordingly. Secondly, since utilities are not modelled as streams in the superstructure, utility heat exchangers cannot be placed in series. If heat exchange between a process stream and a utility would occur in two stages, the heat exchangers would be placed in parallel on the utility stream and thus each exchange would utilise the full temperature range of this utility. As a consequence some feasible solutions are excluded a priori.

To narrow down the solution space and improve convergence of simultaneous energy system synthesis problems with multiple utilities, Na *et al.* [82] proposed an MINLP model alternative to the one of Ponce-Ortega *et al.* [81]. Between the conventional stages, they inserted utility substages in which multiple utilities can exchange heat with process streams. In each substage, utilities are placed in series, following a predefined sequence according to decreasing temperature levels, while conventional stages contain no utilities. This implicates that, in contrast to [95], a process-process heat exchanger cannot be placed in parallel on a certain process stream with a process-utility heat exchanger. Their present model formulation is not able to cope with isothermal streams, but this could easily be adapted.

3.2.4. Comparison of features of simultaneous methods

Table 5 summarises the main differences between the simultaneous HEN synthesis approaches that start from the superstructure of Yee *et al.* [84]. In all of these methods, utility costs are directly proportional to their heat loads, so no distinction is made between investment, fuel, and operation and maintenance costs.

	Yee et al. [84]	***Aaltola [80]***	***Verheyen et al. [71]***	***Ponce-Ortega et al. [81]***	***Na et al. [82]***
time	single period	multi period	multi period	single period	single period
area cost	area cost single period	average area cost over periods	maximum area cost over periods	area cost single period	area cost single period
objective	non-linear	non-linear	non-linear	non-linear	non-linear
constraints	linear	linear	non-linear	linear	linear
LMTD *approxim.*	in obj. function Chen. [96]	in obj. function Paterson [97]	in constraints Paterson [97]	in obj. function Chen. [96]	in constraints Chen. [96]
utilities	1 type hot and cold at ends of structure	1 type hot and cold at ends of structure	1 type hot and cold at ends of structure	selection from multiple types in each stage	selection from multiple types in each utility substage
isothermal streams	no	no	no	yes	no

Table 5: Comparison of features of simultaneous HEN synthesis methods

3.3. Two-staged method

The energy model *Syn-E-Sys* follows a two-staged method, that combines elements of the sequential and the simultaneous approach. More specifically, the configuration of utility system and energy storage is optimised using the heat cascade model that correponds to the first step of the sequential approach (Fig. 23). Based on these results, the HEN is designed using the MINLP model of the simultaneous approach.

In stage 1, heat exchange between hot and cold process streams is maximised for a given $\Delta Tmin$. Simultaneously, utility and storage units are optimally integrated and designed to fulfil the remaining energy requirements in every period at minimum total annualised costs (fuel, operation and maintenance, investment). This requires optimising selection, size and operation of utility and storage units. For this purpose, a multi-period MILP heat cascade model is equipped with a generic superstructure that embeds all feasible utility system and energy storage configurations (see Chapter 4). The synthesis of the utility system and energy storage is not influenced by the heat exchanger properties. This can be considered as a safe approach in the predesign phase, when heat exchanger properties are not accurately specified.

In stage 2, heat loads of utility and storage units are fixed at their values obtained in the first stage and an optimal heat exchanger network configuration is calculated using a multi-period MINLP model (see Chapter 4). This involves optimising heat exchanger placement and heat exchanger area and in a HEN superstructure. The proposed two-staged approach avoids the need for identification of pinch point locations and partitioning into subnetworks.

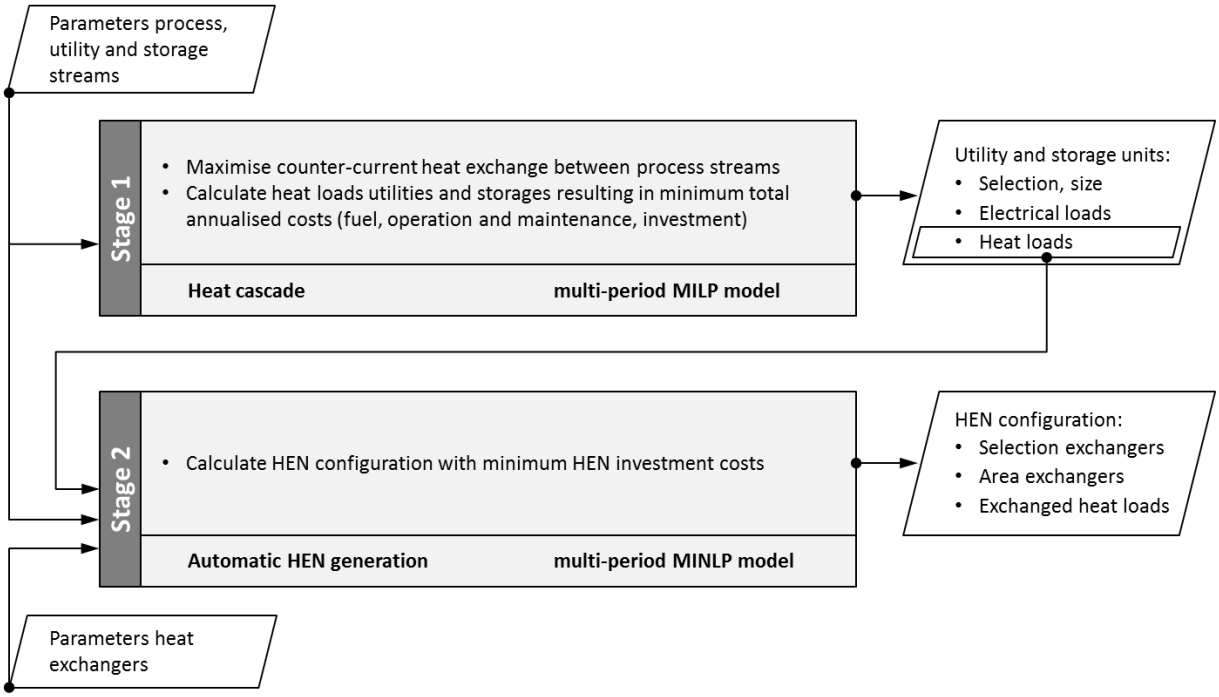

Fig. 23: Steps in two-staged method for energy system synthesis

If the entire energy system synthesis problem would be formulated as a simultaneous multi-period MINLP model, the complexity and the solution time would drastically increase when it is extended with additional equations and variables. By decomposing the synthesis problem in an MILP part in stage 1 and an MINLP part in stage 2, complexity can be better managed. However, the trade-off between utility and heat exchanger network costs is not taken into account.

4. Development of a holistic energy system synthesis model

In this Chapter, the essential features for energy system modelling on business park scale are combined into one holistic model for cost-optimal energy system synthesis, called *Syn-E-Sys*. The model follows the two-staged method proposed in Chapter 3. The relation between the essential features introduced throughout this chapter and the interaction between the sub-models is schematically represented in Fig. 24.

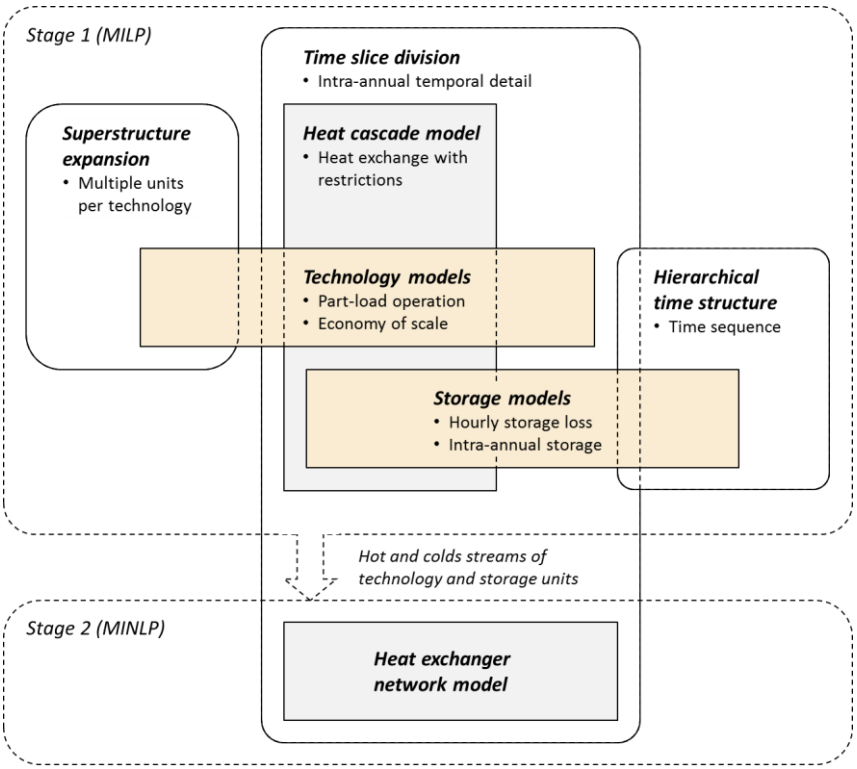

Fig. 24: Scheme of interaction between model features in the two stages of Syn-E-Sys

Section 4.1 provides an overall view on the assembly of the model and a schematic representation of the model's superstructure. Section 4.2 deals with the representation of time in the model. Time series can be condensed into empirically defined time slices, or clustered into typical days using cluster optimisation algorithms. A hierarchical time structure is set up that introduces time sequence needed for modelling of energy storage. In section 4.3, a generic model for energy technologies (utilities) is developed, adopted from Voll *et al.* [50] and elaborated in order to connect it to the thermodynamic energy balances governing the energy system (see section 4.4). The technology model simulates part-load behaviour and accounts for the effects of economy of scale on investment costs. Furthermore, specific technology models are derived from the generic model by adding extra equations.

Section 4.4 first provides a brief introduction into energy integration techniques. These methods are used to calculate the potential of heat recovery between thermal process streams and the resulting minimum energy requirements, and assist in optimal integration of energy technologies to fulfil the remaining electrical and thermal energy demands. Next, the basic heat cascade model is described

[70, 85], which is a mathematical tool for energy integration. An extended version of this model takes into account heat exchange restrictions by subdividing the energy system a priori into subsystems connected to a joint heat transfer system, containing common utilities and heat networks [62]. Subsequently, a multi-period version of the heat cascade model with heat exchange restrictions is developed, which forms the core of *Syn-E-Sys*. Moreover, the formulation is adapted to accept isothermal streams.

The fact that heat networks can form a self-sustaining energy loop is highlighted in this work as an important limitation to the extended heat cascade model. This phenomenon is referred to here as phantom heat and two strategies are explored and evaluated to avoid it. A first approach exists in adding extra equations to block phantom heat, while the second approach exists in choosing heat networks with temperature ranges that are embedded within a precalculated heat transfer unit envelope [62]. However, the envelope formulation and its calculation strategy are discussed and improved in this work in order to integrate the trade-off between utility and heat network costs. Finally, thermal and electrical storage units are integrated in the multi-period heat cascade model with heat exchange restrictions, with and without envelope. Carbon emissions of fuel-driven utilities are accumulated over all time slices and limited by a specified emission cap.

In section 4.5, the effect of considering multiple units per technology type is discussed. All technology units to be considered during optimisation have to be embedded in the model's superstructure. Because the number of units in the optimal configurations is not known before, this can lead to unnecessary large superstructures. Therefore, a procedure for automated superstructure expansion [50] is incorporated into the model.

Section 4.6 deals with the modelling of electrical and thermal energy storage units. To simulate the evolution of storage levels, time sequence needs to be added to the yearly time slice division. Therefore, a three-layered hierarchical time structure is set up consisting of seasons, daytypes and daily time brackets, to which each time slice is assigned [48]. Storage levels need to stay between predefined limits in each time step, but to avoid having to check them in each time step, critical points in time are identified at which extreme storage levels can occur. When hourly storage losses are taken into account, the energy system's operation must be calculated in every single hour to enable correct calculation of the storage level, leading to excessive model sizes. In this section, however, a novel approach is proposed that enables correct storage level calculation subject to hourly loss, while keeping the time dimension of the model at time slice level. Consequently, this method can be used to facilitate the integration of energy storage in current energy system optimisation models. A more detailed model for thermal storage is conceived of a series of interconnected virtual tanks [98]. We modified this model and applied the aforementioned method for storage level calculation with hourly loss to calculate the mass levels of the virtual tanks. As a result, the virtual tank model is no longer confined to daily storage [98], but can be used to simulate storage at any arbitrary time scale over the year. Finally, the models for electrical and thermal storage and for thermal storage with virtual tanks are integrated into the heat cascade model.

Section 4.7 describes the design of the heat exchanger network that enables all required heat exchanges between thermal streams. The method uses a multi-period MINLP model, based on a stagewise superstructure [71]. Section 4.8 explains the architecture of the model code, indicating the different building blocks.

4.1. Model assembly

To construct the MILP model in stage 1, a multi-period version of the heat cascade model with heat exchange restrictions proposed by Becker *et al.* [62] is combined with a generic superstructure that embeds all feasible utility system and energy storage configurations. This superstructure is based on a generic technology model similar to Voll *et al.* [50], that includes part-load operation and investment cost subject to economy of scale, and a generic energy storage model inspired by Welsch *et al.* [48]. The former is used as a building block to model more complex technologies (e.g. heat pump, heat engine, heat network, etc.). The latter is modified to cover electrical as well as thermal storage and to account for the effect of hourly energy losses on the storage level. In addition, a more complex model for sensible heat storage is elaborated and integrated into the heat cascade. Furthermore, the automated superstructure expansion procedure proposed by Voll *et al.* [50] is incorporated into the optimisation. The optimisation of the MILP model in the first stage delivers optimised thermal storage and utility loads, which serve as input to the MINLP model in the second stage, together with the known thermal process streams. In this stage, the HEN is optimised, using a multi-period HEN design model derived from the one proposed by Verheyen *et al.* [71] and adapted to enable representation of isothermal streams analogous to the formulation of Ponce-Ortega *et al.* [81]. Sections 3.1 to 3.5 elaborate the development of the MILP model of stage 1, while Section 4.7 deals with the MINLP model of stage 2.

In the superstructure of the MILP model in stage 1, utility units, energy storage units and energy demands are not connected by a one-to-one relation. Instead, they are connected indirectly through the thermal energy balances in the heat cascade and the overall electricity balance (Fig. 25). Optimising the system's configuration implicates selecting the utility and storage units to be installed, determining their size within the available capacity ranges, and calculating in and output energy loads, in such a way that total annualised costs are minimised. The superstructure corresponding to the MINLP model in stage 2 is described in Section 4.7.

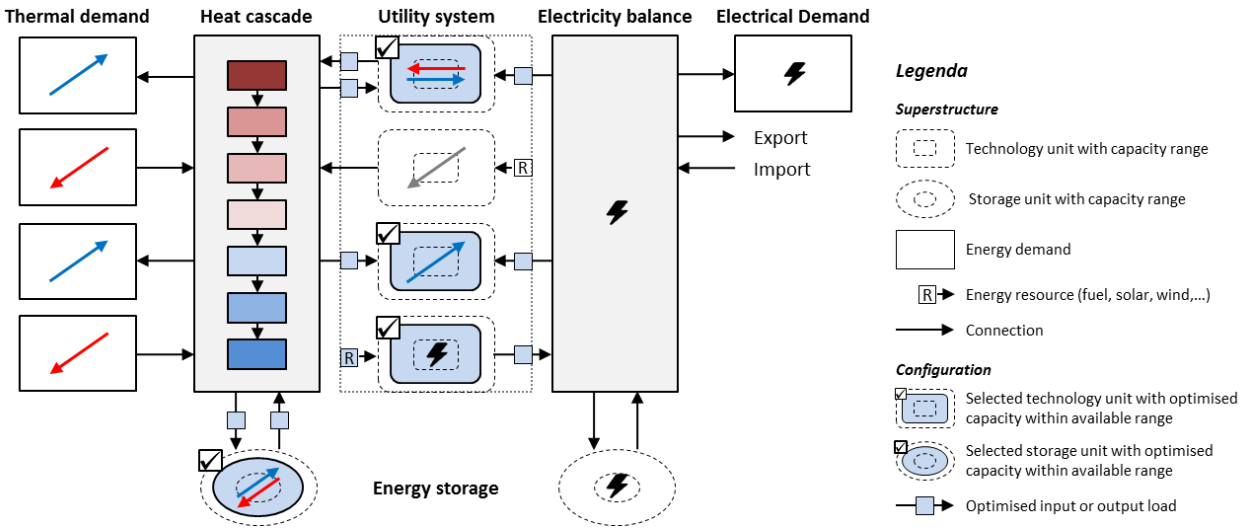

Fig. 25: Schematic representation of stage 1 MILP model superstructure (no heat exchange restrictions) and example of optimised configuration

In this chapter, variables are indexed with sets: $varname_{set}$, refers to all instances set_j in set of that variable, whereas specific instances of a variable are referred to by $varname_{set_j}$. The same is valid for parameters. Furthermore, to avoid confusing notations, the name of a variable or parameter does not contain any sub or superscript. Instead, subscripts are reserved for the set or set element that serve as variable indexes.

4.2. Temporal detail

Electrical and thermal demand loads, electricity prices, temperature levels of processes and utilities and the availability of non-dispatchable renewable energy sources are subject to variations over the year. To capture the key characteristics of these yearly time profiles, energy models need to integrate sufficient temporal detail. However, higher temporal detail comes at the expense of higher computational demands, since every time segment introduces a number of continuous and integer variables into the optimisation problem [99]. In order to limit the number of time segments to be analysed, the year can be condensed into a set of empirically defined time slices. Alternatively, when time series of hourly data are available, clustering optimisation algorithms can be employed to cluster time segments into typical days. Domínguez-Muñoz *et al.* [99] and Fazlollahi *et al.* [100] reviewed empirical and optimisation methods for clustering of energy demand data. In *Syn-E-Sys*, the year is divided into empirically defined time slices, which are labelled according to a hierarchical time structure. This allows introducing time sequence required for modelling of energy storage. In the following subsections, the time slice division with hierarchical time structure on the one hand, and the time division based on typical days on the other hand, are described. In the final subsection, the ability to integrate time sequence is discussed for both approaches.

4.2.1. Time division based on time slices and hierarchical time structure

To limit the number of time segments to be analysed in the optimisation problem, the year can be divided into a number of time slices, which are non-sequential collections of time intervals with similar conditions for energy supply and demand in the energy system. As an example, all summer weekday mornings could be represented by one single time slice, provided that the conditions occurring during these time intervals are comparable. In each time slice, steady state conditions are assumed and thus no dynamic effects are considered within or between time slices.

In addition to the time slice division, a hierarchical time structure is set up to introduce the time sequence needed for modelling of energy storage, following the approach of Welsch *et al.* [48] (for more details, see subsection 4.6.3). This structure divides the year into a number of seasons, daytypes and daily time brackets, containing a specified number of weeks, days and hours respectively. Time slices are assigned to seasons, daytypes and daily time brackets. As a consequence, every week of the year follows the same division into daytypes and days, and every day follows an identical division into daily time brackets and hours. This empirical method is adequate when time profiles are derived from daily, weekly and seasonal trends in energy supply and demand or from process operating schedules, and data is specified accordingly. The energy model developed in this work is based on this approach.

The hierarchical time structure can be manipulated at will by changing the number of seasons, daytypes and hourly time brackets, and the number of weeks, days and hours that they contain. For example, to model a year with time slices of arbitrary duration, it must be conceived as 1 'season' containing 1 'week', divided in 1 daytype containing 1 'day'. The hourly time brackets can then be used to represent time slices of arbitrary length. If storage is included, these hourly time brackets, and the time slices that they represent, are interpreted by the model as consecutive time intervals each containing a sequence of hours. The input data per time slice must be specified accordingly.

4.2.2. Time division based on typical days

When measured yearly profiles are available, the clustering of time intervals can be optimised to better capture key characteristics, such as peak demands and profile trends. Based on the k-medoids clustering algorithm, Domínguez-Muñoz *et al.* [99] developed an optimisation method to downsize a set of yearly time profiles to a number of representative days. In this method, similar days are clustered and for each cluster the most representative day, also referred to as the typical day, is identified. Extreme demand days are treated as separate clusters. As a consequence, all days of the year can be replaced by a few typical days, which are repeated throughout the year. The clustering is optimised by minimising the dissimilarity from all days in a cluster to the typical day of that cluster for an a priori specified number of typical days. To distinguish the best typical day division between alternatives with a different number of typical days, quality indexes are calculated. Starting from the k-means clustering algorithm, Fazlollahi *et al.* [100] proposed a multi-objective optimisation clustering method, that simultaneously minimises the number of typical periods and maximises the clustering quality. Additionally, the 24 hours in each typical day can be optimally clustered in order to further reduce the time slices to be modelled.

4.2.3. Time division and time sequence

A typical day does not have inherent time sequence, as the represented time intervals may be disorderly dispersed over the year. The same is valid for the daily segments calculated in the method of Fazlollahi *et al.* [100]. Empirical time slice division combined with assignment to season, daytype and hourly type, however, embeds time sequence. Indeed, time intervals belonging to a certain time slice are dispersed over the year in an priori known and structured order. This allows us to follow evolution of storage levels over time (see Subsection 4.6.3). For this reason, in *Syn-E-Sys*, the year is divided in empirically defined time slices that are allocated to a hierarchical time structure.

4.3. Technology models

Optimisation models for large scale energy systems, such as TIMES [36], employ a reference energy system or superstructure with averaged technology models. Each averaged technology represents a large group of technology units of similar type, and features averaged operating efficiency and specific investment cost. On the scale of business park energy systems, a representation with more detail on technology unit level is required. At unit level, energy conversion technologies (utilities), show non-linear part-load behaviour, while economy of scale results in lower specific investment costs at larger sizes. Therefore, a generic technology model is employed that is able to represent these features.

The layout of the generic technology model is presented in the subsection 4.3.1. In subsection 4.3.2, equations are developed to include selection of utility units and part-load operation in the optimisation problem. Equations for investment costs subject to economy of scale within the available capacity range are developed in subsection 4.3.3. In subsection 4.3.4, the generic model is extended to take into account the features of some specific energy technologies.

4.3.1. Generic technology model

The various thermal and electrical energy conversion technologies in the utility system are represented by a generic technology model, featuring part-load operation and investment costs subject to economy of scale. For this purpose, the equipment model developed by Yokoyama *et al.* [69] and used by Voll *et al.* [50] is adapted for integration in the heat cascade model. The conversion from energy input $\dot{Q}in$ to energy output $\dot{Q}$ is governed by the part-load operation curve, while the output is limited by the nominal load $\dot{Q}nom$ (Fig. 26). Investment costs Inv are linked to the nominal load via the investment cost curve. If a technology is driven by fossil fuel combustion, a specific fuel cost cF and a carbon emission factor $iCO2$ are allocated to its energy input $\dot{Q}in$. A specific operation and maintenance cost cOM is allocated to the energy output $\dot{Q}$.

As it forms an essential part of the MILP model, the generic technology model [50, 69] is reformulated here according to the mathematical terminology used in this work. It is described for technologies (utilities) generating thermal streams (U), but it is analogous for technologies generating electricity (E). Note that in this section, thermal loads are not modelled with temperature levels. This will be required when utilities are integrated into the heat cascade as will be explained in section 4.4.

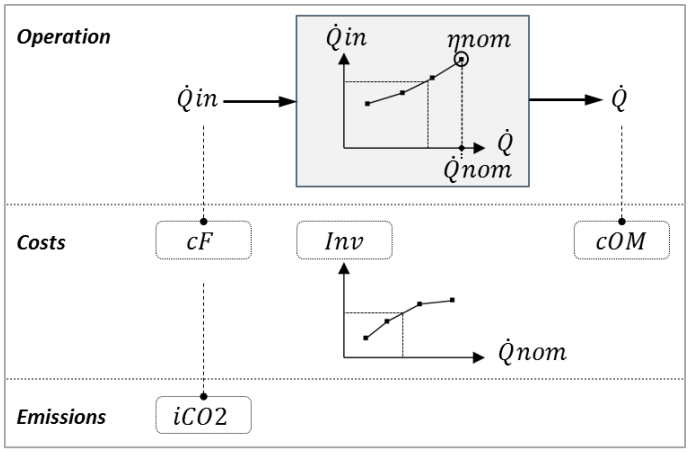

Fig. 26: Scheme of the generic technology model

4.3.2. Part-load operation

The conversion efficiency of most energy technologies is not constant, but varies with the output load. Boilers and CHP engines for example, reach maximum efficiencies at full load, whereas the coefficient of performance (COP) of compression and absorption chillers peaks before the nominal load is attained [50]. This non-linear part-load behaviour can be described by a piecewise linear curve between subsequent reference points R (see Fig. 27), representing the relation between energy input $\dot{Q}in$ and energy output $\dot{Q}$.

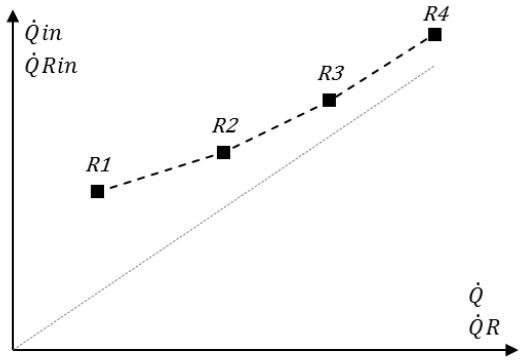

Fig. 27: Part-load operation curve

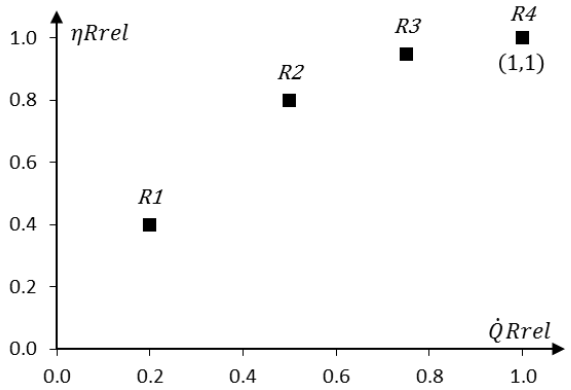

Fig. 28: Specification reference points part-load curve

Each reference point is specified in terms of fractions of nominal output load and nominal efficiency ($\dot{Q}Rrel$ and $\eta Rrel$) as shown in Fig. 28. Note that the relation between relative output load and relative efficiency will not be linear. It is assumed that all units of a certain technology show the same normalised part-load behaviour. The nominal output load $\dot{Q}nom$ (also referred to as equipment size or capacity) is a decision variable in the optimisation, whereas the nominal efficiency ηnom is a known parameter, independent of $\dot{Q}nom$. The nominal efficiency ηnom indicates the efficiency at full output load equal to $\dot{Q}nom$. Consequently, both $\dot{Q}Rrel$ and $\eta Rrel$ equal 1 at the last reference point. Expressions for energy input $\dot{Q}Rin$ and output $\dot{Q}R$ in each reference point and for the operation in each line segment L_i between subsequent reference points R_i and R_{i+1} are derived:

Part-load operation in $\boldsymbol{L_i = [R_i, R_{i+1}]}$

$$\eta R_i = \eta Rrel_i \cdot \eta nom$$

$$\dot{Q}R_i = \dot{Q}Rrel_i \cdot \boldsymbol{\dot{Q}nom}$$

$$\dot{Q}Rin_i = \frac{\dot{Q}R_i}{\eta R_i}$$

$$\boldsymbol{\dot{Q}in_i} = \dot{Q}Rin_i + \left(\boldsymbol{\dot{Q}_i} - \dot{Q}R_i\right) \cdot \tan\gamma_i$$

$$\boldsymbol{\dot{Q}_i} \geq \dot{Q}R_i$$

$$\boldsymbol{\dot{Q}_i} \leq \dot{Q}R_{i+1}$$

$$\boldsymbol{\dot{Q}in_i, \dot{Q}_i, \dot{Q}nom} \in \mathbb{R}^+$$

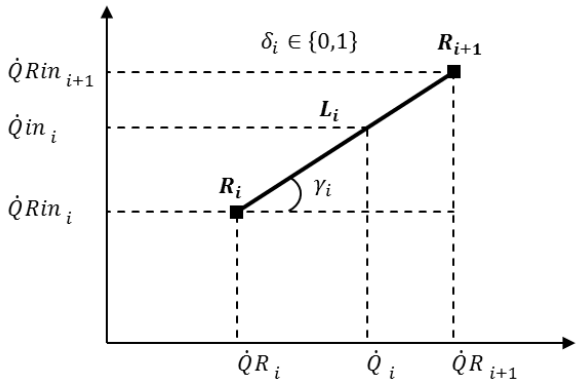

Fig. 29: Part-load operation in line segment L_i

Known parameters are bundled into coefficients α_i and β_i, calculated by utility parameter equations UP1 and UP2. To indicate whether or not the operation point lies on line segment $\boldsymbol{L_i}$, a binary decision variable $\boldsymbol{\delta_i}$ is introduced into the formulation (equations U1, U2, U3). Another binary decision variable $\boldsymbol{sel}$ determines the selection of the technology in the overall system configuration. In an active segment ($\boldsymbol{\delta_i} = 1$), the load is embedded between the segment's lower and upper boundary, while it is forced to zero in a non-active segment ($\boldsymbol{\delta_i} = 0$) by equations U2 and U3. Equation U4 ensures that at most one line segment is active when the technology is selected, and no segments are activated when the technology is not included in the optimised system. Equations U5' and U6' confine the nominal load between upper and lower boundaries $\dot{Q}nommin$ and $\dot{Q}nommax$, if a line segment is active. If no segment is active, total costs minimisation will turn $\dot{Q}nom$ to zero.

UP1 $\quad \forall i: \alpha_i = \dfrac{\dot{Q}Rrel_i}{\eta Rrel_i \cdot \eta nom}$

UP2 $\quad \forall i: \beta_i = \tan\gamma_i = \dfrac{1}{\eta nom} \cdot \dfrac{\dot{Q}Rrel_{i+1}/\eta Rrel_{i+1} - \dot{Q}Rrel_i/\eta Rrel_i}{\dot{Q}Rrel_{i+1} - \dot{Q}Rrel_i}$

U1 $\quad \forall i: \boldsymbol{\dot{Q}in_i} = \alpha_i \cdot (\boldsymbol{\delta_i} \cdot \boldsymbol{\dot{Q}nom}) + \beta_i \cdot \boldsymbol{\dot{Q}_i} - \beta_i \cdot \dot{Q}Rrel_i \cdot (\boldsymbol{\delta_i} \cdot \boldsymbol{\dot{Q}nom})$

U2 $\quad \forall i: \boldsymbol{\dot{Q}_i} \geq \dot{Q}Rrel_i \cdot (\boldsymbol{\delta_i} \cdot \boldsymbol{\dot{Q}nom})$

U3 $\quad \forall i: \boldsymbol{\dot{Q}_i} \leq \dot{Q}Rrel_{i+1} \cdot (\boldsymbol{\delta_i} \cdot \boldsymbol{\dot{Q}nom})$

U4 $\quad \sum_i \boldsymbol{\delta_i} \leq \boldsymbol{sel}$

U5'-U6' $\quad \forall i: \boldsymbol{\delta_i}.\dot{Q}nommin \leq (\boldsymbol{\delta_i}.\boldsymbol{\dot{Q}nom}) \leq \boldsymbol{\delta_i}.\dot{Q}nommax$

$\boldsymbol{\delta_i}, \boldsymbol{sel} \in \{0,1\}, \boldsymbol{\dot{Q}in_i}, \boldsymbol{\dot{Q}_i}, \boldsymbol{\dot{Q}nom} \in \mathbb{R}^+$

The formulation above is not linear due to the product of the binary decision variable $\boldsymbol{\delta_i}$ and the continuous decision variable $\boldsymbol{\dot{Q}nom}$. However, this problem can be tackled with the reformulation strategy described by Voll *et al.* [50]. The bilinear product $\boldsymbol{\delta_i}.\boldsymbol{\dot{Q}nom}$ is substituted in equations U1-U3 by a single continuous (positive) decision variable $\boldsymbol{\chi_i}$ and linear constraints are developed guaranteeing that the behaviour of the bilinear product is reproduced correctly (equations U5-U8). For a non-active line segment ($\boldsymbol{\delta_i} = 0$), equations U5-U6 force $\boldsymbol{\chi_i}$ to be zero and equations U7-U8 translate into $0 \leq \boldsymbol{\dot{Q}nom} \leq \dot{Q}nommax$. With $\boldsymbol{\chi_i} = 0$, equations U1-U3 ensure that the utility unit is not operated in that segment. If the segment is active ($\boldsymbol{\delta_i} = 1$), equations U7-U8 set $\boldsymbol{\chi_i}$ equal to $\boldsymbol{\dot{Q}nom}$, while equations U5-U6 ensure that $\dot{Q}nommin \leq \boldsymbol{\dot{Q}nom} \leq \dot{Q}nommax$. As a result, $\boldsymbol{\chi_i}$ behaves in the same way as the original bilinear product $\boldsymbol{\delta_i} \cdot \boldsymbol{\dot{Q}nom}$.

The thermal generic technology model needs to be integrated in the heat cascade model, which will be described in detail in subsection 4.4.2. Therefore, equation CN1 is introduced to connect the variable $\boldsymbol{\dot{Q}_i}$, denoting the thermal output load in each line segment $\boldsymbol{L_i}$ of the part-load curve, to the variable $\boldsymbol{\dot{Q}U}$, indicating thermal load in the thermal energy balances of the heat cascade. Note that by default, the output load of a thermal utility is integrated in the heat cascade and not the input load. Alternatively, the variable $\boldsymbol{\dot{Q}U}$ could be substituted in the heat cascade with its expression CN1. Such substitution is applied to couple part-load operation of electrical utilities to the overall electricity balance.

When the year is divided into **multiple time slices**, the variables indicating the position of the operation point on the part-load performance curve are time slice dependent. Consequently, they

receive an extra index S: $\dot{\boldsymbol{Q}}\boldsymbol{in}_{S,i}$, $\dot{\boldsymbol{Q}}_{S,i}$, $\boldsymbol{\delta}_{S,i}$ and $\boldsymbol{\chi}_{S,i}$ while equations U1-U8 and CN1 need to be fulfilled in every time slice.

U5-U6 $\forall i: \boldsymbol{\delta_i} \cdot \dot{Q}nommin \leq \boldsymbol{\chi_i} \leq \boldsymbol{\delta_i} \cdot \dot{Q}nommax$

U7-U8 $\forall i: 0 \leq \dot{\boldsymbol{Q}}\boldsymbol{nom} - \boldsymbol{\chi_i} \leq (1 - \boldsymbol{\delta_i}) \cdot \dot{Q}nommax$

CN1 $\dot{\boldsymbol{Q}}\boldsymbol{U} = \sum_i \dot{\boldsymbol{Q}}_i$

4.3.3. Investment cost subject to economy of scale

Due to economy of scale, technology investment cost curves are often non-linear and are therefore approximated by piecewise linearisation. Analogous to the part-load operation curve, a piecewise linear curve between subsequent reference points Rc (see Fig. 30), represents the relation between investment cost Inv and nominal load $\dot{Q}nomL$, equivalent to the technology unit's size.

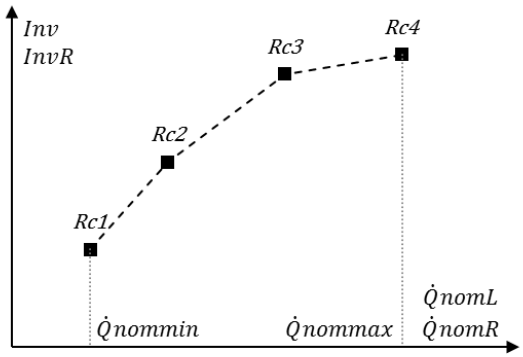

Fig. 30: Investment cost curve

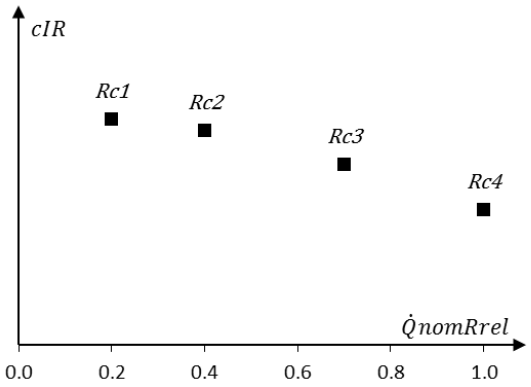

Fig. 31: Specification reference points investment cost curve

Each reference point is specified in terms of fraction of maximal nominal load and specific investment cost ($\dot{Q}nomRrel$ and cIR) as shown in Fig. 31, which are both known parameters. At the first reference point, $\dot{Q}nomRrel = \dot{Q}nommin/\dot{Q}nommax$, while at the last one, $\dot{Q}nomRrel = 1$. Expressions for nominal load $\dot{Q}nomR_i$ and investment cost $InvR_i$ in each reference point and for the points on each line segment Lc_i between subsequent reference points Rc_i and Rc_{i+1} are derived:

Investment cost in $\boldsymbol{Lc_i} = [\boldsymbol{Rc_i}, \boldsymbol{Rc_{i+1}}]$

$\dot{Q}nomR_i = \dot{Q}nomRrel_i \cdot \dot{Q}nommax$

$InvR_i = cIR_i \cdot \dot{Q}nomR_i$

$\boldsymbol{Inv_i} = InvR_i + \tan\theta_i \cdot \left(\dot{\boldsymbol{Q}}\boldsymbol{nomL_i} - \dot{Q}nomR_i\right)$

$\dot{\boldsymbol{Q}}\boldsymbol{nomL_i} \geq \dot{Q}nomR_i$

$\dot{\boldsymbol{Q}}\boldsymbol{nomL_i} \leq \dot{Q}nomR_{i+1}$

$\boldsymbol{Inv_i}, \dot{\boldsymbol{Q}}\boldsymbol{nomL_i} \in \mathbb{R}^+$

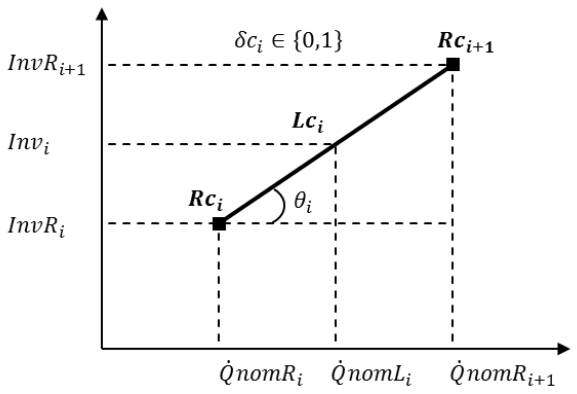

Fig. 32: Investment costs in line segment Lc_i

The inclination of each line segment is calculated by parameter equation CUP1. To indicate whether or not the investment point lies on line segment $\boldsymbol{Lc_i}$, a binary decision variable $\boldsymbol{\delta c_i}$ is introduced (equations CU1, CU2, CU3), while equation CU4 ensures that exactly one line segment is activated when the utility is selected. In each active segment ($\boldsymbol{\delta c_i} = 1$), the nominal load is embedded between the segment's lower and upper boundaries, while it is forced to zero in a non-active segment ($\boldsymbol{\delta c_i} = 0$) by equations CU2 and CU3. Equation CU5 connects the nominal load $\dot{Q}nom$, used in the part-load operation formulation, to the nominal load $\boldsymbol{\dot{Q}nomL_i}$ in the active segment $\boldsymbol{Lc_i}$.In this way, a non-linear relationship between utility size and investment cost is taken into account. To model investment costs of electrical utilities, a completely analogous formulation can be set up.

CUP1 $$\forall i: der_i = \tan\theta_i = \frac{cIR_{i+1} \cdot \dot{Q}nomRrel_{i+1} - cIR_i \cdot \dot{Q}nomRrel_i}{\dot{Q}nomRrel_{i+1} - \dot{Q}nomRrel_i}$$

CU1 $$\forall i: Inv_i = cIR_i.\dot{Q}nomRrel_i \cdot \dot{Q}nommax \cdot \boldsymbol{\delta c_i} + der_i \cdot \boldsymbol{\dot{Q}nomL_i} - der_i \cdot \dot{Q}nomRrel_i \cdot \dot{Q}nommax \cdot \boldsymbol{\delta c_i}$$

CU2 $$\forall i: \boldsymbol{\dot{Q}nomL_i} \geq \boldsymbol{\delta c_i} \cdot \dot{Q}nomRrel_i \cdot \dot{Q}nommax$$

CU3 $$\forall i: \boldsymbol{\dot{Q}nomL_i} \leq \boldsymbol{\delta c_i} \cdot \dot{Q}nomRrel_{i+1} \cdot \dot{Q}nommax$$

CU4 $$\sum_i \boldsymbol{\delta c_i} = \boldsymbol{sel}$$

$\boldsymbol{\delta c_i} \in \{0,1\}, \boldsymbol{\dot{Q}nomL_i} \in \mathbb{R}^+$

CU5 $$\dot{Q}nom = \sum_i \boldsymbol{\dot{Q}nomL_i}$$

4.3.4. Specific technologies

The generic technology model can only handle one input and one output load. More specifically, the thermal generic model is set up for technologies, such as boilers, which have an external energy source as input and induce a thermal stream in the heat cascade of the energy system. The electrical generic model converts an external energy source to an electrical load that is included as a supply to the system's electricity balance. For utilities with two inputs or outputs (e.g. cogeneration, heat pump, heat network, heat engine), two instances (submodels) of the generic thermal or electrical utility model are set up and interconnected by means of additional equations to reproduce the correct technology behaviour. In other words, the generic technology models are used as building blocks to construct more complex technology models. Moreover, for thermal utilities with one input and one output load, driven by heat (e.g. absorption chiller) or electricity (e.g. electrical boiler, compression chiller, cooling water), the generic thermal technology model needs to be adapted.

The equations in this subsection are initially composed disregarding time slice division. When extending these equations to **multiple time slices**, the variables related to the operation point on the part-load curve receive an extra index S: $\boldsymbol{\dot{Q}in_{S,i}}$, $\boldsymbol{\dot{Q}_{S,i}}$, $\boldsymbol{\dot{Q}U_{S,i}}$, $\boldsymbol{\dot{Q}in\_el_{S,i}}$, and equations containing these variables need to be fulfilled in every time slice (equations CHP2, HP2, HE2 and CN2 in following subsections).

4.3.4.1. Cogeneration unit

A cogeneration or combined heat and power (CHP) unit converts its energy input $\dot{Q}F$ into a thermal load $\dot{Q}h$ and an electrical load $\dot{W}$. It is modelled by coupling the generic model for thermal utilities to that for electrical utilities by means of additional equations, as shown in Fig. 33. The thermal submodel describes the relation between $\dot{Q}F$ and $\dot{Q}h$, wheras the electrical submodel deals with the relation between $\dot{Q}F$ and $\dot{W}$.

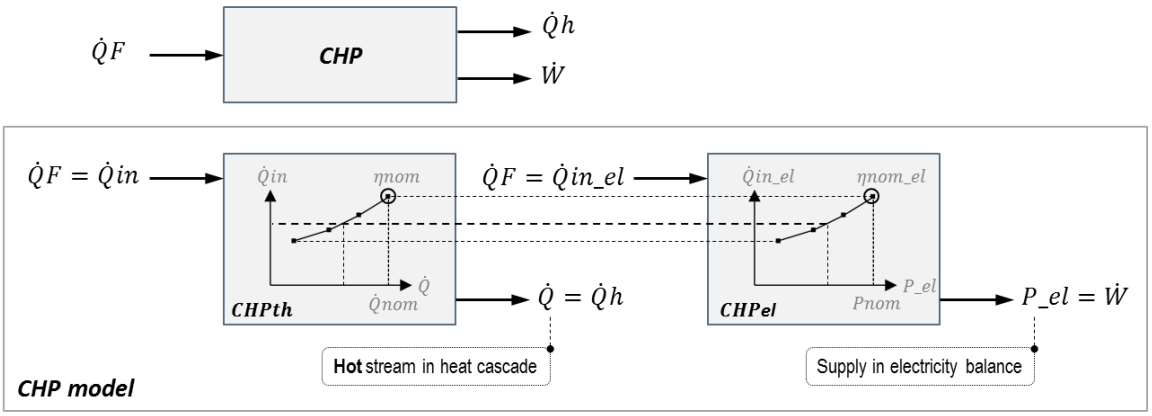

Fig. 33: Technology model for CHP

Parameter equations CHP_a and CHP_b derive the allowable range for the electrical nominal load from the range specified for the thermal nominal load. The range of the input load must be the same for both submodels, and consequently the first and the last reference points (R_1 and R_{final}) of their part-load curves need to have the same ordinates, as indicated in Fig. 33 and expressed by equation CHP1a. Since at the last reference point all relative parameters in this equation are equal to 1, it can be rewritten as equation CPH1. By substituting CPH1 in CPH1a written out for the first reference point, parameter equation CHP_c is obtained. Moreover, both submodels operate at the same input load (equation CHP2) and are simultaneously selected in the energy system configuration (equation CHP3). In summary, the CHP model consists of parameter equations CHPa, CHPb and CHPc, and optimisation constraints CHP1, CHP2 and CHP3. Investment and operation and maintenance costs and CO_2 emissions are only assigned to the thermal submodel.

CHP_a $$Pnommax = \frac{\eta nom\_el}{\eta nom} \cdot \dot{Q}nommax$$

CHP_b $$Pnommin = \frac{\eta nom\_el}{\eta nom} \cdot \dot{Q}nommin$$

CHP_c $$\eta Rrel\_el_1 = \eta Rrel_1 \cdot \frac{PRrel_1}{\dot{Q}Rrel_1}$$

CHP1a $$for\ i = 1 \text{ and } i = i_{final}$$

$$\dot{Q}Rin_i = \dot{Q}Rin\_el_i \Leftrightarrow \frac{\dot{Q}Rrel_i \cdot \boldsymbol{\dot{Q}nom}}{\eta Rrel_i \cdot \eta nom} = \frac{PRrel_i \cdot \boldsymbol{Pnom}}{\eta Rrel\_el_i \cdot \eta nom\_el}$$

CHP1 $$\boldsymbol{Pnom} = \frac{\eta nom\_el}{\eta nom} \cdot \boldsymbol{\dot{Q}nom}$$

CHP2 $$\sum_i \boldsymbol{\dot{Q}in}_i = \sum_i \boldsymbol{\dot{Q}in\_el}_i$$

CHP3 $$\boldsymbol{sel} = \boldsymbol{sel\_el}$$

4.3.4.2. Heat pump

A heat pump (HP) extracts heat $\dot{Q}c$ from the energy system by evaporation of its working fluid. It lifts the fluid to a higher temperature level by mechanical compression, while using an electrical load $\dot{W}$, and delivers an increased amount of heat $\dot{Q}h$ back to the system by condensation of the fluid. The heat pump model is conceived of two instances of the generic thermal utility model, as shown in Fig. 34, that are interconnected by additional equations.

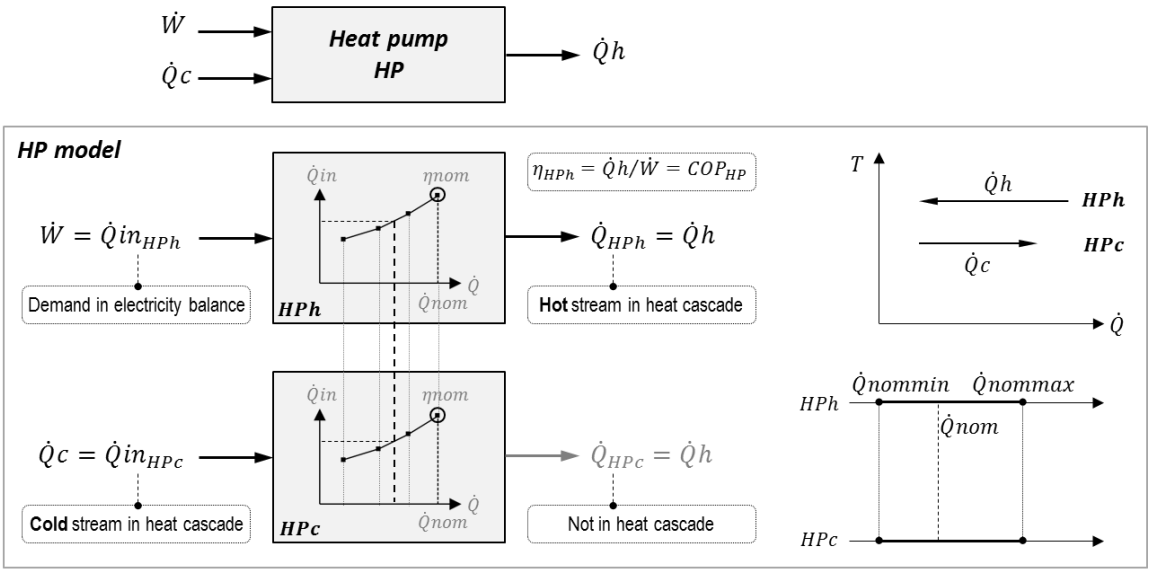

Fig. 34: Technology model for heat pump

Submodel HPh describes the relation between $\dot{W}$ and $\dot{Q}h$, while submodel HPc deals with the relation between $\dot{Q}c$ and $\dot{Q}h$. The part-load curves representing these relations are defined by linear segments between subsequent reference points R. In both submodels, these points need to have the same abscissa, given by $\dot{Q}Rrel \cdot \dot{Q}nom$. Therefore, the relative heat loads in submodel HPc are set equal to those specified for submodel HPh, using parameter equation HP_a, and the nominal loads of both models are forced to be equal by equation HP1. Moreover, the output load of both submodels must be the same (equation HP2). Additionally, the allowable range for the nominal load needs to be identical for both submodels (parameter equations HP_b and HP_c).

The efficiency of submodel HPh is equivalent to the heat pump's coefficient of performance (COP), which is specified in the reference points as fractions of a specified nominal value. An equation can be derived expressing the efficiency of submodel HPc as a function of the efficiency of submodel HPh. Therefore, the law of energy conservation is combined with the definitions of nominal efficiency in both submodels (HP_d1 - HP_d3), leading to parameter equation HP_d. An analogue relation is valid at each reference point (HP_e1) and is reformulated as parameter equation HP_e to calculate the relative efficiencies of submodel HPc. Both submodels are simultaneously selected in the system configuration (equation HP3)

HP_a $\dot{Q}Rrel_{HPc,i} = \dot{Q}Rrel_{HPh,i}$

HP_b $\dot{Q}nommin_{HPc} = \dot{Q}nommin_{HPh}$

HP_c $\dot{Q}nommax_{HPc} = \dot{Q}nommax_{HPh}$

HP_d1 $\dot{Q}h = \dot{Q}c + \dot{W}$

HP_d2 $\eta nom_{HPh} = \frac{\dot{Q}h}{\dot{W}} = \frac{\dot{Q}h}{\dot{Q}h - \dot{Q}c}$

HP_d3 $\eta nom_{HPc} = \frac{\dot{Q}h}{\dot{Q}c}$

HP_d $\eta nom_{HPc} = \frac{\eta nom_{HPh}}{\eta nom_{HPh} - 1}$

HP_e1 $\eta R_{HPc} = \frac{\eta R_{HPh}}{\eta R_{HPh} - 1} = \eta Rrel_{HPc} \cdot \eta nom_{HPc}$

HP_e $\eta Rrel_{HPc} = \frac{1}{\eta nom_{HPc}} \cdot \frac{\eta Rrel_{HPh} \cdot \eta nom_{HPh}}{\eta Rrel_{HPh} \cdot \eta nom_{HPh} - 1}$

HP1 $\boldsymbol{\dot{Q}nom_{HPc} = \dot{Q}nom_{HPh}}$

HP2 $\boldsymbol{\dot{Q}_{HPc,i} = \dot{Q}_{HPh,i}}$

HP3 $\boldsymbol{sel_{HPh} = sel_{HPc}}$

CN2 $\boldsymbol{\dot{Q}U_{HPc} = \sum_i \dot{Q}in_{HPc,i}}$

The electricity consumption $\dot{W}$ is included in the overall electricity balance of the system, while the thermal loads $\dot{Q}h$ and $\dot{Q}c$ are integrated into the system's heat cascade as respectively a hot and a cold stream. Equation CN1, developed in subsection 4.3.2, interprets the output load of a thermal utility as the heat load of a thermal stream in the heat cascade. In submodel HPc however, the thermal stream must be assigned to the input load. Therefore, CN1 is deactivated for this submodel and a new equation CN2 connects the input load to the heat cascade. Investment and operation and maintenance costs are only associated with submodel HPh.

4.3.4.3. Heat network

A heat network (Hnw) consists of a closed loop of heat transfer liquid. When flowing through the cold side of the loop, the fluid heats up by extracting heat $\dot{Q}c$ from the energy system. During the hot part of the loop, the fluid is cooled down by releasing the same amount of heat $\dot{Q}h$ back into the system. An electrical load $\dot{W}$ is required to overcome friction losses and circulate the fluid. Similar to the technology model for the heat pump, the heat network model consists of two interconnected thermal utility submodels $Hnwh$ and $Hnwc$, as shown in simplified form in Fig. 35.

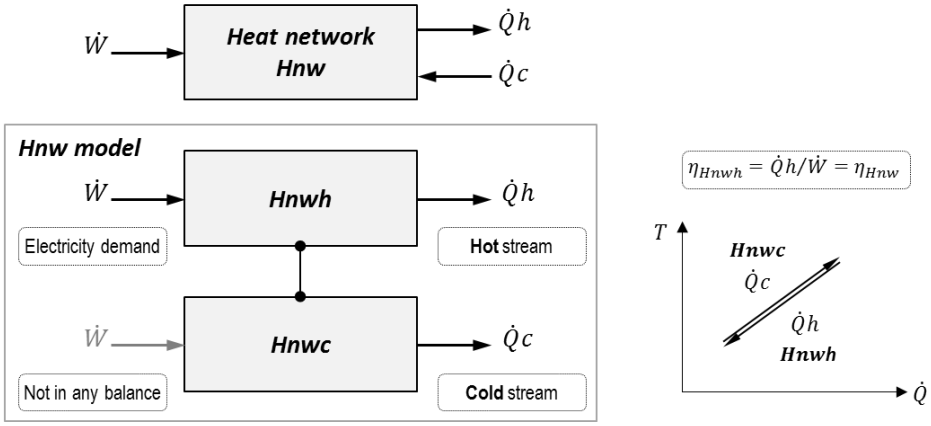

Fig. 35: Technology model for heat network

They are interconnected by equations completely analogous to expressions HP_a, HP_b, HP_c, HP1, HP2 and HP3 describing the heat pump model. However, unlike the heat pump, the relative efficiencies in the reference points of submodel $Hnwc$ and its nominal efficiency are identical to the corresponding values specified for submodel $Hnwh$ (equations Hnw_d and Hnw_e).

Hnw_d $\eta nom_{Hnwc} = \eta nom_{Hnwh}$

Hnw_e $\eta Rrel_{Hnwc} = \eta Rrel_{Hnwh}$

The electricity consumption $\dot{W}$ is included in the overall electricity balance of the system, while the thermal loads $\dot{Q}c$ and $\dot{Q}h$ are integrated into the system's heat cascade as respectively a hot and a cold stream. The efficiencies of both submodels are equivalent to the 'efficiency' of the heat network, expressing the ratio of transferred heat load over required pumping power. Investment and operation and maintenance costs are only associated with submodel $Hnwh$.

4.3.4.4. Heat engine

A heat engine (HE) extracts heat $\dot{Q}h$ from the energy system, produces electrical work $\dot{W}$, and delivers a smaller amount of heat $\dot{Q}c$ back to the system at a lower temperature level. Similar to the heat pump, the heat engine model is conceived of two interconnected thermal utility submodels HEh and HEc, as shown in simplified form in Fig. 36.

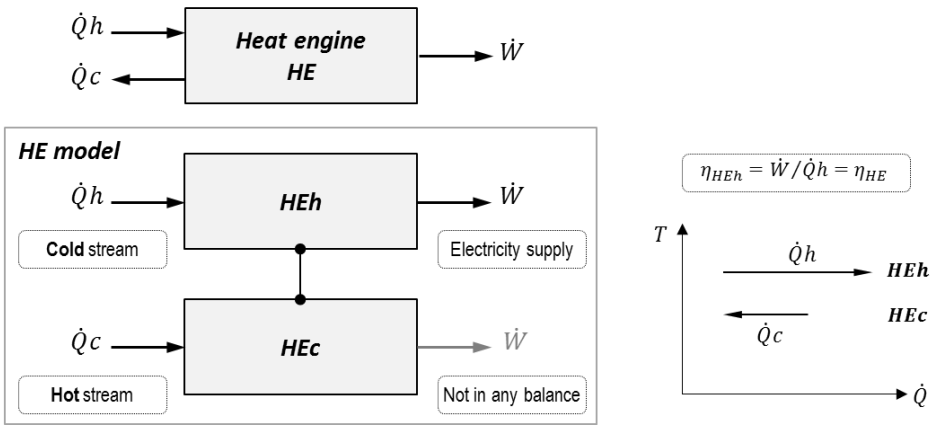

Fig. 36: Technology model for heat engine

Equations completely analogous to expressions HP_a, HP_b, HP_c, HP1, HP2 and HP3 for the heat pump model interconnect both submodels. However, equations HE_d and HE_e expressing the relative efficiencies in the reference points of submodel HEc and its nominal efficiency, as a function of the corresponding values specified for submodel HEh, differ from the heat pump model. Nonetheless, they are derived following similar intermediary steps as for the heat pump (HE_d1 - HE_d3 and HE_e1). The electricity production $\dot{W}$ is included as a supply to the overall electricity balance, while the thermal loads $\dot{Q}h$ and $\dot{Q}c$ are integrated into the heat cascade as respectively a cold and a hot stream. Since these thermal loads are inputs to the submodels and not outputs, the default equation CN1 (subsection 4.3.2) needs to be deactivated. Instead, equation CN2 for the heat pump is extended to additionally connect the input loads of submodels HEh and HEc to the heat cascade. The efficiency of submodel HEh is equivalent to the efficiency of the heat engine. Investment and operation and maintenance costs are only associated with submodel HEh.

HE_d1 $\dot{Q}h = \dot{Q}c + \dot{W}$

HE_d2 $\eta nom_{HEh} = \frac{\dot{W}}{\dot{Q}h} = \frac{\dot{W}}{\dot{Q}c + \dot{W}}$

HE_d3 $\eta nom_{HEc} = \frac{\dot{W}}{\dot{Q}c}$

HE_d $\eta nom_{HEc} = \frac{\eta nom_{HEh}}{1 - \eta nom_{HEh}}$

HE_e1 $\eta R_{HEc} = \frac{\eta R_{HEh}}{1 - \eta R_{HEh}} = \eta Rrel_{HEc} \cdot \eta nom_{HEc}$

HE_e $\eta Rrel_{HEc} = \frac{1}{\eta nom_{HEc}} \cdot \frac{\eta Rrel_{HEh} \cdot \eta nom_{HEh}}{1 - \eta Rrel_{HEh} \cdot \eta nom_{HEh}}$

CN2 $\boldsymbol{\dot{Q}U_{HEh}} = \sum_i \boldsymbol{\dot{Q}in}_{HEh,i}$

$\boldsymbol{\dot{Q}U_{HEc}} = \sum_i \boldsymbol{\dot{Q}in}_{HEc,i}$

4.3.4.5. Absorption chiller

An absorption chiller (AC) extracts heat $\dot{Q}c$ from the energy system by evaporation of its working fluid, lifts it to a higher temperature level by thermochemical compression, and releases an increased amount of heat $\dot{Q}h$ outside the system by condensation of the fluid. The thermochemical compression extracts heat $\dot{Q}h'$ from the energy system and releases a reduced amount of heat $\dot{Q}c'$ outside the system at a lower temperature (Fig. 37). In the absorber, the refrigerant is dissolved in cold water. Subsequently, the pressure of this strong solution is increased with a pump. In the generator, the solution is heated up to separate the refrigerant from the water.

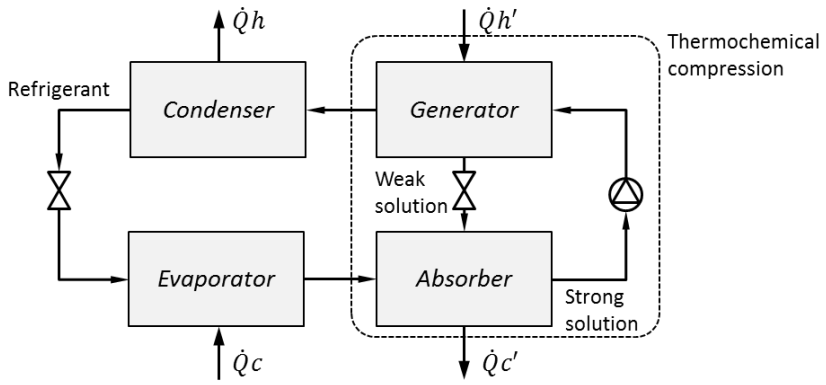

Fig. 37: Scheme absorption chiller

The absorption chiller model shown in Fig. 38 is similar to the heat network model, and is composed of analogous parameter equations and optimisation constraints. It is assumed that the condenser and the absorber release their heat loads $\dot{Q}h$ and $\dot{Q}c'$ to the environment, and therefore these heat loads are not included in the model. The electrical load for pumping is also not taken into account.

The parameter equations and constraints force the part-load curves, the output loads and the nominal loads of both submodels to be identical. As a consequence, the efficiency of either submodel is equivalent to the coefficient of performance of the absorption chiller. Both thermal loads $\dot{Q}h'$ and $\dot{Q}c$ are included in the heat cascade as cold streams. This implicates that equation CN2 is extended to include the absorption chiller submodel ACc. If the heat for thermochemical compression is not

extracted from the energy system, but resulting from fuel combustion, the AC can be modelled by the generic thermal utility model. Costs are associated with the submodel ACh.

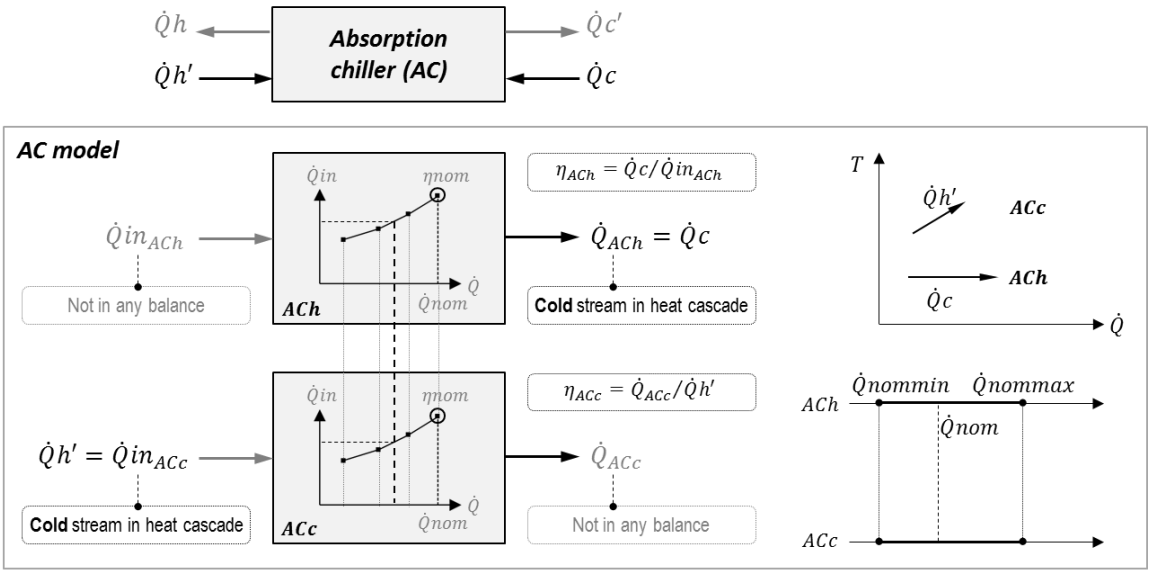

Fig. 38: Technology model for absorption chiller

4.3.4.6. Compression chiller, cooling water

A compression chiller (CC) extracts heat $\dot{Q}c$ from the energy system by evaporation of its working fluid, lifts it to a higher temperature level by compression, while using an electrical load $\dot{W}$, and releases an increased amount of heat outside the system by condensation of the fluid. The compression chiller can be modelled using the generic thermal utility model, as shown in Fig. 39. The electricity use $\dot{W}$ is included in the overall electricity balance of the system, thermal load $\dot{Q}c$ is integrated into the system's heat cascade as a cold stream.

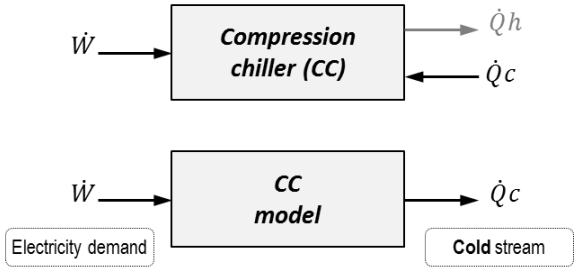

Fig. 39: Technology model for compression chiller

A cooling water loop (CW) extracts a heat load $\dot{Q}c$ from the energy system and releases it outside the system. To pump around the water, a an electrical load $\dot{W}$ is required. The technology model is identical to that of the compression chiller (see Fig. 39), but appropriate values for efficiency need to be specified.

4.3.4.7. Non-dispatchable utilities

The operation of energy technologies such as wind turbines and photovoltaic or thermal solar panels depends on the availability of their energy source, which cannot be controlled. These technologies are modelled by extending the generic utility formulation with an additional equation (NDPU or NDPE) that fixes the output load in each time slice S to a predefined fraction fEa_S of a prescribed annual output per capacity unit $Ea1$. Note that $Ea1$ cannot exceed the number of hours in the year hrs_y multiplied by 1 kW and that the summation of the fractions fEa_S over all time slices S must equal 1.

NDPU $\quad \forall S: \sum_i \boldsymbol{\dot{Q}}_{S,i} = \left(fEa_S \cdot Ea1 \cdot \dot{Q}nom\right)/hrs\_S_S$

NDPE $\quad \forall S: \sum_i \boldsymbol{P\_el}_{S,i} = (fEa\_el_S \cdot Ea1\_el \cdot Pnom)/hrs\_S_S$

4.3.4.8. Summary of specific technology models

The integration of the default generic model as well as of the specific technology models into the thermal and electrical energy balances is given in

Table 6, together with the related cost components. The second column indicates whether the utility input load, the output load or both loads are integrated into the system's heat cascade. The third column shows the integration of the input or output load as either demand or supply in the system's electrical energy balance. The final column assigns cost types to the utilities.

Utility	*Thermal energy balances*	*Electrical energy balance*		*Costs*
$DefaultU$	$\dot{Q}$	-		fuel, O&M, Inv
$DefaultE$		P_el	supply	fuel, O&M, Inv
$CHPth$	$\dot{Q}$	-		fuel, O&M, Inv
$CHPel$		P_el	supply	
HPh	$\dot{Q}$	$\dot{Q}in$	demand	O&M, Inv
HPc	$\dot{Q}in$	-		
$Hnwh$	$\dot{Q}$	$\dot{Q}in$	demand	O&M, Inv
$Hnwc$	$\dot{Q}$	-		
HEh	$\dot{Q}in$	$\dot{Q}$	supply	O&M, Inv
HEc	$\dot{Q}in$	-		
CC	$\dot{Q}$	$\dot{Q}in$	demand	O&M, Inv
AC	$\dot{Q}$ and $\dot{Q}in$	-		fuel, O&M, Inv
CW	$\dot{Q}$	$\dot{Q}in$	demand	O&M, Inv

Table 6: integration of technology models into the thermal and electrical energy balances of the heat cascade model

4.3.5. Formulation of technology models

In this subsection, the equations for part-load operation and investment costs constituting the technology models are formulated in full form and the necessary parameters and variables are defined. Equations are derived for thermal utilities (U) in Subsections 4.3.2 and 4.3.3, but are analogous for electrical utilities. Since the operation of technologies must be optimised in every time slice, a number of variables and equations are indexed with time slice S. Another index (Ins) is added to indicate the different technology units (utility instances) that may be installed in the system configuration when the superstructure is gradually expanded as described in section 4.5.

4.3.5.1. Sets and parameters

Sets

Notation: $El_1: first\ set\ element\ of\ uploaded\ set$
$El_f: final\ set\ element\ of\ uploaded\ set$

S	$= S_1..S_f$	time slices
U	$= U_1..U_f$	thermal utilities
E	$= E_1..E_f$	electrical utilities
R	$= R_1..R_f$	reference points part-load operation
Rc	$= Rc_1..Rc_f$	reference points specific investment costs
Ins	$= Ins_1..Ins_{100}$	instances (of utilities)

Subsets

$L(R)$	$= R_1..R_{f-1}$	lines between reference points part-load operation
$Lc(Rc)$	$= Rc_1..Rc_{f-1}$	lines between reference points specific investment costs
$DefaultU(U)$	$= U\|TypeU_U = 0$	default thermal utilities (e.g. gas-fired boiler)
$DefaultE(E)$	$= E\|TypeE_E = 0$	default electrical utilities (e.g. diesel generator)
$CHPth(U)$	$= U\|TypeU_U = 1$	thermal submodels CHPs
$CHPel(E)$	$= E\|TypeE_E = 1$	electrical submodels CHPs
$CC(U)$	$= U\|TypeU_U = 2$	compression chillers
$HPh(U)$	$= U\|TypeU_U = 3$	submodels heat pumps
$HPc(U)$	$= U\|TypeU_U = 4$	submodels heat pumps
$Hnwh(U)$	$= U\|TypeU_U = 5$	submodels heat networks
$Hnwc(U)$	$= U\|TypeU_U = 6$	submodels heat networks
$HEh(U)$	$= U\|TypeU_U = 8$	submodels heat engines
$HEc(U)$	$= U\|TypeU_U = 9$	submodels heat engines
$ACh(U)$	$= U\|TypeU_U = 10$	submodels absorption chillers
$ACc(U)$	$= U\|TypeU_U = 11$	submodels absorption chillers
$CW(U)$	$= U\|TypeU_U = 12$	cooling water loops
$ndU(U)$	$= U\|TypeU_U = 7$	non-dispatchable thermal utilities (sun)
$ndE(E)$	$= E\|TypeE_E = 7$	non-dispatchable electrical utilities (sun, wind)

Parameters

Time

hrs_S_S	number of hours in time slice S

Thermal utilities

$TypeU_U$	type of thermal utility
$\dot{Q}Rrel_{U,R}$	relative thermal load utility U at reference point R
$\eta Rrel_{U,R}$	relative efficiency (or COP) utility U at reference point R
ηnom_U	nominal efficiency (or COP) utility U
$\dot{Q}nommin_U$	minimal nominal thermal load utility U (kW)
$\dot{Q}nommax_U$	maximal nominal thermal load utility U (kW)
$\alpha_{U,R}$	normalised energy input utility U at reference point R
$\beta_{U,R}$	inclination thermal part-load curve utility U between reference points R and R+1
iU_U	number of instances of utility U

$\dot{Q}nomRrel_{U,Rc}$	relative thermal nominal load utility U at reference point Rc
$cIR_{U,Rc}$	specific investment cost utility U at reference point Rc (€/kW)
$der_{U,Rc}$	derivative investment cost curve utility U at reference point Rc
Electrical utilities	
$TypeE_E$	type of electrical utility
$PRrel_{E,R}$	relative electrical load utility E at reference point R
$\eta Rrel\_el_{E,R}$	relative electrical efficiency utility E at reference point R
ηnom_el_E	nominal electrical efficiency of utility E
$Pnommin_E$	minimal nominal electrical load utility E (kW)
$Pnommax_E$	maximal nominal electrical load utility E (kW)
$\alpha el_{E,R}$	normalised energy input utility E at at reference point R
$\beta el_{E,R}$	inclination electrical part-load curve utility E between reference points R and R+1
iE_E	number of instances of utility E
$PnomRrel_{E,Rc}$	relative electrical nominal load utility E at reference point Rc
$cIR\_el_{E,Rc}$	specific investment cost utility E at reference point Rc (€/kW)
$der\_el_{E,Rc}$	derivative investment cost curve utility E at reference point Rc (€/kW)

4.3.5.2. Variables

Thermal utilities: Part-load operation and selection

$\boldsymbol{\dot{Q}in}_{U,Ins,S,R}$	$\mathbb{R}^+$	energy supplied to utility U, instance Ins, in line segment L in time slice S (kW)
$\boldsymbol{\dot{Q}}_{U,Ins,S,R}$	$\mathbb{R}^+$	thermal load of utility U, instance Ins, in line segment L in time slice S (kW)
$\boldsymbol{\dot{Q}nom}_{U,Ins}$	$\mathbb{R}^+$	nominal thermal load of utility U, instance Ins (kW)
$\boldsymbol{\chi}_{U,Ins,S,R}$	$\mathbb{R}^+$	nominal power of utility U, instance Ins, in line segment L in time slice S
$\boldsymbol{sel}_{U,Ins}$	$\{0,1\}$	indicates whether utility U, instance Ins, is selected in the configuration
$\boldsymbol{\delta}_{U,Ins,S,R}$	$\{0,1\}$	indicates whether utility U, instance Ins, is operated in line segment L in time slice S

Electrical utilities: Part-load operation and selection

$\boldsymbol{\dot{Q}in\_el}_{E,Ins,S,R}$	$\mathbb{R}^+$	energy supplied to utility E, instance Ins, in line segment L in time slice S (kW)
$\boldsymbol{P\_el}_{E,Ins,S,R}$	$\mathbb{R}^+$	electrical load of utility E, instance Ins, in line segment L in time slice S (kW)
$\boldsymbol{Pnom}_{E,Ins}$	$\mathbb{R}^+$	nominal electrical load of utility E, instance Ins (kW)
$\boldsymbol{\chi el}_{E,Ins,S,R}$	$\mathbb{R}^+$	nominal power of utility E, instance Ins, in line segment L in time slice S
$\boldsymbol{sel\_el}_{E,Ins}$	$\{0,1\}$	indicates whether utility E, instance Ins, is selected in the configuration
$\boldsymbol{\delta el}_{E,Ins,S,R}$	$\{0,1\}$	indicates whether utility E, instance Ins, is operated in line segment L in time slice S

Thermal utilities: Size-dependent specific investment costs

$\boldsymbol{Inv}_{U,Ins,Rc}$	$\mathbb{R}^+$	investment costs utility U, instance Ins, in line segment Lc (€)
$\boldsymbol{\delta c}_{U,Ins,Rc}$	$\mathbb{R}^+$	]
$\boldsymbol{\dot{Q}nomL}_{U,Ins,Rc}$	$\mathbb{R}^+$	nominal thermal load utility U, instance Ins, line segment Lc (kW)

Electrical utilities: Size-dependent specific investment costs

$\boldsymbol{Inv\_el}_{E,Ins,Rc}$	$\mathbb{R}^+$	investment costs utility E, instance Ins, in line segment Lc (€)
$\boldsymbol{\delta c_{el}}_{E,Ins,Rc}$	$\mathbb{R}^+$	
$\boldsymbol{PnomL}_{E,Ins,Rc}$	$\mathbb{R}^+$	nominal electrical load utility E, instance Ins, line segment Lc (kW)

4.3.5.3. Equations

Parameter equations

Thermal utilities: Part-load operation and selection

UP1 $\quad \forall\, U, R|L(R): \alpha_{U,R} = \dfrac{\dot{Q}Rrel_{U,R}}{\eta Rrel_{U,R} \cdot \eta nom_U}$

UP2 $\quad \forall\, U, R|L(R):$

$$\beta_{U,R} = \left(\frac{\dot{Q}Rrel_{U,R+1}}{\eta Rrel_{U,R+1}} - \frac{\dot{Q}Rrel_{U,R}}{\eta Rrel_{U,R}}\right) \Big/ \left(\dot{Q}Rrel_{U,R+1} - \dot{Q}Rrel_{U,R}\right) \cdot \frac{1}{\eta nom_U}$$

EP1 $\forall\ E,R|L(R)\colon \alpha el_{E,R} = \dfrac{\dot{P}Rrel_{E,R}}{\eta Rrel\_el_{E,R}\ \cdot\ \eta nom\_el_{E}}$

EP2 $\forall\ E,R|L(R)\colon$

$$\beta el_{E,R} = \left(\frac{\dot{P}Rrel_{E,R+1}}{\eta Rrel\_el_{E,R+1}} - \frac{\dot{P}Rrel_{E,R}}{\eta Rrel\_el_{E,R}}\right) \Big/ \left(\dot{P}Rrel_{E,R+1} - \dot{P}Rrel_{E,R}\right) \cdot \frac{1}{\eta nom\_el_{E}}$$

Thermal utilities: Size-dependent specific investment costs

CUP1 $\forall\ U,Rc|Lc(Rc)\colon$

$$der_{U,Rc} = \frac{cIR_{U,Rc+1} \cdot \dot{Q}nomRrel_{U,Rc+1} - cIR_{U,Rc} \cdot \dot{Q}nomRrel_{U,Rc}}{\dot{Q}nomRrel_{U,Rc+1} - \dot{Q}nomRrel_{U,Rc}}$$

Electrical utilities: Size-dependent specific investment costs

CEP1 $\forall\ E,Rc|Lc(Rc)\colon$

$$der\_el_{E,Rc} = \frac{cIR\_el_{E,Rc+1} \cdot PnomRrel_{E,Rc+1} - cIR\_el_{E,Rc} \cdot PnomRrel_{E,Rc}}{PnomRrel_{E,Rc+1} - PnomRrel_{E,Rc}}$$

Technology-specific parameter equations

CHP

For CHP_a-CHP_b: $CHPth.pos = CHPel.pos$

CHP_a $\forall\ CHPth, CHPel\colon \quad Pnommax_{CHPel} = \frac{\eta nom\_el_{CHPel}}{\eta nom_{CHPth}} \cdot \dot{Q}nommax_{CHPth}$

CHP_b $\forall\ CHPth, CHPel\colon \quad Pnommin_{CHPel} = \frac{\eta nom\_el_{CHPel}}{\eta nom_{CHPth}} \cdot \dot{Q}nommin_{CHPth}$

CHP_c $\forall\ CHPth, CHPel, R = R_1\colon \eta Rrel\_el_{CHPel,R} = \eta Rrel_{CHPth,R} \cdot \frac{PRrel_{CHPel,R}}{\dot{Q}Rrel_{CHPth,R}}$

HP

For HP_a-HP_e: $HPc.pos = HPh.pos$

Hp_a $\forall\ HPc, HPh, R\colon \quad \dot{Q}Rrel_{HPc,R} = \dot{Q}Rrel_{HPh,R}$

HP_b $\forall\ HPc, HPh\colon \quad \dot{Q}nommin_{HPc} = \dot{Q}nommin_{HPh}$

HP_c $\forall\ HPc, HPh\colon \quad \dot{Q}nommax_{HPc} = \dot{Q}nommax_{HPh}$

HP_d $\forall\ HPc, HPh\colon \quad \eta nom_{HPc} = \frac{\eta nom_{HPh}}{\eta nom_{HPh}-1}$

HP_e $\forall\ HPc, HPh, R\colon \quad \eta Rrel_{HPc,R} = \frac{1}{\eta nom_{HPc}} \cdot \frac{\eta Rrel_{HPh,R} \cdot \eta nom_{HPh}}{\eta Rrel_{HPh,R} \cdot \eta nom_{HPh}-1}$

Hnw

For HNW_a-HNW_c: $Hnwc.pos = Hnwh.pos$

HNW_a $\forall\ Hnwc, Hnwh, R\colon \quad \dot{Q}Rrel_{Hnwc,R} = \dot{Q}Rrel_{Hnwh,R}$

HNW_b $\forall\ Hnwc, Hnwh\colon \quad \dot{Q}nommin_{Hnwc} = \dot{Q}nommin_{Hnwh}$

HNW_c $\forall\ Hnwc, Hnwh\colon \quad \dot{Q}nommax_{Hnwc} = \dot{Q}nommax_{Hnwh}$

HNW_d $\forall\ Hnwc, Hnwh\colon \quad \eta nom_{Hnwc} = \eta nom_{Hnwh}$

HNW_e $\forall\ Hnwc, Hnwh, R\colon \quad \eta Rrel_{Hnwc,R} = \eta Rrel_{Hnwh,R}$

HE

For HE_a-HE_e: $HEc.pos = HEh.pos$

HE_a $\forall\ HEc, HEh, R\colon \quad \dot{Q}Rrel_{HEc,R} = \dot{Q}Rrel_{HEh,R}$

HE_b $\forall\ HEc, HEh$: $\dot{Q}nommin_{HEc} = \dot{Q}nommin_{HEh}$

HE_c $\forall\ HEc, HEh$: $\dot{Q}nommax_{HEc} = \dot{Q}nommax_{HEh}$

HE_d $\forall\ HEc, HEh$: $\eta nom_{HEc} = \frac{\eta nom_{HEh}}{1-\eta nom_{HEh}}$

HE_e $\forall\ HEc, HEh, R$: $\eta Rrel_{HEc,R} = \frac{1}{\eta nom_{HEc}} \cdot \frac{\eta Rrel_{HEh,R} \cdot \eta nom_{HEh}}{1-\eta Rrel_{HEh,R} \cdot \eta nom_{HEh}}$

AC: *parameter equations analogous to Hnw*

Constraints

Thermal utilities: Part-load operation and selection

For U1-U8: $R|L(R), Ins.ord \leq iU(U)$

U1 $\forall\ U, Ins, S, R$: $\boldsymbol{\dot{Q}in}_{U,Ins,S,R} = \alpha_{U,R} \cdot \boldsymbol{\chi}_{U,Ins,S,R} + \beta_{U,R} \cdot \boldsymbol{\dot{Q}}_{U,Ins,S,R} - \beta_{U,R} \cdot \dot{Q}Rrel_{U,R} \cdot \boldsymbol{\chi}_{U,Ins,S,R}$

U2 $\forall\ U, Ins, S, R$: $\boldsymbol{\dot{Q}}_{U,Ins,S,R} \geq \dot{Q}Rrel_{U,R} \cdot \boldsymbol{\chi}_{U,Ins,S,R}$

U3 $\forall\ U, Ins, S, R$: $\boldsymbol{\dot{Q}}_{U,Ins,S,R} \leq \dot{Q}Rrel_{U,R+1} \cdot \boldsymbol{\chi}_{U,Ins,S,R}$

U4 $\forall\ U, Ins, S$: $\sum_R \boldsymbol{\delta}_{U,Ins,S,R} \leq \boldsymbol{sel}_{U,Ins}$

U5 $\forall\ U, Ins, S, R$: $\boldsymbol{\chi}_{U,Ins,S,R} \leq \boldsymbol{\delta}_{U,Ins,S,R} \cdot \dot{Q}nommax_U$

U6 $\forall\ U, Ins, S, R$: $\boldsymbol{\chi}_{U,Ins,S,R} \geq \boldsymbol{\delta}_{U,Ins,S,R} \cdot \dot{Q}nommin_U$

U7 $\forall\ U, Ins, S, R$: $\boldsymbol{\chi}_{U,Ins,S,R} \leq \boldsymbol{\dot{Q}nom}_{U,Ins}$

U8 $\forall\ U, Ins, S, R$: $\boldsymbol{\chi}_{U,Ins,S,R} \geq \left(\boldsymbol{\delta}_{U,Ins,S,R} - 1\right) \cdot \dot{Q}nommax_U + \boldsymbol{\dot{Q}nom}_{U,Ins}$

Connection part-load and heat cascades

For CN1,CN2: $Ins.ord \leq iU(U)$

CN1 $\forall\ U \notin \{Hpc, HEh, HEc, ACc\}, Ins, S$: $\boldsymbol{\dot{Q}U}_{U,Ins,S} = \sum_L \boldsymbol{\dot{Q}}_{U,Ins,S,L}$

CN2 $\forall\ U \in \{Hpc, HEh, HEc, ACc\}, Ins, S$: $\boldsymbol{\dot{Q}U}_{U,Ins,S} = \sum_L \boldsymbol{\dot{Q}in}_{U,Ins,S,L}$

Electrical utilities: Part-load operation and selection

For E1-E8: $R|L(R), Ins.ord \leq iE(E)$

E1 $\forall\ E, Ins, S, R$:

$\boldsymbol{\dot{Q}in\_el}_{E,Ins,S,R} = \alpha el_{E,R} \cdot \boldsymbol{\chi el}_{E,Ins,S,R} + \beta el_{E,R} \cdot \boldsymbol{P\_el}_{E,Ins,S,R} - \beta el_{E,R} \cdot PRrel_{E,R} \cdot \boldsymbol{\chi el}_{E,Ins,S,R}$

E2 $\forall\ E, Ins, S, R$: $\boldsymbol{P\_el}_{E,Ins,S,R} \geq PRrel_{E,R} \cdot \boldsymbol{\chi el}_{E,Ins,S,R}$

E3 $\forall\ E, Ins, S, R$: $\boldsymbol{P\_el}_{E,Ins,S,R} \leq PRrel_{E,R+1} \cdot \boldsymbol{\chi el}_{E,Ins,S,R}$

E4 $\forall\ E, Ins, S$: $\sum_R \boldsymbol{\delta el}_{E,Ins,S,R} \leq \boldsymbol{sel\_el}_{E,Ins}$

E5 $\forall\ E, Ins, S, R$: $\boldsymbol{\chi el}_{E,Ins,S,R} \leq \boldsymbol{\delta el}_{E,Ins,S,R} \cdot Pnommax_E$

E6 $\forall\ E, Ins, S, R$: $\boldsymbol{\chi el}_{E,Ins,S,R} \geq \boldsymbol{\delta el}_{E,Ins,S,R} \cdot Pnommin_E$

E7 $\forall\ E, Ins, S, R$: $\boldsymbol{\chi el}_{E,Ins,S,R} \leq \boldsymbol{Pnom}_{E,Ins}$

E8 $\forall\ E, Ins, S, R$: $\boldsymbol{\chi el}_{E,Ins,S,R} \geq \left(\boldsymbol{\delta el}_{E,Ins,S,R} - 1\right) \cdot Pnommax_E + \boldsymbol{Pnom}_{E,Ins}$

Thermal utilities: Size-dependent specific investment costs

For CU1-CU5: $Rc|Lc(Rc), Ins.ord \leq iU(U)$

CU1 $\forall\, U, Ins, Rc$:

$$\boldsymbol{Inv}_{U,Ins,Rc} = cIR_{U,Rc} \cdot \dot{Q}nomRrel_{U,Rc} \cdot \dot{Q}nommax_{U} \cdot \boldsymbol{\delta c}_{U,Ins,Rc} + der_{U,Rc} \cdot \boldsymbol{\dot{Q}nomL}_{U,Ins,Rc} - der_{U,Rc} \cdot \dot{Q}nomRrel_{U,Rc} \cdot \dot{Q}nommax_{U} \cdot \boldsymbol{\delta c}_{U,Ins,Rc}$$

CU2 $\forall\, U, Ins, Rc$: $\boldsymbol{\dot{Q}nomL}_{U,Ins,Rc} \geq \boldsymbol{\delta c}_{U,Ins,Rc} \cdot \dot{Q}nomRrel_{U,Rc} \cdot \dot{Q}nommax_{U}$

CU3 $\forall\, U, Ins, Rc$: $\boldsymbol{\dot{Q}nomL}_{U,Ins,Rc} \leq \boldsymbol{\delta c}_{U,Ins,Rc} \cdot \dot{Q}nomRrel_{U,Rc+1} \cdot \dot{Q}nommax_{U}$

CU4 $\forall\, U, Ins$: $\sum_{Rc} \boldsymbol{\delta c}_{U,Ins,Rc} = \boldsymbol{sel}_{U,Ins}$

CU5 $\forall\, U, Ins$: $\boldsymbol{\dot{Q}nom}_{U,Ins} = \sum_{Rc} \boldsymbol{\dot{Q}nomL}_{U,Ins,Rc}$

Electrical utilities: Size-dependent specific investment costs

For CE1-CE5: $Rc|Lc(Rc), Ins \leq iE(E)$

CE1 $\forall\, E, Ins, Rc$:

$$\boldsymbol{Inv\_el}_{E,Ins,Rc} = cIR_{el_{E,Rc}} \cdot PnomRrel_{E,Rc} \cdot Pnommax_{E} \cdot \boldsymbol{\delta c\_el}_{E,Ins,Rc} + der\_el_{E,Rc} \cdot \boldsymbol{PnomL}_{E,Ins,Rc} - der\_el_{E,Rc} \cdot PnomRrel_{E,Rc} \cdot Pnommax_{E} \cdot \boldsymbol{\delta c\_el}_{E,Ins,Rc}$$

CE2 $\forall\, E, Ins, Rc$: $\boldsymbol{PnomL}_{P,Ins,Rc} \geq \boldsymbol{\delta c\_el}_{E,Ins,Rc} \cdot PnomRrel_{E,Rc} \cdot Pnommax_{E}$

CE3 $\forall\, E, Ins, Rc$: $\boldsymbol{PnomL}_{E,Ins,Rc} \leq \boldsymbol{\delta c\_el}_{E,Ins,Rc} \cdot PnomRrel_{E,Rc+1} \cdot Pnommax_{E}$

CE4 $\forall\, E, Ins$: $\sum_{Rc} \boldsymbol{\delta c\_el}_{E,Ins,Rc} = \boldsymbol{sel\_el}_{E,Ins}$

CE5 $\forall\, E, Ins$: $\boldsymbol{Pnom}_{E,Ins} = \sum_{Rc} \boldsymbol{PnomL}_{E,Ins,Rc}$

Technology-specific equations

CHP

For CHP1-CHP2: $Ins \leq Ins.ord \leq iU(CHPth), CHPth.pos = CHPel.pos$

CHP1 $\forall\, CHPth, CHPel, Ins$: $\boldsymbol{Pnom}_{CHPel,Ins} = \frac{\eta nom\_el_{CHPel}}{\eta nom_{CHPth}} \cdot \boldsymbol{\dot{Q}nom}_{CHPth,Ins}$

CHP2 $\forall\, CHPth, CHPel, Ins, S$: $\sum_{L} \boldsymbol{\dot{Q}in}_{CHPth,Ins,S,L} = \sum_{L} \boldsymbol{\dot{Q}in\_el}_{CHPel,Ins,S,L}$

CHP3 $\forall\, CHPth, CHPel, Ins$: $\boldsymbol{sel}_{CHPth,Ins} = \boldsymbol{sel\_el}_{CHPel,Ins}$

HP

For HP1-HP3: $Ins \leq Ins.ord \leq iU(HPh), HPc.pos = HPh.pos$

HP1 $\forall\, HPc, HPh, Ins$: $\boldsymbol{\dot{Q}nom}_{HPc,Ins} = \boldsymbol{\dot{Q}nom}_{HPh,Ins}$

HP2 $\forall\, HPc, HPh, Ins, S, L$: $\boldsymbol{\dot{Q}}_{HPc,Ins,S,L} = \boldsymbol{\dot{Q}}_{HPh,Ins,S,L}$

HP3 $\forall\, HPc, HPh, Ins$: $\boldsymbol{sel}_{HPc,Ins} = \boldsymbol{sel}_{HPh,Ins}$

Hnw, HE, AC*: analogous to HP*

Non-dispatchable technologies

NDPU $\forall\, U, Ins, S|ndU(U), Ins.ord \leq iU(U)$: $\sum_{L} \dot{Q}_{U,Ins,S,L} = \frac{fEa_{U,S} \cdot Ea1_{U} \cdot \dot{Q}nom_{U,Ins}}{hrs\_S_{S}}$

NDPE $\forall\, E, Ins, S|ndE(E), Ins.ord \leq iE(E)$: $\sum_{L} P_{E,Ins,S,L} = \frac{fEa\_el_{E,S} \cdot Ea1\_el_{E} \cdot Pnom_{E,Ins}}{hrs\_S_{S}}$

4.4. Energy integration

The energy consumption of a process, company, business park or district can be significantly reduced by applying energy integration techniques in the design or retrofit phase. In a broad sense, energy integration aims at maximum heat recovery between process streams and optimal integration of energy technologies to fulfil remaining energy demands. In this section, a model formulation for energy integration is gradually developed, starting from existing mathematical programming methods for minimum utility cost targeting in Pinch Technology.

Pinch Technology is a well-known methodology for energy integration in industrial processes. The first subsection gives a brief overview of the sequential steps in Pinch Technology and highlights key concepts. In the two following subsections, the heat cascade model is described, which enables mathematical application of the analysis steps within Pinch Technology, also referred to as Pinch Analysis. The basic version of the heat cascade model assumes that all streams are available for direct counter-current heat exchange, whereas a more elaborated version is able to take into account restrictions for heat exchange between certain streams. This extended heat cascade model forms the core of *Syn-E-Sys*. Next, the construction of an envelope curve for heat transfer units and the corresponding model formulation are described. The final subsection deals with a shortcoming of the extended heat cascade model, referred to as phantom heat.

4.4.1. Pinch Technology

This subsection provides a brief overview of Pinch Technology, derived from a more elaborated introduction presented by Linhoff [18]. Naming of parameters, variables and equations correspond to the terminology used in the formulation of *Syn-E-Sys*.

Thermal processes in industrial companies can be considered as mass flows with constant heat capacities that either need to be heated up (cold streams) or cooled down (hot streams) from a source to a target temperature by absorbing or releasing heat. Besides industrial processes, also energy services, such as space cooling, space heating or hot sanitary water can be conceived as hot or cold process streams. Significant reductions in cooling and heating demands can be achieved by recovering excess heat from hot streams and using it to heat up cold streams. Pinch Technology provides a practical tool to assess the energy saving potential thereof.

In Pinch Technology, heating and cooling demands are minimised by maximising counter-current heat exchange between process streams. Next, thermal energy conversion technologies (utilities) are optimally integrated to fulfil the remaining demands at minimum costs. Finally, the heat exchanger network, enabling all required heat exchanges, is designed. Moreover, Pinch Technology facilitates the detection of modifications to process operation conditions that can reduce energy demands even further. The method comprises different steps, which are described in following subsections and illustrated by means of a simple example taken from CANMET [101]. Note that the steps prior to the heat exchanger network design are referred to as Pinch Analysis.

4.4.1.1. Minimum hot and cold utility targets

This subsection describes the steps in Pinch technology for calculation of the minimum hot and cold utility requirements. Firstly, thermodynamic calculation of the entire process is performed (heat and mass balance) and for all streams the heating or cooling loads in function of temperature are extracted. The source and target temperatures, thermal loads and heat capacity rates (TsP, TtP, QP and $mcpP$) of the process streams (P) in the guiding example are listed in Table 7 and graphically presented in Fig. 40, step 1. Next, the heat-temperature profiles of all hot and all cold process streams are combined to form respectively the Hot Composite Curve (HCC) and the Cold Composite Curve (CCC), as shown in Fig. 40, step 2. In each temperature interval, the heat capacity rate of the HCC (CCC) is obtained by adding up the ones of the hot (cold) streams present in that interval.

In a following step, the Hot and Cold Composite Curves are shifted towards each other along the heat axis until a fixed minimum temperature difference ΔT_{min} is reached, as depicted in Fig. 40, step 3. In this way, sufficient driving force for counter-current heat exchange is ensured. The point of closest approach is referred to as the pinch point or pinch. On the heat axis, the overlap between HCC and CCC indicates the maximum heat exchange $\dot{Q}exmax$ that can be attained, while the residual heat loads indicate the minimum hot and cold utility requirements $\dot{Q}hmin$ and $\dot{Q}cmin$. The pinch point divides the entire process in two distinct parts. Above the pinch, the process acts as a heat sink that requires external heating, while beneath the pinch it behaves as a heat source that needs to be cooled. Minimum energy requirement targets can only be achieved if no heat is transferred downwards across the pinch and if no cold utilities above nor hot utilities below the pinch are used. Assuming a ΔT_{min} of 10 °C, 4850 kW of heat can be exchanged between the HCC and the CCC of the example process, resulting in a minimum hot and cold utility of 900 kW and 750 kW respectively. This implicates a reduction of 4850 kW on the initial heating and cooling demands of 5750 kW and 5600 kW.

In a next step, the Grand Composite Curve (GCC) is constructed by shifting the Cold and Hot Composite Curves towards each other along the temperature axis over a distance $\Delta T_{min}/2$ and plotting the heat load difference α between those curves, as shown in Fig. 40, step 4. The temperature shift fixes a temperature difference of ΔT_{min} between the hot and cold stream segments in each interval of the shifted temperature range. The GCC graphically represents how much external heating (cooling) is needed in the temperature range between a certain temperature level above (below) the pinch and the pinch temperature. In other words, the GCC shows how the heating (cooling) requirements are accumulated over the shifted temperature range upwards (downwards) form the pinch point. Using the Problem Table algorithm, the GCC be calculated algebraically [102].

Process stream	**Stream type**	**TsP** °C	**TtP** °C	**QP** kW	**mcpP** kW/°C
h1	hot	200	100	2000	20
h2	hot	150	60	3600	40
c1	cold	80	120	3200	80
c2	cold	50	220	2550	15

Table 7: Process data of the guiding example [101]

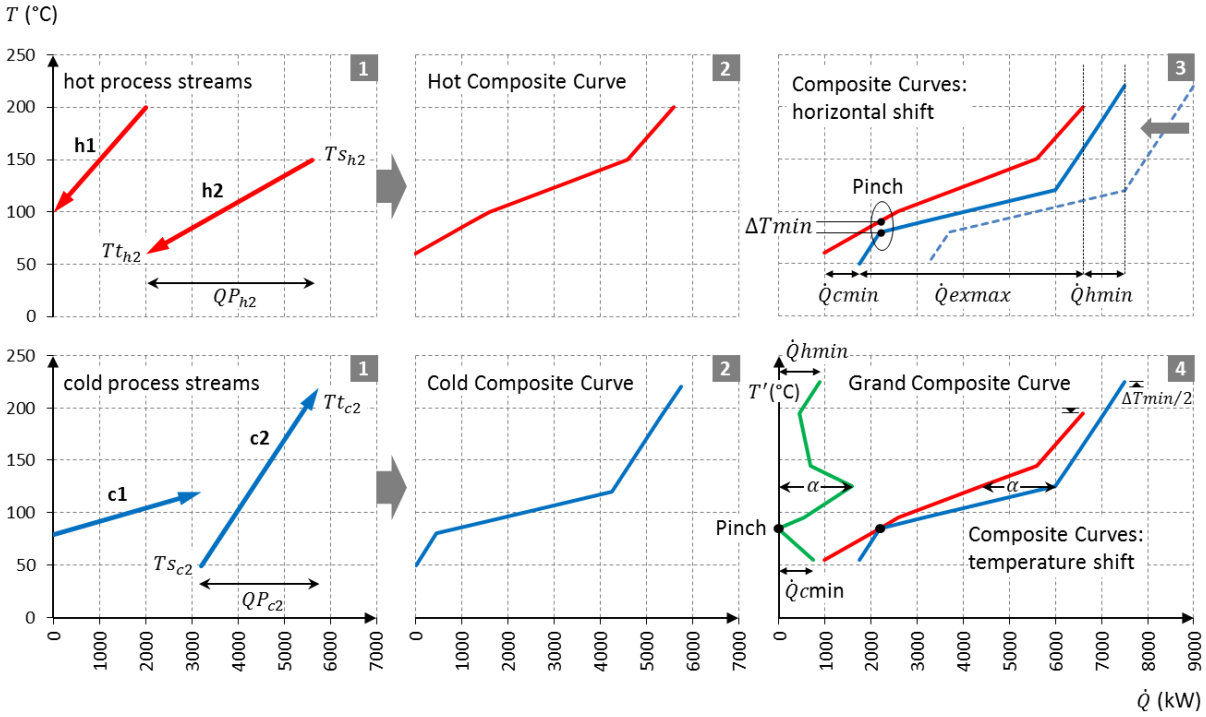

Fig. 40: Steps in Pinch Analysis for the guiding example: from thermal stream data to GCC

In some cases, a more slender shape of the Grand Composite Curve can be obtained by shifting hot streams from below to above the pinch and cold streams from above to below the pinch (the plus-minus principle), which may result in a reduction of minimum hot and cold utilities. This involves modifying the operation conditions (pressure or temperature) of some process streams.

4.4.1.2. Utility integration

Multiple hot and cold utilities (U) can be employed to fulfil the process's minimum energy requirements, such as steam at different temperature and pressure levels, furnace flue gas, hot oil, cooling water, refrigeration, etc. Selection and integration of utilities can be easily optimised starting from the GCC. Similar to process streams, utility streams are integrated with their shifted heat-temperature profiles. To achieve minimum energy costs, cheapest utilities are selected first and their flow rates are increased until utility pinch points are activated, as highlighted in Fig. 41, step 5. Such a pinch point occurs when a utility's heat-temperature profile touches the GCC (disregarding the pockets in the GCC). The utilities available in the guiding example are defined in Table 8. Low pressure steam (LP) is integrated prior to high pressure steam (HP), both with a heat load of 450 kW to fulfil the minimum hot utility requirement of 900 kW. Cooling water (CW) fulfils the complete cooling demand of 750 kW. The minimum total operation cost amounts 354780 €/year. Results are shown in Table 8 and in Fig. 41, step 5. If flue gasses of a furnace (FG) are added as third hot utility, it is selected instead of HPS due to the lower energy costs (see Fig. 42, step 5 and Table 9).

When minimum loss of thermodynamic quality is aimed at, hot and cold utilities are selected and integrated in such a way that their temperature-heat profiles approach the GCC as close as possible. This can be achieved by consecutively maximising the heat provided above the pinch at the lowest temperatures and the heat extracted below the pinch at the highest temperatures, until utility pinch points are activated.

Eventually, the joint curve of hot and cold utility streams must completely close the process grand composite curve. The composition of both curves delivers the heat cascade (HC) (Fig. 41, step 6) which graphically represents the residual heat above each temperature level of the shifted temperature range. Optimal integration of utilities can be performed graphically as explained in this subsection or by means of the mathematical programming formulation described in Subsection 4.4.2.

Data					*Results*	
Utility stream	**Stream type**	**TsU** °C	**TtU** °C	**cost** €/kWh	**QU** kW	**cost** €/year
HPS	hot	250	250	0.05	450 (+)	197100
LPS	hot	120	120	0.04	450 (+)	157680
CW	cold	15	30	0	750 (-)	0
						354780

Table 8: Utility data and optimal results

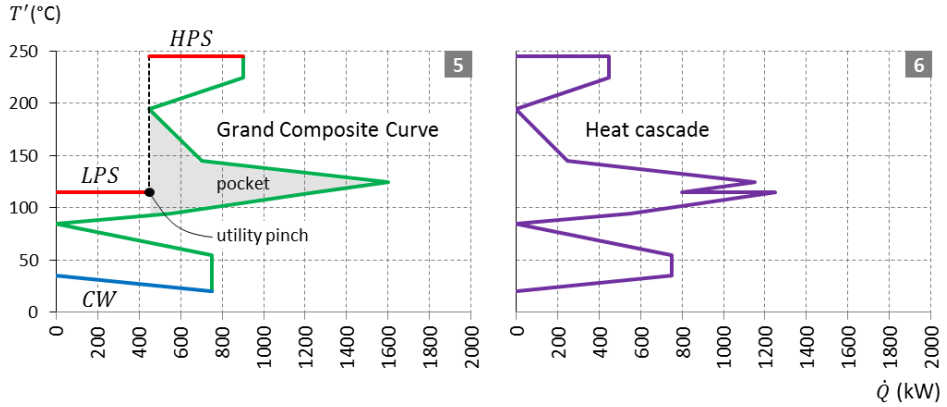

Fig. 41: Integration of different steam levels in the GCC and graphic representation of the HC

Data					*Results*	
Utility stream	**Stream type**	**TsU** °C	**TtU** °C	**cost** €/kWh	**QU** kW	**cost** €/year
HPS	hot	250	250	0.05	0 (+)	0
LPS	hot	120	120	0.04	437 (+)	153175
CW	cold	15	30	0	750 (-)	0
FG	hot	1950	150	0.045	463 (+)	182458
						335633

Table 9: Utility data and optimal results

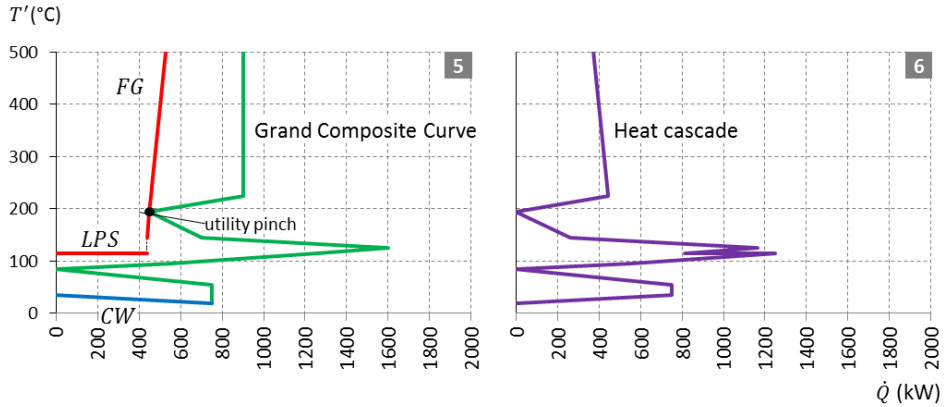

Fig. 42: Integration of low pressure steam and flue gasses in the GCC and graphic representation of the HC

Heat pumps (HP) are employed to extract low temperature waste heat and lift it to a higher temperature level, so that it can be used to heat up cold process streams. A heat pump needs to be placed across the pinch point in order to extract heat from below the pinch, where the process acts as a heat source, and release it above the pinch, where the process is a heat sink. A sharp, pointed nose in the GCC at the pinch indicates an opportunity for heat pump placement, because lifting a large heat load over a small temperature difference can be done with high efficiency. The integration of a heat pump with coefficient of performance (COP) 4.5 into the example process is shown in Table 10 and Fig. 43. A refrigeration cycle is analogous to a heat pump, except that its cold stream is below environmental temperature.

Data					*Results*	
Utility stream	**Stream type**	**TsU** °C	**TtU** °C	**cost** €/kWh	**QU** kW	**cost** €/year
HPS	hot	250	250	0.05	450 (+)	197100
CW	cold	15	30	0	412.5 (-)	0
HPh	hot	100	100	0.01	450 (+)	9855
Hpc	cold	45	45	0	337.5 (-)	0
						206955

Table 10: Utility data and optimal results

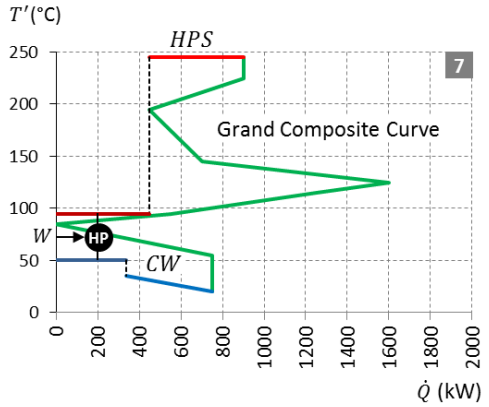

Fig. 43: Integration HP

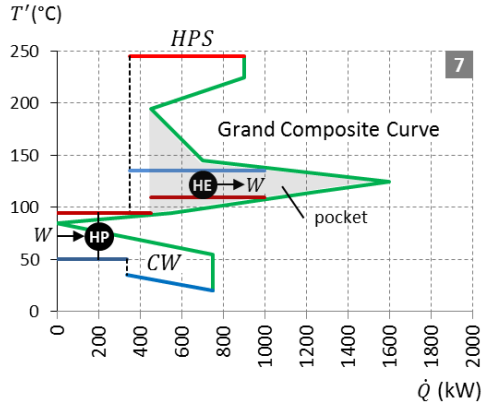

Fig. 44: Integration HP and HE

A heat engine (HE) extracts heat from a hot reservoir, converts part of it to mechanical work e.g. to drive an electricity generator, and releases the residual heat to a cold reservoir. The pockets in the GCC offer opportunities for integration of a heat engine. In the temperature range corresponding to the upper part of a pocket, more heat is available from hot process streams than required by cold process streams. This excess heat is cascaded down to be absorbed by the cold process streams in the temperature range corresponding to the lower part of the pocket. However, this heat can intermediately be used to drive a heat engine, inducing a new cold stream for heat extraction and a new hot stream to deliver its waste heat back to the process. Appropriate placement is at either side of the pinch, but not across the pinch.

4.4.1.3. Trade-off between utility and heat exchanger area costs

The minimum temperature approach ΔT_{min} represents the trade-off between utility costs and heat exchanger area costs. The lower ΔT_{min}, the lower the minimum utility requirements and corresponding fuel or operation costs, but the higher the investment costs for heat exchangers, as

lower temperature differences require larger heat transfer areas. Vice versa, a higher ΔT_{min}, implies higher utility costs, but lower heat exchanger investment costs. Hence, the choice for ΔT_{min} is of key importance. A list of experience based values for various processes is provided by Linhoff [18]. However, the optimal value of ΔT_{min} resulting in minimum total costs can be estimated prior to the actual design of the heat exchanger network. Therefore, utility costs as well as heat exchanger area costs need to be plotted against ΔT_{min}. The optimal ΔT_{min} value can then be identified from the aggregated curve.

The curve for utility costs can be obtained by performing Pinch Analysis for a range of ΔT_{min} values. For that purpose, the heat cascade model described in subsection 4.4.2 can be employed. To construct the curve of required heat exchanger area costs versus minimum temperature approach, cost estimations are made for a range of ΔT_{min} values. Following the basic principle of spaghetti design [103, 104], a minimum heat exchanger area target for a certain ΔT_{min} is obtained when assuming vertical heat exchange between the composite curve of all hot process and utility streams and the composite curve of all cold process and utility streams. A heat exchanger is placed in each interval along the heat axis between two subsequent nods in either one of the composite curves. The required heat exchanger areas are calculated, and summed up to deliver the minimum total heat exchanger area. Furthermore, the minimum number of heat exchangers at each side of the process pinch can be calculated as the total number of streams minus one. By dividing the minimum total heat exchanger area by the total minimum number of units, the mean area is obtained, for which the investment cost can be determined. By multiplying this cost with the minimum number of heat exchangers, an estimation of the total heat exchanger area cost is obtained. Equations to calculate heat exchanger area and related costs are given in subsection 4.7.1.

4.4.1.4. Heat exchanger network design

In the final step of Pinch Technology, the heat exchanger network is designed, starting from the known process streams and the optimised utility flows. This network physically enables the exchange of heat between process streams, but also between process and utility streams. The design is performed using the Pinch Design Method [89], which is built upon a set of heuristic rules.

To avoid cross-pinch heat exchange and to maintain minimum energy requirements, the Pinch Design Method is applied separately above and below the pinch. At each side of the pinch, the design starts with the streams present at pinch temperature and then moves away from the pinch. Since external cooling above the pinch needs to be avoided, all hot streams in that region need to be cooled down by the cold streams. Similarly, external heating must be avoided below the pinch, so all cold streams need to be heated up by hot streams. For both pinch sides, this implicates that the number of streams going out from the pinch needs to be greater or equal to the number of ingoing streams (*number of streams rule*). To satisfy this condition, outgoing streams may have to be split. When a heat exchanger is placed between an ingoing and an outgoing stream, both present at the pinch, away from the pinch their heat-temperature profiles must diverge in order to maintain sufficient driving force for heat exchange. Consequently, the heat capacity rate of the outgoing stream must be greater or equal than that of the ingoing stream (*cp rule*). If this is not the case, the ingoing stream needs to be split. In each match between two streams starting at the pinch, the maximum possible heat load is exchanged (*tick-off rule*) When all matches comply with these heuristic rules, the design can be further refined by shifting heat loads along heat load loops and paths in order to eliminate heat exchangers or utilities.

4.4.2. Basic heat cascade model

The graphical procedures for minimum utility targets and optimal integration of multiple utilities starting from the GCC are described in subsections 4.4.1.1 and 4.4.1.2. A mathematical alternative is provided by the heat cascade model, that has been proposed as an LP transshipment model by Papoulias *et al.* [85] or as a MILP formulation by Maréchal *et al.* [70]. By solving the MILP heat cascade model, counter-current heat exchange between hot and cold process streams is maximised for a given $dTmin$. Simultaneously, utilities are optimally integrated to fulfil the resulting minimum energy requirements at minimum total utility costs. Optimal utility integration implies computation of the optimal values of the decision variables for utility selection, size (nominal load) and operation. In essence, the heat cascade consists of a series of sequentially coupled thermal energy balances. Such an energy balance is set up for each interval of the shifted temperature domain. The basic version of the heat cascade model assumes that there are no external constraints to direct heat exchange between streams.

In the following subsections, the basic heat cascade model formulation is presented. First, the temperature shift and the calculation of the required parameters per temperature interval (heat capacity rate and heat load) are described. Next, the equations constituting the heat cascade formulation are elaborated. Naming of parameters, variables and equations corresponds to the terminology used in the formulation of *Syn-E-Sys*.

4.4.2.1. Composition of shifted temperature list

Hot (cold) streams are defined in the model as non-isothermal streams with a higher (lower) source than target temperature, or as isothermal streams labelled as hot (cold) stream by the analyst. Firstly, all hot (cold) streams are shifted downwards (upwards) along the temperature axis over a distance of $\Delta Tmin/2$ (see Fig. 45). Next, the shifted source and target temperatures are included in a list that is then sorted in ascending order, while removing duplicates. Subsequently, all temperatures in the list related to isothermal streams are duplicated once. The resulting temperature list is tagged with the index set $k = k_1..k_{max}$, from the lowest to the highest temperature. The basic principle of the heat cascade is that heat can be transferred from any hot stream in a certain temperature interval to any cold stream in the same or in a lower interval. To ensure the positive temperature difference required for spontaneous heat transfer, all hot (cold) streams are shifted downwards (upwards) by $\Delta Tmin/2$, as shown in Fig. 45. This temperature shift can be specified for each stream separately.

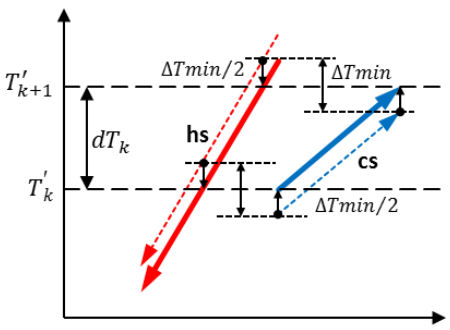

Fig. 45: Driving force for heat exchange by temperature shift

4.4.2.2. Calculation of heat capacity rates and thermal loads per temperature interval

To set up an energy balance in each shifted temperature interval $[T'_k, T'_{k+1}]$, the heat loads of streams crossing that interval need to be calculated, starting from their heat capacity rates. For a non-isothermal process stream, the heat capacity rate $mcpP_P$ is calculated by dividing the stream's heat load $QP_P(\geq 0)$ by the difference between its source and target temperatures $(TsP_P - TtP_P)$ (equation MCPP1). As a consequence, hot (cold) streams feature positive (negative) heat capacity rates. However, for non-isothermal utility streams, heat loads are decision variables that have to be optimised. Therefore, the heat capacity rates $mcpU1_U$ of these streams are normalised to their total heat loads (equation MCPU1). For isothermal streams, the heat capacity rate is not calculated since its value is infinite.

The heat load $dQP_{k,P}$ in a temperature interval $[T'_k, T'_{k+1}]$ of a non-isothermal process stream is calculated by multiplying the interval's temperature range $dT_k = T'_{k+1} - T'_k$ with the stream's heat capacity rate $mcpP_P$ provided that the stream crosses that interval (equation HLP1). For a non-isothermal utility stream, the normalised heat load per temperature interval $dQU1_{k,U}$ is derived by multiplying the temperature range dT_k with the normalised heat capacity rate $mcpU1_U$ (equation HLU1). For an isothermal process stream, the heat load assigned to the infenitesimal temperature interval in which the stream appears is equal to the stream's overall heat load (equation HLP2). In case of an isothermal utility stream, the heat load is equal to +/-1, while the sign is specified by the labels hcP_P or hcU_U defined by the analyst (equation HLU2). All hot streams have positive (normalised) heat loads, whereas for cold streams they are negative. The calculation of (normalised) heat capacity rate and (normalised) heat load per temperature interval is visualised in Fig. 46.

Calculation stream parameters

for non-isothermal streams:

MCPP1		$mcpP_P = QP_P/(TsP_P - TtP_P)$
MCPU1		$mcpU1_U = 1/(TsU_U - TtU_U)$
HLP1	P crossing $[T'_k, T'_{k+1}]$	$dQP_{k,P} = dT_k \cdot mcpP_P$
HLU1	U crossing $[T'_k, T'_{k+1}]$	$dQU1_{k,U} = dT_k \cdot mcpU1_U$

for isothermal streams

HLP2	P crossing $[T'_k, T'_{k+1}]$	$dQP_{k,P} = QP_P \cdot sign(hcP_P)$
HLU2	U crossing $[T'_k, T'_{k+1}]$	$dQU1_{k,U} = 1 \cdot sign(hcU_U)$

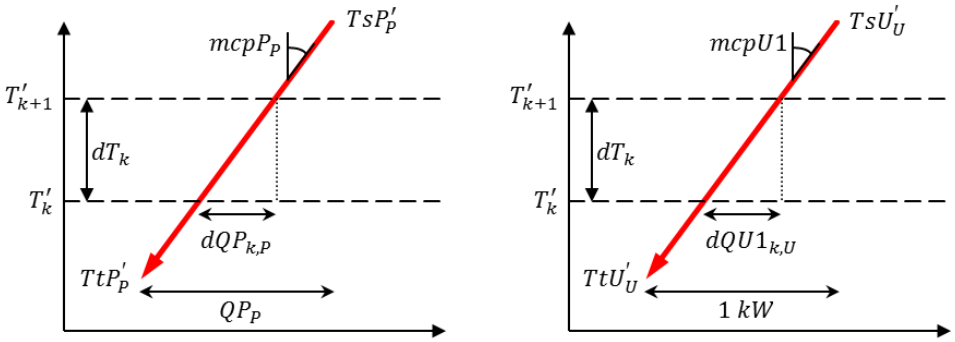

Fig. 46: Heat capacity rate and heat load per temperature interval for non-isothermal process and utility streams

4.4.2.3. Equations composing the basic heat cascade model

In the MILP model of Maréchal *et al.* [70], a continuous and a binary variable are associated to every utility and represent flowrate and selection. The utility flowrate serves as a multiplication factor for the heat loads that result from thermodynamic analysis of that utility in a reference situation. This analysis can be performed prior to optimisation, or simultaneously by incorporating technology models as linearised constraints into the optimisation problem. These technology models describe the relation between the different flowrates associated with that technology and the corresponding heat (and electricity) loads.

The formulation presented in this subsection is based on the general formulation of Maréchal *et al.* [70], but is simplified in terms of technology modelling. Instead of a series of complex specific technology models, a simplified generic technology model is used, based on the equipment model of Voll *et al.* [50] (see Section 4.3). As a consequence, technology operation is not represented by flowrate as in [70], but directly by thermal (or electrical) load. Additionally, the original equations in [70] constraining the flowrate of a selected utility between a minimum and maximum value, as well as the objective function are replaced by an equivalent formulation integrating the generic technology model. Moreover, for practical modelling reasons, a distinction is made between utilities generating electricity (E) and utilities generating thermal streams (U).

The constraints of the heat cascade model comprise a series of coupled thermal energy balances, one for each interval in the shifted temperature domain, as depicted in Fig. 47. In a certain temperature interval $[T'_k, T'_{k+1}]$, hot process and utility streams supply heat to the balance, whereas cold streams extract heat from it. Furthermore, a heat load is received from the interval above and residual heat is transferred to the interval below (equation HC1). Heat loads originating from process streams are calculated a priori and denoted as $d\dot{Q}P_{k,P}$. The heat load of a utility is expressed as the product of its known normalised heat load $dQU1_{k,U}$ and its total heat load $\boldsymbol{\dot{Q}U}_U$, which is a decision variable to be optimised. Heat residuals entering and leaving the interval are denoted as $\boldsymbol{R}_{k+1}$ and $\boldsymbol{R}_k$. At both ends of the shifted temperature range, the heat residual must be equal to zero (equations HC3 and HC4). In contrast to the coupled series of thermal balances, a single balance suffices for electrical energy, as shown in Fig. 48. Equations EB1 and EB2 ensure that electricity import $\boldsymbol{Imp\_el}$ from the grid and electricity production by utilities balance overall electricity demand dem_el of the process, electricity usage by utilities and electricity export $\boldsymbol{Exp\_el}$ to the grid. It must be noted that equation EB1 is redundant, since it is automatically fulfilled when EB2 is fulfilled.

Technology equations are developed in subsections 4.3.2 and 4.3.3. Equation U4 ensures that, when a utility is selected, at most one of the line segments of its part-load curve is active, while equation U2 and U3 demand that the utility load is embedded between the boundaries of the active segment, similar to the corresponding equation in [70] The same is valid for electricity generating utilities (E).

The objective function OBJ expresses the total annual costs over all utilities to be minimised. Utility costs consist of fuel costs, proportional to the energy input ($\boldsymbol{\dot{Q}in}_{U,R}$ or $\boldsymbol{\dot{Q}in\_el}_{E,R}$) of that utility, operation and maintenance costs, proportional to the utility load ($\boldsymbol{\dot{Q}U}_U$ or $\boldsymbol{P\_el}_{E,R}$) and investment costs subject to economy of scale. The investment costs are annualised by means of a factor $Anf = [i \cdot (1+i)^n]/[(1+i)^n - 1]$ with i indicating the fractional interest rate per year and n the economic lifetime in years [105]. Note that not all utility types have all cost types, so for every utility, only the relevant costs must be included in the objective function (see 4.4.4 for more details).

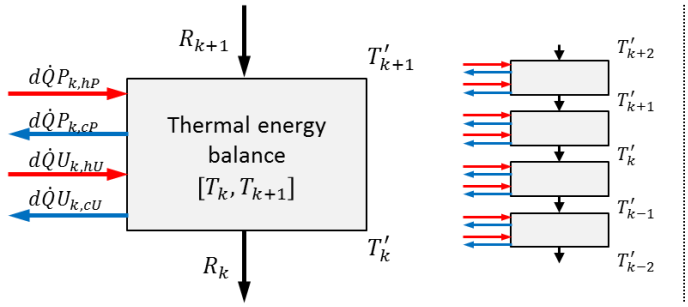

For full notation:

$\forall P \in \{hP, cP\}$: replace $d\dot{Q}P_{k,P}$ with $\sum_P d\dot{Q}P_{k,P}$

$\forall U \in \{hU, cU\}$: replace $d\dot{Q}U_{k,U}$ with $\sum_U \dot{Q}U_U \cdot d\dot{Q}U1_{k,U}$

Fig. 47: Coupled thermal energy balances (simplified notation)

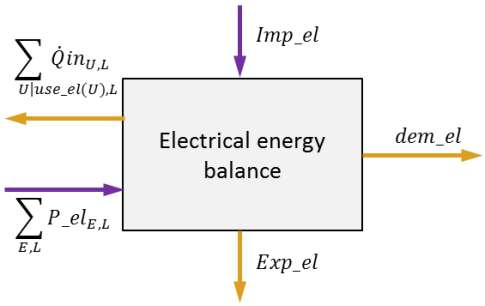

Fig. 48: Electrical energy balance

The heat cascade formulation given in this subsection only serves as a starting point for the development of the energy system synthesis model *Syn-E-Sys*. It is modified and extended as more features are integrated into the model.

Thermal energy balances

HC1 $$\forall k < k_{max}: \boldsymbol{R}_{k+1} - \boldsymbol{R}_k + \sum_P d\dot{Q}P_{k,P} + \sum_U \boldsymbol{\dot{Q}U}_U \cdot d\dot{Q}U1_{k,U} = 0$$

HC3 $$\boldsymbol{R}_{k_1} = 0$$

HC4 $$\boldsymbol{R}_{k_{max}} = 0$$

Electrical energy balance

EB1 $$\boldsymbol{Imp\_el} + \sum_{E,L} \boldsymbol{P\_el}_{E,L} \geq dem\_el + \sum_{U|use\_el(U),L} \boldsymbol{\dot{Q}in}_{U,L}$$

EB2 $$\boldsymbol{Imp\_el} + \sum_{E,L} \boldsymbol{P\_el}_{E,L} = \boldsymbol{Exp\_el} + dem\_el + \sum_{U|use\_el(U),L} \boldsymbol{\dot{Q}in}_{U,L}$$

Technology models

technology equations described in subsections 4.3.2 and 4.3.3

Objective function

OBJ $$\boldsymbol{cost} = hrs\_y \cdot (\boldsymbol{Imp\_el}.cost\_el - \boldsymbol{Exp\_el}.revs\_el)$$
$$+ hrs\_y \cdot \left(\sum_{U,L} \boldsymbol{\dot{Q}in}_{U,L} \cdot cF_U + \sum_U \boldsymbol{\dot{Q}U}_U \cdot cOM_U + \sum_{E,L} \boldsymbol{\dot{Q}in\_el}_{E,L} \cdot cF\_el_E + \sum_{E,L} \boldsymbol{P\_el}_{E,L} \cdot cOM\_el_E \right)$$
$$+ Anf. \left(\sum_{U,Lc} \boldsymbol{Inv}_{U,Lc} + \sum_{E,Lc} \boldsymbol{Inv\_el}_{E,Lc} \right)$$

$$\boldsymbol{\dot{Q}U}_U, \boldsymbol{R}_k, \boldsymbol{Imp\_el}, \boldsymbol{Exp\_el}, \boldsymbol{\dot{Q}in}_{U,L}, \boldsymbol{P\_el}_{E,L}, \boldsymbol{Inv}_{U,Rc}, \boldsymbol{Inv\_el}_{E,Rc} \in \mathbb{R}^+, \boldsymbol{cost} \in \mathbb{R}$$

4.4.2.4. Multi-period

The heat cascade formulation developed in the previous subsection is extended to multi-period and is similar to the multi-period heat cascade model proposed by Maréchal *et al.* [61]. Note that periods are referred to here as time slices (S).Thermal and electrical energy demands vary over the different time slices, while source and target temperatures of thermal process and utility streams keep constant values. The composition of the shifted temperature list (see 4.4.2.1) remains unchanged, but for the process streams, heat capacity rates and thermal loads per temperature interval (see 4.4.2.2) need to be calculated in every time slice separately. Since energy demands need to be fulfilled in every single time slice, thermal and electrical energy balances (HC1, HC3, HC4, EB1, EB2) have to be generated separately for each time slice. Accordingly, the equations expressing technology behaviour (U1-U8, CN1, CN2, E1-E8) are set up in each time slice. In contrast, the technology equations calculating the investment cost remain unchanged. Furthermore, parameters related to thermal process and utility streams and to electrical energy demand, and all variables except the investment cost and the binary selection variable are additionally indexed with S. The objective function is adapted to accumulate the variable costs over all periods and the one-off annualised investment costs.

4.4.2.5. Variable stream temperatures

When stream temperatures demonstrate a priori defined variations over time, a separate shifted temperature list needs to be generated for every time slice. Each temperature list is tagged with the index set $k = k_1..k_{max,S}$, in which $k_{max,S}$ indicates the position of the highest temperature in the temperature list related to time slice S. Moreover, for process as well as utility streams, heat capacity rates and thermal loads per temperature interval are calculated in every time slice separately, and the corresponding parameters are additionally indexed with the set of time slices.

4.4.3. Extended heat cascade model with heat exchange restrictions

The basic heat cascade model starts from the assumption that all hot streams can be matched with all cold streams to exchange heat. However, within an industrial site or company, some matches might be forbidden due to product quality or safety issues, because of non-simultaneous processes operation, or because the distance between certain streams is too large, resulting in excessive heat exchanger network costs. On business park scale, companies might be opposed to direct heat exchange with other companies, because of various operational, economic or strategic reasons. Obviously, there is a need for energy system models that are able to deal with specific restrictions in heat exchange.

Total Site Analysis, initially proposed by Dhole and Linnhoff [106], is a method to set minimum energy requirement targets for an industrial site, consisting of different production processes that can only exchange heat via a central utility system. Becker *et al.* [62] developed an alternative approach by extending the single period version of the basic heat cascade model to take into account restricted matches. Therefore, they divided the energy system into different subsystems that are connected to a central heat transfer system. In each subsystem, heat exchange between hot and cold streams is unconstrained, but direct heat exchange between streams of different subsystems is not allowed. However, subsystems can exchange heat with each other via heat transfer units located in the heat transfer system (e.g. hot water loop, steam network). Common utilities included in the heat transfer system (e.g. boiler, cooling water) are directly available to all streams, while utilities located

in subsystems are limited to direct heat exchange with local streams. The heat transfer system itself may also contain process streams.

In essence, the heat cascade model with restricted matches consists of heat cascades for all subsystems that are connected in every temperature interval to the heat cascade of the heat transfer system as depicted in Fig. 49. By optimally employing the heat transfer units, the increase in energy costs due to the heat exchange restrictions is minimised. Moreover, Becker *et al.* [62] provided the heat cascade model with an envelope composite curve that facilitates the selection of optimal temperature ranges for heat transfer units, as will be discussed in subsection 4.4.6.

If the different companies in a business park are represented by different subsystems, the model allows us to perform energy integration in each company separately, while simultaneously optimising heat exchange between different companies via heat networks and joint energy production via common utilities. The heat network and the joint energy production facilities could be owned and managed by an energy service company.

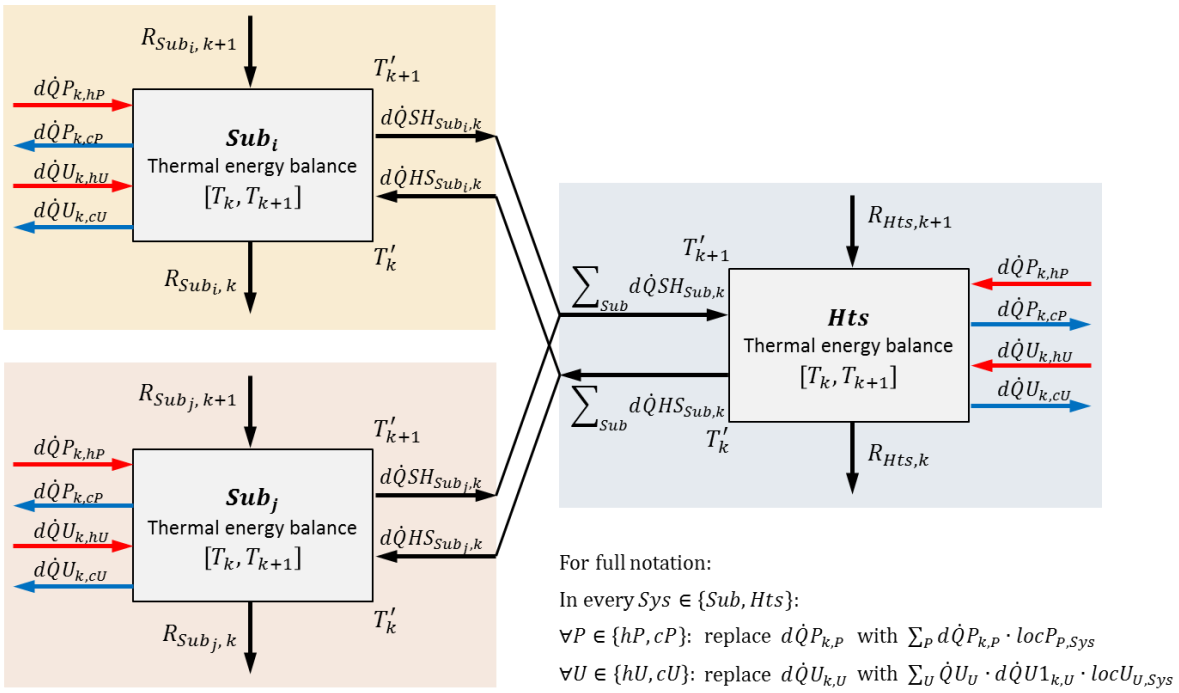

Fig. 49: Heat cascade model with restricted matches: interconnected thermal energy balances in temperature interval k (simplified notation). arrow color code: red/blue = hot/cold P or U streams, black = heat transfers within system

4.4.3.1. Equations composing the extended heat cascade model

The heat cascade formulation incorporated in *Syn-E-Sys* is based on the approach of Becker *et al.* [62]. It is customised to integrate the generic technology model equations, in a similar way as for the basic heat cascade model. The composition of the shifted temperature list and the calculation of stream parameters, as described in Subsections 4.4.2.1 and 4.4.2.2, remain unchanged. The thermal energy balances from Subsection 4.4.2.3 are composed for all system sections (Sys) including the heat transfer system (Hts) and all subsystems (Sub), leading to equations HC1, HC2, HC3 and HC4 below.

A graphical representation of the interconnected thermal energy balances of subsystems and heat transfer system in temperature interval $[T_k, T_{k+1}]$ is given in Fig. 49. Note that in this figure, process and utility heat loads are not indicated with correct expressions, for the sake of readability. Streams are assigned to a certain system section by a priori specified binary location parameters ($locU_{U,Sub}$, $locP_{P,Sub}$, $locU_{U,Hts}$ and $locP_{P,Hts}$).

Next, the heat transfer loads between subsystems and heat transfer system are added to the thermal balances in each temperature interval. The variable $\boldsymbol{d\dot{Q}SH}_{Sub,k}$ represents the heat transferred from a subsystem to the heat transfer system (**S**ub to **H**ts) in temperature interval k, while $\boldsymbol{d\dot{Q}HS}_{Sub,k}$ indicates the heat transfer in the opposite sense (**H**ts to **S**ub). Furthermore, the heat residuals $\boldsymbol{R}$ are now additionally indexed with the system section (Sys, Sub or Hts). The heat residual of the total system at a certain temperature is derived by summing up the heat residuals of all system sections at that temperature (HC5).

Thermal energy balances

HC1 $\forall\, Sub, k < k_{max}$:

$$\boldsymbol{R}_{Sub,k+1} - \boldsymbol{R}_{Sub,k} + \sum_{P} d\dot{Q}P_{k,P} \cdot locP_{P,Sub} + \sum_{U} \boldsymbol{\dot{Q}U}_{U} \cdot d\dot{Q}U1_{k,U} \cdot locU_{U,Sub} - \boldsymbol{d\dot{Q}SH}_{Sub,k} + \boldsymbol{d\dot{Q}HS}_{Sub,k} = 0$$

HC2 $\forall\, k < k_{max}$:

$$\boldsymbol{R}_{Hts,k+1} - \boldsymbol{R}_{Hts,k} + \sum_{P} d\dot{Q}P_{k,P} \cdot locP_{P,Hts} + \sum_{U} \boldsymbol{\dot{Q}U}_{U}.d\dot{Q}U1_{k,U} \cdot locU_{U,Hts} + \sum_{Sub} \boldsymbol{d\dot{Q}SH}_{Sub,k} - \sum_{Sub} \boldsymbol{d\dot{Q}HS}_{Sub,k} = 0$$

HC3 $\forall\, Sys: \boldsymbol{R}_{Sys,k_1} = 0$

HC4 $\forall\, Sys: \boldsymbol{R}_{Sys,k_{max}} = 0$

HC5 $\forall\, k \leq k_{max}: \boldsymbol{Rtot}_k = \sum_{Sys} \boldsymbol{R}_{Sys,k}$

$\boldsymbol{\dot{Q}U}_{U}, \boldsymbol{R}_{Sys,k}, \boldsymbol{d\dot{Q}SH}_{Sub,k}, \boldsymbol{d\dot{Q}HS}_{Sub,k} \in \mathbb{R}^{+}$

To avoid that heat received by the Hts from a subsystem in a certain temperature interval is directly passed on to another subsystem, while bypassing all utilities and heat transfer units in the Hts, additional equations are required per temperature interval. The hot stream balances demand that in each temperature interval the total heat load transferred from the Hts to all subsystems can completely be delivered by the hot streams in the Hts in that temperature interval (HC6). Analogously, cold stream balances are set up for every interval (HC7), demanding that in each temperature interval the total heat load received by the Hts from all subsystems can completely be absorbed by the Hts cold streams in that temperature interval.

Hot and cold stream balances

HC6 $\forall\, k < k_{max}$:

$$\sum_{Sub} \boldsymbol{d\dot{Q}HS}_{Sub,k} \leq \sum_{hP} d\dot{Q}P_{k,hP} \cdot locP_{hP,Hts} + \sum_{hU} \boldsymbol{\dot{Q}U}_{hU} \cdot d\dot{Q}U1_{k,hU} \cdot locU_{hU,Hts}$$

HC7 $\forall\, k < k_{max}$:

$$\sum_{Sub} \boldsymbol{d\dot{Q}SH}_{Sub,k} \leq -\sum_{cP} d\dot{Q}P_{k,cP} \cdot locP_{cP,Hts} - \sum_{cU} \boldsymbol{\dot{Q}U}_{cU} \cdot d\dot{Q}U1_{k,cU} \cdot locU_{cU,Hts}$$

$\boldsymbol{\dot{Q}U}_{U}, \boldsymbol{d\dot{Q}SH}_{Sub,k}, \boldsymbol{d\dot{Q}HS}_{Sub,k} \in \mathbb{R}^{+}$

Due to these balances the cascading of heat loads of processes and utilities is performed in the subsystems rather than in the heat transfer system. In other words, the heat transferred from a subsystem to the Hts in a certain temperature interval is completely absorbed by the cold streams in the Hts in that temperature interval and not sent to a lower interval. In a similar way, the heat transferred from the Hts to a subsystem in a certain temperature interval is completely supplied by the hot streams in the Hts in that temperature interval and not received from a higher interval. Consequently, the hot and cold stream balances tighten the solution space of the optimisation problem. Note that, unlike Becker *et al.* [62], I did not include the heat residuals $\boldsymbol{R}_{Hts,k+1}$ and $\boldsymbol{R}_{Hts,k}$ into the hot and cold stream balances HC6 and HC7. It can be proven that the combination of the thermal energy balances of the Hts (HC2) with the modified hot and cold stream balances is equivalent to the combination with the original balances. The heat cascade constraints for the model with restricted matches are given by equations HC1-HC7 below.

The equations expressing the electricity balance, the generic technology model equations, and the objective function are identical to the basic heat cascade model and are not reproduced here. Indeed, the formulation of these expressions is not influenced by the system subdivision and the heat exchange constraints.

4.4.3.2. Multi-period, and varying stream temperatures

The extension of the heat cascade model to multi-period is completely analogue to the multi-period extension of the basic heat cascade model, described in subsection 4.4.2.4. The optimisation constraints are set up for each period separately and the relevant parameters and variables are additionally indexed with the set S. When stream temperatures change over time, the model formulation is modified in the same way as described in subsection 4.4.2.5 for the basic heat cascade model.

4.4.4. Formulation extended heat cascade model

This subsection describes the parameters, variables and equations in the formulation of the multi-period heat cascade model with heat exchange restrictions, accounting for variable stream temperatures that follow a priori defined variations.

The parameters describing the characteristics of the thermal streams per time slice include stream temperatures per time slice, location in the system, and for process streams, heat load per time slice. Other parameters represent the heat capacity rates and heat loads per temperature interval, the temperature range in each interval, labels for the stream type of isothermal streams, the overall electricity demand per time slice and specific utility costs. Note that in this subsection the letter S is used instead of the apostrophe (') to indicate shifted temperatures. Decision variables are the heat residuals cascaded in every system section, the heat transfers between subsystems and heat transfer system, and electricity import and export. The variables related to the technology selection, operation and investment and parameters, sets and variables mentioned in subsection 4.3.5 are not repeated here.

The parameter equations for calculation of heat capacity rates and thermal heat loads per temperature interval, related to process and utility streams, are developed in subsection 4.4.2.2 and reformulated here for every time slice. The electrical balances and the objective function are composed in subsections 4.4.2.3, and the thermal balances are presented in 4.4.3.1. These equations are all extended here to multi-period, as explained in subsection 4.4.3.2. Technology equations are not reproduced here. Next to index S, a number of variables and equations is indexed with the set of technology instances, related to the automated superstructure expansion as discussed in subsection 4.5.4.

4.4.4.1. Sets and parameters

Sets

Sys	$= Hts, Sub_1 .. Sub_f$	heat transfer system, subsystems
P	$= P_1 .. P_f$	thermal processes
k	$= k_1 .. k_{100}$	temperatures

Subsets

$Sub(Sys)$	$= Sub_1 .. Sub_f$	subsystems
$Hts(Sys)$	$= Hts$	heat transfer system
$hp(P)$	$= \{P \mid TsP_{P,S_1} > TtP_{P,S_1}, P \mid (TsP_{P,S_1} = TtP_{P,S_1}\ and\ hcP_P > 0)\}$	hot processes
$cp(P)$	$= \{P \mid TsP_{P,S_1} < TtP_{P,S_1}, P \mid (TsP_{P,S_1} = TtP_{P,S_1}\ and\ hcP_P < 0)\}$	cold processes
$hu(U)$	$= \{U \mid TsU_{U,S_1} > TtU_{U,S_1}, P \mid (TsU_{U,S_1} = TtU_{U,S_1}\ and\ hcU_U > 0)\}$	hot utilities
$cu(U)$	$= \{U \mid TsU_{U,S_1} < TtU_{U,S_1}, P \mid (TsU_{U,S_1} = TtU_{U,S_1}\ and\ hcU_U < 0)\}$	cold utilities

$use\_el(U)$	$= U \mid [U \in \{HPh, Hnwh, CC, CW\}\ and\ presU(U) = 1]$ thermal utilities using electricity
$gen\_elU(U)$	$= U \mid [U \in \{HEh\}\ and\ presU(U) = 1]$ thermal utilities generating electricity
$use\_fuelU(U)$	$= U \mid [U \in \{DefaultU, CHPth\}\ and\ presU(U) = 1]$ thermal utilities using fuel
$use\_fuelE(E)$	$= E \mid [E \in \{DefaultE\}\ and\ presE(E) = 1]$ thermal utilities using fuel
$OMcostU(U)$	$= U \mid [U \notin \{HPc, Hnwc, HEc\}\ and\ presU(U) = 1]$ thermal utilities with operation and maintenance costs

$OMcostE(E)$ $= U|[E \notin \{CHPel\}\ and\ presE(E) = 1]$
electrical utilities with operation and maintenance costs

$fcostU(U)$ $= U|[U \notin \{HPc, Hnwc, HEc\}\ and\ presU(U) = 1]$
thermal utilities with investment costs

$fcostE(E)$ $= E|[E \notin \{CHPel\}\ and\ presE(E) = 1]$
electrical utilities with investment costs

Parameters

Time

hrs_S_S number of hours in time slice S

Processes

$TsP_{P,S}$ source temperature process P in time slice S (°C)
$TtP_{P,S}$ target temperature process P in time slice S (°C)
$TsPS_{P,S}$ shifted source temperature process P in time slice S (°C)
$TtPS_{P,S}$ shifted target temperature process P in time slice S (°C)
hcP_P indicates whether isothermal process P is hot $hcP_P > 0$ or cold stream $hcP_P < 0$
$QP_{P,S}$ thermal energy demand process P in time slice S (kW)
$mcp_{P,S}$ heat capacity rate process P in time slice S (kW/K)
$locP_{P,Sys}$ connection process P to system
$presP_P$ $\forall P| \left(\sum_{Sys} locP_{P,Sys} \geq 1\right) : presP_P = 1$

Thermal utilities

$TsU_{U,S}$ source temperature utility U in time slice S (°C)
$TtU_{U,S}$ target temperature utility U in time slice S (°C)
$TsUS_{U,S}$ shifted source temperature utility U in time slice S (°C)
$TtUS_{U,S}$ shifted target temperature utility U in time slice S (°C)
hcU_U indicates whether isothermal utility U is hot $hcU_U > 0$ or cold stream $hcU_U < 0$
$mcpU1_{U,S}$ normalised heat capacity rate utility U in time slice S (kW/K/1kW)
$locU_{U,Sys}$ connection utility U to system
cF_U fuel cost utility U (€/kWh)
cOM_U O&M cost utility U (€/kWh)
$presU_U$ $\forall U| \left(\sum_{Sys} locU_{U,Sys} \geq 1\right) : presU_U = 1$

Electrical utilities

cF_el_E fuel cost utility E (€/kWh)
cOM_el_E O&M cost utility E (€/kWh)

Electricity

dem_el_S overall electricity demand in time slice S (kW)
$cost\_el_S$ costs electricity (€/kWh)
$revs\_el_S$ revenues electricity (€/kWh)

Minimum temperature difference

$dTPmin_P$ minimum temperature difference for heat exchange with process P (°C)
$dTUmin_U$ minimum temperature difference for heat exchange with utility U (°C)

Economic parameters

Anf annualisation factor

4.4.4.2. Variables

Objective function

$\boldsymbol{cost}$	$\mathbb{R}$	total cost as objective function (€)

Thermal balances

$\boldsymbol{R}_{Sys,k,S}$	$\mathbb{R}^+$	heat exchange between temperature intervals [Tk, Tk+1] and [Tk-1, Tk] in system Sys in time slice S (kW)
$\boldsymbol{Rtot}_{k,S}$	$\mathbb{R}^+$	heat exchange between temperature intervals [Tk, Tk+1) and [Tk-1, Tk] in overall system in time slice S (kW)
$\dot{\boldsymbol{QU}}_{U,Ins,S}$	$\mathbb{R}^+$	absolute value actual thermal load of utility U, instance Ins, in time slice S (kW)
$d\dot{\boldsymbol{QSH}}_{Sub,k,S}$	$\mathbb{R}^+$	heat transfer from subsystem Sub to heat transfer system in time slice S (kW)
$d\dot{\boldsymbol{QHS}}_{Sub,k,S}$	$\mathbb{R}^+$	heat transfer from heat transfer system to subsystem Sub in time slice S (kW)

Electrical energy balances

$\boldsymbol{Imp\_el}_S$	$\mathbb{R}^+$	electricity import in time slice S (kW)
$\boldsymbol{Exp\_el}_S$	$\mathbb{R}^+$	electricity export in time slice S (kW)

4.4.4.3. Equations

Parameter equations

Calculation heat capacity rates

MCPP1 $\forall\, P,S \big| \left(TsP_{P,S_1} \neq TtP_{P,S_1}\right): mcpP_{P,S} = QP_{P,S} / \left(TsP_{P,S} - TtP_{P,S}\right)$

MCPU1 $\forall\, U,S \big| \left(TsU_{U,S_1} \neq TtU_{U,S_1}\right): mcpU1_{U,S} = 1 / \left(TsU_{U,S} - TtU_{U,S}\right)$

Calculation heat loads per temperature interval [TS_k,TS_{k+1}]

HLP1a $\forall\, P,S,k \big| \left(k < k_{max,S}, TsP_{P,S} > TtP_{P,S}, TsPS_{P,S} \geq TS_{k+1,S}, TtPS_{P,S} \leq TS_{k,S}\right)$:
$dQP_{k,P,S} = dT_{k,S} \cdot mcpP_{P,S}$

HLP1b $\forall\, P,S,k \big| \left(k < k_{max,S}, TsP_{P,S} < TtP_{P,S}, TtPS_{P,S} \geq TS_{k+1,S}, TsPS_{P,S} \leq TS_{k,S}\right)$:
$dQP_{k,P,S} = dT_{k,S} \cdot mcpP_{P,S}$

HLP2 $\forall\, P,S,k \big| \left(k < k_{max,S}, TsP_{P,S} = TtP_{P,S}, TtPS_{P,S} = TS_{k+1,S}, TsPS_{P,S} = TS_{k,S}\right)$:
$dQP_{k,P,S} = QP_{P,S} \cdot sign(hcP_P)$

HLU1a $\forall\, U,S,k \big| \left(k < k_{max,S}, TsU_{U,S} > TtU_{U,S}, TsUS_{U,S} \geq TS_{k+1,S}, TtUS_{U,S} \leq TS_{k,S}\right)$:
$dQU1_{k,U,S} = dT_{k,S} \cdot mcpU1_{U,S}$

HLU1b $\forall\, U,S,k \big| \left(k < k_{max,S}, TsU_{U,S} < TtU_{U,S}, TtUS_{U,S} \geq TS_{k+1,S}, TsUS_{U,S} \leq TS_{k,S}\right)$:
$dQU1_{k,U,S} = dT_{k,S} \cdot mcpU1_{U,S}$

HLU2 $\forall\, U,S,k \big| \left(k < k_{max,S}, TsU_{U,S} = TtU_{U,S}, TtUS_{U,S} = TS_{k+1,S}, TsUS_{U,S} = TS_{k,S}\right)$:
$dQU1_{k,U,S} = 1 \cdot sign(hcU_U)$

Constraints

Thermal energy balances

For HC1-HC5: $Ins.ord \leq iU(U)$, HC6: $Ins.ord \leq iU(hU)$, HC7: $Ins.ord \leq iU(cU)$

HC1 $\forall\, Sub,S,k \big| k < k_{max,S}$:

$$\boldsymbol{R}_{Sub,k+1,S} - \boldsymbol{R}_{Sub,k,S} + \sum_{P} d\dot{Q}P_{k,P,S} \cdot locP_{P,Sub} + \sum_{U,Ins} \dot{\boldsymbol{QU}}_{U,Ins,S} \cdot d\dot{Q}U1_{k,U,S} \cdot locU_{U,Sub} - d\dot{\boldsymbol{QSH}}_{Sub,k,S} + d\dot{\boldsymbol{QHS}}_{Sub,k,S} = 0$$

HC2 $\forall\, Hts, S, k \big| k < k_{max,S}$:

$$\boldsymbol{R}_{Hts,k+1,S} - \boldsymbol{R}_{Hts,k,S} + \sum_{P} d\dot{Q}P_{k,P,S} \cdot locP_{P,Hts} + \sum_{U,Ins} \dot{\boldsymbol{Q}}\boldsymbol{U}_{U,Ins,S} \cdot d\dot{Q}U1_{k,U,S} \cdot locU_{U,Hts}$$
$$+ \sum_{sub} \boldsymbol{d\dot{Q}SH}_{sub,k,S} - \sum_{sub} \boldsymbol{d\dot{Q}HS}_{sub,k,S} = 0$$

HC3 $\forall\, Sys, S, k | k = k_1$: $\boldsymbol{R}_{Sys,k,S} = 0$

HC4 $\forall\, Sys, S, k \big| k = k_{max,S}$: $\boldsymbol{R}_{Sys,k,S} = 0$

HC5 $\forall\, S, k \big| k \le k_{max,S}$: $\boldsymbol{Rtot}_{k,S} = \sum_{Sys} \boldsymbol{R}_{Sys,k,S}$

HC6 $\forall\, Hts, S, k \big| k < k_{max,S}$:

$$\sum_{Sub} \boldsymbol{d\dot{Q}HS}_{Sub,k,S} \le \sum_{hP} d\dot{Q}P_{k,hP,S} \cdot locP_{hP,Hts} + \sum_{hU,Ins} \dot{\boldsymbol{Q}}\boldsymbol{U}_{hU,Ins,S} \cdot d\dot{Q}U1_{k,hU,S} \cdot locU_{hU,Hts}$$

HC7 $\forall\, Hts, S, k \big| k < k_{max,S}$:

$$\sum_{Sub} \boldsymbol{d\dot{Q}SH}_{Sub,k,S} \le -\sum_{cP} d\dot{Q}P_{k,cP,S} \cdot locP_{cP,Hts} - \sum_{cU,Ins} \dot{\boldsymbol{Q}}\boldsymbol{U}_{cU,Ins,S} \cdot d\dot{Q}U1_{k,cU,S} \cdot locU_{cU,Hts}$$

Electrical energy balances

For EB1, EB2: $Ins.ord \le iU(U), Ins.ord \le iE(E)$

EB1 $\forall\, S$:

$$\boldsymbol{Imp\_el}_S + \sum_{E,Ins,L} \boldsymbol{P\_el}_{E,Ins,S,L} + \sum_{\substack{U,Ins,L| \\ gen\_elU(U)}} \dot{\boldsymbol{Q}}_{U,Ins,S,L} \ge dem\_el_S + \sum_{\substack{U,Ins,L| \\ use\_elU(U)}} \dot{\boldsymbol{Q}}\boldsymbol{in}_{U,Ins,S,L}$$

EB2 $\forall\, S$:

$$\boldsymbol{Imp\_el}_S + \sum_{E,Ins,L} \boldsymbol{P\_el}_{E,Ins,S,R} + \sum_{\substack{U,Ins,L| \\ gen\_elU(U)}} \dot{\boldsymbol{Q}}_{U,Ins,S,L} = dem\_el_S + \sum_{\substack{U,Ins,L| \\ use\_elU(U)}} \dot{\boldsymbol{Q}}\boldsymbol{in}_{U,Ins,S,L} + \boldsymbol{Exp\_el}_S$$

Objective

OBJ $Ins.ord \le iU(U), Ins.ord \le iE(E)$

$$\boldsymbol{cost} =$$
$$\sum_{U|usefuelU(U),Ins,S,L} \dot{\boldsymbol{Q}}\boldsymbol{in}_{U,Ins,S,L} \cdot hrs\_S_S \cdot cF_U + \sum_{E|usefuelE(E),Ins,S,L} \dot{\boldsymbol{Q}}\boldsymbol{inel}_{E,Ins,S,L} \cdot hrs\_S_S \cdot cF\_el_E$$
$$+ \sum_{U|OMcostU(U),Ins,S,L} \dot{\boldsymbol{Q}}_{U,Ins,S,L} \cdot hrs\_S_S \cdot cOM_U + \sum_{E|OMcostE(E),Ins,S,L} \boldsymbol{Pel}_{E,Ins,S,L} \cdot hrs\_S_S . cOM\_el_E$$
$$+ Anf \cdot \sum_{U|fcostU(U),Ins,Lc} \boldsymbol{Inv}_{U,Ins,Lc} + Anf \cdot \sum_{E|fcostE(E),Ins,Lc} \boldsymbol{Inv\_el}_{E,Ins,Lc}$$
$$+ \sum_{S} (\boldsymbol{Imp\_el}_S \cdot hrs\_S_S \cdot cost\_el_S - \boldsymbol{Exp\_el}_S \cdot hrs\_S_S \cdot revs\_el_S)$$

4.4.5. Phantom heat

The thermal energy balances and the hot and cold stream balances per temperature interval, composing the heat cascade formulation, do not prevent that heat is being transferred from a hot to a cold utility stream in a certain temperature interval. This can be problematic for a thermal utility that consists of a hot and a cold stream with overlapping temperature ranges, such as a heat network (see subsection 4.3.4.3).

4.4.5.1. Occurrence of phantom heat

When the temperature range of a heat network is ill chosen, heat will be transferred from its hot to its cold stream in one or more temperature intervals. This phenomenon is referred to as phantom heat, because the heat network is feeding itself with heat that is actually not available in the energy system. In this subsection, the occurrence of phantom heat is illustrated with a simple example calculated with *Syn-E-Sys*.

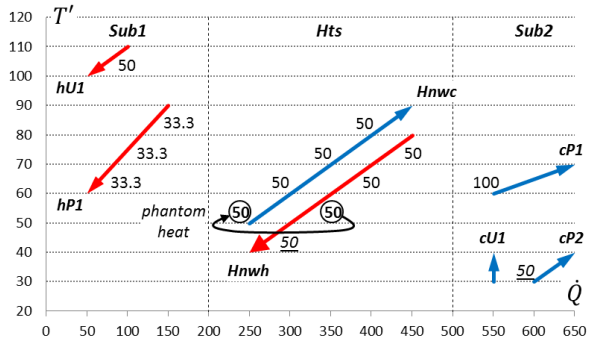

Fig. 50: Example with ill-chosen Hnw temperature range

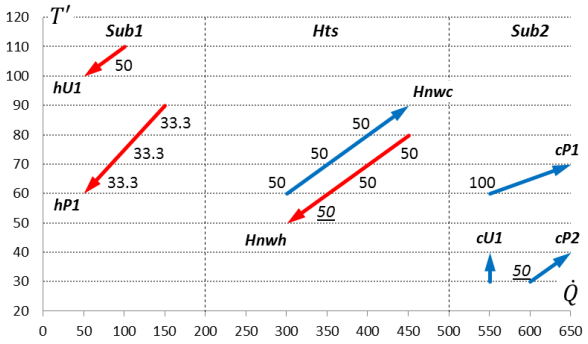

Fig. 51: Example with well-chosen Hnw temperature range

Fig. 50 shows an example of an energy system with two subsystems connected by a heat transfer system. The first subsystem (Sub1) contains a hot process (hP1) of 100 kW and a hot utility (hU1), the second one (Sub2) includes two cold process streams (cP1 and cP2) of respectively 100 kW and 50 kW and a cold utility (cU1), and the heat transfer system (Hts) contains a heat network (Hnw). Thermal streams are represented with their shifted temperatures taking into account a $\Delta Tmin$ of 10 °C. hU1 needs to generate a 50 kW heat load, which is added to the 100 kW available from hP1. The resulting 150 kW is absorbed by the heat network's cold stream (Hnwc) and subsequently released by its hot stream (Hnwh) to supply cP1 and cP2. Since cP1 requires 100 kW of heat above 60 °C, the heat load of Hnwh above this temperature is fixed to 100 kW, and consequently the temperature-heat profiles of Hnwc and Hnwh are determined. The lowest part of the heat network's hot stream delivers a heat load of 50 kW to cold process stream cP2. Both heat network streams require a heat load of 200 kW to keep their temperature-heat curves linear. Therefore, 50 kW will be transferred from its hot to its cold stream, which is referred to as phantom heat (see Fig. 50). In the heat network technology model, the total heat load absorbed by its cold stream is entirely sent to its hot stream ($\dot{\boldsymbol{Q}}_{Hnwc,i} = \dot{\boldsymbol{Q}}_{Hnwh,i}$). Consequently, the 50 kW added to the cold stream is simultaneously added to the hot stream and a self-sustaining loop is created.

Cost minimisation will chose phantom heat over an increase in hot and cold utility loads, because no costs are assigned to phantom heat. This implicates that phantom heat obstructs correct calculation of the utility requirements, as will be discussed in more detail in subsection 4.4.6.1. If phantom heat could somehow be blocked, a feasible solution for the system in Fig. 50 is obtained by increasing the heat load of hU1 to 100 kW and installing a cold utility cU1 to evacuate the remaining 50 kW from Hnwh. As can be observed in Fig. 51, a better choice of the heat network's temperature range avoids phantom heat.

4.4.5.2. Avoiding phantom heat

Two alternative approaches are explored to tackle the phantom heat problem. In the first approach described in this subsection, the heat cascade formulation is extended with equations in order to block phantom heat. In a second approach, appropriate temperature ranges for heat networks are identified that will not induce phantom heat and additionally avoid the increase in utility requirements that results from heat exchange restrictions. These temperature ranges are determined using the heat transfer unit envelope curves developed by Becker *et al.* [62], which we modified in subsection 4.4.6. If the temperature ranges of the available heat networks are chosen in such a way that the optimised heat network composite curves are embedded within this envelope, no phantom heat is induced, while the energy penalty is completely avoided.

The hot and cold stream balances in the heat cascade formulation (equations HC6 and HC7) prevent that heat received by the heat transfer system from a subsystem in a certain temperature interval is directly passed on to another subsystem, while bypassing all utilities and heat transfer units in the Hts. However, these equations do not prevent the heat exchange between the hot and cold stream of a heat network in the Hts at a certain temperature interval (route 1 in Fig. 52). To facilitate understanding, the equations treated in this subsection are written in a simplified, single-period form based on Fig. 52.

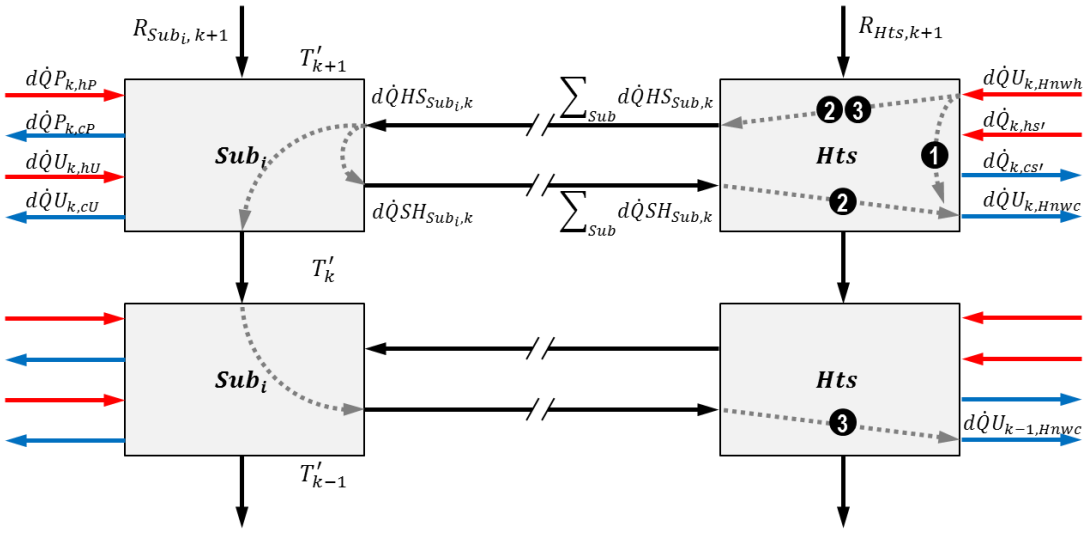

For full notation:
In Hts: replace $d\dot{Q}_{k,hs'}$ with $\sum_{hP} d\dot{Q}P_{k,hP} \cdot locP_{hP,Hts} + \sum_{hU \in \{Hnwh\}} \dot{Q}U_{hU} \cdot d\dot{Q}U1_{k,hU} \cdot locU_{hU,Hts}$
In Hts: replace $d\dot{Q}_{k,cs'}$ with $\sum_{cP} d\dot{Q}P_{k,cP} \cdot locP_{cP,Hts} + \sum_{cU \in \{Hnwc\}} \dot{Q}U_{cU} \cdot d\dot{Q}U1_{k,cU} \cdot locU_{cU,Hts}$
In Sub_i: $\forall P \in \{hP, cP\}$: replace $d\dot{Q}P_{k,P}$ with $\sum_{P} d\dot{Q}P_{k,P} \cdot locP_{P,Sub_i}$
In Sub_i: $\forall U \in \{hU, cU\}$: replace $d\dot{Q}U_{k,U}$ with $\sum_{U} \dot{Q}U_{U} \cdot d\dot{Q}U1_{k,U} \cdot locU_{U,Sub_i}$

Fig. 52: Phantom heat routes (simplified notation)

In order to block phantom heat route **1**, extra equations are developed. Equation EXT1 demands that, in each temperature interval, the heat released by the heat network's hot stream can either be send out to a subsystem or be absorbed by to the other cold streams in the Hts. In a similar way, equation EXT2 demands that, in each temperature interval, the heat absorbed by the heat network's cold stream is either received from a subsystem or supplied by the other hot streams in the Hts. Note that the heat residuals R are not included in the equation. It can be proven that equations EXT1 and EXT2 with or without the heat residuals, in combination with the thermal energy balances of the Hts, are equivalent, in analogy with the cold and hot stream balances. However, these extra equations cannot avoid that heat sent out by the heat network's hot stream to a subsystem is immediately send back to the Hts and subsequently absorbed by the heat network's cold stream in that same temperature interval (route 2 in Fig. 52).

Hot and cold stream balances *(simplified notation)*

HC6 $\quad \forall k < k_{max}: \sum_{Sub} \boldsymbol{d\dot{Q}HS}_{Sub,k} \leq \boldsymbol{d\dot{Q}}_{k,hs'} + \boldsymbol{d\dot{Q}U}_{k,Hnwh}$

HC7 $\quad \forall k < k_{max}: \sum_{Sub} \boldsymbol{d\dot{Q}SH}_{Sub,k} \leq -\boldsymbol{d\dot{Q}}_{k,cs'} - \boldsymbol{d\dot{Q}U}_{k,Hnwc}$

Extra equations to avoid phantom heat *(simplified notation)*

EXT1 $\quad \forall k < k_{max}: \boldsymbol{d\dot{Q}U}_{k,Hnwh} \leq \sum_{Sub} \boldsymbol{d\dot{Q}HS}_{Sub,k} - \boldsymbol{d\dot{Q}}_{k,cs'}$

EXT2 $\quad \forall k < k_{max}: -\boldsymbol{d\dot{Q}U}_{k,Hnwc} \leq \sum_{Sub} \boldsymbol{d\dot{Q}SH}_{Sub,k} + \boldsymbol{d\dot{Q}}_{k,hs'}$

EXT3 $\quad \forall k < k_{max}: \boldsymbol{d\dot{Q}SH}_{Sub,k} \leq R_{Sub,k+1} + \boldsymbol{d\dot{Q}P}_{k,hP} + \boldsymbol{d\dot{Q}U}_{k,hU}$

EXT4 $\quad \forall k < k_{max}: \boldsymbol{d\dot{Q}HS}_{Sub,k} \leq R_{Sub,k} - \boldsymbol{d\dot{Q}P}_{k,cP} - \boldsymbol{d\dot{Q}U}_{k,cU}$

To tackle this problem, another set of equations is added to the formulation. Equation EXT3 demands that for a subsystem in a certain temperature interval the heat sent out to the Hts can be delivered either by the heat residual from the temperature interval above or by the subsystem's hot streams. Similarly, equation EXT4 demands that for a subsystem in a certain temperature interval the heat received from the Hts can be either cascaded to the temperature interval below or absorbed by the subsystem's cold streams. Note that in equation EXT4 the heat residual is included in order to allow a heat load received from the Hts to be cascaded down in the subsystem before being absorbed by cold streams. Analogously, equation EXT3 allows that heat from hot streams in the subsystem can first be cascaded down before it is sent to the Hts. However, additional equations EXT1-EXT4 cannot prevent phantom heat in every situation. Indeed, the heat network's hot stream could send a heat load to a subsystem, where it is cascaded to the interval below, and in that interval immediately sent back to the Hts before being absorbed by the heat network's cold stream (route 3 in Fig. 52). It can be concluded that the heat cascade formulation is insufficient to prohibit phantom heat, even with the set of additional equations discussed in this subsection.

The LP transshipment model of Papoulias *et al.* [85] for calculation of minimum utility costs with restricted matches (RP1) could offer a solution, because streams with restrictions are treated separately from streams without restrictions. However, it is outside the scope of the present work to completely reconfigure the heat cascade formulation.

4.4.5.3. Formulation of extra equations to avoid phantom heat

The additional equations are not included in the final model, because they are not sufficient to block phantom heat. Nonetheless, their complete multi-period formulation is given below.

Extra equations to avoid phantom heat (full notation)

For EXT1-EXT4: $Ins.ord \leq iU(cU), Ins.ord \leq iU(hU)$

EXT1 $\forall\, Hts, S, k \big| k < k_{max,S}$:

$$\sum_{Hnwh,Ins} \boldsymbol{\dot{Q}U}_{Hnwh,Ins,S} \cdot d\dot{Q}U1_{k,Hnwh,S} \cdot locU_{Hnwh,Hts} \leq \sum_{Sub} \boldsymbol{d\dot{Q}HS}_{Sub,k,S} - \sum_{cU \notin \{Hnwc\},Ins} \boldsymbol{\dot{Q}U}_{cU,Ins,S} \cdot d\dot{Q}U1_{k,cU,S} \cdot locU_{cU,Hts} - \sum_{cP} d\dot{Q}P_{k,cP,S} \cdot locP_{cP,Hts}$$

EXT2 $\forall\, Hts, S, k \big| k < k_{max,S}$:

$$-\sum_{Hnwc,Ins} \boldsymbol{\dot{Q}U}_{Hnwc,Ins,S} \cdot d\dot{Q}U1_{k,Hnwc,S} \cdot locU_{Hnwc,Hts} \leq \sum_{Sub} \boldsymbol{d\dot{Q}SH}_{Sub,k,S} + \sum_{hU \notin \{Hnwh\},Ins} \boldsymbol{\dot{Q}U}_{hU,Ins,S} \cdot d\dot{Q}U1_{k,hU,S} \cdot locU_{hU,Hts} + \sum_{hP} d\dot{Q}P_{k,hP,S} \cdot locP_{hP,Hts}$$

EXT3 $\forall\, Sub, S, k \big| k < k_{max,S}$:

$$\boldsymbol{d\dot{Q}SH}_{Sub,k,S} \leq \boldsymbol{R}_{Sub,k+1,S} + \sum_{hP} d\dot{Q}P_{k,hP,S} \cdot locP_{hP,Sub} + \sum_{hU,Ins} \boldsymbol{\dot{Q}U}_{hU,Ins,S} \cdot d\dot{Q}U1_{k,hU,S} \cdot locU_{hU,Sub}$$

EXT4 $\forall\, Sub, S, k \big| k < k_{max,S}$:

$$\boldsymbol{d\dot{Q}HS}_{Sub,k,S} \leq \boldsymbol{R}_{Sub,k,S} - \sum_{cP} d\dot{Q}P_{k,cP,S} \cdot locP_{cP,Sub} - \sum_{cU,Ins} \boldsymbol{\dot{Q}U}_{cU,Ins,S} \cdot d\dot{Q}U1_{k,cU,S} \cdot locU_{cU,Sub}$$

4.4.6. Heat transfer unit envelope curve

In an energy system, restrictions to direct heat exchange between (groups of) thermal streams limit the heat recovery potential and increase the system's minimum energy requirement targets, compared to the situation without restrictions. However, this energy penalty can be decreased by integrating heat networks. The heat transfer unit envelope developed by Becker *et al.* [62] assists in choosing appropriate temperature ranges for heat networks that completely avoid the energy penalty. The envelope is integrated into the heat cascade formulation as a fictive heat network, enabling indirect heat exchange between thermal streams of different subsystems. Its hot and cold stream can separately adopt different heat loads at each temperature interval, and these heat loads are calculated in such a way that the energy penalty is completely avoided. In other words, the optimised envelope removes the heat exchange restrictions, and utilities operate at the levels that would be obtained when optimising the system without restrictions. The envelope's cold (hot) stream forms an upper (lower) limiting curve for the cold (hot) composite curve of the optimal heat networks.

The envelope for the example described in subsection 4.4.5.1 is shown in Fig. 53 and Fig. 54. Obviously, the envelope cold (hot) stream corresponds to certain hot (cold) streams in the system. A set of heat networks with shifted temperature ranges that are perfectly enclosed by the envelope completely avoids the energy penalty. Moreover, a heat network encompassed by the envelope is not prone to phantom heat, because the heat load of its cold (hot) stream can be completely supplied (absorbed) by the heat loads of the thermal streams in the subsystems, calculated for the situation without heat exchange restrictions (Fig. 54). In contrast, if the hot and cold stream of a heat network are not embedded in the envelope, phantom heat can occur (Fig. 53).

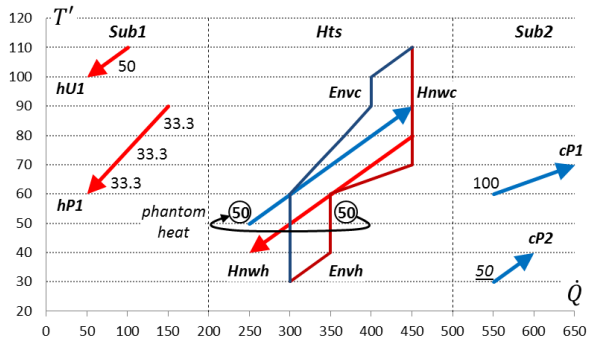

Fig. 53: Hot and cold stream of heat network not embedded in envelope, phantom heat possible

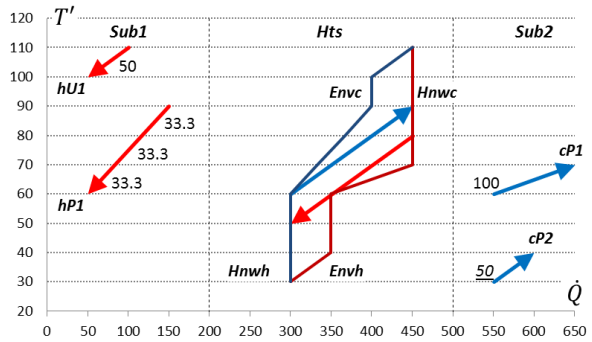

Fig. 54: Hot and cold stream of heat network embedded in envelope, no phantom heat

4.4.6.1. Influence of phantom heat on calculation of energy penalty

The disruptive influence of phantom heat on the calculation of the energy penalty can be better understood by means of a simple example. Consider an energy system consisting of two subsystems connected by a heat transfer system. The first subsystem (Sub1) includes two hot process streams (hP1 and hP2), both with a heat load of 100 kW. The second subsystem (Sub2) contains a cold process stream (cP1) of 200 kW, while the heat transfer system (Hts) contains a heat network (Hnw), a hot utility (hU1) and a cold utility (cU1). All stream data is depicted in Fig. 57 in the shifted temperature domain, taking into account a $\Delta Tmin$ of 10°C. In this simple example, there is no heat recovery in the subsystems because Sub 1 only contains hot streams and Sub 2 only a cold stream, but the reasoning is analogue for more complex systems.

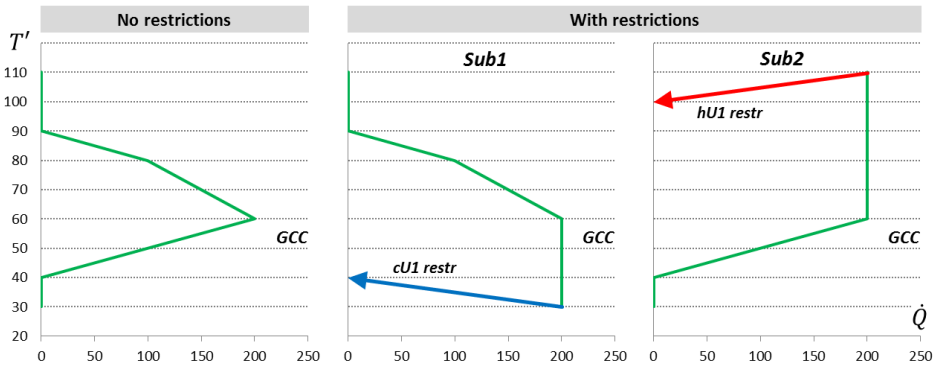

Fig. 55: Utility requirement with and without heat exchange restrictions

If no heat exchange restrictions are taken into account, the energy system does not require any utility. But with restrictions and without heat network, a cold utility of 200 kW in Sub1 and a hot utility of 200 kW in Sub 2 are needed (see Fig. 55). This energy penalty of 200 kW is visualised in Fig. 56.

When the hot and cold stream of the heat network are embedded in the envelope, the hot processes in Sub 1 transfer heat to the cold process in Sub 2 via the heat network, and no hot or cold utility is required (see Fig. 57). As a result, the energy penalty is reduced to zero. Cost optimisation will select and operate the heat network rather than the hot and cold utilities, as long as the heat network costs stay sufficiently low in comparison to the utility costs.

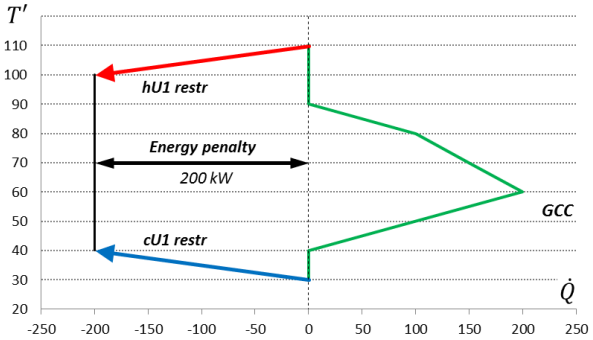

Fig. 56: Energy penalty due to heat exchange restrictions

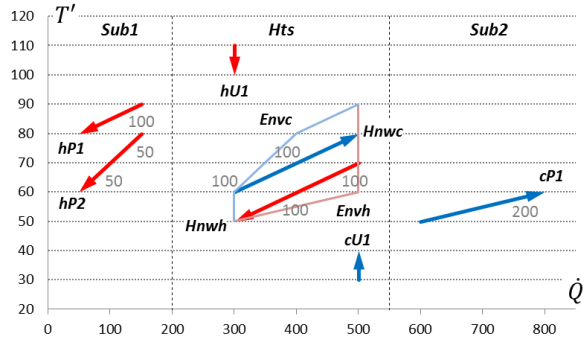

Fig. 57: Energy system with heat network embedded in the envelope to avoid the energy penalty

A heat network with a temperature range for which the heat network hot and cold streams are not embedded in the envelope, however, induces extra utility requirements or phantom heat, as shown in parts A-D of Fig. 58. In the current example, phantom heat appears when both hot and cold stream of the heat network fall outside the envelope (see parts B and D of Fig. 58). If beneficial, the optimisation model choses free phantom heat over increased utility loads, which involve extra costs. Due to phantom heat, the real utility loads in situations B and D, and thus the energy penalty, cannot be calculated correctly by the heat cascade model.

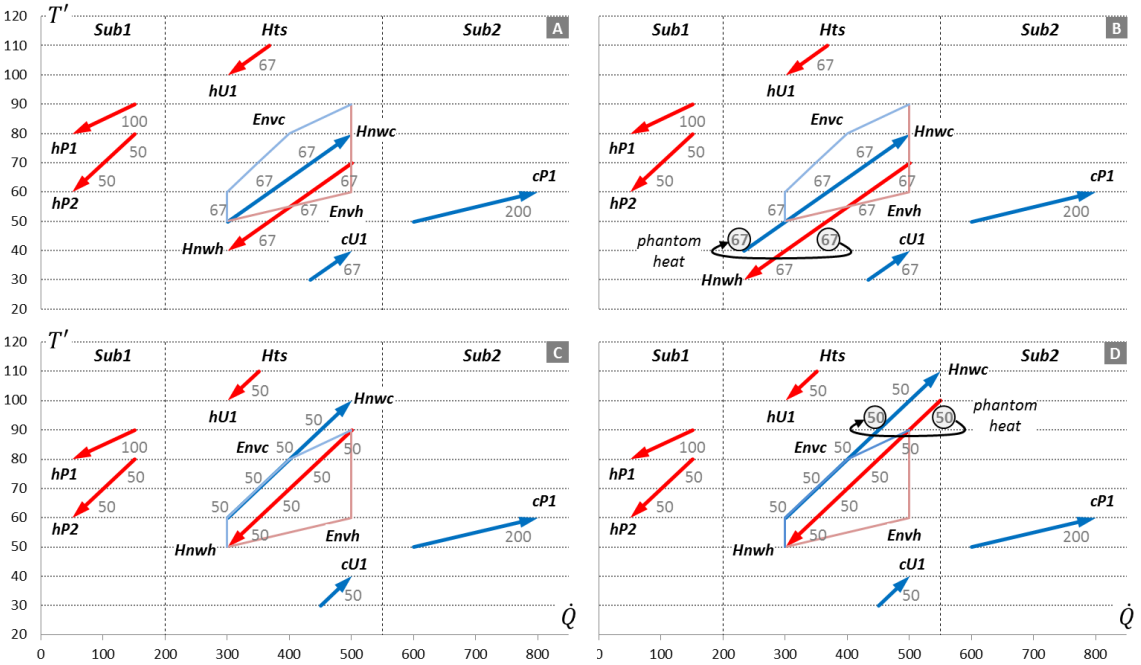

Fig. 58: Occurrence of phantom heat and influence on the calculation of the energy penalty for different heat network temperature ranges

(Parameter values: hU1: cI = 0 €/kW, cF = 0,05 €/kWh, η = 1; Hnw: cI = 100 €/kW, η = 4, , $cost\_el$ = 0.01 €/kWh)

4.4.6.2. Trade-off between utility and heat network costs in envelope calculation

The methodology described by Becker *et al.* [62] performs well for the example described in their publication. But, when investment or operation costs are assigned to heat networks or when their electricity consumption is taken into account, the model formulation to calculate the envelope needs to be modified. Indeed, the original formulation does not assign any costs or electricity usage to the envelope. However, the envelope and the composite curves of the embedded heat networks can only be equivalent if they induce identical costs into the objective function. In other words the trade-off between utility costs and heat network costs already needs to be made at the stage of the envelope calculation. The optimisation could increase utility loads and decrease heat network loads if this would results in lower total costs.

If this trade-off is not equivalent for both envelope and heat networks, it cannot be guaranteed that the composite curves of the heat networks will be perfectly enclosed by the envelope curve, even if their temperature ranges are adequately chosen, based on the envelope. Therefore, *Syn-E-Sys* uses a modified version of the original envelope calculation approach, which is presented and evaluated in the next subsection.

4.4.6.3. Integration envelope in heat cascade model

The heat cascade model to calculate the envelope is derived from the formulation developed in subsection 4.4.3.1, by modifying and adding equations. The envelope is integrated into the heat cascade in a similar way as thermal utility streams (see Fig. 59), but induces more decision variables. For a thermal utility U, the heat loads $d\dot{Q}U_{k,U}$ per temperature interval are a function of one decision variable $\boldsymbol{\dot{Q}U}_U$ expressing the utility's overall heat load: $d\dot{Q}U_{k,U} = \boldsymbol{\dot{Q}U}_U \cdot d\dot{Q}U1_{k,U} \cdot locU_{U,Sub}$. The envelope's hot and cold stream on the other hand, can separately adopt a different heat load at each temperature interval, each corresponding to a separate decision variable.

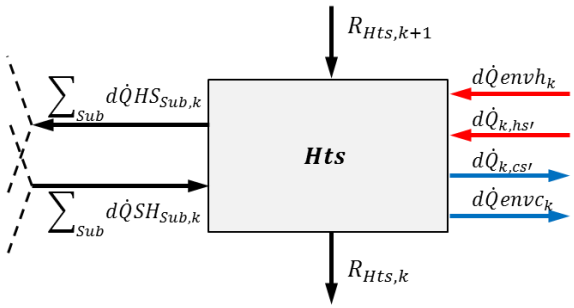

For full notation:
replace $d\dot{Q}_{k,hs'}$ with $\sum_{hP} d\dot{Q}P_{k,hP} \cdot locP_{hP,Hts} + \sum_{hU \in \{Hnwh\}} \dot{Q}U_{hU} \cdot d\dot{Q}U1_{k,hU} \cdot locU_{hU,Hts}$
replace $d\dot{Q}_{k,cs'}$ with $\sum_{cP} d\dot{Q}P_{k,cP} \cdot locP_{cP,Hts} + \sum_{cU \in \{Hnwc\}} \dot{Q}U_{cU} \cdot d\dot{Q}U1_{k,cU} \cdot locU_{cU,Hts}$

Fig. 59: Integration of heat loads per temperature interval for envelope hot and cold streams in the heat cascade of the heat transfer system

The thermal balances HC2, HC6 and HC7 of the model in subsection 4.4.3.1 are modified to integrate the envelope heat loads $\boldsymbol{d\dot{Q}envh}_k$ and $\boldsymbol{d\dot{Q}envc}_k$, resulting in respectively equations ENV1, ENV2 and ENV3. Equation ENV4 is added to ensure that the envelope's hot and cold stream represent the same total heat load. Furthermore, the envelope cold stream must be hotter than the hot stream, which is guaranteed by equation ENV5. Equation ENV6 calculates the nominal load of the envelope, to which

investment can be assigned. Furthermore, the electrical energy balances EB1 and EB2 are adapted to include the electricity consumption that can be associated with the envelope hot stream (ENV7 and ENV8). The envelope's efficiency η_env expresses the ratio of transported heat load to electricity load required for pumping (see subsection 4.3.4.3), and is equal to the (maximum) efficiency of the heat networks that will be integrated. Finally, the specific investment (cI_env) and operation and maintenance costs (cOM_env) that can be related to the envelope are inserted in the objective function (ENV9). These specific costs are equal to the (minimum of the) corresponding costs for heat networks.

Obviously, minimisation of operation costs corresponds to minimising the total heat load of the envelope, and therefore a value for the specific operation cost must always be specified. In order to obtain an envelope cold stream with the highest and a hot stream with the lowest temperatures possible, the summation of the total system's heat residuals ($\boldsymbol{Rtot}_k = \sum_{Sys} \boldsymbol{R}_{Sys,k}$) must be minimised. It is included in the objective function with a factor 10^{-5} to avoid significant influence on the objective value. A higher factor could result in a different, sub-optimal system configuration after optimisation. Note that, since the hot and cold stream balances demand that heat is cascaded in the subsystems rather than in the heat transfer system, $\boldsymbol{R}_{Hts,k}$ will be zero and ENV9 will minimise $\sum_{Sub} \boldsymbol{R}_{Sub,k}$. The formulation is easily extended to multi-period and varying stream temperatures, analogous to subsection 4.4.3.2.

Thermal energy balances

ENV1 $\forall\, k < k_{max}$:

$$\boldsymbol{R}_{Hts,k+1} - \boldsymbol{R}_{Hts,k} + \sum_{P} d\dot{Q}P_{k,P} \cdot locP_{P,Hts} + \sum_{U} \dot{\boldsymbol{Q}}\boldsymbol{U}_{U} . d\dot{Q}U1_{k,U} \cdot locU_{U,Hts} + \sum_{Sub} \boldsymbol{d\dot{Q}SH}_{Sub,k} - \sum_{Sub} \boldsymbol{d\dot{Q}HS}_{Sub,k} + \boldsymbol{d\dot{Q}envh}_k - \boldsymbol{d\dot{Q}envc}_k = 0$$

ENV2 $\forall\, k < k_{max}$:

$$\sum_{Sub} \boldsymbol{d\dot{Q}HS}_{Sub,k} \leq \sum_{hP} d\dot{Q}P_{k,hP} \cdot locP_{hP,Hts} + \sum_{hU} \dot{\boldsymbol{Q}}\boldsymbol{U}_{hU} \cdot d\dot{Q}U1_{k,hU} \cdot locU_{hU,Hts} + \boldsymbol{d\dot{Q}envh}_k$$

ENV3 $\forall\, k < k_{max}$:

$$\sum_{Sub} \boldsymbol{d\dot{Q}SH}_{Sub,k} \leq -\sum_{cP} d\dot{Q}P_{k,cP} \cdot locP_{cP,Hts} - \sum_{cU} \dot{\boldsymbol{Q}}\boldsymbol{U}_{cU} \cdot d\dot{Q}U1_{k,cU} \cdot locU_{cU,Hts} + \boldsymbol{d\dot{Q}envc}_k$$

ENV4 $$\sum_{k<k_{max}} \boldsymbol{d\dot{Q}envh}_k = \sum_{k<k_{max}} \boldsymbol{d\dot{Q}envc}_k$$

ENV5 $\forall\, k < k_{max}$: $$\sum_{k^*|k\leq k^*<k_{max}} \boldsymbol{d\dot{Q}envh}_{k^*} \leq \sum_{k^*|k\leq k^*<k_{max}} \boldsymbol{d\dot{Q}envc}_{k^*}$$

ENV6 $$\dot{\boldsymbol{Q}}\boldsymbol{nom\_env} \geq \sum_{k|k<k_{max}} \boldsymbol{d\dot{Q}envh}_k$$

Electrical energy balances

ENV7 $$\boldsymbol{Imp\_el} + \sum_{E,L} \boldsymbol{P\_el}_{E,L} + \sum_{HEh,L} \dot{\boldsymbol{Q}}_{HEh,L} \geq dem\_el + \sum_{U|use\_elU(U),L} \dot{\boldsymbol{Q}}\boldsymbol{in}_{U,L} + \sum_{k|k<k_{max}} \frac{\boldsymbol{d\dot{Q}envh}_k}{\eta_{env}}$$

ENV8 $$\boldsymbol{Imp\_el} + \sum_{E,L} \boldsymbol{P\_el}_{E,L} + \sum_{HEh,L} \dot{\boldsymbol{Q}}_{HEh,L} = dem\_el + \sum_{U|use\_elU(U),L} \dot{\boldsymbol{Q}}\boldsymbol{in}_{U,L} + \sum_{k|k<k_{max}} \frac{\boldsymbol{d\dot{Q}envh}_k}{\eta_{env}} + \boldsymbol{Exp\_el}$$

Objective

ENV9

$$\begin{aligned}
\boldsymbol{cost_env} = & \sum_{U|usefuelU(U),L} \dot{\boldsymbol{Q}}\boldsymbol{in}_{U,Ins,S,L} \cdot hrs_y \cdot cF_U + \sum_{E|usefuelE(E),L} \dot{\boldsymbol{Q}}\boldsymbol{in_el}_{E,L} \cdot hrs_y \cdot cF_el_E \\
& + \sum_{U|OMcostU(U)} \dot{\boldsymbol{Q}}\boldsymbol{U}_U \cdot hrs_y \cdot cOM_U + \sum_{E|OMcostE(E),L} \boldsymbol{P_el}_{E,L} \cdot hrs_y \cdot cOM_el_E \\
& + Anf \cdot \sum_{U|fcostU(U),Lc} \boldsymbol{Inv}_{U,Lc} + Anf \cdot \sum_{E|fcostE(E),Lc} \boldsymbol{Inv_el}_{E,Lc} \\
& + \boldsymbol{Imp_el} \cdot hrs_y \cdot cost_el - \boldsymbol{Exp_el}_S \cdot hrs_y \cdot revs_el \\
& + \sum_{k<k_{max}} \left(\boldsymbol{d\dot{Q}envh}_k \cdot hrs_y \cdot cOM_env\right) + Anf \cdot \dot{\boldsymbol{Q}}\boldsymbol{nom_env} \cdot cI_env + 10^{-5} \cdot \sum_{k<k_{max}} \boldsymbol{Rtot}_k
\end{aligned}$$

$$\boldsymbol{d\dot{Q}envh}_k, \boldsymbol{d\dot{Q}envc}_k, \dot{\boldsymbol{Q}}\boldsymbol{nom\_env} \in \mathbb{R}^+, \boldsymbol{cost\_env} \in \mathbb{R}$$

The original objective function in the formulation of [62], is expressed in equation ORIG below using the terminology of *Syn-E-Sys*, in order to better indicate the modifications

ORIG

$$\begin{aligned}
\boldsymbol{cost_env} = & \sum_{U|usefuelU(U),L} \dot{\boldsymbol{Q}}\boldsymbol{in}_{U,Ins,S,L} \cdot hrs_y \cdot cF_U + \sum_{E|usefuelE(E),L} \dot{\boldsymbol{Q}}\boldsymbol{in_el}_{E,L} \cdot hrs_y \cdot cF_el_E \\
& + \sum_{U|OMcostU(U)} \dot{\boldsymbol{Q}}\boldsymbol{U}_U \cdot hrs_y \cdot cOM_U + \sum_{E|OMcostE(E),L} \boldsymbol{P_el}_{E,L} \cdot hrs_y \cdot cOM_{el_E} \\
& + \boldsymbol{Imp_el} \cdot hrs_y \cdot cost_el - \boldsymbol{Exp_el}_S \cdot hrs_y \cdot revs_el \\
& + 10^7 \cdot \left(\sum_{k<k_{max}} \left(\boldsymbol{d\dot{Q}envh}_k \cdot 1\right) + \sum_{k<k_{max}} \boldsymbol{Rtot}_k \right)
\end{aligned}$$

4.4.6.4. Calculation Strategy

The envelope calculation method proposed by Becker *et al.* [62] comprises three phases (Fig. 60).

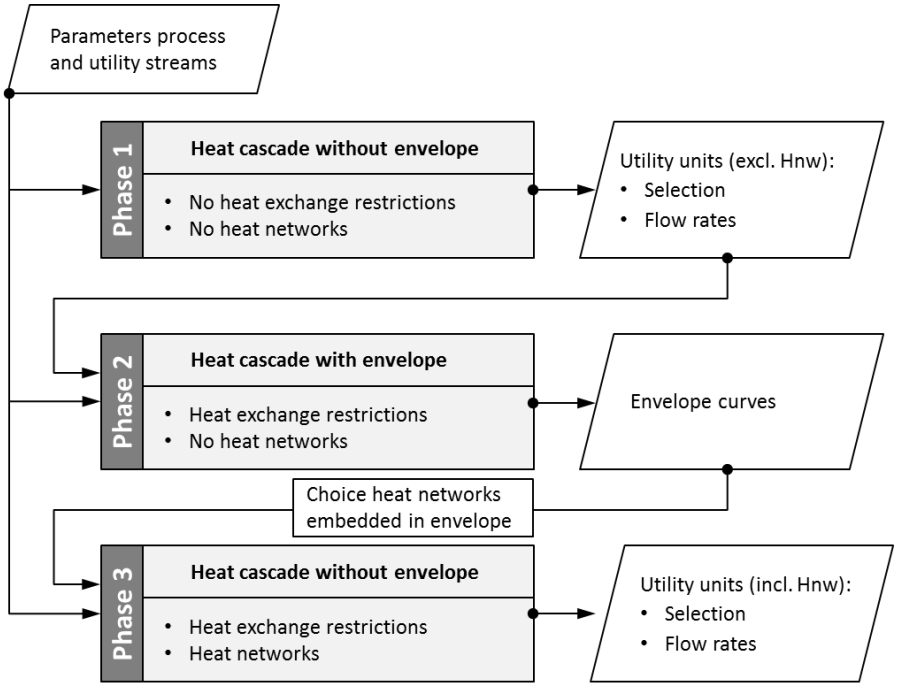

Fig. 60: Envelope calculation strategy proposed by Becker *et al.* [62]

In the first phase, all heat exchange restrictions are removed and the energy system is optimised using the heat cascade model without envelope, excluding heat networks. In the second phase, all utility flow rates are fixed at their optimal values obtained in the first phase and the system is optimised using the heat cascade model with envelope, taking into account the heat exchange restrictions. The resulting envelope assists in choosing appropriate heat networks and their temperature ranges. In the third phase, the energy system including the chosen heat networks is optimised using the heat cascade model without envelope and with restrictions.

However, as explained before, this solution strategy is not sufficient when investment or operation costs are assigned to heat networks or when their electricity consumption is taken into account. In that case, the trade-off between utility costs and heat network costs must also be made when calculating the envelope. To enable this trade-off, the utility heat loads cannot be fixed when calculating the envelope.

Therefore, the proposed strategy comprises only two phases (Fig. 61). In the first phase, the envelope and the utility system without heat networks are simultaneously optimised taking account the heat exchange restrictions. Specific costs cOM_env and cI_env and electrical efficiency η_{env} are assigned to the envelope, equivalent with the costs and efficiency of the initially proposed heat networks. In the second phase, the heat cascade model without envelope and with the proposed heat networks is optimised, subject to heat exchange restrictions. If heat network temperature ranges in the shifted temperature domain are embedded within the envelope, the solution is satisfactory. If not, the heat network temperature ranges need to be adapted to fall within the envelope.

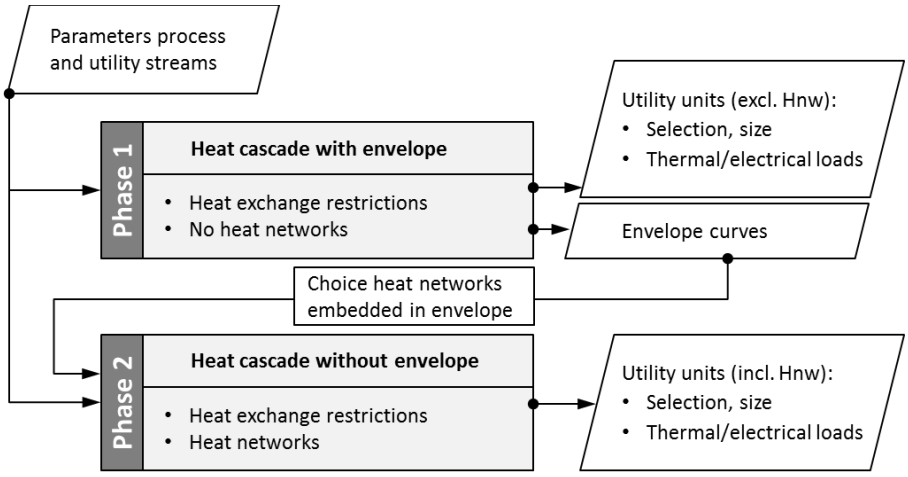

Fig. 61: Modified envelope calculation strategy

In a multi-period situation, each time slice corresponds to a different envelope in which the heat networks must be embedded to avoid the energy penalty and to cancel out phantom heat. As a consequence, the heat network temperature ranges need to vary with the time slices.

For the modified envelope calculation strategy a number of limitations have to be considered. Firstly, since only one efficiency, specific investment cost and specific operation and maintenance cost can be assigned to the envelope, all heat networks that are integrated in the second phase need to have the same specific cost and efficiency. Moreover, heat network investment costs cannot be subject to

economy of scale, but must feature a constant specific investment cost. As the envelope's efficiency is represented by a single constant value, the heat networks must feature a linear part-load curve.

The second limitation is only relevant for multi-period and when two or more heat networks are integrated with non-zero investment costs. The nominal value of the envelope, inducing investment costs in the objective function, is equal to the maximum total heat load of the envelope over all time slices. The heat networks on the other hand, can each attain their maximum heat load in different time slices. Consequently, the combined investment cost of the heat networks can be greater than the investment cost related to the envelope. As a result, different utility system configurations could be found by the heat cascade models in both calculation stages.

Thirdly, the trade-off between the costs of the utility system and the costs related to the envelope (representing heat network costs) significantly increases the number of decision variables in the optimisation model, leading to higher computation times compared to [62].

As a fourth point of concern, the envelope calculation and the heat network optimisation can result in different alternative solutions with the same objective value. In that case, it is possible that the heat network temperature-heat curves are not embedded in the envelope.

Finally, if the minimum temperature approach between the hot (cold) heat network stream and other cold (hot) streams is smaller than or equal to the minimum temperature approach between these other streams, it is guaranteed that a shifted heat network temperature range can be found that can be embedded in the envelope.

In conclusion, the equivalence between envelope and heat network composite curves is guaranteed for a generic problem when a number of conditions are fulfilled: Specific operation costs (or alternatively specific electricity consumption) need to be the same for all heat networks. In addition, for multi-period problems, specific investment costs need to be zero for all heat networks. If these conditions are not met, there is no guarantee that the envelope indicates appropriate heat network temperature ranges that avoid the energy penalty and cancel out phantom heat. However, the heat cascade model can still be used to optimise the system and integrate heat networks. But, the solution needs to be checked for phantom heat and if it occurs, an appropriate heat network temperature ranges need to be determined by trial and error.

A steam network is not prone to phantom heat because the shifted temperature-heat curves of its hot and cold stream are horizontal and do not overlap on the temperature axis.

4.4.7. Formulation extended heat cascade model with envelope

This subsection describes the parameters, variables and equations in the formulation of the multi-period heat cascade model with heat exchange restrictions, equipped with the heat transfer envelope, accounting for variable stream temperatures that follow a priori defined variations.

4.4.7.1. Sets and parameters

Parameters

Envelope

η_{env}	efficiency envelope, equivalent to efficiency heat networks
cOM_env	O&M cost envelope [€/kWh]
cI_env	specific investment cost envelope (€/kW)

4.4.7.2. Variables

Objective function

$\boldsymbol{cost\_env}$	$\mathbb{R}$	objective heat cascade model with envelope

Thermal balances

$\boldsymbol{d\dot{Q}envh_{k,S}}$	$\mathbb{R}^+$	heat load hot stream envelope in temperature interval k, time slice S (kW)
$\boldsymbol{d\dot{Q}envc_{k,S}}$	$\mathbb{R}^+$	electricity export in time slice S (kW)

4.4.7.3. Equations

Thermal energy balances

For ENV1: $Ins.ord \leq iU(U)$, ENV2: $Ins.ord \leq iU(hU)$, ENV3: $Ins.ord \leq iU(cU)$

ENV1 $\forall\, Hts, S, k \big| k < k_{max,S}$:

$$\boldsymbol{R}_{Hts,k+1,S} - \boldsymbol{R}_{Hts,k,S} + \sum_{P} d\dot{Q}P_{k,P,S} \cdot locP_{P,Hts} + \sum_{U,Ins} \boldsymbol{\dot{Q}U}_{U,Ins,S} \cdot d\dot{Q}U1_{k,U,S} \cdot locU_{U,Hts}$$
$$+ \sum_{sub} \boldsymbol{d\dot{Q}SH}_{sub,k,S} - \sum_{sub} \boldsymbol{d\dot{Q}HS}_{sub,k,S} + \boldsymbol{d\dot{Q}envh}_{k,S} - \boldsymbol{d\dot{Q}envc}_{k,S} = 0$$

ENV2 $\forall\, Hts, S, k \big| k < k_{max,S}$:

$$\sum_{Sub} \boldsymbol{d\dot{Q}HS}_{Sub,k,S} \leq \sum_{hP} d\dot{Q}P_{k,hP,S} \cdot locP_{hP,Hts} + \sum_{hU,Ins} \boldsymbol{\dot{Q}U}_{hU,Ins,S} \cdot d\dot{Q}U1_{k,hU,S} \cdot locU_{hU,Hts}$$
$$+ \boldsymbol{d\dot{Q}envh}_{k,S}$$

ENV3 $\forall\, Hts, S, k \big| k < k_{max,S}$:

$$\sum_{Sub} \boldsymbol{d\dot{Q}SH}_{Sub,k,S} \leq -\sum_{cP} d\dot{Q}P_{k,cP,S} \cdot locP_{cP,Hts} - \sum_{cU,Ins} \boldsymbol{\dot{Q}U}_{cU,Ins,S} \cdot d\dot{Q}U1_{k,cU,S} \cdot locU_{cU,Hts}$$
$$+ \boldsymbol{d\dot{Q}envc}_{k,S}$$

ENV4 $\forall\, S$:

$$\sum_{k|k<k_{max,S}} \boldsymbol{d\dot{Q}envh}_{k,S} = \sum_{k|k<k_{max,S}} \boldsymbol{d\dot{Q}envc}_{k,S}$$

ENV5 $\forall\, S, k \big| k < k_{max,S}$:

$$\sum_{k^*|k\leq k^*<k_{max,S}} \boldsymbol{d\dot{Q}envh}_{k^*,S} \leq \sum_{k^*|k\leq k^*<k_{max,S}} \boldsymbol{d\dot{Q}envc}_{k^*,S}$$

ENV6 $\forall\, S$:

$$\boldsymbol{\dot{Q}nom\_env} \geq \sum_{k|k<k_{max,S}} \boldsymbol{d\dot{Q}envh}_{k,S}$$

Electrical energy balances

For ENV7, ENV8: $Ins.ord \leq iU(U), Ins.ord \leq iE(E)$

ENV7 $\forall S$:

$$\boldsymbol{Imp\_el}_S + \sum_{E,Ins,L} \boldsymbol{P\_el}_{E,Ins,S,L} + \sum_{\substack{U,Ins,L| \\ gen\_elU(U)}} \dot{\boldsymbol{Q}}_{U,Ins,S,L} \geq$$

$$dem\_el_S + \sum_{\substack{U,Ins,L| \\ use\_elU(U)}} \dot{\boldsymbol{Q}}\boldsymbol{in}_{U,Ins,S,L} + \sum_{k|k<k_{max,S}} \frac{\boldsymbol{d\dot{Q}envh}_{k,S}}{\eta_{env}}$$

ENV8 $\forall S$:

$$\boldsymbol{Imp\_el}_S + \sum_{E,Ins,L} \boldsymbol{P\_el}_{E,Ins,S,L} + \sum_{\substack{U,Ins,L| \\ gen\_elU(U)}} \dot{\boldsymbol{Q}}_{U,Ins,S,L} = \boldsymbol{Exp\_el}_S +$$

$$dem\_el_S + \sum_{\substack{U,Ins,L| \\ use\_elU(U)}} \dot{\boldsymbol{Q}}\boldsymbol{in}_{U,Ins,S,L} + \sum_{k|k<k_{max,S}} \frac{\boldsymbol{d\dot{Q}envh}_{k,S}}{\eta_{env}}$$

Objective

ENV9 $Ins.ord \leq iU(U), Ins.ord \leq iE(E)$

$$\boldsymbol{cost\_env} =$$

$$\sum_{U|usefuelU(U),Ins,S,L} \dot{\boldsymbol{Q}}\boldsymbol{in}_{U,Ins,S,L} \cdot hrs\_S_S \cdot cF_U + \sum_{E|usefuelE(E),Ins,S,L} \dot{\boldsymbol{Q}}\boldsymbol{in\_el}_{E,Ins,S,L} \cdot hrs\_S_S \cdot cF\_el_E$$

$$+ \sum_{U|OMcostU(U),Ins,S,L} \dot{\boldsymbol{Q}}_{U,Ins,S,L} \cdot hrs\_S_S \cdot cOM_U + \sum_{E|OMcostE(E),Ins,S,L} \boldsymbol{P\_el}_{E,Ins,S,L} \cdot hrs\_S_S \cdot cOM\_el_E$$

$$+ Anf \cdot \sum_{U|fcostU(U),Ins,Lc} \boldsymbol{Inv}_{U,Ins,Lc} + Anf \cdot \sum_{E|fcostE(E),Ins,Lc} \boldsymbol{Inv\_el}_{E,Ins,Lc}$$

$$+ \sum_{S} (\boldsymbol{Imp\_el}_S \cdot hrs\_S_S \cdot cost\_el_S - \boldsymbol{Exp\_el}_S \cdot hrs\_S_S \cdot revs\_el_S)$$

$$+ \sum_{S,k|k<k_{max,S}} \boldsymbol{d\dot{Q}envh}_{k,S} \cdot hrs\_S_S \cdot cOM\_env + Anf \cdot \dot{\boldsymbol{Q}}\boldsymbol{nom\_env} \cdot cI\_env$$

$$+10^{-5} \cdot \sum_{S,k|k<k_{max,S}} \boldsymbol{Rtot}_{k,S}$$

4.4.8. Integrating storage in heat cascade models

The integration of storage into the heat cascade model is similar to the integration of utilities. On the one hand, equations describing the technology behaviour of storage units are added as constraints. On the other hand, the equations in the heat cascade model describing thermal and electrical balances and the objective function are adapted to include the storage charge and discharge loads. More details are given in section 4.6.

4.4.9. Emission cap

Energy technologies driven by fossil fuel combustion generate carbon dioxide emissions proportional to the fuel input. To force the energy system optimisation model to design energy systems with lower carbon emissions, an equation (EM1) is added to the extended heat cascade formulations (with and without envelope) that keeps the total emission weight below a specified value. The carbon emissions per kW of fuel input are provided as input data to the model.

Total annual CO_2 emissions are calculated by summing up the carbon emissions from fuel combustion of all thermal (U) and all electrical utilities (E) over all time slices S the year, and adding the carbon emissions related to imported electricity.

Parameters

$iUCO2_U$	carbon intensity utility U (kg CO_2/kWh)
$iECO2_E$	carbon intensity utility E (kg CO_2/kWh)
$iCO2grid$	carbon intensity of electricity imported from the grid (kg CO_2/kWh)
$CO2cap$	upper limit to overall carbon emissions of the energy system (kg CO_2)

Constraints

Emissions

EM1: $Ins.ord \leq iU(U), Ins.ord \leq iE(E)$

$$\sum_{U|usefuelU(U),\ Ins,S,L} \boldsymbol{\dot{Q}in}_{U,Ins,S,L} \cdot hrs\_S_S \cdot iUCO2_U + \sum_{E|usefuelE(E),\ Ins,S,L} \boldsymbol{\dot{Q}inel}_{E,Ins,S,L} \cdot hrs\_S_S \cdot iECO2_E + \sum_S \boldsymbol{Imp\_el}_S \cdot hrs\_S_S \cdot iCO2grid \leq CO2cap$$

4.5. Automated superstructure expansion

4.5.1. Considering multiple units per technology type

As pointed out by Voll *et al.* [50], optimising the design of an energy system is a complex task, because multiple trade-offs have to be considered simultaneously. Energy technology units must be selected, sized and operated in such a way that energy demands can be fulfilled at each time slice. Due to economy of scale effects on technology investment costs, larger sized units will be promoted over smaller ones in order to curb the overall system cost. Furthermore, it is advantageous to size technologies in such a way that they can be operated near full load, as (in general) their efficiencies rise with increasing relative output load. Moreover, the relative load must be above a minimum threshold (typically 20%) and size must be within the economically available capacity range.

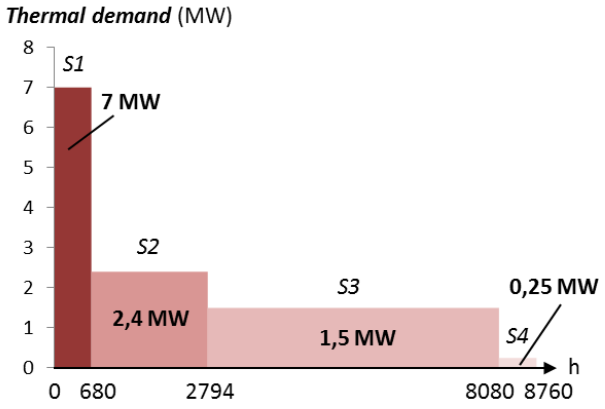

Fig. 62: Thermal energy demand illustrative energy system

As an illustration, *Syn-E-Sys* is applied on a simple energy system similar to the motivating example presented by Voll *et al.* [50]. Consider a system in which the time-varying thermal energy demand shown in Fig. 62, must be fulfilled by boiler units of type 'BoilerA'. For this technology type, the non-linear equations (Eq. a and Eq. b) characterising efficiency and investment cost are adopted from Voll [75], appendix A.

Eq. a $$\eta rel = \frac{C_1 + C_2 \cdot \dot{Q}rel + C_3 \cdot \dot{Q}rel^2 + C_4 \cdot \dot{Q}rel^3}{C_5 + C_6 \cdot \dot{Q}rel + C_7 \cdot \dot{Q}rel^2 + C_8 \cdot \dot{Q}rel^3}$$

values of constants $C_1 - C_8$ taken from [75]

Eq. b $$Inv = Inv_B \cdot \left(\dot{Q}nomL/\dot{Q}B\right)^M \Leftrightarrow cI = \frac{Inv}{\dot{Q}nomL} = \frac{Inv_B \cdot \left(\dot{Q}nomLrel \cdot \dot{Q}nommax\right)^{M-1}}{\dot{Q}B^M}$$

values of constants $Inv_B, \dot{Q}B, M$ taken from [75], $\dot{Q}nommax = 14MW$

The technology model developed in section 4.3 is calibrated by fitting the reference points for part-load operation (R) and investment cost (Rc) as close as possible to these non-linear curves, as shown by the squares in Fig. 63 and Fig. 64. Fuel costs of 0.05 €/kWh are assumed and available boiler sizes range from $\dot{Q}nommin$ = 0.1 MW to $\dot{Q}nommax$ = 14 MW. When only one boiler unit would be available, a capacity of 7MW is required to fulfil the peak demand in time slice S1. Consequently, its

minimum part-load threshold, specified as 20% of the capacity, equals 1.4 MW, which surpasses the 0.25 MW required in time slice S4. Since no cold utility is available to evacuate the excess heat from the system, the optimisation problem is infeasible. But if the heat demand in S4 is changed to 1.4 MW, a total cost of 1302 k€ is obtained, including an annual fuel cost of 1157 k€ and an investment cost of 145 k€.

Without restrictions to the number of boiler units (instances), the optimisation results in a system configuration with three boiler instances of different sizes. Except for unit 1 at time slice S2, all units work at full load in every time slice (see Table 11). These loads are indicated with dots on the part-load curve of Fig. 63. Obviously, the largest boiler unit features the lowest specific investment cost as indicated by the red dot in Fig. 64. The total system costs amount 1214 k€, including 1002 k€ of annual fuel costs and 212 k€ of investment costs. Comparing this result with the solution of the single-unit system proves that multiple units per technology type have to be considered to find the minimum cost solution. Clearly, a trade-off exists between total system cost and number of units per technology.

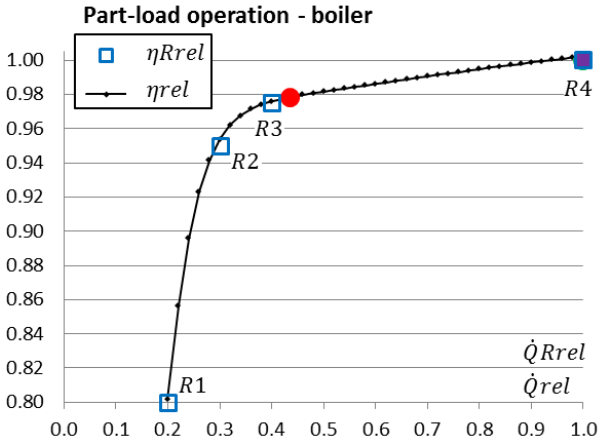

	R1	R2	R3	R4
$\dot{Q}Rrel$	0.200	0.300	0.400	1
$\eta Rrel$	0.800	0.950	0.975	1

Fig. 63: Fitting reference points to non-linear part-load curve boiler and indication optimised operation points

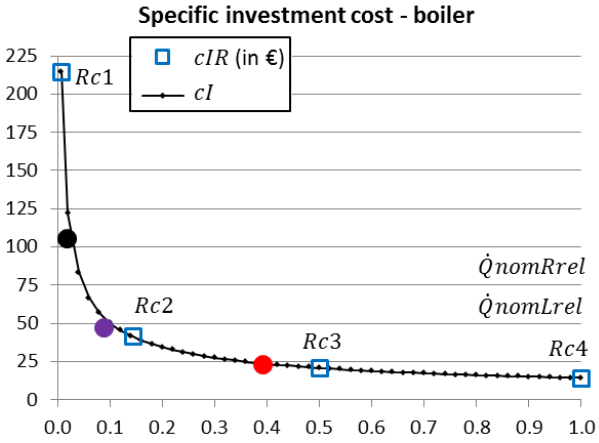

	Rc1	Rc2	Rc3	Rc4
$\dot{Q}nomRrel$	0.007	0.143	0.500	1
cIR	214.8	41.37	20.78	14.19

Fig. 64: Fitting reference points to non-linear specific investment curve boiler and indication optimised cost points:

(in MW)		$\dot{Q}nom$	$\dot{Q}U_{S1}$	$\dot{Q}U_{S2}$	$\dot{Q}U_{S3}$	$\dot{Q}U_{S4}$
BoilerA	*Ins1*	5.5	5.5	2.4		
BoilerA	*Ins2*	1.25	1.25		1.25	
BoilerA	*Ins3*	0.25	0.25		0.25	0.25

Table 11: Results

4.5.2. Concept of stepwise superstructure expansion

The number of units per technology type in the optimal energy system configuration, and in the superstructure embedding this configuration, is not known a priori. One way to cope with this is to provide a sufficiently large, fixed number of units per technology in the model's superstructure. However, this would considerably increase size and complexity of the optimisation problem, even when finally only a small number of units are used in the optimal solution. Therefore, Voll *et al.* [50] proposed a more efficient approach in which the model's superstructure is gradually expanded. In

this calculation method, a first optimisation run is performed on a superstructure containing a single unit per technology type. Subsequently, for every technology selected in the optimal configuration, one unit is added in the superstructure and a second optimisation run is started. If the objective value (representing total costs) resulting from the second run is lower than in the first run, again one unit is added to the superstructure for every technology for which all units are selected in the optimal solution and a third run is started. This procedure is repeated until there is no significant improvement in objective value compared to the previous run. A schematic representation of this procedure for automated superstructure expansion is given in Fig. 65.

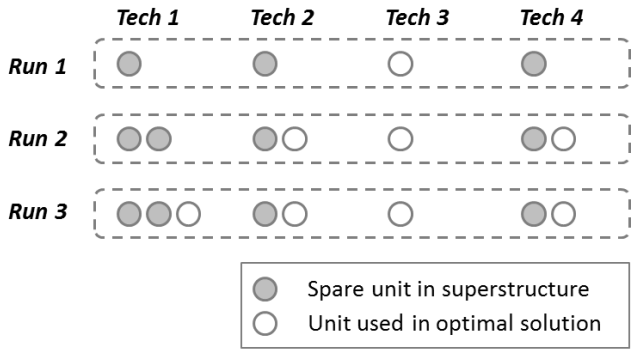

Fig. 65: schematic representation of automated superstructure expansion adopted from [50]

4.5.3. Calculation procedure

To integrate multiple instances (units) per technology type, all variables related to energy technologies (utilities) are additionally indexed with the set of instances Ins, and all equations constituting the generic or specific technology models are generated for every instance of each technology. Additionally, in the thermal energy balances, the hot and cold stream balances, the electrical energy balances and the objective function, summations over technology types are extended with the set of technology instances. The number of instances incorporated in the superstructure for each utility is indicated by parameters iU_U and iE_E. Note that energy storage technologies are not included yet in the automated superstructure expansion, and in subsequent optimisation runs, only one unit per storage technology is included in the superstructure.

The procedure for automated superstructure expansion explained below employs parameters $InsmaxU_U$ and $InsmaxE_E$ to indicate the maximum allowed number of instances, whereas parameters $contU_U$ and $contE_E$ are used to control loop structures. The value of the optimised system cost is indicated with $cost^l$. Fig. 66 represents the procedure by means of a flowchart consisting of 5 main steps. For the sake of conciseness, only thermal utilities are included in the chart. In a first step, all utilities present in the superstructure are each represented by 1 unit, their control parameters are activated, and the model is solved. If this superstructure does not embed any feasible configuration that can fulfil energy demands, the superstructure is gradually expanded by the loop in step 2, until a feasible solution is found or until all control parameters are deactivated. In every run-through, utilities that have not yet reached a predefined maximum number of units get one extra unit, but if this maximum is reached their control parameter is deactivated. As long as at least one control parameter is active, an optimisation run is performed. In step 3, the superstructure

is cleaned up by removing utility units that have not been selected in the last calculated configuration, while leaving at least one unit per utility. Next, all utility control parameters are reactivated. Step 4 contains the core of the automated superstructure expansion procedure as described in the previous subsection. If a feasible solution is obtained in step 1 or 2, the superstructure is gradually expanded in a loop, until the objective function shows no more improvement or until all control parameters are deactivated. During every run-through, a utility receives one extra unit in the superstructure if all available units are selected in the optimised configuration and the maximum number is not yet reached. If not all units are selected or if the maximum number is attained, the corresponding control parameter is deactivated. As long as there is one active control parameter, an optimisation run is performed. If the objective value is not lower than the one obtained in the previous run, the loop is terminated. In step 5, the superstructure is refreshed by removing all utility instances that have not been used in the last calculated configuration and a final optimisation is performed.

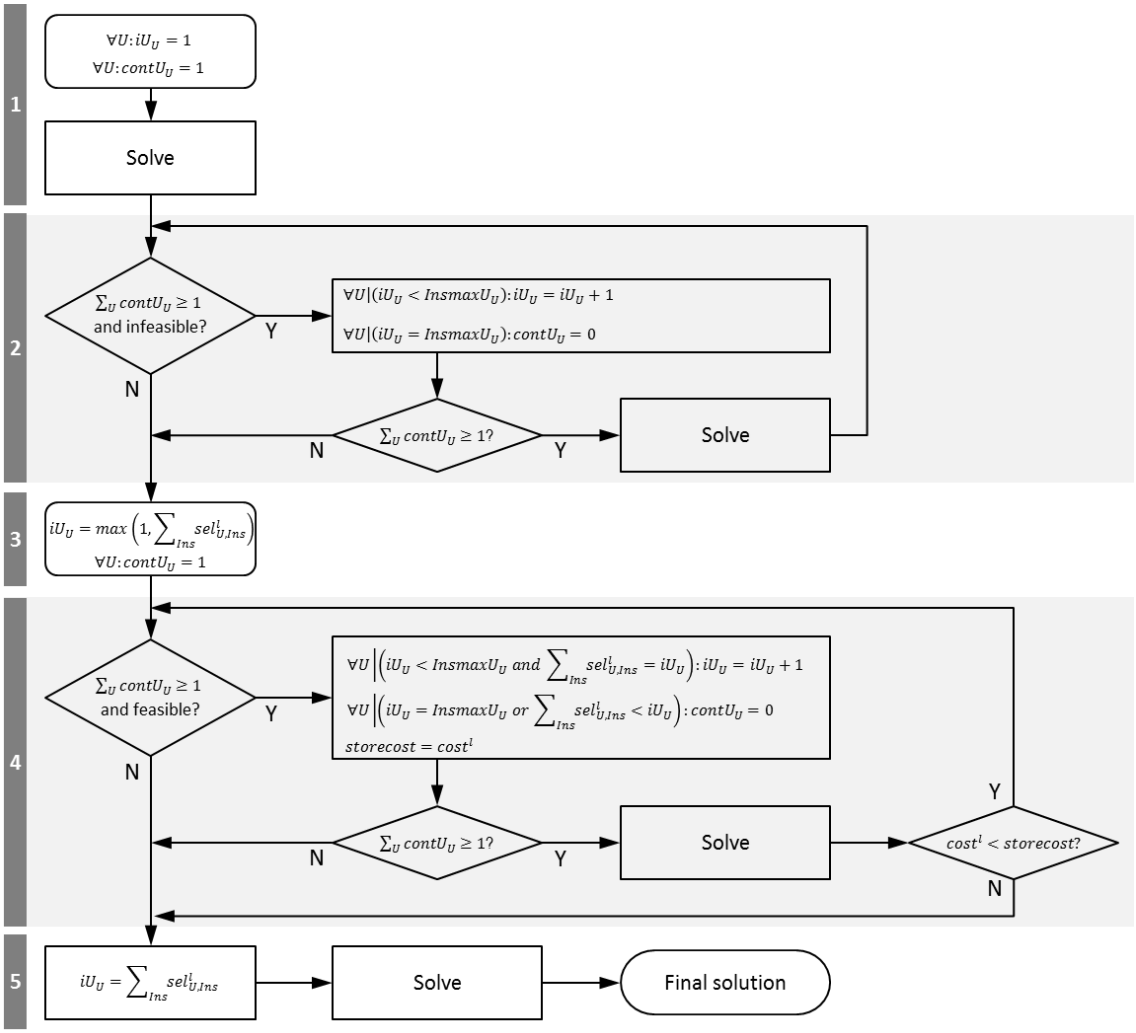

Fig. 66: flowchart of implementation automated superstructure expansion

4.5.4. Formulation of superstructure expansion procedure

In this subsection, the calculation procedure for automated superstructure expansion is implemented in *Syn-E-Sys*. Both the extended heat cascade MILP model with and the one without envelope calculation are subjected to the this procedure.

Initialise control parameters

$\forall U|(presU_U = 1): iU_U = 1$

$\forall E|(presE_E = 1): iE_E = 1$

$\forall U|(presU_U = 1): contU_U = 1$

$\forall E|(presE_E = 1): contE_E = 1$

Initial calculation

solve the MILP model by minimising the variable $cost$

If the model is infeasible, increase the number of instances (within given limits) for all utilities until a feasible solution is obtained

while $\sum_U contU_U + \sum_E contE_E \geq 1$ and optimisation model is infeasible:

$\forall U|(iU_U < InsmaxU_U): iU_U = iU_U + 1$

$\forall U|(iU_U = InsmaxU_U): contU_U = 0$

analogue expressions for electrical utilities E

if $\sum_U contU_U + \sum_E contE_E \geq 1$: **solve** the MILP model by minimising the variable $cost$

Remove unused utility instances, but keep at least one instance per utility

$$\forall U|(presU_U = 1): iU_U = max\left(1, \sum_{Ins|\dot{Q}nom^l_{U,Ins}>0} sel^l_{U,Ins}\right)$$

$$\forall E|(presE_E = 1): iE_E = max\left(1, \sum_{Ins|Pnom^l_{E,Ins}>0} sel\_el^l_{E,Ins}\right)$$

$\forall U|(presU_U = 1): contU_U = 1$

$\forall E|(presE_E = 1): contE_E = 1$

When all instances of a utility are used, increase the number of instances within given limits

while $\sum_U contU_U + \sum_E contE_E \geq 1$ and the optimisation model is feasible:

$storecost = cost^l$

$$\forall U|\left(iU_U < InsmaxU_U \; and \sum_{Ins|\dot{Q}nom^l_{U,Ins}>0} sel^l_{U,Ins} = iU_U\right): iU_U = iU_U + 1$$

$$\forall U|\left(iU_U = InsmaxU_U \; or \sum_{Ins|\dot{Q}nom^l_{U,Ins}>0} sel^l_{U,Ins} < iU_U\right): contU_U = 0$$

analogue expressions for electrical utilities E

if $\sum_U contU_U + \sum_E contE_E \geq 1$, **solve** EI using MIP minimizing cost

if $cost^l \geq storecost$: $\forall U: contU_U = 0, \forall E: contE_E = 0$

clean up lst file and solve

$$\forall U|(presU_U = 1): iU_U = \sum_{Ins|\dot{Q}nom^l_{U,Ins}>0} sel^l_{U,Ins}$$

$$\forall E|(presE_E = 1): iE_E = \sum_{Ins|Pnom^l_{E,Ins}>0} sel\_el^l_{E,Ins}$$

If $\sum_{U|(presU_U=1)} InsmaxU_U > \sum_U presU_U$, **solve** EI using MIP minimizing cost

last actualisation number of instances

$$\forall U|(presU_U = 1): iU_U = \sum_{Ins|\dot{Q}nom^l_{U,Ins}>0} sel^l_{U,Ins}$$

$$\forall E|(presE_E = 1): iE_E = \sum_{Ins|Pnom^l_{E,Ins}>0} sel\_el^l_{E,Ins}$$

4.6. Energy storage

Excess energy in a certain time period can be stored by means of storage technologies in order to be used in later periods with energy deficit. These technologies facilitate the introduction of non-dispatchable renewable energy, such as solar and wind, in the energy system. Moreover, they allow to shift part of the energy production to times with lower utility operation costs. Therefore, storage can play an important role in low carbon business park energy systems.

Welsch *et al.* [48] extended the OSeMOSYS modelling framework in order to incorporate storage, next to prioritising of demands and demand side management. They proposed a simplified storage model and introduced time sequence to enable calculation of storage levels over time. However, their formulation does not support thermodynamic simulation of thermal storage, and disregards storage losses over time. Becker [98] proposed a model for sensible heat storage consisting of a series of virtual tanks. Although the model can deal with daily storage, it is not suited for storage over a larger (e.g. seasonal) time span. To eliminate these shortcomings a novel approach is presented. The method of Welsch *et al.* [48] is modified and extended to integrate electrical as well as thermal storage. Moreover, storage losses over time are taken into account, while maintaining the time dimensionality of the optimisation problem by a priori calculating time discount factors. Subsequently, a modified version of the thermal storage model of Becker [98] is integrated in the proposed method in order to enable simulation of intra-annual storage with storage losses over time.

In the following subsections, simple models for electrical and thermal storage units are presented and time sequence is added to the overall model in order to enable correct calculation of storage levels. Next, a novel approach is proposed for dealing with hourly storage loss without extending the time dimension of the decision variables. This approach is integrated into a model for sensible heat storage consisting of a series of virtual tanks. For all storage models, sets, parameters and variables are defined, followed by the formulation of equations that describe the behaviour of storage technologies and their integration into the overall energy system.

4.6.1. Electrical storage model

An electrical storage unit is used to extract electrical energy from the energy system, store it in a reservoir over a certain time span and release it at a later point in time (see Fig. 67). The conversion of electrical energy to an energy form that is stored and vice versa may induce conversion losses. Therefore, the actual filling rate of the storage reservoir is lower than the electrical charge load $\boldsymbol{Pin}_S$ of the storage unit, and the draining rate of the reservoir is higher than the storage unit's discharge load $\boldsymbol{Pout}_S$. The filling and draining rate are calculated by respectively multiplying $\boldsymbol{Pin}_S$ with and dividing $\boldsymbol{Pout}_S$ by a conversion efficiency factor ηc. The charge level $\boldsymbol{lev}(t)$, indicating the instantaneous energy content of the reservoir, varies over time as electrical energy is added or extracted. However, this level can also gradually decrease due to time-dependent energy losses in the reservoir, which can be modelled by means of an hourly storage efficiency factor ηh. The nominal storage capacity $\boldsymbol{Capsto\_nom}$ is the maximum energy content of the storage reservoir and forms an absolute limit to the storage level. Additionally, the storage level can be constraint by an upper and lower limit that are both specified as fractions ($lolimlev\_rel$ and $uplimlev\_rel$) of the nominal storage capacity. In contrast to utilities, no direct relation exists between the energy input and

output of a storage unit, making part-load equations irrelevant. No economy of scale effects on storage unit investment costs are taken into account and the specific investment cost cI_Sto is expressed relative to the energy capacity of the storage (in €/kWh). The proposed model can be readily used to simulate a variety of electrical storages, such as batteries, compressed air tanks, pumped hydro storage, flywheels, etc.

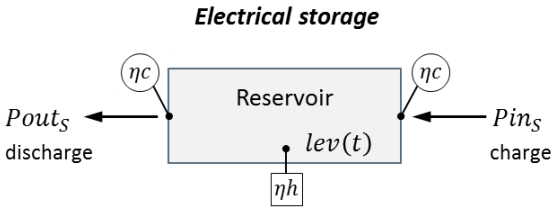

Fig. 67: Electrical storage model

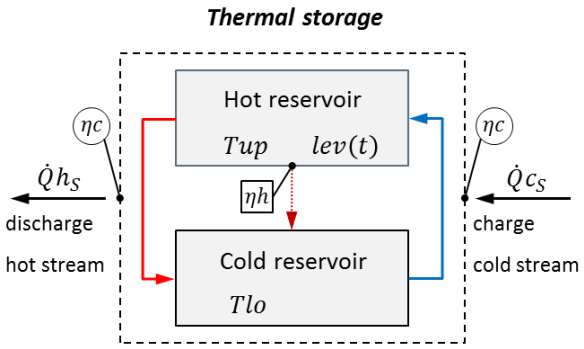

Fig. 68: Thermal storage model

4.6.2. Thermal storage model

The thermal storage model represents a stratified thermal storage tank, but can be manipulated to simulate other types of thermal storage (see 4.6.2.1). The model is conceived as a hot reservoir at temperature Tup that is connected to a cold reservoir at temperature Tlo via a cold and a hot stream (see Fig. 68). The cold stream can extract a heat load $\dot{\boldsymbol{Q}}\boldsymbol{c}_S$ by countercurrent heat exchange with hot process or utility streams, while its temperature is raised from Tlo to Tup. In a similar way, by cooling down the hot stream from Tup to Tlo, a heat load $\dot{\boldsymbol{Q}}\boldsymbol{h}_S$ can be delivered to cold streams in the energy system. These thermal streams correspond to mass flows of the heat storage medium between the two reservoirs. The charge level $\boldsymbol{lev}(t)$ of the storage unit indicates the instantaneous amount of stored heat, representing the amount of heat that could be extracted by cooling down the heat storage medium present in the hot reservoir, from Tup to Tlo. An upper limit to this level is given by the nominal storage capacity $\boldsymbol{Capsto\_nom}$, which depends on the total mass of heat storage medium. Due to heat loss in heat exchangers, the actual charge rate of the storage is lower than the charge load $\dot{\boldsymbol{Q}}\boldsymbol{c}_S$, while the actual discharge rate of the storage is higher than the discharge load $\dot{\boldsymbol{Q}}\boldsymbol{h}_S$. This is taken into account by means of a conversion efficiency factor ηc, in a similar way as for electrical storage. The charge level (of the hot reservoir) varies over time as heat is added to or extracted from the storage unit. Moreover, the charge level can gradually decrease because of time-dependent heat loss, which is taken into account via an hourly storage efficiency factor ηh. This heat loss can be interpreted as a leaking mass flow from the hot to the cold reservoir.

It is obvious that a strong analogy exists between the electrical and the thermal storage model. Hence, the thermal storage model shares equations with the electrical storage model. Extra equations are introduced to shift from the electrical charge and discharge loads $\boldsymbol{Pin}_S$ and $\boldsymbol{Pout}_S$ to the thermal charge and discharge loads $\dot{\boldsymbol{Q}}\boldsymbol{c}_S$ and $\dot{\boldsymbol{Q}}\boldsymbol{h}_S$. These storage hot and cold streams are integrated into the heat cascade in the same way as utility streams. Furthermore, an equation is added to prevent the storage to act as a heat transfer unit by simultaneous charging and discharging when located in the heat transfer system. Note that the storage model assumes steady state operation in each hour, disregarding limits to charge and discharge rate or variations in capacity over

time. The specific investment cost cI_Sto is specified in €/kWh. When different temperature ranges of a latent heat storage unit need to be compared, the analyst should adapt the value of cI_Sto correspondingly, to keep a constant cost per kg of storage medium.

4.6.2.1. Types of thermal storage

In their review of thermal storage systems in power generation plants, Gil *et al.* [107] distinguished sensible, latent and chemical heat storage. All these types of thermal storage can be simulated in a simplified way by manipulating the model described above. For example, in a thermocline thermal storage tank, hot liquid accumulates in the upper part, corresponding to the model's hot reservoir, while the physical phenomenon of stratification separates it from the cold liquid in the lower part of the tank, represented by the cold reservoir. Alternatively, a dual tank system consists of two separate tanks, one with cold and another containing hot liquid, corresponding to the hot and cold reservoirs of the model. Both single tank thermocline and dual tank systems with molten salt are often used in solar power plants [108]. In a similar way, the model could be used for thermal energy storage in underground aquifers. Latent heat storage utilises phase change materials that change from solid to liquid phase and vice versa when heat is added or extracted [107]. The solid phase is equivalent to the cold reservoir, whereas the liquid phase corresponds to the hot reservoir, both reservoirs having equal temperatures. In a thermochemical storage unit, heat can be stored via a reversible endothermic chemical reaction [107]. A chemical compound is decomposed into two substances by absorbing heat, which can be released again by recombining these substances. The cold reservoir is equivalent with the original compound, while the hot reservoir represents both decomposed substances.

4.6.2.2. Hourly storage efficiency

For the specific case of a cylindrical sensible heat storage unit, an expression for the hourly storage efficiency can be derived. It is assumed that the cylindrical volume of heat transfer medium in the hot reservoir loses heat to the environment through its mantle area. This is equivalent to a mass flow from the hot to the cold reservoir at environmental temperature (see discussion 7.2.3). The mantle area Am (in m²) can be written as a function of diameter D (in m), density ρ (in kg/m³) and the total instantaneous mass of heat transfer medium in the hot reservoir $M(t)$ (in kg) at time t (Eq 1). The heat loss rate $\dot{Q}hl$ (in W) can be expressed as heat transfer through the containment wall with heat transfer coefficient k (in W/m².K) (Eq. 2), but also as mass flow to the cold reservoir with specific heat capacity cp (in J/kg.K) (Eq. 3), both driven by temperature difference $Tup - Tlo$ (in K). Moreover, the heat loss per hour from the volume to the environment can be calculated by means of the hourly storage efficiency ηh (Eq. 4). By combining equations 1, 2 and 3 on the one hand, and equations 3 and 4 on the other hand, two alternative expressions for mhl are obtained (Eqs. 5 and 6). From these expressions a formula for ηh can be derived (Eq. 7).

Eq. 1 $$Am = \frac{4 \cdot M}{\rho \cdot D}$$

Eq. 2 $$\dot{Q}hl = k \cdot Am \cdot (Tup - Tlo)$$

Eq. 3 $$\dot{Q}hl = mhl \cdot cp \cdot (Tup - Tlo)$$

Eq. 4 $$\dot{Q}hl \,.3600 = M \cdot cp \cdot (Tup - Tlo) \cdot (1 - \eta h)$$

Eq. 5 $$mhl = k \cdot \frac{4.M}{\rho \cdot D \cdot cp}$$

Eq. 6 $$mhl = \frac{M \cdot (1 - \eta h)}{3600}$$

Eq. 7 $$\eta h = 1 - 3600 \cdot \frac{4 \cdot k}{\rho \cdot D \cdot cp}$$

4.6.3. Introduction of time sequence

Within each time slice S, the parameters for generation and demand (utilities and processes) keep constant values. As a result, the charge or discharge load of a storage unit in the energy system does not vary within a time slice. However, the charge level is not constant within a time slice, because energy is supplied to or extracted from the storage over sequential time steps of the year. Indeed, a time slice has no inherent time sequence, as it is a collection of time intervals with identical conditions spread across the year. Consequently, a yearly time division based on time slices is ill suited to simulate the evolution of the storage level. Therefore, Welsch *et al.* [48] introduced an additional time structure in the OSeMOSYS modelling framework that allows to calculate the storage level and keep it between predefined limits over sequential hourly time steps.

The time division used in this work is adopted from Welsch *et al.* [48]. The year is divided by the modeller into a number of seasons, weeks, daytypes, days, daily time brackets and hours, as shown in Fig. 69. Daytypes can be used to distinguish between weekdays and days in the weekend, while daily time brackets divide the day into distinct representative parts, such as morning, midday, afternoon, evening and night. More specifically, the year consists of a set of seasons (ls) and each season comprises a certain number of weeks (wks_ls_{ls}). All weeks follow the same predefined division into a set of successive daytypes (ld), while each daytype contains a specified number of days ($days\_ld_{ld}$). All days have an identical partitioning according to a set of consecutive daily time brackets (lh), each comprising a certain number of sequential hours (hrs_lh_{lh}). The time step class ls_i, ld_j, lh_k is defined as the collection of all time steps that fall within season ls_i, daytype ld_j and daily time bracket lh_k. Each time slice is attributed to a specific time step class (season, daytype, daily time bracket) by means of binary 'conversion parameters' $conv\_s_{S,ls}$, $conv\_d_{S,ld}$ and $conv\_h_{S,lh}$. (e.g., see Appendix A.1). A time step can be defined as the time interval in one day that belongs to one time step class, which can also be referred to as a daily time bracket. It consists of a series of consecutive hourly time steps.

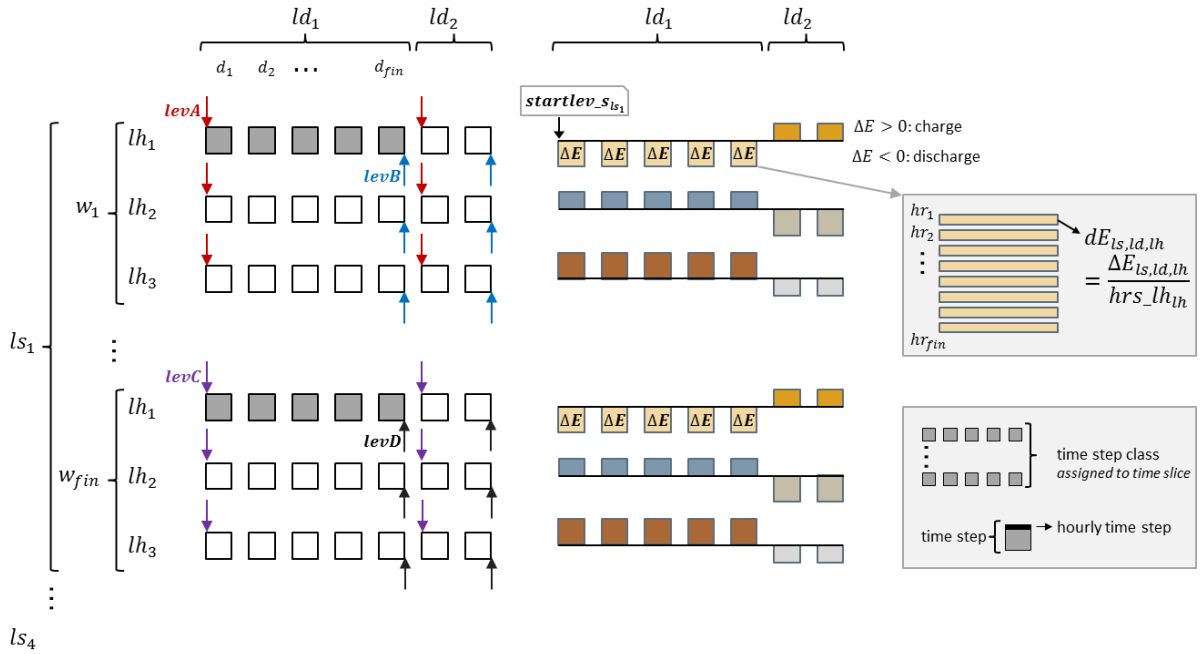

Fig. 69: Exemplary time division, positions in time of critical storage levels and net energy charges storage

As an illustration, the time steps belonging to time step class ls_1, ld_1, lh_1 are shaded with a grey colour in the left part of Fig. 69. During all these time steps the storage charge and discharge loads (electrical: $\boldsymbol{Pin}_S$ and $\boldsymbol{Pout}_S$ or thermal: $\dot{\boldsymbol{Q}}\boldsymbol{c}_S$ and $\dot{\boldsymbol{Q}}\boldsymbol{h}_S$) and consequently also the resulting net energy charge of the storage reservoir per time step $\Delta \boldsymbol{E}_{Sto,ls,ld,lh}$ takes a constant value (see right part of Fig. 69). Note that a year following a time structure with weeks of 7 days counts 364 instead of 365 days.

4.6.4. Position of critical storage levels

The charge level of a storage unit must lie between a given lower and upper bound, both specified as a fraction of the nominal capacity of the storage reservoir. Although these conditions need to be fulfilled in every hourly time step, it suffices to impose them only in hourly time steps where extreme storage levels may occur. Therefore, the positions in time (over the year) of these critical storage levels need to be determined.

Since a daily time bracket is a sequence of hours with the same net hourly energy charges, extreme storage levels can only appear in the beginning or at the end of the daily time bracket. Similarly, a daytype is a sequence of identical days, while a season is a series of identical weeks, which implicates that extreme storage levels appear in the first and final day of the daytype and in the first and final week of the season. This statement also holds when hourly energy losses are taken into account, but in this work no mathematical proof is given. More specifically, the critical storage levels of a storage unit occurring in time step class ls_i, ld_j, lh_k are the level at the start of the first hour of daily time bracket lh_k in the first day of daytype ld_j and the level at the end of the final hour of daily time bracket lh_k in the final day of daytype ld_j in both the first and the final week of season ls_i (see Fig. 69 and Fig. 70). In other words, per storage unit Sto four critical storage levels exist in every time step class ls, ld, lh, which are denoted as $\boldsymbol{levA}_{Sto,ls,ld,lh}$, $\boldsymbol{levB}_{Sto,ls,ld,lh}$, $\boldsymbol{levC}_{Sto,ls,ld,lh}$ and $\boldsymbol{levD}_{Sto,ls,ld,lh}$ respectively.

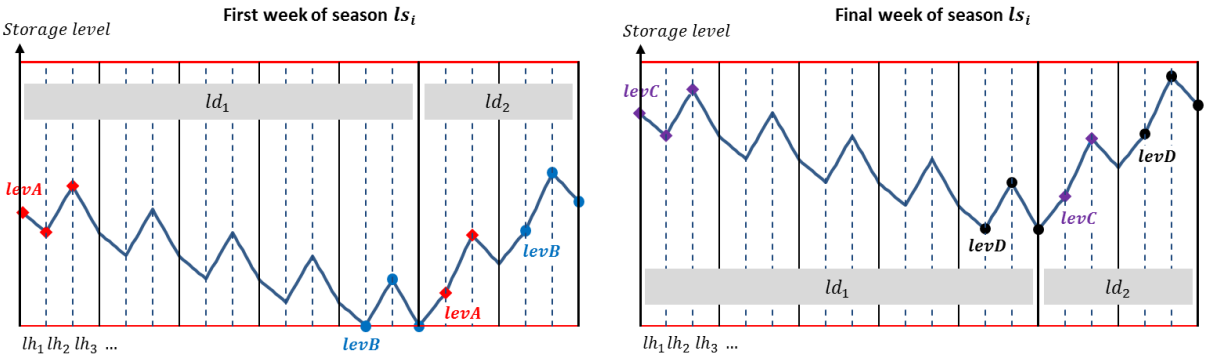

Fig. 70: positions in time of critical storage levels

The positions in time (over the year) at which these critical levels occur are denoted as $posA_{ls,ld,lh}$, $posB_{ls,ld,lh}$, $posC_{ls,ld,lh}$ and $posD_{ls,ld,lh}$ and are calculated by means of a multi-layered loop (POS). For each season separately, the loop chronologically runs through the time structure from one hour to the next. Meanwhile, it keeps track of the current hourly time step (numbered per season) and of the current location in the time structure in terms of week, daytype, day, daily time bracket and hour. When arriving at a time location where a specific critical level occurs, as described above, the

index of the current hourly time step is assigned to the position in time of that level. As an example, the location in the time structure corresponding to critical level A of time step class ls_i, ld_j, lh_k is reached at the **start** of the **first hour** of daily time bracket lh_k in the **first day** of daytype ld_j in the **first week** of season ls_i. Furthermore, each hourly time step $hstep$ is allocated to the time step class ls, ld, lh to which it belongs by setting the value of the parameter $assign_{hstep,ls,ld,lh}$ to 1.

When hourly heat losses are disregarded, it is not required to first explicitly calculate the positions of the critical storage levels, because the critical levels can be calculated implicitly using the equations proposed by Welsch *et al.* [48] which are given in more detail in his thesis [109] and presented in Subsection 4.6.6.

POS
$loop(\ ls,$
$i = 1$
$for(w = 1\ to\ wks\_ls_{ls}$
$loop(\ ld,$
$for(d = 1\ to\ days\_ld_{ld}$
$loop(\ lh,$
$for(h = 1\ to\ hrs\_lh_{lh}$
$assign_{hstep_i,ls,ld,lh} = 1$
$if(w = 1\ and\ d = 1\ and\ h = 1,$
$posA_{ls,ld,lh} = i)$
$if(w = 1\ and\ d = days_{ld\,ld}\ and\ h = hrs\_lh_{lh},$
$posB_{ls,ld,lh} = i)$
$if(w = wks_{ls_{ls}}\ and\ d = 1\ and\ h = 1,$
$posC_{ls,ld,lh} = i)$
$if(w = wks_{ls_{ls}}\ and\ \mathrm{d} = days_{ld\,ld}\ and\ h = hrs\_lh_{lh},$
$posD_{ls,ld,lh} = i)$
$i = i + 1$
))))))

4.6.5. Integration of storage loss over time

The formulation of Welsch *et al.* [48] is not developed to deal with storage losses over time. To tackle this shortcoming, an alternative formulation is proposed in which the effects of hourly storage losses are concentrated into time discount factors that are calculated before optimisation. These factors form the coefficients of equations that express the critical storage levels in the optimisation problem. In this way, incorporating storage loss over time does not intensify the complexity of the optimisation model. The proposed formulation is illustrated with an example.

4.6.5.1. Concept of time discount factors

To introduce the concept of time discount factors, assume that all hourly time steps over the year belong to a single time step class. Note that in this work net hourly energy charges are added to the storage at the start of each hourly time step, which implies a safe overestimation of energy losses. Consequently, the storage level $\boldsymbol{lev}_{h_n}$ at the end of a certain hourly time step is equal to the sum of the storage level $\boldsymbol{lev}_{h_{n-1}}$ at the end of the previous hour and the net hourly energy charge $\boldsymbol{dE}$ in the current hour, multiplied with the hourly storage efficiency ηh: $\boldsymbol{lev}_{h_n} = \left(\boldsymbol{lev}_{h_{n-1}} + \boldsymbol{dE}\right) \cdot \eta h$. By applying this recursive formula from the initial to the current hourly time step, following expression

is obtained: $\boldsymbol{lev}_{h_n} = \boldsymbol{lev}_{h_0} \cdot (\eta h^n) + \boldsymbol{dE} \cdot \left(\sum_{i=1}^{n} \eta h^i\right)$. The coefficients in this function can be readily calculated and are referred to as time discount factors, denoted αi and α. Consequently, the storage level is expressed as a linear function of the initial storage level and the hourly net energy charge, using discount factors as coefficients: $\boldsymbol{lev}_{h_n} = \boldsymbol{lev}_{h_0} \cdot \alpha i + \boldsymbol{dE} \cdot \alpha$. However, when time steps over the year belong to different time step classes, a more complex formulation is required.

4.6.5.2. Expressions for critical storage levels and time discount factors

In this subsection, mathematical expressions are developed for the critical storage levels A,B,C and D of a storage unit in an arbitrary time step class. Each expression is formulated as a linear function of the initial storage level at the start of the season and the net hourly energy charges in each time step class. The coefficients are referred to as time discount factors and can be calculated before system optimisation.

The critical level A of a storage unit in a certain time step class is reached at the start of the hourly time step with index $i = posA_{ls,ld,lh}$ in season ls. An expression for this critical level is obtained by summing up the contributions, devaluated over the elapsed time, of the level at the start of the season and of the net energy charges over all hourly time steps preceding the critical one. More specifically, the startlevel is devaluated over the time span Δt elapsed between the start of the season and the start of the critical hourly time step i, by a factor $\eta h^{\Delta t}$, with $\Delta t = i - 1$. Similarly, the net energy charge at the start of each hourly time step j preceding the critical one ($1 \leq j \leq i - 1$), is devaluated over the elapsed time span Δt by a factor $\eta h^{\Delta t}$, with $\Delta t = i - j$. The devaluated energy charges related to hourly time steps within one specific time step class are accumulated, and their devaluation factors are bundled in a time discount factor. Consequently, the critical level A in time step class ls, ld, lh can be expressed as a linear function of the initial level of the season $\boldsymbol{startlev\_s}_{Sto,ls}$ and the net energy charges $\boldsymbol{dE}_{Sto,ls,ld^*,lh^*}$ related to all time step classes ls, ld^*, lh^*, as presented in equation B_LV1. The corresponding time discount factors $\alpha Ai_{Sto,ls,ld,lh}$ and $\alpha A_{Sto,ls,ld,lh,ld^*,lh^*}$ can be calculated prior to the optimisation.

B_LV1 $\forall\, Sto, ls, ld, lh$:

$$\boldsymbol{levA}_{Sto,ls,ld,lh} = \boldsymbol{startlev\_s}_{Sto,ls} \cdot \alpha Ai_{Sto,ls,ld,lh} + \sum_{ld^*,lh^*} \boldsymbol{dE}_{Sto,ls,ld^*,lh^*} \cdot \alpha A_{Sto,ls,ld,lh,ld^*,lh^*}$$

Time discount factor $\alpha A_{Sto,ls,ld,lh,ld^*,lh^*}$ related to the critical level A of a certain time step class ls, ld, lh, and that has to be applied to the net hourly energy charge of a certain time step class ls, ld^*, lh^*, can be calculated using equation *DCF*. This expression sums up all devaluation factors ηh^{i-j} over all hourly time steps j ($hstep_j$) preceding the critical hourly time step i ($hstep_i$) and belonging to the respective time step class ls, ld^*, lh^*.

The time discount factor $\alpha Ai_{Sto,ls,ld,lh}$ that has to be applied to the startlevel of the season is given by parameter equation *DCFi*.

DCF $\forall\, Sto, ls, ld, lh, ld^*, lh^*$:

$$\alpha A_{Sto,ls,ld,lh,ld^*,lh^*} = \sum_j \eta h_{Sto}{}^{(i-j)}$$

with $1 \le j \le i-1$ and $assign_{hstep_j,ls,ld^*,lh^*} = 1$

$i = posA_{ls,ld,lh}$

DCFi $\forall\, Sto, ls, ld$:

$$\alpha Ai_{Sto,ls,ld,lh} = \eta h_{Sto}{}^{(i-1)}$$

with $i = posA_{ls,ld,lh}$

However, the formulation used in the actual model does not rely on parameter equations to calculate the discount factors, but uses multi-layered loops. The discount factors related to critical level A are calculated by means of the loop TDF1 and an analogous loop is used for the coefficients related to critical level C. For determination of critical level B, loop TDF2 is employed and a similar loop is used for level D. Note these loops are only activates for storage units with hourly storage efficiencies lower than 1.

TDF1
$\alpha A_{Sto,ls,ld,lh,ld^*,lh^*} = 0$
$loop(\ (Sto, ls, ld, lh)$
$i = posA_{ls,ld,lh}$
$\Delta t = i - 1$
$\alpha Ai_{Sto,ls,ld,lh} = \eta h_{Sto}{}^{\Delta t}$
$for\ (\ j = 1\ to\ i-1$
$loop(\ (ld^*, lh^*)$
$if(\ assign_{hstep_j,ls,ld^*,lh^*} = 1,$
$\Delta t = i - j$
$\alpha A_{Sto,ls,ld,lh,ld^*,lh^*} = \alpha A_{Sto,ls,ld,lh,ld^*,lh^*} + \eta h_{Sto}{}^{\Delta t}$
))))

TDF3: equation for critical level C, analogue to TDF1

TDF2
$\alpha B_{Sto,ls,ld,lh,ld^*,lh^*} = 0$
$loop(\ (Sto, ls, ld, lh)$
$i = posB_{ls,ld,lh}$
$\Delta t = i$
$\alpha Bi_{Sto,ls,ld,lh} = \eta h_{Sto}{}^{\Delta t}$
$for\ (\ j = 1\ to\ i$
$loop(\ (ld^*, lh^*)$
$if(\ assign_{hstep_j,ls,ld^*,lh^*} = 1,$
$\Delta t = i - j + 1$
$\alpha B_{Sto,ls,ld,lh,ld^*,lh^*} = \alpha B_{Sto,ls,ld,lh,ld^*,lh^*} + \eta h_{Sto}{}^{\Delta t}$
))))

TDF4: equation for critical level D, analogue to TDF2

When the time structure is based on **typical days** and **daily time segments** (see subsection 4.2.2), an extended version of the critical storage level approach could be used, provided that each typical day represents a chronologic sequence of days and each daily time segment represents a chronologic sequence of hours.

4.6.5.3. Example

As an example, let us consider a fictive time division with two daytypes ld_1 and ld_2 containing respectively 2 and 5 days. Each fictive day is divided in three hourly time brackets lh_1, lh_2 and lh_3 comprising respectively 2, 2 and 3 hours, as depicted in Fig. 71. The aim is to calculate all discount factors that appear in the expression for critical storage level A in time step class $ls_1 ld_2 lh_3$. This critical level is attained at the start of the hourly time step with index i = 19 in season ls_1, which can be derived from Fig. 71. The critical position $posA_{ls_1 ld_2 lh_3}$ can also be calculated using the loop POS given in Subsection 4.6.4. Using equation B_LV1, the critical level can be expressed as a linear function of the initial level at the start of the season and of the net hourly energy charges in each time step class of the season. The time discount factors in this expression can be calculated either with the mathematical formulas *DCF* and *DCFi* or using the loop *TDF1* developed in Subsection 4.6.5.2. Results are displayed in Fig. 71 in which ηh_{Sto} is denoted as η for the sake of conciseness.

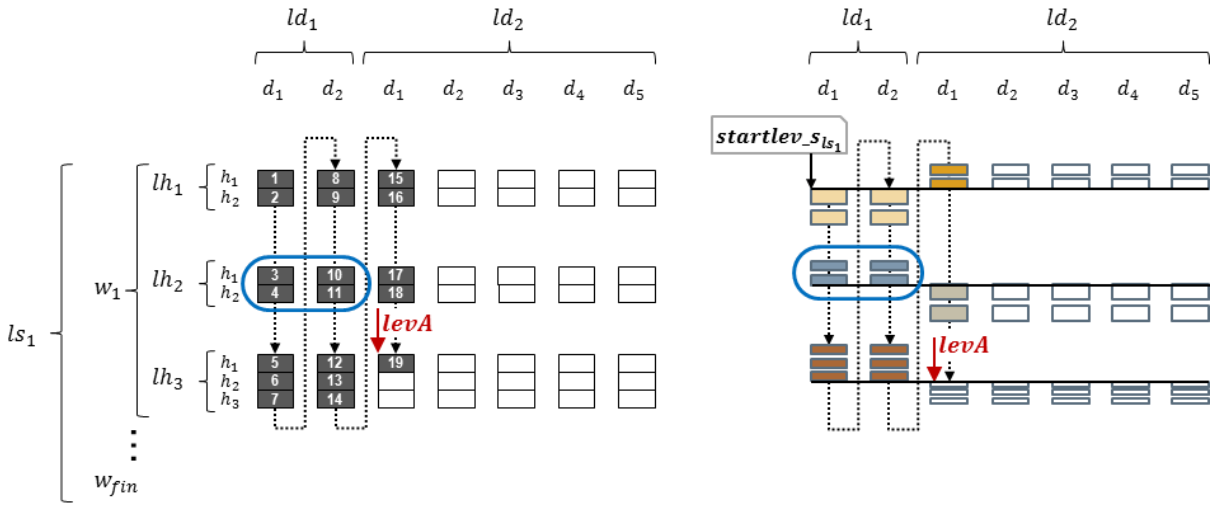

$$
\begin{aligned}
&levA_{Sto,ls_1 ld_2 lh_3} = \\
&\boldsymbol{startlev\_s}_{Sto,ls_1} \cdot \alpha Ai_{Sto,ls_1,ld_2,lh_3} \\
&+\boldsymbol{dE}_{Sto,ls_1,ld_1,lh_1} \cdot \alpha A_{Sto,ls_1,ld_2,lh_3,ld_1^*,lh_1^*} \\
&+\boldsymbol{dE}_{Sto,ls_1,ld_1,lh_2} \cdot \alpha A_{Sto,ls_1,ld_2,lh_3,ld_1^*,lh_2^*} \\
&+\boldsymbol{dE}_{Sto,ls_1,ld_1,lh_3} \cdot \alpha A_{Sto,ls_1,ld_2,lh_3,ld_1^*,lh_3^*} \\
&+\boldsymbol{dE}_{Sto,ls_1,ld_2,lh_1} \cdot \alpha A_{Sto,ls_1,ld_2,lh_3,ld_2^*,lh_1^*} \\
&+\boldsymbol{dE}_{Sto,ls_1,ld_2,lh_2} \cdot \alpha A_{Sto,ls_1,ld_2,lh_3,ld_2^*,lh_2^*} \\
&+\boldsymbol{dE}_{Sto,ls_1,ld_2,lh_3} \cdot \alpha A_{Sto,ls_1,ld_2,lh_3,ld_2^*,lh_3^*}
\end{aligned}
$$

with time-discount factors:

$$
\begin{aligned}
\alpha Ai_{Sto,ls_1,ld_2,lh_3} &= \eta^{18} \\
\alpha A_{Sto,ls_1,ld_2,lh_3,ld_1^*,lh_1^*} &= \eta^{18} + \eta^{17} + \eta^{11} + \eta^{10} \\
\alpha A_{Sto,ls_1,ld_2,lh_3,ld_1^*,lh_2^*} &= \eta^{16} + \eta^{15} + \eta^{9} + \eta^{8} \\
\alpha A_{Sto,ls_1,ld_2,lh_3,ld_1^*,lh_3^*} &= \eta^{14} + \eta^{13} + \eta^{12} + \eta^{7} + \eta^{6} + \eta^{5} \\
\alpha A_{Sto,ls_1,ld_2,lh_3,ld_2^*,lh_1^*} &= \eta^{4} + \eta^{3} \\
\alpha A_{Sto,ls_1,ld_2,lh_3,ld_2^*,lh_2^*} &= \eta^{2} + \eta \\
\alpha A_{Sto,ls_1,ld_2,lh_3,ld_2^*,lh_3^*} &= 0
\end{aligned}
$$

Fig. 71: Example calculation of time discount factors

To illustrate the procedure, the calculation of time discount factor $\alpha A_{Sto,ls_1,ld_2,lh_3,ld_1^*,lh_2^*}$ is given in more detail. This factor needs to be applied to the net hourly energy charge dE of time step class ls_1, ld_1^*, lh_2^* (circled in blue in Fig. 71). It is the summation of the different factors that devaluate the net energy charges dE in every hour j that precedes the position i of the critical level and that belongs to time step class ls_1, ld_1^*, lh_2^*. The devaluation factors in such hourly time steps are equal to $\eta^{\Delta t}$, with $\Delta t = i - j$ representing the time elapsed between that hour and the position i of the critical level.

Applying equation *DCF* gives:

$$\alpha A_{Sto,ls_1,ld_2,lh_3,ld_1^*,lh_2^*} = \sum_j \eta^{(i-j)}$$

with $1 \leq j \leq i-1$ and hourly time step j belonging to time step class ls_1, ld_1^*, lh_2^*

$i = posA_{ls_1 ld_2 lh_3}$ = 19

$$\Longrightarrow \alpha A_{Sto,ls_1,ld_2,lh_3,ld_1^*,lh_2^*} = \eta^{(19-3)} + \eta^{(19-4)} + \eta^{(19-10)} + \eta^{(19-11)} = \eta^{16} + \eta^{15} + \eta^{9} + \eta^{8}$$

4.6.6. Formulation electrical and thermal storage model

Storage without energy loss over time is modelled using the formulation presented by Welsch *et al.* [48]. For storage with hourly losses, an alternative formulation is proposed, in which the expressions of critical storage levels are based on precalculated time discount factors (see Subsections 4.6.3 to 4.6.5. Both approaches have a similar setup and share a number of parameters, sets and variables.

The parameters describing the properties of each storage unit are specified by the modeller and include its location in the system, minimum and maximum limits to the nominal storage capacity, minimum and maximum bounds to the storage level as fractions of the nominal capacity, conversion and hourly storage efficiencies and the specific investment cost. Additionally, for a thermal storage the temperatures of the cold and hot reservoir and the minimum temperature approach for heat exchange with process or utility streams are given. Simultaneous charge and discharge in one time slice can be activated or deactivated. The decision variables related to a storage unit include a binary selection variable and a number of continuous variables representing charge and discharge loads related to time slices or time step classes, net energy charges per time step , critical storage levels and the nominal capacity.

Cold and hot streams of thermal storages are processed analogously to utility streams to determine the normalised heat capacity rates and heat loads per temperature interval. For units with energy loss over time, the position of critical storage levels and the corresponding time discount factors are calculated via parameter equations prior to the optimisation. The equations that describe the behaviour of storage units and their integration into the energy system form constraints to the overall optimisation problem. They involve calculation of net energy charges and critical levels, ensure that critical levels lie between upper and lower boundaries and that simultaneous charge and discharge is avoided. The latter prevents the storage to act as a heat transfer unit when it is located in the heat transfer system. Other equations deal with the limitation of nominal capacity, the integration of the units into the energy system's thermal energy balances and hot and cold stream balances and with the selection of the unit in the energy system configuration. Investment costs are introduced into the overall objective function and electrical charge and discharge loads are incorporated in the overall electricity balance.

4.6.6.1. Sets and parameters

Sets

Notation:	$El_1: first\ set\ element\ of\ uploaded\ set$ $El_f: final\ set\ element\ of\ uploaded\ set$	
Sto_th	$= Sto\_th_1..Sto\_th_f$	thermal storages
Sto_el	$= Sto\_el_1..Sto\_el_f$	electrical storages
Sto	$= Sto\_th + Sto\_el$	thermal and electrical storages
ls	$= ls_1..ls_f$	season
ld	$= ld_1..ld_f$	day type
lh	$= lh_1..lh_f$	daily time bracket
$step$	$= h_1..h_{10000}$	hourly time step

Subsets

$elSto(Sto)$	$= Sto \in \{Sto\_el\}$

Parameters

Time structure

$conv\_s_{S,ls}$	time slice S: season label
$conv\_d_{S,ld}$	time slice S: daytype label
$conv\_h_{S,lh}$	time slice S: daily time bracket label
wks_ls_{ls}	number of weeks in season ls
$days\_ld_{ld}$	number of days in daytype ld
hrs_lh_{lh}	number of hours in daily time bracket lh
$hrs\_sdh_{ls,ld,lh}$	$= wks\_ls_{ls} \cdot days\_ld_{ld} \cdot hrs\_lh_{lh}.$
hrs_S_S	$= \sum_{ls,ld,lh} hrs\_sdh_{ls,ld,lh} \cdot conv\_s_{S,ls} \cdot conv\_d_{S,ld} \cdot conv\_h_{S,lh}$
$days\_w$	$= \sum_{ld} days\_ld_{ld}$
hrs_d	$= \sum_{lh} hrs\_lh_{lh}$
hrs_y	$= \sum_{ls}(wks\_ls_{ls} \cdot days_w \cdot hrs\_d)$

Thermal storage

$locSto\_th_{Sto\_th,Sys}$	connection of storage Sto_th to system
$presSto\_th_{Sto\_th}$	$\forall Sto\_th \mid \left(\sum_{Sys} locSto\_th_{Sto\_th,Sys} \geq 1\right): presSto\_th_{Sto\_th} = 1$
$TsStoc_{Sto\_th,S}$	(*) source temperature cold stream storage Sto_th in time slice S (°C)
$TtStoc_{Sto\_th,S}$	(*) target temperature cold stream storage Sto_th in time slice S (°C)
$TsStocS_{Sto\_th,S}$	(*) shifted source temperature cold stream storage Sto_th in time slice S (°C)
$TtStocS_{Sto\_th,S}$	(*) shifted target temperature cold stream storage Sto_th in time slice S (°C)
$mcpStoc1_{Sto\_th,S}$	(*) normalised heat capacity rate cold stream storage Sto_th in time slice S (kW/K/1kW)
$d\dot{Q}Stoc1_{k,Sto\_th,S}$	(*) fraction of heat load cold stream storage Sto_th situated in temperature interval k in time slice S (kW/1kW)

(*) *analogue parameters related to hot stream storage Sto_th*

$OpSto\_th_{Sto\_th}$	= 1: no simultaneous charging and discharging allowed

Minimum temperature difference

$dTStomin_{Sto\_th}$	minimum temperature difference for heat exchange with storage Sto_th (°C)

Storage (data electrical and thermal storage merged)

$lolimlev\_rel_{Sto}$	lower limit to relative storage level as fraction of nominal capacity
$uplimlev\_rel_{Sto}$	upper limit to relative storage level as fraction of nominal capacity
$CapSto\_min_{Sto}$	lower limit to storage capacity (kWh)
$CapSto\_max_{Sto}$	upper limit to storage capacity (kWh)
$presSto_{Sto}$	presence of storage in superstructure (given for Sto_el, calculated for Sto_th)
cI_Sto_{Sto}	specific investment cost of storage (€/kWh)
ηc_{Sto}	efficiency of conversion to and from storage
ηh_{Sto}	hourly storage efficiency

parameters related to critical storage levels

$test_{step,ls,ld,lh}$	connection between hourly steps and time step class ls,ld,lh
$posA_{ls,ld,lh}$	(*) hourly time step critical level A
exp	number of hours over which an amount of energy is discounted over time'
$\alpha Ai_{Sto,ls,ld,lh}$	(*) time discount factor related to critical level A in time step class $lsldlh$ to be applied to the storage level at the start of the season
$\alpha A_{Sto,ls,ld,lh,ld^*,lh^*}$	(*) time discount factor related to critical level A in time step class $lsldlh$ to be applied to the net hourly energy charge of time step class $lsld^*lh^*$

(*) *analogue parameters related to critical storage levels B, C, D*

4.6.6.2. Variables

Variables

Variables for connection thermal storage to heat cascade constraints

$\boldsymbol{\dot{Q}Stoh}_{Sto\_th,S}$	$\mathbb{R}^+$	discharge load of thermal storage Sto_h in time slice S (kW)
$\boldsymbol{\dot{Q}Stoc}_{Sto\_th,S}$	$\mathbb{R}^+$	charge load of thermal storage Sto_h in time slice S (kW)

Variables for both (A) no energy loss over time and (B) energy loss over time

$\boldsymbol{PSto\_in\_S}_{Sto,S}$	$\mathbb{R}^+$	charge load to storage Sto in time slice S (kW)
$\boldsymbol{PSto\_out\_S}_{Sto,S}$	$\mathbb{R}^+$	discharge load from storage Sto in time slice S (kW)
$\boldsymbol{PSto\_in\_sdh}_{Sto,ls,ld,lh}$	$\mathbb{R}^+$	charge load to storage Sto in time step with label (ls,ld,lh) (kW)
$\boldsymbol{PSto\_out\_sdh}_{Sto,ls,ld,lh}$	$\mathbb{R}^+$	discharge load from storage Sto in time step with label (ls,ld,lh) (kW)
$\Delta\boldsymbol{E}_{Sto,ls,ld,lh}$	$\mathbb{R}$	energy charge (+) or discharge (-) in storage Sto in time step with label (ls,ld,lh) (kWh)
$\Delta\boldsymbol{E\_y}_{Sto,ls,ld,lh}$	$\mathbb{R}$	energy charge (+) or discharge (-) in storage Sto in time step with label (ls,ld,lh) accumulated over the year (kWh)
$\boldsymbol{startlev\_s}_{Sto,ls}$	$\mathbb{R}^+$	charge level at start season ls (kWh)
$\boldsymbol{startlev\_y}_{Sto}$	$\mathbb{R}^+$	storage level at start of the year
$\boldsymbol{endlev\_y}_{Sto}$	$\mathbb{R}^+$	storage level at end of the year
$\boldsymbol{CapSto\_nom}_{Sto}$	$\mathbb{R}^+$	nominal capacity storage Sto (kWh)
$\boldsymbol{sel\_Sto}_{Sto\_th}$	$\{0,1\}$	selection of storage
$\boldsymbol{d\_Sto}_{Sto\_th,S}$	$\{0,1\}$	charge = 1 or discharge = 0

Variables (A) no energy loss over time

$\boldsymbol{startlev\_d}_{Sto,ls,ld}$	$\mathbb{R}^+$	charge level at start first day of daytype ld in first week of season ls (kWh)
$\boldsymbol{endlev\_d}_{Sto,ls,ld}$	$\mathbb{R}^+$	charge level at end last day of daytype ld in last week of season ls (kWh)

Variables (B) energy loss over time

$\boldsymbol{levA}_{Sto,ls,ld,lh}$	$\mathbb{R}^+$	(*) critical storage level A in time step class ls,ld,lh (kWh)

(*) *analogue variables for critical storage levels B, C, D*

4.6.6.3. Equations

Preparation hot and cold stream parameters thermal storage

The shifted source and target temperatures of the streams related to thermal storages, utilities and processes are simultaneously sorted to compose the shifted temperature list. In each time slice, the normalised heat capacity rates and the normalised heat loads per temperature interval for both the hot and the cold stream of a thermal storage unit are obtained with parameter equations analogue to the ones for utilities (see subsections 4.4.2.1 and 4.4.2.2).

Parameter equations

Calculation heat capacity rates

MCPSTh $\forall\ Sto\_th, S \left| TsStoh_{Sto\_th,S} \neq TtStoh_{Sto\_th,S}\right.$:

$$mcpStoh1_{Sto\_th,S} = 1/\left(TsStoh_{Sto\_th,S} - TtStoh_{Sto\_th,S}\right)$$

MCPSTc $\forall\ Sto\_th, S \left| TsStoc_{Sto\_th,S} \neq TtStoc_{Sto\_th,S}\right.$:

$$mcpStoc1_{Sto\_th,S} = 1/\left(TsStoc_{Sto\_th,S} - TtStoc_{Sto\_th,S}\right)$$

Calculation heat loads per temperature interval [T_k,T_{k+1}]

HLSTh1 $\forall\ Sto\_th, S, k|$

$$\left(k < k_{max,S}, TsStoh_{Sto\_th,S} > TtStoh_{Sto\_th,S}, TsStoh_{Sto\_th,S} \geq TS_{k+1,S}, TtStoh_{Sto\_th,S} \leq TS_{k,S}\right):$$

$$d\dot{Q}Stoh1_{k,Sto\_th,S} = dT_{k,S} \cdot mcpStoh1_{Sto\_th,S}$$

HLSTc1 $\forall\ Sto\_th, S, k|$

$$\left(k < k_{max,S}, TtStoc_{Sto\_th,S} > TsStoc_{Sto\_th,S}, TtStoc_{Sto\_th,S} \geq TS_{k+1,S}, TsStoc_{Sto\_th,S} \leq TS_{k,S}\right):$$

$$d\dot{Q}Stoc1_{k,Sto\_th,S} = dT_{k,S} \cdot mcpStoc1_{Sto\_th,S}$$

HLSTh2 $\forall\ Sto\_th, S, k|$

$$\left(k < k_{max,S}, TsStoh_{Sto\_th,S} = TtStoh_{Sto\_th,S}, TsStoh_{Sto\_th,S} = TS_{k+1,S}, TS_{k+1,S} = TS_{k,S}\right):$$

$$d\dot{Q}Stoh1_{k,Sto\_th,S} = 1$$

HLSTc2 $\forall\ Sto\_th, S, k|$

$$\left(k < k_{max,S}, TsStoc_{Sto\_th,S} = TtStoc_{Sto\_th,S}, TsStoc_{Sto\_th,S} = TS_{k+1,S}, TS_{k+1,S} = TS_{k,S}\right):$$

$$d\dot{Q}Stoc1_{k,Sto\_th,S} = -1$$

Connection thermal storage to heat cascade

Equations ST1 and ST2 convert the charge and discharge loads resulting from the general (electrical) storage model to thermal charge and discharge loads, that are integrated in the heat cascade constraints related to the subsystems and the heat transfer system. Equations ST3 and ST4 are required to prevent the storage to act as a heat transfer unit by simultaneous charging and discharging when located in the heat transfer system.

Constraints

Thermal storage: connection to heat cascade constraints, operation

ST1 $\forall\ Sto\_th, S$: $\boldsymbol{\dot{Q}Stoc}_{Sto\_th,S} = \boldsymbol{PSto\_in\_S}_{Sto\_th,S}$

ST2 $\forall\ Sto\_th, S$: $\boldsymbol{\dot{Q}Stoh}_{Sto\_th,S} = \boldsymbol{PSto\_out\_S}_{Sto\_th,S}$

ST3 $\forall\ Sto_{th}, S$: $\boldsymbol{\dot{Q}Stoc}_{Sto\_th,S} \leq \boldsymbol{d\_Sto}_{Sto\_th,S} \cdot CapSto\_max_{Sto\_th}$

ST4 $\forall\ Sto_{th}, S$: $\boldsymbol{\dot{Q}Stoh}_{Sto\_th,S} \leq \left(1 - \boldsymbol{d\_Sto}_{Sto\_th,S}\right) \cdot CapSto\_max_{Sto\_th}$

Storage without heat loss (A): calculation of and constraints to critical storage levels

To enable the calculation of storage levels, the variables representing charge and discharge loads in a specific time slice need to be converted to equivalent variables in the corresponding time step class (equations A_LD1 and A_LD2). From these loads, the net energy charge during a time step with label ls, ld, lh and the net energy charge over the entire time step class ls, ld, lh in one year are derived, taking into account the conversion efficiency $\eta conv_{Sto}$ (A_LD3 and A_LD4). Subsequently, these variables are used to build expressions for storage levels.

In the formulation of Welsch *et al.* [48] the variables representing storage levels are related to start and end of year, season and daytype, but not to daily time brackets. As a first condition, the charge level at the start of the first season equals the one at the start of the year (A_LV1). For following seasons, the startlevel is obtained by adding the sum of net energy charges over all time step classes ls, ld, lh of the previous season to the startlevel of that season (A_LV2). The startlevel of the first daytype of a season equals the startlevel of that season (A_LV3). For subsequent daytypes, the startlevel is calculated by adding the sum of the net energy charges per time step over all daily time brackets in all days of the previous daytype to the startlevel of that daytype (A_LV4).

The endlevel of the last daytype in the last season is equal to the endlevel of the year (A_LV5). For all seasons but the last, the endlevel of the final daytype equals the startlevel of the next season (A_LV6). Furthermore, for all daytypes but the last, the endlevel is found by subtracting the sum of the net energy charges per time step over all daily time brackets in all days of the next daytype form the endlevel of that daytype (A_LV7). Equation A_LV8 ensures that the difference between start and endlevel of the year is equal to the total net energy charge, while equation A_LV9 implies that after a year, the storage reservoir is at the same level again.

A following set of equations ensures that all critical storage levels of each time step class lie between the specified upper and lower limits (A_LM1- A_LM8). Since in the present formulation no variables exist for storage levels at daily time bracket level, they are calculated implicitly. The startlevel of a daily time bracket in the first day of a daytype in the first week of a season is equal to startlevel of that daytype plus the sum of net energy charges over all preceding daily time brackets in that day (A_LM1 and A_LM2). The endlevel of a daily time bracket in the last day of the first week of a season is equal to the startlevel of that daytype, plus the sum of net energy charges over all daily time brackets in all days but the last of that daytype, plus the net energy charges over all preceding daily time brackets in the last day including the present one (A_LM3 and A_LM4). The startlevel of a daily time bracket in the first day of a daytype in the last week of a season is equal to the endlevel of that daytype minus the sum of net energy charges over all daily time brackets in all days but the first of that daytype, minus the net energy charges over all succeeding daily time brackets in the first day including the present one (A_LM5 and A_LM6). The endlevel of a daily time bracket in the last day of a daytype in the last week of a season is equal to the endlevel of that daytype minus the net energy charges over all succeeding daily time brackets in the last day (A_LM7 and A_LM8). When a storage unit is chosen in the configuration, its nominal capacity is embedded between a minimum and a maximum value (A_LM9 and A_LM10).

It must be noted that the original equations in the work of Welsch *et al.* [48] corresponding to equations A_LM3, A_LM4, A_LM5 and A_LM6 neglect to check the endlevels of daily time brackets in the last day of the last daytype in the first week of the season and the startlevels for daily time brackets in the first day of the first daytype of the last week of the season. However, it has been observed that even at these time locations peaks in storage level can appear under specific circumstances. Therefore, the proposed equations are modified versions of the original ones, that do limit these storage levels.

Constraints

Storage (thermal and electrical) without heat loss

For all equations A_***: $Sto|nohloss(Sto)$

calculation (dis)charge load and net energy charge in time step and time step class

A_LD1 $\forall\, Sto, ls, ld, lh$:

$$\boldsymbol{PSto\_in\_sdh}_{Sto,ls,ld,lh} = \sum_{S} \boldsymbol{PSto\_in\_S}_{Sto,S} \cdot conv\_s_{S,ls} \cdot conv\_d_{S,ld} \cdot conv\_h_{S,lh}$$

A_LD2 $\forall\, Sto, ls, ld, lh$:

$$\boldsymbol{PSto\_out\_sdh}_{Sto,ls,ld,lh} = \sum_{S} \boldsymbol{PSto\_out\_S}_{Sto,S} \cdot conv\_s_{S,ls} \cdot conv\_d_{S,ld} \cdot conv\_h_{S,lh}$$

A_LD3 $\forall\, Sto, ls, ld, lh$:

$$\Delta \boldsymbol{E}_{Sto,ls,ld,lh} = hrs\_lh_{lh} \cdot \left(\boldsymbol{PSto\_in\_sdh}_{Sto,ls,ld,lh} \cdot \eta c_{Sto} - \boldsymbol{PSto\_out\_sdh}_{Sto,ls,ld,lh} / \eta c_{Sto}\right)$$

A_LD4 $\forall\, Sto, ls, ld, lh$:

$$\Delta \boldsymbol{E\_y}_{Sto,ls,ld,lh} = hrs\_sdh_{ls,ld,lh} \cdot \left(\boldsymbol{PSto\_in\_sdh}_{Sto,ls,ld,lh} \cdot \eta c_{Sto} - \boldsymbol{PSto\_out\_sdh}_{Sto,ls,ld,lh} / \eta c_{Sto}\right)$$

calculation startlevels

A_LV1 $\forall\, Sto, ls = ls_1$: $\boldsymbol{startlev\_s}_{Sto,ls_1} = \boldsymbol{startlev\_y}_{Sto}$

A_LV2 $\forall\, Sto, ls \neq ls_1$: $\boldsymbol{startlev\_s}_{Sto,ls} = \boldsymbol{startlev\_s}_{Sto,ls-1} + \sum_{ld,lh} \Delta \boldsymbol{E\_y}_{Sto,ls-1,ld,lh}$

A_LV3 $\forall\, Sto, ls, ld = ld_1$: $\boldsymbol{startlev\_d}_{Sto,ls,ld_1} = \boldsymbol{startlev\_s}_{Sto,ls}$

A_LV4 $\forall\, Sto, ls, ld \neq ld_1$:

$$\boldsymbol{startlev\_d}_{Sto,ls,ld} = \boldsymbol{startlev\_d}_{Sto,ls,ld-1} + \sum_{lh} \Delta \boldsymbol{E}_{Sto,ls,ld-1,lh} \cdot days\_ld_{ld-1}$$

calculation endlevels

A_LV5 $\forall\, Sto, ls = ls_f, ld = ld_f$: $\boldsymbol{endlev\_d}_{Sto,ls_f,ld_f} = \boldsymbol{endlev\_y}_{Sto}$

A_LV6 $\forall\, Sto, ls \neq ls_f, ld = ld_f$: $\boldsymbol{endlev\_d}_{Sto,ls,ld_f} = \boldsymbol{startlev\_s}_{Sto,ls+1}$

A_LV7 $\forall\, Sto, ls, ld \neq ld_f$:

$$\boldsymbol{endlev\_d}_{Sto,ls,ld} = \boldsymbol{endlev\_d}_{Sto,ls,ld+1} - \sum_{lh} \Delta \boldsymbol{E}_{Sto,ls,ld+1,lh} \cdot days\_ld_{ld+1}$$

storage balance

A_LV8 $\forall\, Sto$: $\boldsymbol{endlev\_y}_{Sto} = \boldsymbol{startlev\_y}_{Sto} + \sum_{ls,ld,lh} \Delta \boldsymbol{E\_y}_{Sto,ls,ld,lh}$

A_LV9 $\forall\, Sto$: $\boldsymbol{startlev\_y}_{Sto} = \boldsymbol{endlev\_y}_{Sto}$

constraints to critical storage levels

A_LM1 $\forall\, Sto, ls, ld, lh$:

$$lolimlev\_rel_{Sto} \cdot \boldsymbol{CapSto\_nom}_{Sto} \leq \boldsymbol{startlev\_d}_{Sto,ls,ld} + \sum_{lh^* < lh} \Delta \boldsymbol{E}_{Sto,ls,ld,lh^*}$$

A_LM2 $\forall\, Sto, ls, ld, lh$:

$$uplimlev\_rel_{Sto} \cdot \boldsymbol{CapSto\_nom}_{Sto} \geq \boldsymbol{startlev\_d}_{Sto,ls,ld} + \sum_{lh^* < lh} \Delta \boldsymbol{E}_{Sto,ls,ld,lh^*}$$

A_LM3 $\forall\, Sto, ls, ld, lh$:

$$lolimlev\_rel_{Sto} \cdot \boldsymbol{CapSto\_nom}_{Sto} \leq \boldsymbol{startlev\_d}_{Sto,ls,ld} + (days\_ld_{ld} - 1) \cdot \sum_{lh^*} \Delta \boldsymbol{E}_{Sto,ls,ld,lh^*} + \sum_{lh^* \leq lh} \Delta \boldsymbol{E}_{Sto,ls,ld,lh^*}$$

A_LM4 $\forall\, Sto, ls, ld, lh$:

$$uplimlev\_rel_{Sto} \cdot \boldsymbol{CapSto\_nom}_{Sto} \geq \boldsymbol{startlev\_d}_{Sto,ls,ld} + (days\_ld_{ld} - 1) \cdot \sum_{lh^*} \Delta \boldsymbol{E}_{Sto,ls,ld,lh^*} + \sum_{lh^* \leq h} \Delta \boldsymbol{E}_{Sto,ls,ld,lh^*}$$

A_LM5 $\forall\, Sto, ls, ld, lh$:

$$lolimlev\_rel_{Sto} \cdot \boldsymbol{CapSto\_nom}_{Sto} \leq \boldsymbol{endlev\_d}_{Sto,ls,ld} - (days\_ld_{ld} - 1) \cdot \sum_{lh^*} \Delta \boldsymbol{E}_{Sto,ls,ld,lh^*} - \sum_{lh^* \geq lh} \Delta \boldsymbol{E}_{Sto,ls,ld,lh^*}$$

A_LM6 $\forall\, Sto, ls, ld, lh$:

$$uplimlev_{rel_{Sto}} \cdot \boldsymbol{CapSto\_nom}_{Sto} \geq \boldsymbol{endlev\_d}_{Sto,ls,ld} - (days\_ld_{ld} - 1) \cdot \sum_{lh^*} \Delta \boldsymbol{E}_{Sto,ls,ld,lh^*} - \sum_{lh^* \geq lh} \Delta \boldsymbol{E}_{Sto,ls,ld,lh^*}$$

A_LM7 $\forall\, Sto, ls, ld, lh$:

$$lolimlev\_rel_{Sto} \cdot \boldsymbol{CapSto\_nom}_{Sto} \leq \boldsymbol{endlev\_d}_{Sto,ls,ld} - \sum_{lh^* > lh} \Delta \boldsymbol{E}_{Sto,ls,ld,lh^*}$$

A_LM8 $\forall\, Sto, ls, ld, lh$:

$$uplimlev\_rel_{Sto} \cdot \boldsymbol{CapSto\_nom}_{Sto} \geq \boldsymbol{endlev\_d}_{Sto,ls,ld} - \sum_{lh^* > lh} \Delta \boldsymbol{E}_{Sto,ls,ld,lh^*}$$

constraints to nominal capacity

A_LM9 $\forall\, Sto: CapSto\_min_{Sto} \cdot sel\_Sto_{Sto} \leq \boldsymbol{CapSto\_nom}_{Sto}$

A_LM10 $\forall\, Sto: CapSto\_max_{Sto} \cdot sel\_Sto_{Sto} \geq \boldsymbol{CapSto\_nom}_{Sto}$

Storage with heat loss (B): calculation of and constraints to critical storage levels

The positions in time of all critical storage levels are determined by means of the parameter equation POS (see subsection 4.6.4), while the time discount factors for these levels are calculated by parameter equations TDF1-TDF4 (see subsection 4.6.5.2). Equations B_LD1 and B_LD2 convert charge and discharge loads from the time slice to the time step class dimension and are identical to A_LD1- A_LD2. From these loads, the net energy charge during a time step is derived in equation B_LD3, which is identical to A_LD3. The expression for critical storage levels A to D are given by equations B_LV1- B_LV4. Equation B_LV5 expresses that the storage level at the start of the year is equal to the storage level at the start of the first season. Equation B_LV6 allocates level D of the time step class featuring final season, final daytype and final daily time bracket to the endlevel of the year. For all seasons but the last one, the startlevel is equal to level D of the time step class related to the previous season, final daytype and final daily time bracket. Equation B_LV8 ensures that start and endlevel of the year are the same. Next, equations B_LM1- B_LM8 restrict the critical levels to the allowable range. The nominal capacity of a storage unit selected by the optimisation must lie between a minimum and a maximum value (B_LM9 and B_LM10).

Parameter equations

POS calculation positions in time for critical storage levels

TDF1, TDF2, TDF3, TDF4: calculations time discount factors for critical storage levels A, B, C, D

Constraints

Storage (thermal and electrical) with heat loss

For all equations B_***: $Sto = hloss(Sto)$

calculation (dis)charge load and net energy charge in time step and time step class

B_LD1 $\forall\ Sto, ls, ld, lh$:

$$\boldsymbol{PSto\_in\_sdh}_{Sto,ls,ld,lh} = \sum_{S} \boldsymbol{PSto\_in\_S}_{Sto,S} \cdot conv\_s_{S,ls} \cdot conv\_d_{S,ld} \cdot conv\_h_{S,lh}$$

B_LD2 $\forall\ Sto, ls, ld, lh$:

$$\boldsymbol{PSto\_out\_sdh}_{Sto,ls,ld,lh} = \sum_{S} \boldsymbol{PSto\_out\_S}_{Sto,S} \cdot conv\_s_{S,ls} \cdot conv\_d_{S,ld} \cdot conv\_h_{S,lh}$$

B_LD3 $\forall\ Sto, ls, ld, lh$:

$$\Delta \boldsymbol{E}_{Sto,ls,ld,lh} = hrs\_lh_{lh} \cdot \left(\boldsymbol{PSto\_in\_sdh}_{Sto,ls,ld,lh} \cdot \eta c_{Sto} - \boldsymbol{PSto\_out\_sdh}_{Sto,ls,ld,lh} / \eta c_{Sto}\right)$$

calculation critical storage levels

B_LV1 $\forall\ Sto, ls, ld, lh$:

$$\boldsymbol{levA}_{Sto,ls,ld,lh} = \boldsymbol{startlev\_s}_{Sto,ls} \cdot \alpha Ai_{Sto,ls,ld,lh} + \sum_{ld^*,lh^*} \Delta \boldsymbol{E}_{Sto,ls,ld^*,lh^*} / hrs\_lh_{lh^*} \cdot \alpha A_{Sto,ls,ld,lh,ld^*,lh^*}$$

B_LV2, B_LV3, B_LV4: *analogue equations related to critical storage levels B, C, D*

calculation storage levels at start and end of the year

B_LV5 $\forall\ Sto, ls = ls_1$: $\boldsymbol{startlev\_y}_{Sto} = \boldsymbol{startlev\_s}_{Sto,ls_1}$

B_LV6 $\forall\ Sto, ls = ls_f, ld = ld_f, lh = lh_f$: $\boldsymbol{endlev\_y}_{Sto} = \boldsymbol{levD}_{Sto,ls_f,ld_f,lh_f}$

B_LV7 $\forall\ Sto, ls \neq ls_1, ld = ld_f, lh = lh_f$: $\boldsymbol{startlev\_s}_{Sto,ls} = \boldsymbol{levD}_{Sto,ls-1,ld_f,lh_f}$

B_LV8 $\forall\ Sto$: $\boldsymbol{startlev\_y}_{Sto} = \boldsymbol{endlev\_y}_{Sto}$

constraints to critical storage levels

B_LM1 $\forall\ Sto, ls, ld, lh$: $lolimlev\_rel_{Sto} * \boldsymbol{CapSto\_nom}_{Sto} \leq \boldsymbol{levA}_{Sto,ls,ld,lh}$

B_LM2 $\forall\ Sto, ls, ld, lh$: $uplimlev\_rel_{Sto} * \boldsymbol{CapSto\_nom}_{Sto} \geq \boldsymbol{levA}_{Sto,ls,ld,lh}$

B_LM3 - B_LM8: *analogue equations related to critical storage levels B, C, D*

constraints to nominal capacity

B_LM9 $\forall\ Sto$: $CapSto\_min_{Sto} \cdot sel\_Sto_{Sto} \leq \boldsymbol{CapSto\_nom}_{Sto}$

B_LM10 $\forall\ Sto$: $CapSto\_max_{Sto} \cdot sel\_Sto_{Sto} \geq \boldsymbol{CapSto\_nom}_{Sto}$

4.6.7. Thermal storage with virtual tanks model

The thermal storage model described in Subsection 4.6.2, requires the modeller to specify the constant temperature levels of both hot and cold reservoirs, while it is not known a priori which temperature range will deliver the best system. Therefore, Becker [98] proposed a thermal storage model with discretised temperature range, consisting of a stack of interconnected virtual tanks at different constant temperature levels, increasing from the bottom to the top tank. Optimisation will decide up to which temperature level the virtual tanks will be used. The model formulation is set up for daily storage and storage losses are compensated by extra heat demands. However, seasonal storage has not yet been introduced. Therefore, an alternative model is developed in this subsection by combining the model proposed by Becker with the calculation strategy for critical storage levels described in Subsections 4.6.3 to 4.6.5.

4.6.7.1. Existing models

Becker [98] introduced daily thermal storage into the model for energy integration with heat exchange restrictions, developed earlier by Becker *et al.* [62].They divided the time horizon into a number of periods and daily time segments. Each period consists of a repetition of the representative typical day, while each day contains a series of daily time segments. A daily thermal storage is able to store heat in one daily time segment and release it in another segment in the same day. Consequently, a cyclic constraint is required to ensure that the storage level at the start and the end of each day in a period are equal. Becker's model for sensible heat storage consists of a series of virtual tanks at increasing temperature levels, interconnected by hot and cold streams between subsequent tanks. The cold streams can extract heat from hot processes or utilities in the heat cascade by countercurrent heat exchange, while the hot streams can heat up cold process or utility streams. These heat loads are equivalent to mass flows up and down between subsequent tanks with increasing temperatures.

As can be understood from equations 1 and 2. in Subsection 4.6.2.1, the heat loss from each virtual tank at a specific time is proportional to the mass level at that time. Note that to correctly follow up the mass levels, it is required that the daily time segments are collections of successive hours during the day. Becker proposed to compensate storage heat losses by adding corresponding cold streams to the heat cascade of the energy system. Although this approach ensures that storage losses over time are compensated at overall system level, it does not simulate their effect on the evolution of the mass levels in the tanks. Moreover, hot utilities would be activated to compensate thermal storage losses even in periods with no thermal demands. As a consequence, the operation of daily thermal storage subjected to heat losses cannot be accurately modelled. Fazlollahi, Becker and Maréchal [110] modified the method of Becker [98] in order to include the number of virtual tanks in the optimisation process, but kept the same approach for modelling heat losses.

As an alternative, the heat loss from a virtual tank to the environment can be modelled as a mass flow to the tank below [111], as shown in Fig. 72. The same authors attempted to introduce seasonal storage, but did not provide adequate mathematical expressions to calculate the mass levels in each virtual tank. They divided the year into multiple periods that each consist of a repetition of the representative (typical) day. Each day is divided into a number of daily time slices containing a sequential series of hours. Translated to the terminology used here, the year is divided into multiple seasons, one single daytype and multiple daily time brackets.

Equations (44)-(46) in [111], expressed in this time structure, calculate the mass level of a virtual tank related to a certain season and daily time bracket by summing up the net mass flows to that tank over a collection of hourly time steps. This collection includes all hourly time steps belonging to all daily time brackets up to the current one, over all days of all seasons up to the current season. For example, to obtain the mass level corresponding to the first season and the first daily time bracket, the sum of net mass flows over all hours belonging to the first daily time bracket in the first season would be added to the initial mass level. This formulation does not follow the natural sequence of daily time brackets over subsequent days or over subsequent periods. As a consequence, the mass level constraints in equations (40) and (42) are not imposed to real mass levels. Moreover, the calculation of the heat loss mass flows by combining equations (39),(33) and (34) in [111] is incorrect. Rager [112] applied a method similar to [111] to model seasonal storage.

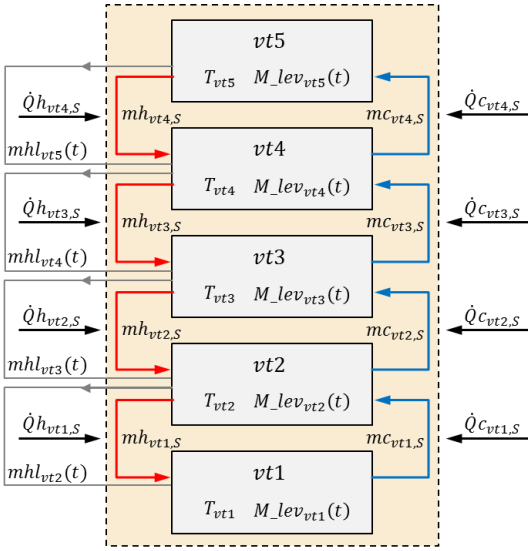

Fig. 72: Thermal storage model with virtual tanks [98, 111]

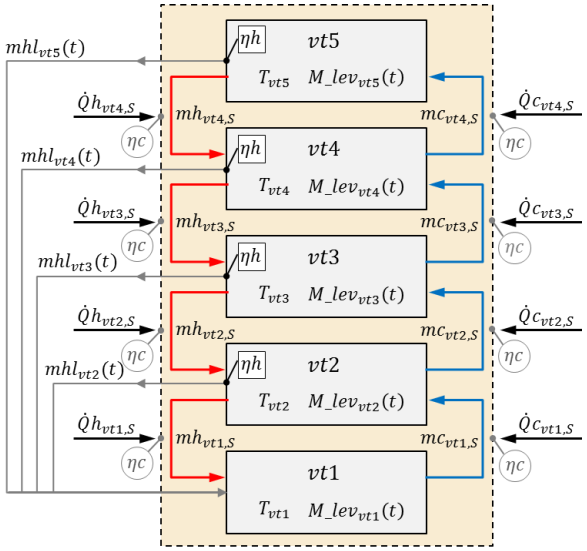

Fig. 73: Proposed thermal storage model with virtual tanks

4.6.7.2. Alternative model for thermal storage with virtual tanks

The short overview above shows that there is a need for a thermal storage model with discretised temperature levels that allows for both seasonal and daily storage and that is able to more accurately simulate heat losses over time. The novel approach presented in this subsection is based on the concept of thermal storage with virtual tanks. In order to introduce time sequence, time slices are attributed to season, daytype and daily time bracket, analogous to Subsection 4.6.3. Closest to reality would be to simulate the heat loss from a certain tank by means of a mass flow to the tank below. In this way, liquid is cascaded down in the storage reservoir while losing heat. However, this results in complex and integrated formulations for the evolution of the mass level of each tank. To tackle this problem, for each virtual tank the heat loss to the environment is conceived as a mass flow directly to the bottom tank, which is at environmental temperature (see Fig. 73).

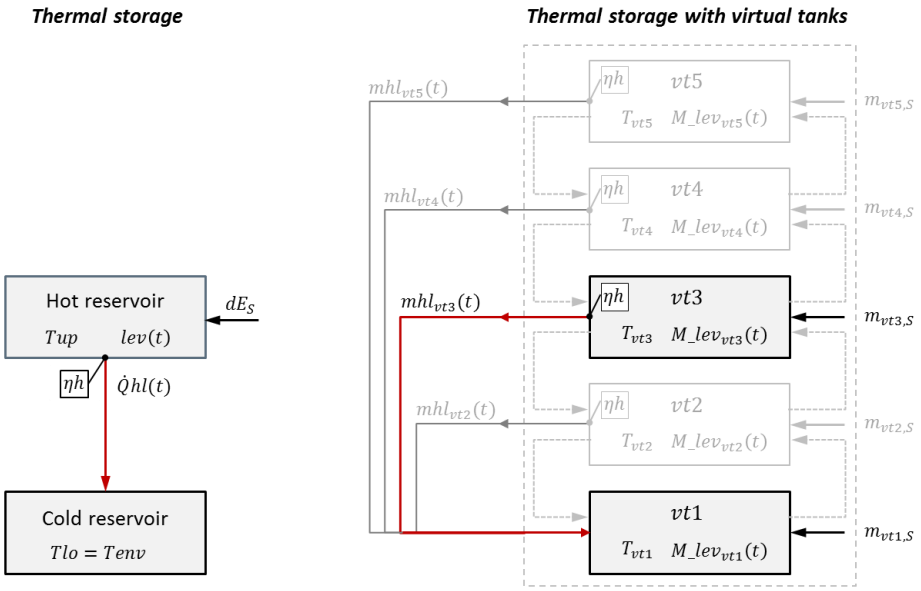

Fig. 74: Analogy between dual reservoir model and virtual tank model

As a result, an analogy exists between the calculation of the mass level in a virtual tank (above the bottom one) and the calculation of the energy charge level (in the hot reservoir) of the simplified thermal storage model (see Fig. 74). Net hourly energy charge dE [kWh/h], energy level $lev(t)$ [kWh], and heat loss $\dot{Q}hl(t)$ [kWh/h], are analogous to net hourly mass flow m_{vt} [kg/h], mass level $M\_lev_{vt}(t)$ [kg] and hourly heat loss mass flow $mhl_{vt}(t)$ [kg/h]. Consequently, the tank's critical mass levels can be formulated using the same time discount factors as defined in Subsections 4.6.4 and 4.6.5. For all virtual tanks vt but the bottom one vt_1, the expressions are completely analogue to the one for the hot reservoir in the dual tank model. However, for the bottom tank a modified formula is required since it is not subjected to heat loss and receives all heat loss mass flows from the tanks above. In case the entire year would be represented by a single time step class (1 time slice), the levels at the end of hour h_n would be given by the expressions VT_LVa and VT_LVb.

VT_LVa $\quad \forall\, vt \neq vt_1$:

$$M\_lev_{vt,h_n} = \left(M\_lev_{vt,h_{n-1}} + m_{vt}\right) \cdot \eta h$$

$$\Leftrightarrow M_{vt,h_n} = M_{vt,h_0} \cdot \eta h^n + m_{vt} \cdot \sum_{i=1}^{n} \eta h^i$$

VT_LVb $\quad \forall\, vt = vt_1$:

$$M_{vt_1,h_n} = \left(M_{vt_1,h_{n-1}} + m_{vt_1}\right) \cdot \eta h + Mtot \cdot (1 - \eta)$$

$$\Leftrightarrow M_{vt_1,h_n} = M_{vt_1,h_0} \cdot \eta h^n + m_{vt_1} \cdot \sum_{i=1}^{n} \eta h^i + Mtot \cdot (1 - \eta h^n)$$

However, time steps belong to different time step classes when running through the year. The expressions for critical mass levels in the virtual tanks can be formulated as a linear function of the mass level $\boldsymbol{Mvt\_startlev\_s}_{Sto\_vt,vt,ls_1}$ at the start of the season and the net hourly mass flow $\boldsymbol{mvt\_sdh}_{Sto\_vt,vt,ls,ld,lh}$ in every time step class within that season (equations VT_LV1 and VT_LV5).

VT_LV1 $\forall\, vt \neq vt_1$:

$$\boldsymbol{Mvt\_levA}_{Sto\_vt,vt,ls_1,ld_2,lh_3} = \boldsymbol{Mvt\_startlev\_s}_{Sto\_vt,vt,ls_1} \cdot \alpha Ai_{Sto\_vt,ls_1,ld_2,lh_3} + \sum_{ld^*,lh^*} \boldsymbol{mvt\_sdh}_{Sto\_vt,vt,ls_1,ld^*,lh^*} \cdot \alpha A_{Sto\_vt,ls_1,ld_2,lh_3,ld^*,lh^*}$$

VT_LV5 $\forall\, vt = vt_1$:

$$\boldsymbol{Mvt\_levA}_{Sto\_vt,vt_1,ls_1,ld_2,lh_3} = \boldsymbol{Mvt\_startlev\_s}_{Sto\_vt,vt_1,ls_1} \cdot \alpha Ai_{Sto\_vt,ls_1,ld_2,lh_3} + \sum_{ld^*,lh^*} \boldsymbol{mvt\_sdh}_{Sto\_vt,vt_1,ls_1,ld^*,lh^*} \cdot \alpha A_{Sto\_vt,ls_1,ld_2,lh_3,ld^*,lh^*} + \boldsymbol{MSto\_tot}_{Sto\_vt} \cdot \left(1 - \alpha Ai_{Sto\_vt,ls_1,ld_2,lh_3}\right)$$

The **time-discount factors**, are calculated by means of the multi-layered loop (TDF1) for levels A and with analogue loops for critical mass levels B,C and D. The hourly storage efficiency appearing in the time discount factor calculations can be calculated with equation 7 in Subsection 4.6.2 in which this parameter is expressed as a function of the storage unit's properties. It is valid for every virtual tank above the bottom one and it is assumed that no heat loss occurs through the lit of the top virtual tank. Since the storage level evolution is followed throughout the year, no distinction between daily and seasonal storage is made and operation of the storage unit is optimised over the year.

4.6.8. Formulation thermal storage model with virtual tanks

The mathematical formulation to model thermal storage with virtual tanks is derived from the one for thermal storage with dual reservoir including hourly losses. The difference is that mass rates have to be introduced to take into account the interconnection between subsequent virtual tanks. Moreover, the critical storage levels of the virtual tanks are related to mass rather than to energy content. However, the same method based on precalculated time discount factors is employed to determine the evolution of the levels in the virtual tanks.

The parameters describing the properties of each storage unit are specified by the modeller and include its location in the system, number of available virtual tanks, minimum and maximum limits to the total mass of heat transfer medium, conversion and hourly storage efficiencies, the specific investment cost and the specific heat capacity of the heat transfer medium. The temperatures of the virtual tanks and the minimum temperature approach for heat exchange with process or utility streams are given. Simultaneous charge and discharge in one time slice can be activated or deactivated per virtual tank.

The decision variables related to a storage unit include a binary selection variable and a number of continuous variables representing for each time slice the mass flow rates and corresponding charge and discharge loads of hot and cold streams between subsequent virtual tanks, net mass flow rates to every virtual tank per time slice and per time step class, critical mass levels and the total mass of the heat transfer liquid.

The real and the shifted source and target temperatures of the hot and cold streams between subsequent virtual tanks are derived from the specified tank temperatures. The cold and hot streams between subsequent virtual tanks are processed analogously to utility streams to determine the normalised heat capacity rates and heat loads per temperature interval. The position of critical mass levels and the corresponding time discount factors are calculated via parameter equations prior to the optimisation. The equations that describe the behaviour of storage units and their integration into the energy system form constraints to the overall optimisation problem. They involve calculation of net mass flow rates to and critical mass levels of every virtual tank, ensure that critical mass levels are lower than the total mass of heat transfer medium and that simultaneous charge and discharge is avoided. Other equations deal with the limitation of total mass, the integration of the units into the heat cascade and with the selection of the unit in the energy system configuration. Investment costs are introduced into the overall objective function.

4.6.8.1. Sets and parameters

Sets

Sto_vt	$= Sto\_vt_1..Sto\_vt_f$	thermal storage with virtual tanks
Sto	$= Sto\_th + Sto\_el + Sto\_vt$	all storage types
vt	$= vt_1..vt_f$	virtual tanks

Parameters

$locStovt_{Sto\_vt,Sys}$	connection of storage Sto_vt to system
$presSto\_vt_{Sto\_vt}$	$\forall Sto\_vt \mid \left(\sum_{Sys} locSto\_vt_{Sto\_vt,Sys} \geq 1\right) : presSto\_vt_{Sto\_vt} = 1$
$Tvt_{Sto\_vt,vt}$	temperature level of virtual tank vt of storage St_vt (in °C)
nvt_{Sto_vt}	number of used virtual tanks
$TsStovtc_{Sto\_vt,vt,S}$	(*) source temperature cold stream tank vt of storage Sto_vt in time slice S (°C)

$TtStovtc_{Sto\_vt,vt,S}$	(*) target temperature cold stream tank vt of storage Sto_vt in time slice S (°C)
$TsStovtcS_{Sto\_vt,vt,S}$	(*) shifted source temperature cold stream from tank vt to vt+1 of storage Sto_vt in time slice S (°C)
$TtStovtcS_{Sto\_vt,vt,S}$	(*) shifted target temperature cold stream from tank vt to vt+1 of storage Sto_vt in time slice S (°C)
$mcpStovtc1_{Sto\_vt,vt,S}$	(*) normalised heat capacity rate of cold stream from tank vt to vt+1 of storage Sto_vt in time slice S (kW/K/1kW)
$d\dot{Q}1Stovtc1_{k,Sto\_vt,vt,S}$	(*) fraction of heat load of cold stream from tank vt to vt+1 of storage Sto_vt situated in temperature interval k in time slice S, (kW/1kW)

(*) *analogue parameters related to hot stream from tank vt+1 to vt of storage Sto_vt*

$dTStomin\_vt_{Sto\_vt}$	minimum temperature difference for heat exchange with storage Sto_vt (°C)
$MStovt\_min_{Sto\_vt}$	lower limit to mass of storage Sto_vt (kg)
$MStovt\_max_{Sto\_vt}$	upper limit to mass of storage Sto_vt (kg)
$presStovt_{Sto\_vt}$	presence of thermal storage Sto_vt
$cI\_Stovt_{Sto\_vt}$	specific investment cost of thermal storage Sto_vt (€/kWh)
ηcvt_{Sto_vt}	efficiency of heat transfer to and from cold and hot streams storage
ηhvt_{Sto_vt}	hourly storage efficiency
$OpSto\_vt_{Sto\_vt}$	= 1: no simultaneous charging and discharging allowed
$cp\_Sto_{Sto\_vt}$	specific heat capacity storage medium (J/kgK)

parameters related to critical mass levels:
identical to thermal dual reservoir and electrical storage

4.6.8.2. Variables

Variables

$\boldsymbol{\dot{Q}Stovth}_{Sto\_vt,vt,S}$	$\mathbb{R}^+$	discharge load of hot stream from tank vt+1 to vt of storage Sto_vt in time slice S (kW)
$\boldsymbol{\dot{Q}Stovtc}_{Sto\_vt,vt,S}$	$\mathbb{R}^+$	charge load of cold stream from tank vt to vt+1 of storage Sto_vt in time slice S (kW)
$\boldsymbol{mvtc}_{Sto\_vt,vt,S}$	$\mathbb{R}^+$	mass flow rate of cold stream (with regard to heat cascade) from vt to vt+1 of storage Sto_vt in time slice S (kg/h)
$\boldsymbol{mvth}_{Sto\_vt,vt,S}$	$\mathbb{R}^+$	mass flow rate of hot stream (with regard to heat cascade) from vt to vt+1 of storage Sto_vt in time slice S (kg/h)
$\boldsymbol{mvt\_S}_{Sto\_vt,vt,S}$	$\mathbb{R}$	net mass flow rate into tank vt of storage Sto_vt in time slice S
$\boldsymbol{mvt\_sdh}_{Sto\_vt,vt,ls,ld,lh}$	$\mathbb{R}$	net mass flow rate into tank vt of storage Sto_vt in time step with label (ls,ld,lh) (kg/h)
$\boldsymbol{MSto\_tot}_{Sto\_vt}$	$\mathbb{R}^+$	total mass in thermal storage Sto_vt (kg)
$\boldsymbol{Mvt\_startlev\_s}_{Sto\_vt,vt,ls}$	$\mathbb{R}^+$	mass level tank vt of storage Sto_vt at start season ls (kg)
$\boldsymbol{Mvt\_startlev\_y}_{Sto\_vt,vt}$	$\mathbb{R}^+$	mass level tank vt of storage Sto_vt at start of the year (kg)
$\boldsymbol{Mvt\_endlev\_y}_{Sto\_vt,vt}$	$\mathbb{R}^+$	mass level tank vt of storage Sto_vt at end of the year (kg)
$\boldsymbol{Mvt\_levA}_{Sto\_vt,vt,ls,ld,lh}$	$\mathbb{R}^+$	(*) critical mass level A in tank vt of storage Sto_vt in time step class ls,ld,lh (kg)

(*) *analogue variables for critical mass levels B, C, D*

$\boldsymbol{sel\_Stovt}_{Sto\_vt}$	$\{0,1\}$	selection of storage
$\boldsymbol{d\_Stovt}_{Sto\_vt,S}$	$\{0,1\}$	charge = 1 or discharge = 0

4.6.8.3. Equations

Preparation hot and cold stream parameters thermal storage with virtual tanks

For a thermal storage with virtual tanks, the hot and cold streams between subsequent tanks are treated in a similar way as for the dual reservoir. This involves the calculation of shifted source and target temperatures and their incorporation into the shifted temperature list. Furthermore, the

normalised heat capacity rates and the normalised heat loads per temperature interval are calculated with parameter equations analogue to the ones for utilities and thermal storages (see subsections 4.4.2.1, 4.4.2.2 and 4.6.6.3.

Parameter equations

Calculation heat capacity rates

MCPVTh $\forall\ Sto\_vt, vt, S \left| TsStovth_{Sto\_vt,vt,S} \neq TtStovth_{Sto\_vt,vt,S}: \right.$

$$mcpStovth1_{Sto\_vt,vt,S} = 1/\left(TsStovth_{Sto\_vt,vt,S} - TtStoh_{Sto\_th,S}\right)$$

MCPVTc $\forall\ Sto\_vt, vt, S \left| TsStovtc_{Sto\_vt,vt,S} \neq TtStovtc_{Sto\_vt,vt,S}: \right.$

$$mcpStovtc1_{Sto\_vt,vt,S} = 1/\left(TsStovtc_{Sto\_vt,vt,S} - TtStoc_{Sto\_th,S}\right)$$

Calculation heat loads per temperature interval [T_k,T_{k+1}]

HLVTh1 $\forall\ Sto\_vt, vt, S, k \left| \begin{pmatrix} k < k_{max,S}, TsStovth_{Sto_{vt},vt,S} > TtStovth_{Sto_{vt},vt,S}, \\ TsStovth_{Sto\_vt,vt,S} \geq TS_{k+1,S}, TtStovth_{Sto\_vt,vt,S} \leq TS_{k,S} \end{pmatrix} \right.:$

$$d\dot{Q}1Stovth1_{k,Sto\_vt,vt,S} = dT_{k,S} \cdot mcpStovth1_{Sto\_vt,vt,S}$$

HLVTc1 $\forall\ Sto\_vt, vt, S, k \left| \begin{pmatrix} k < k_{max,S}, TtStovtc_{Sto\_vt,vt,S} > TsStovtc_{Sto\_vt,vt,S}, \\ TtStovtc_{Sto\_vt,vt,S} \geq TS_{k+1,S}, TsStovtc_{Sto\_vt,vt,S} \leq TS_{k,S} \end{pmatrix} \right.:$

$$d\dot{Q}1Stovtc1_{k,Sto\_vt,vt,S} = dT_{k,S} \cdot mcpStovtc1_{Sto\_vt,vt,S}$$

HLVTh2 $\forall\ Sto\_vt, vt, S, k \left| \begin{pmatrix} k < k_{max,S}, TsStovth_{Sto\_vt,vt,S} = TtStovth_{Sto\_vt,vt,S}, \\ TsStovth_{Sto\_vt,vt,S} = TS_{k+1,S}, TS_{k+1,S} = TS_{k,S} \end{pmatrix} \right.:$

$$d\dot{Q}1Stovth1_{k,Sto\_vt,vt,S} = 1$$

HLVTc2 $\forall\ Sto\_vt, vt, S, k \left| \begin{pmatrix} k < k_{max,S}, TsStovth_{Sto\_vt,vt,S} = TtStovtc_{Sto\_vt,vt,S}, \\ TsStovtc_{Sto\_vt,vt,S} = TS_{k+1,S}, TS_{k+1,S} = TS_{k,S} \end{pmatrix} \right.:$

$$d\dot{Q}1Stovtc1_{k,Sto\_vt,vt,S} = -1$$

Connection thermal storage with virtual tanks to heat cascade

Equations VT1 and VT2 convert the mass flow rates of cold and hot streams between subsequent tanks to corresponding thermal charge and discharge loads that are integrated in the heat cascade. Equations VT3 and VT4 are required to prevent simultaneous charging and discharging.

Constraints

connection to heat cascade, operation

VT1 – VT4: $vt.ord \leq nvt_{Sto\_vt}$

VT1 $\forall\ Sto\_vt, vt, S:$

$$\boldsymbol{\dot{Q}Stovtc}_{Sto\_vt,vt,S} = \frac{\boldsymbol{mvtc}_{Sto\_vt,vt,S}.\, cp\_Sto_{Sto\_vt} \cdot \left(Tvt_{Sto\_vt,vt+1} - Tvt_{Sto\_vt,vt}\right)}{3600000 \cdot \eta cvt_{Sto\_vt}}$$

VT2 $\forall\ Sto\_vt, vt, S:$

$$\boldsymbol{\dot{Q}Stovth}_{Sto\_vt,vt,S} = \frac{\boldsymbol{mvth}_{Sto\_vt,vt,S} \cdot cp\_Sto_{Sto\_vt} \cdot \eta cvt_{Sto\_vt} \cdot \left(Tvt_{Sto\_vt,vt+1} - Tvt_{Sto\_vt,vt}\right)}{3600000}$$

VT3 $\forall\ Sto\_vt, vt, S: \boldsymbol{mvtc}_{Sto\_vt,vt,S} \leq \boldsymbol{d\_Stovt}_{Sto\_vt,S} \cdot MStovt\_max_{Sto\_vt}$

VT4 $\forall\ Sto\_vt, vt, S: \boldsymbol{mvth}_{Sto\_vt,vt,S} \leq \left(1 - \boldsymbol{d\_Stovt}_{Sto\_vt,S}\right) \cdot MStovt\_max_{Sto\_vt}$

Calculation of and constraints to critical mass levels of virtual tanks

The positions in time of all critical mass levels are determined by means of the parameter equation POS (see subsection 4.6.4), while the time discount factors for these levels are calculated by parameter equations TDF1-TDF4 (see subsection 4.6.5.2). For intermediate tanks, as well as for the top and bottom tanks, the net hourly mass flow rate to the tank in a certain time slice is derived from the mass flows of the cold and hot streams between subsequent tanks (VT_MF1 - VT_MF3). Equation VTMF4 converts these net mass flow rates from the time slice to the time step class dimension. The expression for critical storage levels A to D for all tanks but the bottom one are given by equations VT_LV1- VT_LV4, similar to the equations for electrical are thermal storage with dual reservoir (B_LV1- B_LV4). Equations VT_LV5 – VT_LV8 express the critical storage levels A to D for the bottom tank and includes an additional term. Equations VT_LV9 – VT_LV12 provide conditions for storage levels at start and end of the year and at the start of each season, analogous to B_LV5-B_LV8. Next, equations VT_LM1- VT_LM4 restrict the mass level of each virtual tank to the total mass of heat transfer medium. The total mass of the heat transfer medium is equal to the sum of mass levels of all tanks, at all times, for example at the start of the year (VT_LM5). Finally, the total mass in a storage unit selected by the optimisation must lie between a minimum and a maximum value in equations VT_LM6 and VT_LM7 (analogous to B_LM9 and B_LM10).

Constraints

calculation of net hourly mass flow rate to virtual tank in time step S

VT_MF1 $\forall\, Sto\_vt, vt, S \big| 1 < vt.ord < nvt_{Sto\_vt}$:

$$\boldsymbol{mvt\_S}_{Sto\_vt,vt,S} = \boldsymbol{mvtc}_{Sto\_vt,vt-1,S} - \boldsymbol{mvtc}_{Sto\_vt,vt,S} - \boldsymbol{mvth}_{Sto\_vt,vt-1,S} + \boldsymbol{mvth}_{Sto\_vt,vt,S}$$

VT_MF2 $\forall\, Sto\_vt, vt, S \big| vt.ord = nvt_{Sto\_vt}$:

$$\boldsymbol{mvt\_S}_{Sto\_vt,vt,S} = \boldsymbol{mvtc}_{Sto\_vt,vt-1,S} - \boldsymbol{mvth}_{Sto\_vt,vt-1,S}$$

VT_MF3 $\forall\, Sto\_vt, vt, S | vt.ord = 1$:

$$\boldsymbol{mvt\_S}_{Sto\_vt,vt,S} = -\boldsymbol{mvtc}_{Sto\_vt,vt,S} + \boldsymbol{mvth}_{Sto\_vt,vt,S}$$

VT_MF4 $\forall\, Sto\_vt, vt, S \big| vt.ord \leq nvt_{Sto\_vt}$:

$$\boldsymbol{mvt\_sdh}_{Sto\_vt,vt,ls,ld,lh} = \sum_{S} \boldsymbol{mvt\_S}_{Sto\_vt,vt,S} \cdot conv\_s_{S,ls} \cdot conv\_d_{S,ld} \cdot conv\_h_{S,lh}$$

calculation of critical mass levels

virtual tanks 2 to nvt

VT_LV1 $\forall\, Sto\_vt, vt, ls, ld, lh \big| 1 < vt.ord \leq nvt_{Sto\_vt}$:

$$\boldsymbol{Mvt\_levA}_{Sto\_vt,vt,ls,ld,lh} = \boldsymbol{Mvt\_startlev\_s}_{Sto\_vt,vt,ls} \cdot \alpha Ai_{Sto\_vt,ls,ld,lh} + \sum_{ld^*,lh^*} \boldsymbol{mvt\_sdh}_{Sto\_vt,vt,ls,ld^*,lh^*} \cdot \alpha A_{Sto\_vt,ls,ld,lh,ld^*,lh^*}$$

VT_LV2, VT_LV3, VT_LV4: *analogue equations related to critical mass levels B, C, D*

virtual tank 1

VT_LV5 $\forall\, Sto\_vt, vt, ls, ld, lh | vt.ord = 1$:

$$\boldsymbol{Mvt\_levA}_{Sto\_vt,vt,ls,ld,lh} = \boldsymbol{Mvt\_startlev\_s}_{Sto\_vt,vt,ls} \cdot \alpha Ai_{Sto\_vt,ls,ld,lh} + \sum_{ld^*,lh^*} \boldsymbol{mvt\_sdh}_{Sto\_vt,vt,ls,ld^*,lh^*} \cdot \alpha A_{Sto\_vt,ls,ld,lh,ld^*,lh^*} + \boldsymbol{MSto\_tot}_{Sto\_vt} \cdot \left(1 - \alpha Ai_{Sto\_vt,ls,ld,lh}\right)$$

VT_LV6, VT_LV7, VT_LV8: *analogue equations related to critical mass levels B, C, D*

calculation of mass levels at start and end of the year

VT_LV9 - VT_LV12: $vt.ord \leq nvt_{Sto\_vt}$

VT_LV9 $\forall\ Sto\_vt, vt, ls = ls_1$:

$$\boldsymbol{Mvt\_startlev\_y}_{Sto\_vt,vt} = \boldsymbol{Mvt\_startlev\_s}_{Sto\_vt,vt,ls_1}$$

VT_LV10 $\forall\ Sto\_vt, vt, ls = ls_f, ld = ld_f, lh = lh_f$:

$$\boldsymbol{Mvt\_endlev\_y}_{Sto\_vt,vt} = \boldsymbol{Mvt\_levD}_{Sto\_vt,vt,ls_f,ld_f,lh_f}$$

VT_LV11 $\forall\ Sto\_vt, vt, ls \neq ls_1, ld = ld_f, lh = lh_f$:

$$\boldsymbol{Mvt\_startlev\_s}_{Sto\_vt,vt,ls} = \boldsymbol{Mvt\_levD}_{Sto\_vt,vt,ls-1,ld_f,lh_f}$$

VT_LV12 $\forall\ Sto\_vt, vt$:

$$\boldsymbol{Mvt\_startlev\_y}_{Sto\_vt,vt} = \boldsymbol{Mvt\_endlev\_y}_{Sto\_vt,vt}$$

constraints to critical mass levels

VT_LM1 - VT_LM4: $vt.ord \leq nvt_{Sto\_vt}$

VT_LM1 $\forall\ Sto\_vt, vt, ls, ld, lh$: $\boldsymbol{Mvt\_levA}_{Sto\_vt,vt,ls,ld,lh} \leq \boldsymbol{MSto\_tot}_{Sto\_vt}$

VT_LM2 - VT_LM4: *analogue equations related to critical mass levels B, C, D*

constraints to total mass heat transfer medium

VT_LM5 $\forall\ Sto_{vt}$: $\boldsymbol{MSto\_tot}_{Sto\_vt} = \sum_{vt|vt.ord \leq nvt_{Sto\_vt}} \boldsymbol{Mvt\_startlev\_y}_{Sto\_vt,vt}$

VT_LM6 $\forall\ Sto_{vt}$: $\boldsymbol{MSto\_tot}_{Sto\_vt} \geq \boldsymbol{sel\_Stovt}_{Sto\_vt} \cdot MStovt\_min_{Sto\_vt}$

VT_LM7 $\forall\ Sto_{vt}$: $\boldsymbol{MSto\_tot}_{Sto\_vt} \leq \boldsymbol{sel\_Stovt}_{Sto\_vt} \cdot MStovt\_max_{Sto\_vt}$

4.6.9. Integration of thermal and electrical storage in extended heat cascade model

In order to integrate thermal storage units into the formulation of the extended heat cascade model, the equations developed in subsections 4.6.6 and 4.6.8 are added as constraints. Moreover, the thermal energy balances (HC1 and HC2) and the hot and cold stream balances (HC6 and HC7) developed in subsections 4.4.3 and 4.4.4 need to be adapted. More specifically, the thermal loads of the storage hot and cold streams per time slice and temperature interval are added, in an analogous way as for thermal utilities. Furthermore, the charge and discharge loads of electrical storage units are incorporated in the electrical energy balances. In addition, the investment costs related to storage capacities need to be included in the objective function. The extended heat cascade model with envelope is adapted analogously. Note that the investment costs of the storage models in this work are not subject to economy of scale and feature constant specific investment costs.

Heat from hot streams can be stored at a certain time step (time step 1), to be released to a cold utility at a later point in time (time step 2), while it can also be directly cooled away by the cold utility in time step 1. Both pathways for heat transfer are equivalent, if no investment or operation cost are assigned to the cold utility. To prevent in that situation that the first pathway is chosen over the second one, a small specific cost (e.g. 10^{-5} €/kWh) is assigned to the heat entering the storage and the total cost is included in the objective function.

Constraints

Thermal energy balances

For HC1-HC5: $Ins.ord \leq iU(U)$, HC6: $Ins.ord \leq iU(hU)$, HC7: $Ins.ord \leq iU(cU)$

HC1 $\forall\, Sub, S, k \big| k < k_{max,S}$:

$$\boldsymbol{R}_{Sub,k+1,S} - \boldsymbol{R}_{Sub,k,S} + \sum_{P} d\dot{Q}P_{k,P,S} \cdot locP_{P,Sub} + \sum_{U,Ins} \boldsymbol{\dot{Q}U}_{U,Ins,S} \cdot d\dot{Q}U1_{k,U,S} \cdot locU_{U,Sub}$$
$$+ \sum_{Sto\_th} \boldsymbol{\dot{Q}Stoh}_{Sto\_th,S} \cdot d\dot{Q}Stoh1_{k,Sto\_th,S} \cdot locSto\_th_{Sto\_th,Sub}$$
$$+ \sum_{Sto\_th} \boldsymbol{\dot{Q}Stoc}_{Sto\_th,S} \cdot d\dot{Q}Stoc1_{k,Sto\_th,S} \cdot locSto\_th_{Sto\_th,Sub}$$
$$+ \sum_{Sto\_vt,vt} \boldsymbol{\dot{Q}Stovth}_{Sto\_vt,vt,S} \cdot d\dot{Q}1Stovth1_{k,Sto\_vt,vt,S} \cdot locSto\_th_{Sto\_th,Sub}$$
$$+ \sum_{Sto\_vt,vt} \boldsymbol{\dot{Q}Stovtc}_{Sto\_vt,vt,S} \cdot d\dot{Q}1Stovtc1_{k,Sto\_vt,vt,S} \cdot locSto\_th_{Sto\_th,Sub}$$
$$- \boldsymbol{d\dot{Q}SH}_{Sub,k,S} + \boldsymbol{d\dot{Q}HS}_{Sub,k,S} = 0$$

HC2 $\forall\, Hts, S, k \big| k < k_{max,S}$:

$$\boldsymbol{R}_{Hts,k+1,S} - \boldsymbol{R}_{Hts,k,S} + \sum_{P} d\dot{Q}P_{k,P,S} \cdot locP_{P,Hts} + \sum_{U,Ins} \boldsymbol{\dot{Q}U}_{U,Ins,S} \cdot d\dot{Q}U1_{k,U,S} \cdot locU_{U,Hts}$$
$$+ \sum_{Sto\_th} \boldsymbol{\dot{Q}Stoh}_{Sto\_th,S} \cdot d\dot{Q}Stoh1_{k,Sto\_th,S} \cdot locSto\_th_{Sto\_th,Hts}$$
$$+ \sum_{Sto\_th} \boldsymbol{\dot{Q}Stoc}_{Sto\_th,S} \cdot d\dot{Q}Stoc1_{k,Sto\_th,S} \cdot locSto\_th_{Sto\_th,Hts}$$
$$+ \sum_{Sto\_vt,vt} \boldsymbol{\dot{Q}Stovth}_{Sto\_vt,vt,S} \cdot d\dot{Q}1Stovth1_{k,Sto\_vt,vt,S} \cdot locSto\_th_{Sto\_th,Hts}$$
$$+ \sum_{Sto\_vt,vt} \boldsymbol{\dot{Q}Stovtc}_{Sto\_vt,vt,S} \cdot d\dot{Q}1Stovtc1_{k,Sto\_vt,vt,S} \cdot locSto\_th_{Sto\_th,Hts}$$
$$+ \sum_{sub} \boldsymbol{d\dot{Q}SH}_{sub,k,S} - \sum_{sub} \boldsymbol{d\dot{Q}HS}_{sub,k,S} = 0$$

HC6 $\forall\, Hts, S, k \big| k < k_{max,S}$:

$$\sum_{Sub} \boldsymbol{d\dot{Q}HS}_{Sub,k,S} \leq \sum_{hP} d\dot{Q}P_{k,hP,S} \cdot locP_{hP,Hts} + \sum_{hU,Ins} \boldsymbol{\dot{Q}U}_{hU,Ins,S} \cdot d\dot{Q}U1_{k,hU,S} \cdot locU_{hU,Hts}$$
$$+ \sum_{Sto\_th} \boldsymbol{\dot{Q}Stoh}_{Sto\_th,S} \cdot d\dot{Q}Stoh1_{k,Sto\_th,S} \cdot locSto\_th_{Sto\_th,Hts}$$
$$+ \sum_{Sto\_vt,vt} \boldsymbol{\dot{Q}Stovth}_{Sto\_vt,vt,S} \cdot d\dot{Q}1Stovth1_{k,Sto\_vt,vt,S} \cdot locSto\_th_{Sto\_th,Hts}$$

HC7 $\forall\, Hts, S, k \big| k < k_{max,S}$:

$$\sum_{Sub} \boldsymbol{d\dot{Q}SH}_{Sub,k,S} \leq -\sum_{cP} d\dot{Q}P_{k,cP,S} \cdot locP_{cP,Hts} - \sum_{cU,Ins} \boldsymbol{\dot{Q}U}_{cU,Ins,S} \cdot d\dot{Q}U1_{k,cU,S} \cdot locU_{cU,Hts}$$
$$- \sum_{Sto\_th} \boldsymbol{\dot{Q}Stoc}_{Sto\_th,S} \cdot d\dot{Q}Stoc1_{k,Sto\_th,S} \cdot locSto\_th_{Sto\_th,Hts}$$
$$- \sum_{Sto\_vt,vt} \boldsymbol{\dot{Q}Stovtc}_{Sto\_vt,vt,S} \cdot d\dot{Q}1Stovtc1_{k,Sto\_vt,vt,S} \cdot locSto\_th_{Sto\_th,Hts}$$

Electrical energy balances

For EB1, EB2: $R|L(R), Ins.ord \leq iU(U), Ins.ord \leq iE(E)$

EB1 $\forall S$:

$$\boldsymbol{Imp\_el}_S + \sum_{E,Ins,R} \boldsymbol{P\_el}_{E,Ins,S,R} + \sum_{HEh,Ins,R} \dot{\boldsymbol{Q}}_{HEh,Ins,S,R} \geq$$
$$dem\_el_S + \sum_{\substack{U,Ins,R| \\ use\_elU(U)}} \dot{\boldsymbol{Qin}}_{U,Ins,S,R} + \sum_{Sto|elSto(Sto)} \left(\boldsymbol{PSto\_in\_S}_{Sto,S} - \boldsymbol{PSto\_out\_S}_{Sto,S}\right)$$

EB2 $\forall S$:

$$\boldsymbol{Imp\_el}_S + \sum_{E,Ins,R} \boldsymbol{P\_el}_{E,Ins,S,R} + \sum_{HEh,Ins,R} \dot{\boldsymbol{Q}}_{HEh,Ins,S,R} = \boldsymbol{Exp\_el}_S +$$
$$dem\_el_S + \sum_{\substack{U,Ins,R| \\ use\_elU(U)}} \dot{\boldsymbol{Qin}}_{U,Ins,S,R} + \sum_{Sto|elSto(Sto)} \left(\boldsymbol{PSto\_in\_S}_{Sto,S} - \boldsymbol{PSto\_out\_S}_{Sto,S}\right)$$

Objective

OBJ $Ins.ord \leq iU(U), Ins.ord \leq iE(E)$

$$\boldsymbol{cost} =$$
$$\sum_{U|usefuelU(U),Ins,S,L} \dot{\boldsymbol{Qin}}_{U,Ins,S,L} \cdot hrs\_S_S \cdot cF_U + \sum_{E|usefuelE(E),Ins,S,L} \dot{\boldsymbol{Qinel}}_{E,Ins,S,L} \cdot hrs\_S_S \cdot cF\_el_E$$
$$+ \sum_{U|OMcostU(U),Ins,S} \dot{\boldsymbol{QU}}_{U,Ins,S} \cdot hrs\_S_S \cdot cOM_U + \sum_{E|OMcostE(E),Ins,S,L} \boldsymbol{Pel}_{E,Ins,S,L} \cdot hrs\_S_S . cOM\_el_E$$
$$+ Anf \cdot \sum_{U|fcostU(U),Ins,Lc} \boldsymbol{Inv}_{U,Ins,Lc} + Anf \cdot \sum_{E|fcostE(E),Ins,Lc} \boldsymbol{Inv\_el}_{E,Ins,Lc}$$
$$+ Anf \cdot \sum_{\substack{Sto|elSto(Sto) \\ Sto|thSto(Sto)}} cI\_Sto_{Sto} \cdot \boldsymbol{CapSto\_nom}_{Sto} + Anf \cdot \sum_{Sto\_vt} cI\_Sto\_vt_{Sto\_vt} \cdot \boldsymbol{MSto\_tot}_{Sto\_vt}$$
$$+ \sum_S (\boldsymbol{Imp\_el}_S \cdot hrs\_S_S \cdot cost\_el_S - \boldsymbol{Exp\_el}_S \cdot hrs\_S_S \cdot revs\_el_S)$$
$$+ \sum_{Sto\_th,S} \boldsymbol{QStoc}_{Sto\_th,S} \cdot hrs\_S_S \cdot 10^{-5}$$
$$+ \sum_{Sto\_vt,vt,S} \boldsymbol{QSto\_vtc}_{Sto\_vt,vt,S} \cdot hrs\_S_S \cdot 10^{-5}$$

4.7. Heat exchanger network

Since decades heat exchanger networks (HENs) have been key elements in chemical processing plants, as they drastically improve a plant's energy efficiency. In a HEN ,waste heat from processes that need to be cooled down is recovered and transferred to processes that have to be heated up, which can result in significant reductions in process cooling and heating demands. The network is configured by selecting heat exchanger units between hot and cold streams, determining their areas and developing flow paths and interconnections between them (see Fig. 75). When flow rates or temperatures of hot and cold streams vary over time, due to environmental cycles or process operation schedules, a multi-period HEN design method is required [61, 71, 92, 93, 113].

The HEN design is performed in the second stage of the proposed two-staged method. It is formulated as a multi-period superstructure-based MINLP problem, adapted from Yee *et al.* [84], extended to multi-period [71] and modified to include both isothermal and non-isothermal streams [95]. In the next subsections, first the mathematical model of a single heat exchanger is given and next the superstructure used for the HEN design is described, followed by the mathematical formulation of the MINLP problem and strategies to solve it.

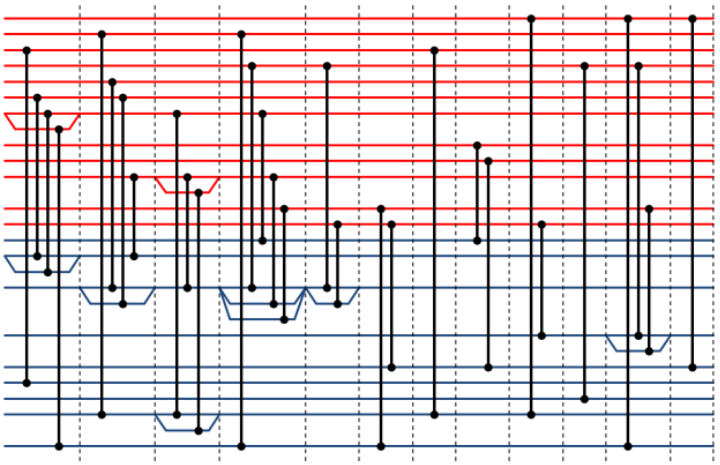

Fig. 75: Exemplary Schematic of a heat exchanger network

4.7.1. Heat exchanger model

A counter current heat exchanger enables heat transfer $\dot{q}_{hs,cs}$ from a hot stream hs to a cold stream cs by bringing both streams into contact over a heat exchange area $A_{hs,cs}$, as shown in Fig. 76. To ensure sufficient driving force (2nd law of Thermodynamics), a practical minimum positive temperature approach $\Delta Tmin$ must be respected. The required area depends on the logarithmic mean temperature difference $LMTD_{hs,cs}$ and on the overall heat transfer coefficient of the heat exchanger $U_{hc,cs}$ (equation hex1). The LMTD can be calculated with equation hex2, but when temperature differences at both sides of the heat exchanger are equal, numerical problems occur as a result of division by zero. Therefore, the approximation of LMTD proposed by Chen [96] is used in this work (equation hex3). The investment cost of the heat exchanger can be estimated by a power law equation (hex4). Multiplication with the annualisation factor Anf delivers the annualised investment cost.

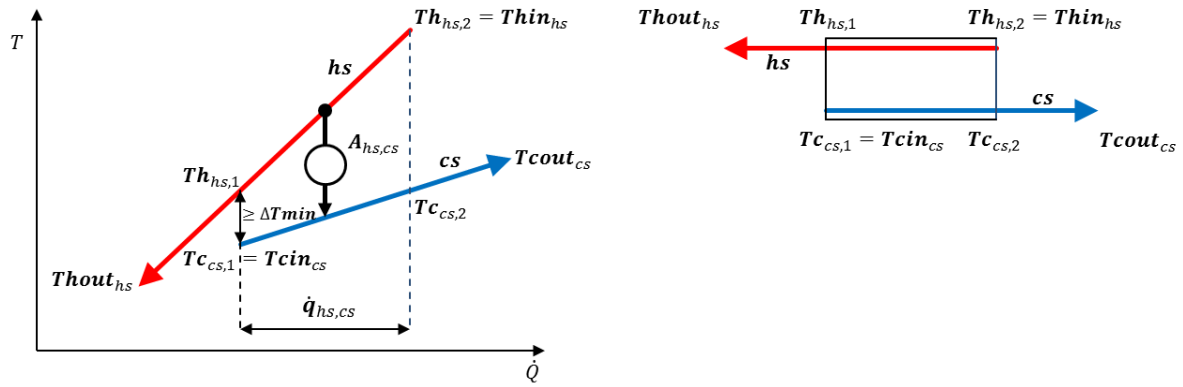

Fig. 76: Heat exchanger

hex1 $$A_{hs,cs} = \frac{\dot{q}_{hs,cs}}{U_{hc,cs} \cdot LMTD_{hs,cs}}$$

hex2 $$LMTD_{hs,cs} = (Th_{hs,1} - Tc_{cs,1})(Th_{hs,2} - Tc_{cs,2}) / \ln\left(\frac{Th_{hs,1} - Tc_{cs,1}}{Th_{hs,2} - Tc_{cs,2}}\right)$$

hex3 $$LMTD_{hs,cs} = \left[(Th_{hs,1} - Tc_{cs,1})(Th_{hs,2} - Tc_{cs,2}) \cdot \frac{1}{2} \cdot \left[(Th_{hs,1} - Tc_{cs,1}) + (Th_{hs,2} - Tc_{cs,2})\right]\right]^{\frac{1}{3}}$$

hex4 $$IC_{ex} = a \cdot (A_{hs,cs})^{exp}$$

The minimum temperature approach $\Delta Tmin$ represents the trade-off between utility costs (operation cost and annualised investment cost) and heat exchanger investment costs (area cost and fixed charges). When considering a system with a hot and a cold process stream exchanging heat, an increase in $\Delta Tmin$ reduces the amount of heat that can be exchanged and increases the hot and cold utility requirement and corresponding costs, while the required heat exchanger area and corresponding investment costs decrease.

4.7.2. Heat exchanger network superstructure

The HEN superstructure is a modified version of the one developed by Yee *et al.* [84]. Since the loads of thermal utilities and storages are fixed at their values obtained in the first stage of the two-staged method, they can be integrated in the superstructure as known streams. Therefore, the utilities at both ends of the superstructure are omitted.

The superstructure is divided into a predefined number of stages (see Fig. 77). All hot streams run from left to right and all cold streams from right to left. At every stage, each hot (cold) stream is split into a number of branches equal to the number of cold (hot) streams. In each stage, heat exchangers connect the hot stream branches with the cold stream branches, in such a way that every hot stream is connected once to every cold stream. At every stage, all branches of a stream are forced to have the same exit temperature after passing through the heat exchangers and are recombined by an isothermal mixer (see Fig. 78).

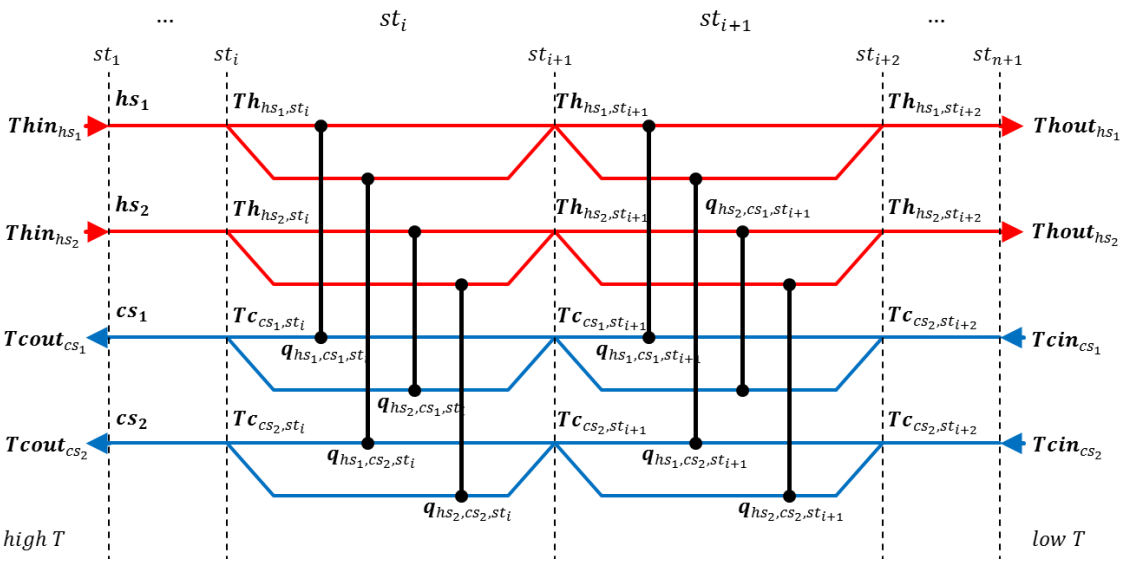

Fig. 77: Multi-stage superstructure hen design (for two hot and two cold steams)

Without isothermal mixing, the thermal energy balance of a heat exchanger on a branch of a split stream would contain a bilinear term of variables, namely mass flow rate through the branch times temperature change in that branch (equations mix1 and mix2). But when for a particular stream and stage, the temperatures of the stream branches after passing the exchangers are forced to be identical, a single overall heat balance for that stream and stage is sufficient (equation mix3). Accordingly, the variables representing the mass flow rates through the branches can be excluded from the optimisation problem and don not have to be actually modelled in the superstructure.

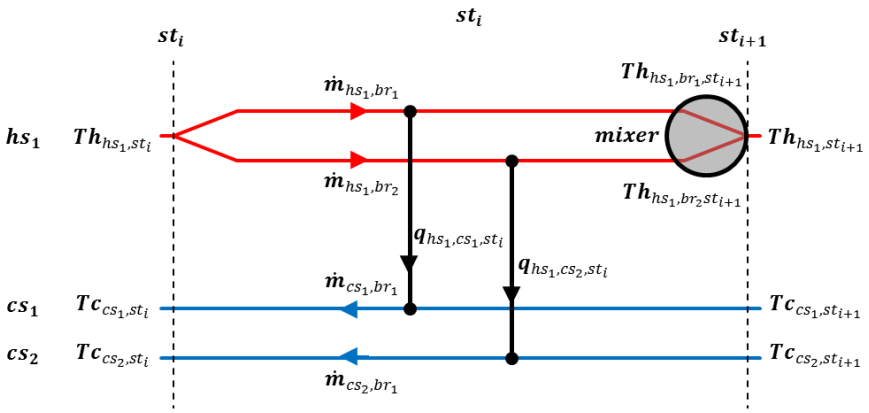

Fig. 78: Explanation of isothermal mixing assumption

mix1 $$q_{hs_1,cs_1,st_i} = \dot{m}_{hs_1,br_1} \cdot \left(Th_{hs_1,st_i} - Th_{hs_1,br_1,st_{i+1}}\right)$$

mix2 $$q_{hs_1,cs_2,st_i} = \dot{m}_{hs_1,br_2} \cdot \left(Th_{hs_1,st_i} - Th_{hs_1,br_2,st_{i+1}}\right)$$

mix3 $$\sum_{cs} q_{hs_1,cs,st_i} = \sum_{br} \dot{m}_{hs_1,br} \cdot \left(Th_{hs_1,st_i} - Th_{hs_1,st_{i+1}}\right) = \dot{m}_{hs_1} \cdot \left(Th_{hs_1,st_i} - Th_{hs_1,st_{i+1}}\right)$$

4.7.3. Formulation heat exchanger network model

Hot and cold streams in the superstructure represent thermal processes, utilities and storages. At the start of the HEN design, all stream parameters (original source and target temperatures and heat loads) are known in each period of operation S, together with the heat exchanger properties (conductivity and costs parameters).

The decision variables in the MINLP model include binaries representing the existence of each heat exchanger in the superstructure, and a number of continuous variables for heat exchanger loads, stage temperatures, approach temperatures and installed exchanger areas. The constraints include overall and stagewise energy balances, assignment of known temperatures, feasibility conditions of stream temperatures, calculation of hot and cold utility loads, constraints related to the existence of a match, calculation of approach temperatures of each match, and constraints to calculate the installed exchanger areas. The objective function to be minimised expresses the annualised costs of installed area and fixed charges for the heat exchangers. Next to the objective function, also some of the constraints are non-linear, namely the expression to determine the maximum area for each heat exchanger over all periods and the equations for calculation of the LMTD.

The number of stages can be varied by the modeller, but to obtain the best objective value the number of stages will normally not be higher than the maximum number of hot or cold streams [84]. As already explained in subsection 3.2.2, in every period the available heat exchanger area is equal to the required area, while in the objective function the maximum area over all periods is taken into account. To enable this in reality, a controllable bypass around each heat exchanger needs to be installed, but these bypasses do not interfere in the optimisation model.

4.7.3.1. Sets and parameters

Following definitions are used in the model formulation. Instance hsI of hot stream hs and instance csI of cold stream csI are denoted as hot stream hs, hsI and cold stream cs, csI

Sets

hs	hot streams (thermal processes, utilities and storages)	
cs	cold streams (thermal processes, utilities and storages)	
hsI	hot stream instances	
csI	cold stream instances	
ks	$= stg_1..stg_{100}$	stages
$st(ks)$	$= stg_1..stg_n$	used stages
$Tst(ks)$	$= stg_1..stg_{n+1}$	temperature locations

Parameters

General

nSt	number of stages

Streams

$Thin_{hs,S}$	source temperature of hot stream hs in time slice S (°C)
$Thout_{hs,S}$	target temperature of hot stream hs in time slice S (°C)
$Tcin_{cs,S}$	source temperature of cold stream cs in time slice S (°C)
$Tcout_{cs,S}$	target temperature of cold stream cs in time slice S (°C)
$fhs_{hs,hsI,S}$	heat capacity flowrate of non-isothermal hot stream hs, hsI in time slice S (kW/K)
$fcs_{cs,csI,S}$	heat capacity flowrate of non-isothermal cold stream cs, csI in time slice S (kW/K)
$Lhh_{hs,hsI,S}$	latent heat load of isothermal hot stream hs, hsI in time slice S (kW)
$Lhc_{cs,csI,S}$	latent heat load of isothermal cold stream cs, csI in time slice S (kW)
ihs_{hs}	number of instances of hot stream hs (for process and storage streams $ihs_{hs} = 1$)

ics_{cs} number of instances of cold stream hs (for process and storage streams $ics_{cs} = 1$)
$lochs_{hs,Sys}$ location of hot stream hs
$loccs_{cs,Sys}$ location of cold stream cs

Heat exchangers

$Uhc_{hs,cs}$ overall heat transfer coefficient of heat exchanger between hot stream hs and cold stream cs (kW/m²K)
$cfix$ fixed charge for heat exchanger (€)
$acoeff$ area cost coefficient for heat exchangers
exp area cost exponent for heat exchangers
$Qmaxhscs_{hs,hsI,cs,csI,S}$ maximum heat exchange between hot stream hs, hsI and cold stream cs, csI in time slice S (kW)
$dTmax_{hs,cs,S}$ upper limit temperature approach between hot stream hs and cold stream cs in time slice S (°C)
$minhex$ minimum number of heat exchangers

4.7.3.2. Variables

Binary variables

$\boldsymbol{z}_{hs,hsI,cs,csI,ks}$ existence heat exchanger between hot stream hs, hsI and cold stream cs, csI in stage st

Positive continuous variables

$\boldsymbol{Th}_{hs,hsI,ks,S}$ temperature of hot stream hs, hsI as it enters stage st in time slice S (°C)
$\boldsymbol{Tc}_{cs,csI,ks,S}$ temperature of cold stream cs, csI as it leaves stage st in time slice S (°C)
$\boldsymbol{qhc}_{hs,hsI,cs,csI,ks,S}$ energy exchanged between hot stream hs, hsI and cold stream cs, csI in stage st in time slice S (kW)
$\boldsymbol{dThc}_{hs,hsI,cs,csI,ks,S}$ temperature approach between hot stream hs, hsI as it enters stage st and cold stream cs, csI as it leaves stage st in time slice S (°C)
$\boldsymbol{Ahc}_{hs,hsI,cs,csI,ks}$ area heat exchanger between hot stream hs, hsI and cold stream cs, csI in stage st (m²)
$\boldsymbol{LMTDhc}_{hs,hsI,cs,csI,ks,S}$ logarithmic mean temperature difference between hot stream hs, hsI and cold stream cs, csI in stage st in time slice S (°C)
$\boldsymbol{numhex}$ number of heat exchangers
$\boldsymbol{hencost}$ hen and utility cost (€)

4.7.3.3. Equations

The equations that describe the superstructure form the constraints of the MINLP problem. In this subsection, (hot or cold) stream refers to (hot or cold) stream instance. For each hot (cold) stream, overall energy balances ensure that in every period the stream's total heat load is equal to the sum over all stages of the heat loads exchanged with all cold (hot) streams. These balances are formulated separately for respectively non-isothermal hot and cold and isothermal hot and cold streams and are indicated as OEB1, OEB2, OEB3, OEB4. For each hot (cold) stream, stage energy balances express that in every period the stream's heat load in a stage is equal to the sum of heat loads exchanged with all cold (hot) streams in that stage. These stagewise balances are formulated for non-isothermal hot and cold streams (SEB1, SEB2), but are not required for isothermal streams, since these streams keep a constant temperature level over all stages.

In each period, stream source and target temperatures can be assigned to both ends of the superstructure (TIO1, TIO2, TIO3, TIO4). In every period, local stream temperatures must monotonically decrease over subsequent stages for a non-isothermal hot stream or increase for a

non-isothermal cold stream (TMO1, TMO2). In case of isothermal hot or cold streams, stream temperatures remain at the same level over all stages (TMO3, TMO4). The heat exchange between a hot and a cold stream in a certain period and stage cannot exceed an upper limit (LIM1). However, if no heat exchanger is required between this pair of streams, the binary variable for selection of that heat exchanger is set to zero, turning the constraint inactive.

For every stage in each period, equations TAP1 and TAP2 express the temperature approaches between a hot and a cold stream at both sides of the stage as a function of the local stream temperatures and the existence of a heat exchanger. When a heat exchanger exists, the difference between the local stream temperatures at each side of the stage must be higher than the temperature approach. In turn, this temperature approach must be greater than a specified minimum value $\Delta Tmin$ (see BND1). However, when no heat exchanger is selected, this lower limit to the local stream temperature difference is deactivated.

The logarithmic mean temperature difference between a hot and a cold stream at a certain stage in a certain period is calculated in equation LMT1 using the approximation proposed by Chen [96]. Since the expression x^c is not defined in GAMS for $x < 0$ nor for $x = 0$ and $0 < c < 1$, the factors in the LMT1 equation must be strictly positive. This explains why this equation is formulated in terms of temperature approaches and not in terms of differences between local stream temperatures. The installed area of a heat exchanger between a hot and a cold stream in a certain stage is the maximum of the areas required in every period (AHC1). Finally, the objective is to minimise the total annualised investment costs of the HEN, consisting of fixed charges and the installed area costs for every heat exchanger (OBJ2). The term 0.001 has been added to avoid numerical problems for x^c with $x = 0$.

All equations: $hsI.ord \leq ihs_{hs},\ csI.ord \leq ics_{cs}$

Constraints

Overall Energy Balances

OEB1 $\forall\ hs, hsI, S \big| hs\_iso_{hs,S} = 0$:

$$\left(Thin_{hs,S} - Thout_{hs,S}\right) \cdot fhs_{hs,hsI,S} = \sum_{cs,csI,st} \boldsymbol{qhc}_{hs,hsI,cs,csI,st,S}$$

OEB2 $\forall\ cs, csI, S \big| cs\_iso_{cs,S} = 0$:

$$\left(Tcout_{cs,S} - Tcin_{cs,S}\right) \cdot fcs_{cs,csI,S} = \sum_{hs,hsI,st} \boldsymbol{qhc}_{hs,hsI,cs,csI,st,S}$$

OEB3 $\forall\ hs, hsI, S \big| hs\_iso_{hs,S} = 1$:

$$Lhh_{hs,hsI,S} = \sum_{cs,csI,st} \boldsymbol{qhc}_{hs,hsI,cs,csI,st,S}$$

OEB4 $\forall\ cs, csI, S \big| cs\_iso_{cs,S} = 1$:

$$Lhc_{cs,csI,S} = \sum_{hs,hsI,st} \boldsymbol{qhc}_{hs,hsI,cs,csI,st,S}$$

Stage Energy Balances

SEB1 $\forall\ hs, hsI, st, S \big| hs\_iso_{hs,S} = 0$:

$$\left(\boldsymbol{Th}_{hs,hsI,st,S} - \boldsymbol{Th}_{hs,hsI,st+1,S}\right) \cdot fhs_{hs,hsI,S} = \sum_{cs,csI} \boldsymbol{qhc}_{hs,hsI,cs,csI,st,S}$$

SEB2 $\forall\ cs, csI, st, S \big| cs\_iso_{cs,S} = 0$:

$$\left(\boldsymbol{Tc}_{cs,csI,st,S} - \boldsymbol{Tc}_{cs,csI,st+1,S}\right) \cdot fcs_{cs,csI,S} = \sum_{hs,hsI} \boldsymbol{qhc}_{hs,hsI,cs,csI,st,S}$$

Assignment in- and outlet temperatures

TIO1 $\forall\, hs, hsI, stg_1, S$: $Thin_{hs,S} = \boldsymbol{Th}_{hs,hsI,stg_1,S}$

TIO2 $\forall\, hs, hsI, stg_{n+1}, S$: $Thout_{hs,S} = \boldsymbol{Th}_{hs,hsI,stg_{n+1},S}$

TIO3 $\forall\, cs, csI, stg_{n+1}, S$: $Tcin_{cs,S} = \boldsymbol{Tc}_{cs,csI,stg_{n+1},S}$

TIO4 $\forall\, cs, csI, stg_1, S$: $Tcout_{cs,S} = \boldsymbol{Tc}_{cs,csI,stg_1,S}$

Conditions stage temperatures

TMO1 $\forall\, hs, hsI, st, S \,|\, hs\_iso_{hs,S} = 0$: $\boldsymbol{Th}_{hs,hsI,st,S} \geq \boldsymbol{Th}_{hs,hsI,st+1,S}$

TMO2 $\forall\, cs, csI, st, S \,|\, cs\_iso_{cs,S} = 0$: $\boldsymbol{Tc}_{cs,csI,st,S} \geq \boldsymbol{Tc}_{cs,csI,st+1,S}$

TMO3 $\forall\, hs, hsI, Tst, S \,|\, hs\_iso_{hs,S} = 1$: $\boldsymbol{Th}_{hs,hsI,Tst,S} = Thin_{hs,S}$

TMO4 $\forall\, cs, csI, Tst, S \,|\, cs\_iso_{cs,S} = 1$: $\boldsymbol{Tc}_{cs,csI,Tst,S} = Tcin_{cs,S}$

Limits to heat transfer

LIM1 $\forall\, hs, hsI, cs, csI, st, S$:

$$\boldsymbol{qhc}_{hs,hsI,cs,csI,st,S} - Qmaxhscs_{hs,hsI,cs,csI,S} \cdot \boldsymbol{z}_{hs,hsI,cs,csI,st} \leq 0$$

Temperature approaches

TAP1 $\forall\, hs, hsI, cs, csI, st, S$:

$$\boldsymbol{dThc}_{hs,hsI,cs,csI,st,S} \leq \boldsymbol{Th}_{hs,hsI,st,S} - \boldsymbol{Tc}_{cs,csI,st,S} + dTmax_{hs,cs,S} \cdot \left(1 - \boldsymbol{z}_{hs,hsI,cs,csI,st}\right)$$

TAP2 $\forall\, hs, hsI, cs, csI, st, S$:

$$\boldsymbol{dThc}_{hs,hsI,cs,csI,st+1,S} \leq \boldsymbol{Th}_{hs,hsI,st+1,S} - \boldsymbol{Tc}_{cs,csI,st+1,S} + dTmax_{hs,cs,S} \cdot \left(1 - \boldsymbol{z}_{hs,hsI,cs,csI,st}\right)$$

Logarithmic mean temperature difference

LMTD $\forall\, hs, hsI, cs, csI, st, S$:

$$\boldsymbol{LMTDhc}_{hs,hsI,cs,csI,st,S} =$$

$$\left(\boldsymbol{dThc}_{hs,hsI,cs,csI,st,S} \cdot \boldsymbol{dThc}_{hs,hsI,cs,csI,st+1,S} \cdot \frac{\boldsymbol{dThc}_{hs,hsI,cs,csI,st,S} + \boldsymbol{dThc}_{hs,hsI,cs,csI,st+1,S}}{2}\right)^{\frac{1}{3}}$$

Maximum heat exchanger area

AHC1 $\forall\, hs, hsI, cs, csI, st, S$:

$$\boldsymbol{Ahc}_{hs,hsI,cs,csI,st} \geq \frac{\boldsymbol{qhc}_{hs,hsI,cs,csI,st,S}}{Uhc_{hc,cs} \cdot \boldsymbol{LMTDhc}_{hs,hsI,cs,csI,st,S}}$$

Objective function

OBJ2

$$\boldsymbol{hencost} = Anf \times \left[\sum_{hs,hsI,cs,csI,st} cfix \cdot \boldsymbol{z}_{hs,hsI,cs,csI,st} + acoeff \cdot \sum_{hs,hsI,cs,csI,st} \left(\boldsymbol{Ahc}_{hs,hsI,cs,csI,st} + 0.001\right)^{exp}\right]$$

The maximum heat exchange between a hot and cold stream in a certain period and stage is equal to the minimum of the total heat loads of both streams in that period. These limits are precalculated for the combinations: non-isothermal hot, non-isothermal cold (QMX1), isothermal hot, non-isothermal cold (QMX2), non-isothermal hot, isothermal cold (QMX2), and isothermal hot, isothermal cold (QMX4). The 'big M values' in equations TAP1 and TAP2 are prespecified by the parameter equations DTMX. These values must prevent, for each period, that the local stream temperatures of a hot and a cold stream in a certain stage are constrained if no heat exchanger exists between these streams. Moreover, the temperature approaches between hot and cold stream at both stage ends cannot be lower than $dTmin$. Therefore, the big M must be bigger than the absolute value of the largest negative temperature difference that could occur between this hot and cold stream plus $dTmin$. The number of stages is taken equal to the maximum number of hot or cold streams [84]

Parameter equations

Maximum heat exchange

QMX1 $\forall\ hs, hsI, cs, csI, S \left| hs\_iso_{hs,S} = 0, cs\_iso_{cs,S} = 0 \right.$:
$Qmaxhscs_{hs,hsI,cs,csI,S} =$
$min\left[\left(Thin_{hs,S} - Thout_{hs,S}\right) \cdot fhs_{hs,hsI,S}, \left(Tcout_{cs,S} - Tcin_{cs,S}\right) \cdot fcs_{cs,csI,S}\right]$

QMX2 $\forall\ hs, hsI, cs, csI, S \left| hs\_iso_{hs,S} = 1, cs\_iso_{cs,S} = 0 \right.$:
$Qmaxhscs_{hs,hsI,cs,csI,S} = min\left[Lhh_{hs,hsI,S}, \left(Tcout_{cs,S} - Tcin_{cs,S}\right) \cdot fcs_{cs,csI,S}\right]$

QMX3 $\forall\ hs, hsI, cs, csI, S \left| hs\_iso_{hs,S} = 0, cs\_iso_{cs,S} = 1 \right.$:
$Qmaxhscs_{hs,hsI,cs,csI,S} = min\left[\left(Thin_{hs,S} - Thout_{hs,S}\right) \cdot fhs_{hs,hsI,S}, Lhc_{cs,csI,S}\right]$

QMX4 $\forall\ hs, hsI, cs, csI, S \left| hs\_iso_{hs,S} = 1, cs\_iso_{cs,S} = 1 \right.$:
$Qmaxhscs_{hs,hsI,cs,csI,S} = \min\left(Lhh_{hs,hsI,S}, Lhc_{cs,csI,S}\right)$

Upper limit temperature approach

DTMX $\forall\ hs, hsI, cs, csI, S \left| hs\_iso_{hs,S} = 1, cs\_iso_{cs,S} = 1 \right.$:
$dTmax_{hs,cs,S} =$
$\mathrm{dTmin} - min\left(0, Thin_{hs,S} - Tcout_{cs,S}, Thout_{hs,S} - Tcin_{cs,S}, Thout_{hs,S} - Tcout_{cs,S}\right)$

4.7.3.4. Bounds

By setting bounds to variables, the solution space of the MINLP problem is reduced. As mentioned above, temperature approaches are subject to a lower bound of $dTmin$ (BND1). Consequently, the same lower bound can be set for the logarithmic mean temperature approaches (BND2). For all hot and cold streams, the local stream temperatures at every temperature location must lie between their source and target temperatures (BND3, BND4, BND5, BND6). Heat cannot be exchanged directly between hot and cold streams of different subsystems. Therefore, a number of heat exchangers in the superstructure are a priori excluded. Their positions are derived from the location in the energy system of the corresponding streams with parameter equation FHE1. At each of these positions, the binary variable corresponding to the existence of the heat exchanger is set to zero (FHE2).

Bounds

All bounds: $hsI \leq ihs_{hs},\ csI \leq ics_{cs}$

Lower bound temperature approaches

BND1 $\forall\ hs, hsI, cs, csI, Tst, S$: $\boldsymbol{dThc}_{hs,hsI,cs,csI,Tst,S} \geq \Delta Tmin$

Lower bound logarithmic mean temperature approaches

Not in A and B-version

BND2 $\forall\ hs, hsI, cs, csI, st, S$: $\boldsymbol{LMTDhc}_{hs,hsI,cs,csI,st,S} \geq \Delta Tmin$

Lower and upper bounds stage temperatures

BND3 $\forall\ hs, hsI, Tst, S$: $\boldsymbol{Th}_{hs,hsI,Tst,S} \leq Thin_{hs,S}$

BND4 $\forall\ hs, hsI, Tst, S$: $\boldsymbol{Th}_{hs,hsI,Tst,S} \geq Thout_{hs,S}$

BND5 $\forall\ cs, csI, Tst, S$: $\boldsymbol{Tc}_{cs,csI,Tst,S} \leq Tcout_{cs,S}$

BND6 $\forall\ cs, csI, Tst, S$: $\boldsymbol{Tc}_{cs,csI,Tst,S} \geq Tcin_{cs,S}$

Forbidden heat exchangers

FHE1 $\forall\, hs, hsI, cs, csI, st \left| \sum_{Sub} \left(lochs_{hs,Sub} + lochs_{hs,Hts}\right).\left(loccs_{cs,Sub} + loccs_{cs,Hts}\right) = 0 \right.$:

$forbiddenhex_{hs,hsI,cs,csI,st} = 1$

FHE2 $\forall\, hs, hsI, cs, csI, st \left| forbiddenhex_{hs,hsI,cs,csI,st} = 1 \right.$:

$\boldsymbol{z}_{hs,hsI,cs,csI,st} = 0$

4.7.3.5. Solution strategies

For more complex energy systems (i.e. more streams, time slices, use of thermal or electrical storage, utilities such as compression chillers, CHPs, heat pumps, heat engines) the MINLP problem requires longer solving times. However, a number of improvements to the model can speed up the calculation.

As a first improvement, the MINLP solve is started from a feasible solution. Therefore, a simplified MILP version (min_NHEX) of the original model (min_TAC) is constructed, in which equations AHC1, and LMTD are omitted. A new objective function is formulated expressing the total number of installed heat exchangers (OBJ1). Based on the solution of min_NHEX (indexed with superscript $l1$), on the installed areas and the mean temperature differences computed with parameter equations AHC2, and LMT2 respectively, a feasible starting point for min_TAC is determined. In GAMS, the decision variable values resulting from min_NHEX are taken as initial values for min_TAC by default. It must be noted that setting initial values for LMTD has no observed effect on the calculation time and can be omitted. In addition, equation NHE1 could be added to the constraints of min_TAC in order to limit the number of heat exchangers to the result obtained in min_NHEX, but also no effect on the solution time was observed.

Improvement 1

$hsI \leq ihs_{hs}, csI \leq ics_{cs}$

Objective function min_NHEX

OBJ1 $$\boldsymbol{numhex} = \sum_{hs,hsI,cs,csI,st} \boldsymbol{z}_{hs,hsI,cs,csI,st}$$

Initialisation min_TAC

Initial values installed heat exchanger areas

AHC2 $\forall\, hs, hsI, cs, csI, st, S \left| z^{l1}_{hs,hsI,cs,csI,st} = 1 \right.$:

$$\boldsymbol{Ahc}_{hs,hsI,cs,csI,st} = \max_{S} \frac{qhc^{l1}_{hs,hsI,cs,csI,st,S}}{Uhc_{hc,cs}.\, LMTDhc^{*}_{hs,hsI,cs,csI,st,S}}$$

with:

$$LMTDhc^{*}_{hs,hsI,cs,csI,st,S} = \left(\boldsymbol{dThc}^{l1}_{hs,hsI,cs,csI,st,S}.\, \boldsymbol{dThc}^{l1}_{hs,hsI,cs,csI,st+1,S}.\, \frac{\boldsymbol{dThc}^{l1}_{hs,hsI,cs,csI,st,S} + \boldsymbol{dThc}^{l1}_{hs,hsI,cs,csI,st+1,S}}{2} \right)^{\frac{1}{3}}$$

Initial values logarithmic mean temperature differences

LMT2 $\forall\, hs, hsI, cs, csI, st, S$:

$$LMTDhc_{hs,hsI,cs,csI,st,S} = \left(\boldsymbol{dThc}^{l1}_{hs,hsI,cs,csI,st,S} \cdot \boldsymbol{dThc}^{l1}_{hs,hsI,cs,csI,st+1,S} \cdot \frac{\boldsymbol{dThc}^{l1}_{hs,hsI,cs,csI,st,S} + \boldsymbol{dThc}^{l1}_{hs,hsI,cs,csI,st+1,S}}{2} \right)^{\frac{1}{3}}$$

Constraint min_TAC

Maximum number of heat exchangers

NHE1 $$\sum_{hs,hsI,cs,csI,st} \boldsymbol{z}_{hs,hsI,cs,csI,st} \leq numhex^{l1}$$

A second and additional improvement consists in fixing all binary decision variables for the selection of heat exchangers in min_TAC at the solution of min_NHEX (BND7). As a consequence, min_TAC is reduced to an NLP problem, which is less complex than an MINLP problem. Moreover, equation NHE1 becomes obsolete. Min_NHEX can have many optimal solutions and selecting only one for further optimisation in min_TAC, may exclude the global optimum. To find all optimal solutions, integer cut constraints have to be added to min_NHEX. As this would dramatically increase the overall solution time, I did not include this technique in the model. In min_TAC, the installed areas of exchangers that have not been selected in min_NHEX can be fixed to zero (BND8). Moreover, equations LMT1 and AHC1 only have to be generated for existing exchangers. Analogously, investment costs must only be included in objective function OBJ2 for existing exchangers and the term 0.001 can be omitted. It was observed that the results obtained by fixed exchanger selection after min_NHEX are similar or better than without fixing.

Improvement 2

$hsI \leq ihs_{hs}, csI \leq ics_{cs}$

Bounds min_TAC

Fixed heat exchanger selection

BND7 $\forall\, hs, hsI, cs, csI, st: \boldsymbol{z}_{hs,hsI,cs,csI,st} = z^{l1}_{hs,hsI,cs,csI,st}$

Fixed heat exchanger areas

BND8 $\forall\, hs, hsI, cs, csI, st \left| z^{l1}_{hs,hsI,cs,csI,st} = 0: \boldsymbol{Ahc}_{hs,hsI,cs,csI,st} = 0 \right.$

Identification exchangers selected in min_NHEX

$\forall\, hs, hsI, cs, csI, st \left| z^{l1}_{hs,hsI,cs,csI,st} = 1: hexpres_{hs,hsI,cs,csI,st} = 1 \right.$

Generation equations min_TAC only for exchangers selected in min_NHEX

LMT1 $\forall\, hs, hsI, cs, csI, st, S \left| hexpres_{hs,hsI,cs,csI,st} = 1 \right.$

AHC1 $\forall\, hs, hsI, cs, csI, st, S \left| hexpres_{hs,hsI,cs,csI,st} = 1 \right.$

OBJ2 $$\ldots \sum_{\substack{hs,hsI,cs,csI,st \\ | hexpres_{hs,hsI,cs,csI,st}=1}} \left(\boldsymbol{Ahc}_{hs,hsI,cs,csI,st} \right)^{exp}$$

Additional improvements can be achieved by eliminating the logarithmic mean temperature difference variable. This requires substituting the LMTD expression in the equation AHC1, which determines the maximum area for each heat exchanger over all periods. Furthermore, equations TAP1 and TAP2 can be combined with bound BND2 in such a way that also the variables for temperature approach can be omitted and substituted by the difference in local stream temperatures. Although the number of variables is decreased, no improvement in solution time was observed.

Note that no problems are encountered resulting from the fact that the energy balances are already closed by fixing the utility streams in stage 1 of the two-staged method.

4.7.4. Extension for thermal storages with virtual tanks

In order to integrate the thermal streams related to thermal storages with virtual tanks, all stream parameters (heat loads and temperatures) are additionally indexed with the set of virtual tanks vt. The number of elements in this set that are active for each hot stream hs or cold stream cs is limited by the parameters $vths_{hs}$ and $vtcs_{cs}$. For hot and cold streams associated with thermal storages with virtual tanks, this number is equal to $nvt_{Sto\_vt} - 1$, corresponding to the number of hot or cold streams between subsequent tanks. However, for streams related to other storage types or utilities, these parameters are equal to 1, since they do not have any meaning. The heat network model is now reformulated by extending the dimension of all variables with the set vt. Moreover, the all parameter equations and model constraints are generated for every active element of the set vt.

4.8. Architecture of the model code

The model code of *Syn-E-Sys* is written in GAMS[72] and built up according to the two-staged method proposed in Chapter 3. In the first stage, energy integration is performed and selection, sizing and operation of the utility and storage units available in the superstructure are optimised to deliver minimum total annualised costs. Starting from these results, the heat exchanger network with minimum annualised investment cost is composed in stage 2.

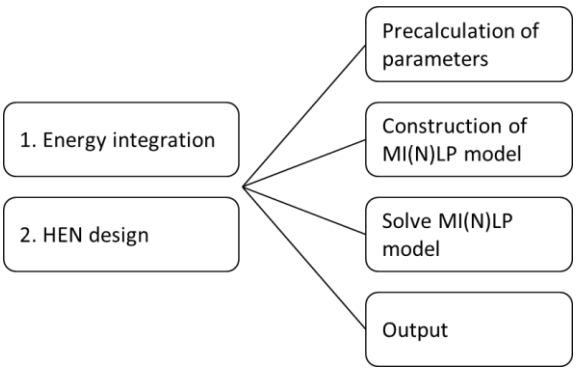

Fig. 79: Model architecture

In each stage the data are read in and restructured into appropriate parameters. Using these parameters, the equations composing the optimisation model are generated. Subsequently, the model is solved with an appropriate solver and finally, the results are post processed and presented in the form of tables or diagrams. The model layout is schematically represented in Fig. 79 and a detailed overview of stage 1 and stage 2 is given in Fig. 80 and Fig. 81, which provide a summary of the equations and calculation procedures that will be developed throughout this chapter.

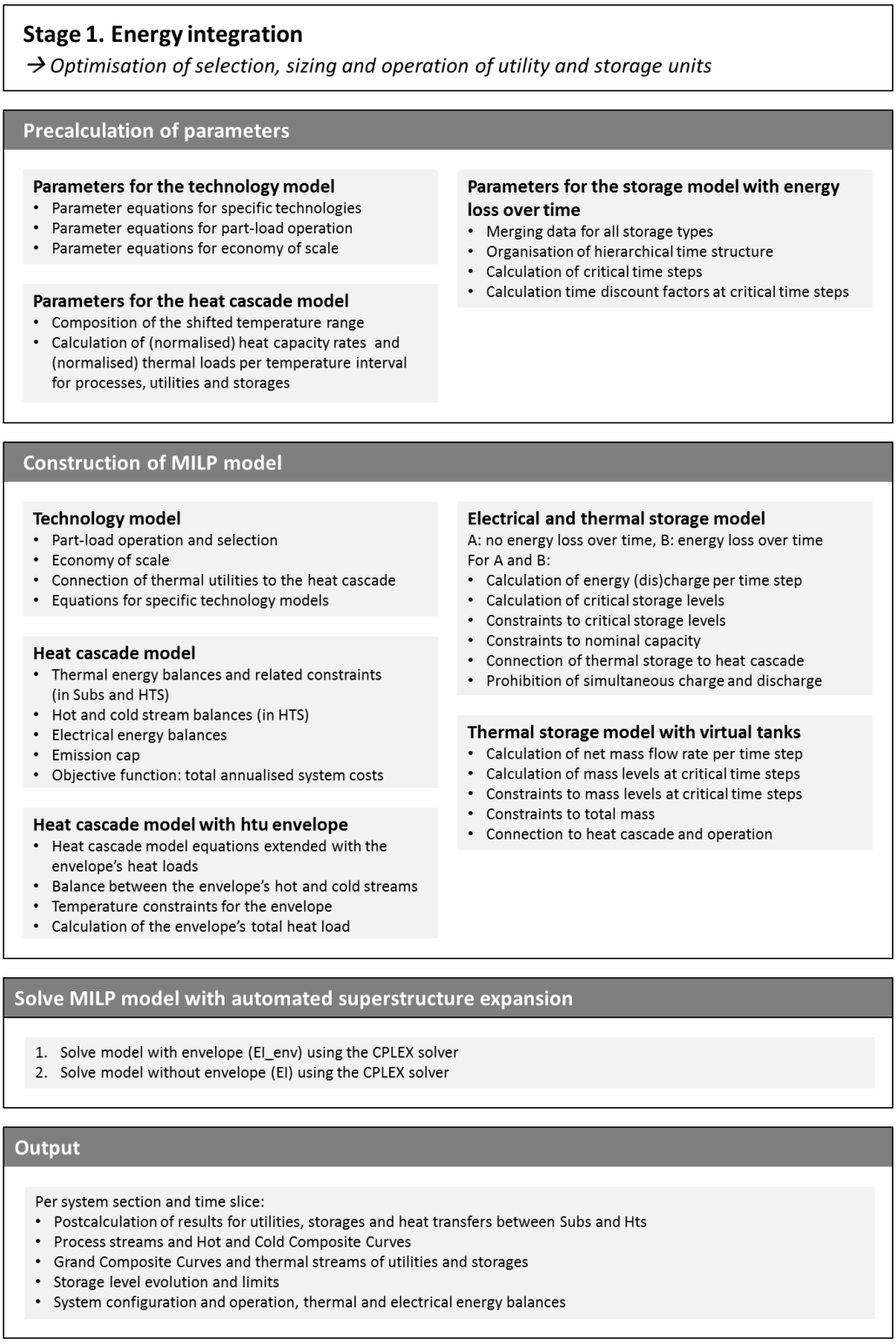

Fig. 80: Model architecture of stage 1

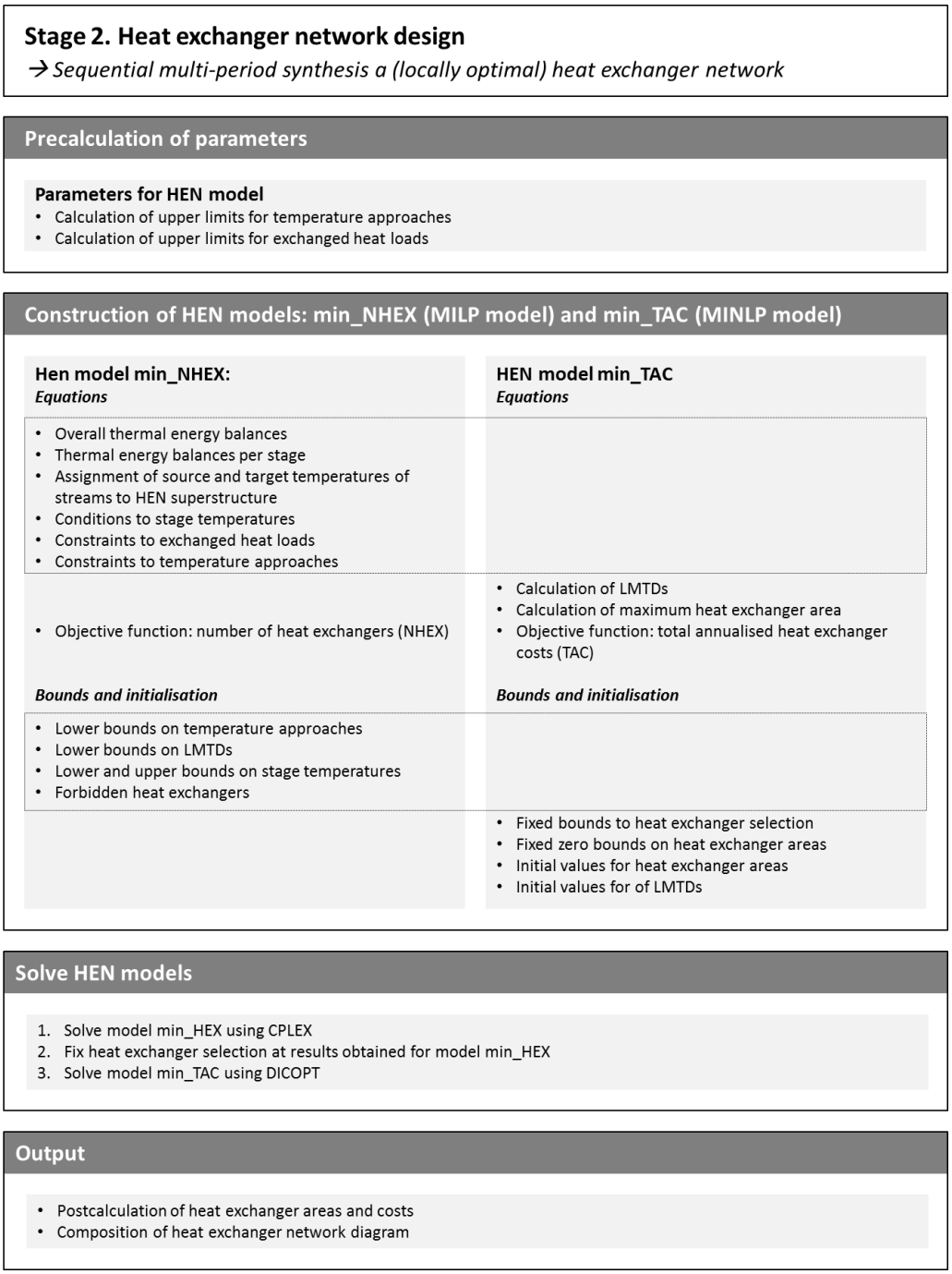

Fig. 81: Model architecture of stage 2

5. Case studies

In this chapter, the performance and features of Syn-E-Sys are demonstrated and discussed. A first example comprises a generic energy system, especially developed to demonstrate storage, renewable energy and a carbon emission cap. As a second example, an energy system optimisation problem from literature [62]is reproduced and gradually extended with new features.

5.1. Case study 1

This section analyses a generic energy system, that is especially set up to demonstrate the modelling of thermal and electrical storage units and non-dispatchable energy technologies subject to an annual carbon emission cap. To allow for multi-period analysis, the year is subdivided into 32 time slices that are each assigned to a specific season, daytype and daily time bracket by means of conversion factors (see Appendix A.1)

5.1.1. Data

The generic energy system in this example (Fig. 93) can be considered as a simplified industrial process and contains one hot and two cold process streams with thermal loads that vary over the year. The hot stream (hP1) is an externally generated waste heat stream that needs to be cooled down from 140 °C to 90 °C. The cold streams (cP1 and cP2) are process streams that need to be heated up from 30 °C to 60 °C and from 30 °C to 50 °C respectively. Furthermore, the system includes a varying electricity demand. The intra-annual variations in heating, cooling and electricity demands are modelled by specifying different parameter values in each time slice (see Appendix A.2).

To fulfil these demands different energy technologies are available: boiler, cooling water (CW), wind turbine (WT) and photovoltaic solar panels (PV). The boiler is modelled as a hot stream (flue gasses) that needs to be cooled down from 1000 °C to 120 °C, while the cooling water is represented by a cold stream between 7 °C and 20 °C. The non-linear curves representing part-load operation and investment cost of the boiler are approximated by piecewise linear curves for normalised part-load operation and specific investment cost (see Appendix A.3). Available boiler sizes range from 0.1 MW to 10 MW, the nominal boiler efficiency is 0.9, and part-load must be at least 20% of full load. In this example, the cost of natural gas is set to 0.0392 €/kWh and the corresponding carbon intensity equals 0.23 kg CO_2/kWh. The electricity consumption for circulating the cooling water is assumed to be 1% of the cooling load

The wind turbine has a fixed capacity of 2000 MW, while no limits are imposed to the capacity of the PV installation. The specific investment costs for solar and wind are assumed to be constant over the capacity range and are respectively 1800 €/kW and 1325 €/kW, while maintenance costs are set at 0.030 €/kWh and 0.025 €/kWh. The specific annual electricity production for the PV installation and the WT are respectively 930 kWh/kW and 2215 kWh/kW. The relative annual energy yield of the PV installation and the WT are listed per time slice and graphically presented in Appendix A.2. Electricity can be imported at a cost of 0.0620 €/kWh and exported with a revenue of 0.0496 €/kWh.

To bridge the asynchrony between the waste heat availability (hP1) and the process heating demands (cP1 and cP2), a thermal storage unit is incorporated in the superstructure. Similarly, an electrical storage unit is included to enable storage of excess electricity from the solar and wind technologies (PV, WT). The thermal storage unit represents a water tank with a diameter of 5 m that is divided by stratification in a lower volume at 40°C and an upper volume at 70°C (see remark below). Setting the heat transfer coefficient of the tank's containment wall equal to 1 W/m²K, an hourly storage efficiency ηh of 0.999312 is obtained using Eq. 7 in subsection 4.6.2.2. By assumption, the specific investment cost of the thermal storage tank in this example is 350 €/m³, which, for a water-filled storage with a temperature range of 30 °C, corresponds to a specific cost of 10 €/kWh. The electrical storage unit represents a hydrogen fuel cell combined with hydrogen production and storage, with a capacity limit of 15 MWh, a specific investment cost of 2 €/kWh, and a charge/discharge efficiency of 0.59, which is equivalent to a conversion efficiency ηc of $\sqrt{0.59}$ The hydrogen fuel cell is not prone to storage losses over time. An overview of technical and economical characteristics of electrical storage is given by Luo *et al.* [114].

Remark: Eq. 7 in subsection 4.6.2.2 is based on the assumption that the bottom tank of the thermal storage model is at environmental temperature. Consequently, the environmental temperature in this case study should be 40 °C. This problem is dealt with in subsection 5.1.4 and an alternative approach eliminating this limitation is proposed in subsection 7.2.3.

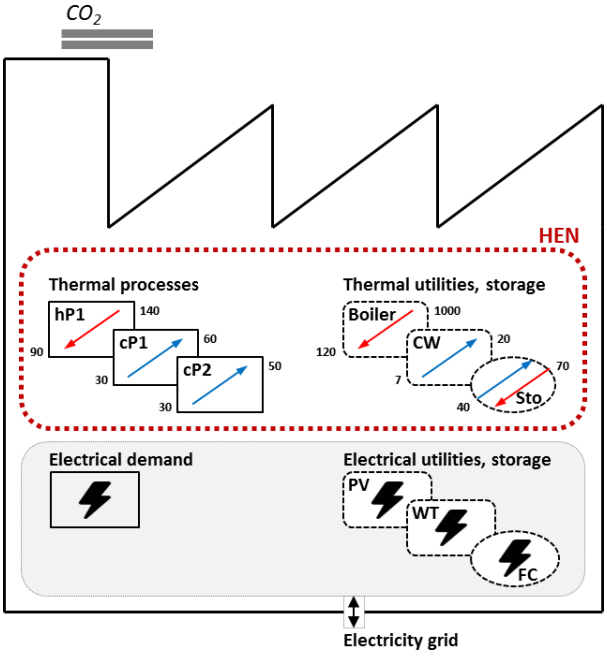

Fig. 82: Schematic representation of energy system in case study 1

The energy system is not subject to heat exchange restrictions and consequently all thermal streams are located in the same system section. For simplification, all thermal stream temperatures keep constant values. A minimum temperature approach $\Delta Tmin$ of 10°C is assumed for all heat exchanges. Investment costs for utilities, storages and heat exchangers are annualised, taking into account an equipment lifetime of 10 years and a discount ratio of 5%. The specific carbon intensity of electricity import from the grid is equal to 0.347 kg CO_2/kWh and the annual CO_2 cap is set at 0.7

kton. Process stream data, utility parameters, storage parameters and specific costs are summarised in Appendix A.2. Optimisation is performed using *Syn-E-Sys* and the results obtained in stage 1 and 2 are described in following subsections.

The expression for the investment cost IC_{hex} of each heat exchanger between a hot stream hs and a cold stream cs comprises a fixed charge C_f and a cost that is an exponential function of the exchanger area $A_{hs,cs}$ (Eq. HEX). The values of the coefficients in this example are Cf = 0, a = 3600, exp = 0.65. The lower limit for temperature approach in each heat exchanger of the HEN superstructure in stage 2 is set to 10°C, equal to the minimum temperature approach in stage 1. As a simplifying assumption, the overall heat transfer coefficient for all heat exchangers is equal to 50 W/m²K.

HEX $$IC_{hex} = Cf + a \cdot \left(A_{hs,cs}\right)^{exp}$$

5.1.2. Results

The optimised configuration contains exactly one unit (instance) of every technology available in the utility system superstructure (1 boiler unit, 1 CW unit, 1 PV unit, 1 WT unit), and the thermal as well as the electrical storage are installed. Total annual carbon emissions reach the predefined emission cap. The installed capacities (nominal loads) are listed in Table 12. In addition, the total annual costs related to installed capacity, fuel consumption, operation and maintenance, electricity import and electricity export are shown. Furthermore, the carbon emissions resulting from fuel combustion and electricity import are given.

Capacities			
Utilities U		$\dot{Q}nom_U$ (kW)	
Boiler	Ins1	1135	
CW	Ins1	2186	
Utilities E		$Pnom_U$ (kW)	
PV	Ins1	589	
WT	Ins1	2000	
Storages		$CapSto\_nom_{Sto}$ (kWh)	
Sto_th1		9689	
Sto_el1		12852	
Costs (k€/y)			**CO_2** (kton)
Investment		525.807	
Fuel		103.919	0.609729
O&M		127.161	
Electricity	import	16.129	0.090271
Electricity	export	-19.936	
Total		753.080	0.700

Table 12: Optimised system configuration, costs and emissions

A detailed tabulation and graphical representation of the system's optimised operation, including thermal and electrical energy balances per time slice is given in Appendix A.5. As an illustration, the thermal energy balances are presented in Fig. 83.

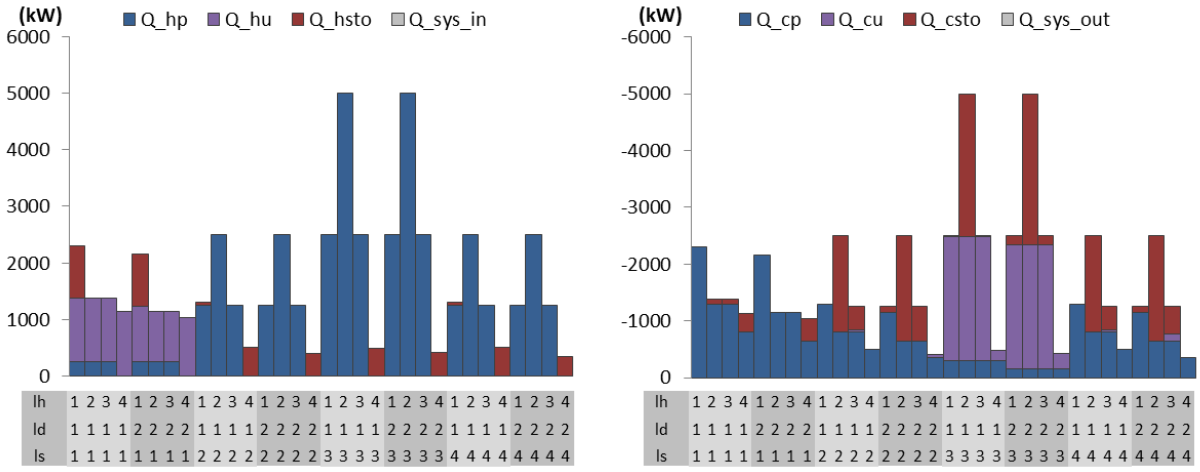

Indexes Q: hp: hot processes, hu: hot utilities, hsto: hot streams storage, cp: cold processes, cu: cold utilities, csto: cold streams storage, sys_in, sys_out: exchange with heat transfer system

Fig. 83: Thermal energy balances – left: hot side, right: cold side

By studying these results, a number of observations can be made: Whenever the waste heat load (hP1) surpasses the cumulative cooling demand (cP1 and cP2), the excess heat is released either to the cold utility (CW), to the thermal storage, or to both. However, in time slices during which the waste heat load is insufficient to fulfil the heating demands, either the boiler, the storage, or both cover the energy deficit. In some of the time slices where the boiler is active, it generates more heat than the deficit in order to charge the thermal storage. On the other hand, in some of the time slices where the storage is discharging, its hot stream releases heat to the cold utility. The reason for this will be explained in Subsection 5.1.3.

Due to the carbon emission cap, electricity is not imported from the grid, but generated in situ by renewable technologies (PV and WT). Electricity is stored when the electrical yield from solar and wind surpasses the demand, and released again at times with insufficient solar and wind resources. When the CW unit is active, an electrical demand is induced in the thermal electricity balance. The evolution of the thermal and electrical storage levels over all subsequent hours of the year are visualised in Appendix A.6. Clearly the intra-annual storage pattern simultaneously embeds daily, weekly, as well as seasonal storage patterns.

The multi-period HEN configuration with the lowest cost of is obtained in a superstructure containing 4 stages and is shown in Fig. 84. This HEN configuration corresponds to an annualised investment cost of 311.392 k€. The transferred heat loads over all time slice are listed in Appendix A.7.

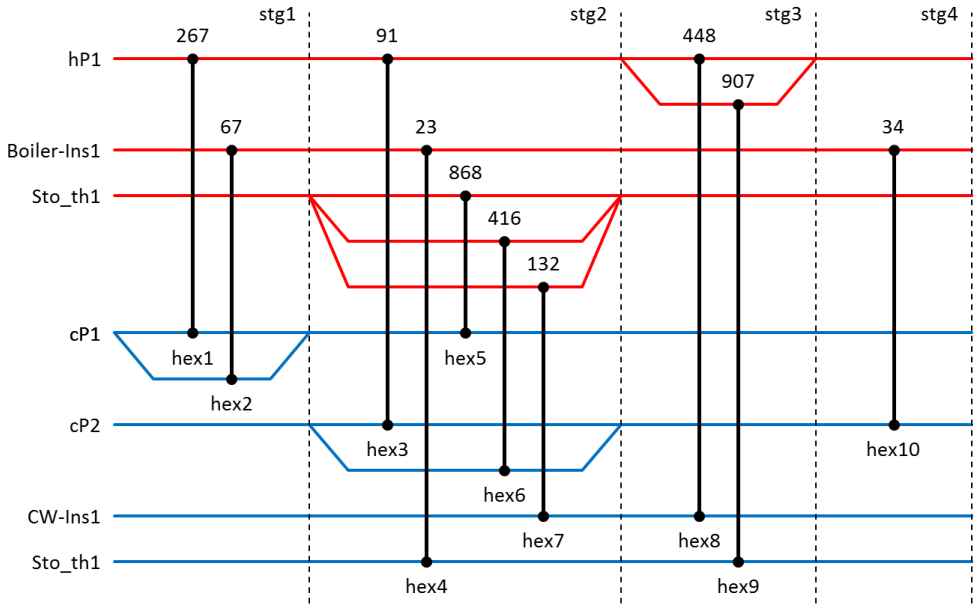

Fig. 84: Optimised heat exchanger network configuration and heat exchanger areas in m

5.1.3. Heat transfer from thermal storage to cold utility

By comparing the hot and cold side of the thermal balances (Appendix A.5), it is observed that the hot stream of the thermal storage transfers heat to the cold utility in some time slices (ls2ld2lh4, ls3ld1lh4 and ls3ld2lh4). Intuitively, it seems useless to store heat in order to release it to the environment at a later point in time. However, the model uses this option to minimise total system costs. Spreading the cooling duty over time may be beneficial to decrease the required nominal capacity of the cold utility. Moreover, if the cold utility's operation costs are lower at a later point in time, part of the cooling duty may be postponed via thermal storage. In the example, the electricity cost of the cooling water is determined in each time slice by the electricity yield of the WT and the PV installation, and by the electricity import from the grid. Besides, the hourly loss in the thermal storage could fulfil a role as free cold utility.

The beneficial influence on the total costs, caused by heat transfer from the thermal storage to the cold utility, can be determined by raising the temperature range of the cold utility to 50°C-80°C. In this way, heat exchange between the storage and the cold utility is impossible, without influencing other heat transfers. As a result, the nominal load of the cold utility increases from 2186 kW to 2439 kW and also its electricity use increases form 26788 kWh to 26810 kWh.

Similar to phantom heat, this phenomenon originates from the nature of the thermal energy balances per temperature interval, in which the heat transfer between a specific hot and a specific cold stream cannot be controlled or prohibited. Analogous to the heat exchange between the overlapping hot and the cold streams of a heat network, leading to phantom heat, the heat transfer from a storage hot stream to a cold utility stream is not prohibited by the heat cascade formulation. In reality, the storage will not be connected to a cold utility, and any surplus heat will increase the upper temperature of the storage.

5.1.4. Application of storage model with virtual tanks

In case study 1, thermal storage is modelled using the dual tank model. Alternatively, the model with virtual tanks can be employed. If only two virtual tanks are included, with temperature levels 40 °C and 70 °C, the optimal energy system configuration obtained with the virtual tank model is identical to that obtained with the dual tank model. Of course, input data need to be equivalent for both cases. For this purpose, the specific investment cost cI_Sto of the dual tank model (10 €/kWh) needs to be converted to an equivalent cost cI_Sto_vt for the virtual tank model using following expression: $cI\_Sto\_vt = cI\_Sto \cdot \Delta T \cdot cp/3600$. Taking into account the temperature range ΔT (30 K) and the specific heat capacity cp of the storage medium (water: 4.187 kJ/kg.K), cI_Sto_vt is equal to 0.349 €/kg.

In both storage models, when heat losses over time are taken into account, the lower tank's temperature needs to represent the average temperature of the environment. In case study 1, a lower tank temperature of 10 °C is therefore more realistic than a temperature of 40 °C. However, the dual tank model is not able to operate in that case, since the stream from the hot (70 °C) to the cold (10 °C) reservoir cannot discharge its entire heat load. Indeed, assuming a $\Delta Tmin$ of 10 °C, the shifted source temperature of the cooling water (12 °C) is higher than the shifted target temperature of the storage discharge stream (5 °C).

This problem can be avoided using the virtual tank model with an appropriate temperature discretisation. By adding an extra tank with a temperature level of 17 °C between the virtual tanks at 10 °C and 70 °C, the hot (discharge) and the cold (charge) streams are each divided into two independent stream segments. As a consequence, the hot stream segment from 70 °C to 17 °C can exchange its heat load below 40 °C (too cold for heat exchange with cP1 and cP2) with the cooling water unit, while the hot stream segment from 17 °C to 10 °C is not activated. More generally, additional virtual tanks divide the storage's hot (cold) stream into segments that can be activated independently, providing the storage unit with a higher operation flexibility.

The list of key virtual tank temperature levels can be composed by shifting the source temperatures of process and utility cold (hot) streams up (down) over $\Delta Tmin$, while adding the prespecified temperatures, if any, for the lower and the upper tank. For case study 1, this list contains following temperature levels for respectively virtual tanks vt1 to vt5: 10 °C, 17 °C, 40 °C, 130° C and 990 °C. In the optimised solution, all tanks but the upper one are used, the total storage mass amounts 92.6 tons, and the minimised total annualised cost is 746.630 k€/y. However, since the maximum temperature for a water storage tank at is about 95 °C, the virtual tank temperature list needs to be limited: 10 °C, 17 °C, 40 °C and 95° C. In this case, all tanks are used, the total mass amounts 151.5 tons, and the total annualised cost is 750.647 k€/y. Extra intermediate tanks do not improve the solution and the optimal temperature discretisation (between 10 °C and 95 °C) is found. In general, the larger the temperature range of the storage, the less mass needed to store a certain amount of heat, and thus the lower the related capital cost.

The installed capacities, the related annual investment costs, fuel costs, operation and maintenance costs, electricity import and export costs and carbon emissions are listed in Table 12. The evolution over the year of the mass levels of the virtual tanks is visualised in Fig. 85. Fig. 86 zooms in on the transition between the first and the second season.

Capacities			
Utilities U		$\dot{Q}nom_U$ (kW)	
Boiler	Ins1	1135	
CW	Ins1	2190	
Utilities E		$Pnom_U$ (kW)	
PV	Ins1	604	
WT	Ins1	2000	
Storages		$CapSto\_nom_{Sto}$ (kWh)	
Sto_vt1		6844/ 151466	
Sto_el1		12875	
Costs (k€/y)			**CO_2** (kton)
Investment		523.556	
Fuel		104.231	0.611557
O&M		127.568	
Electricity	import	15.802	0.088443
Electricity	export	-20.510	
Total		750.647	0.700

Table 13: Optimised system configuration, costs and emissions

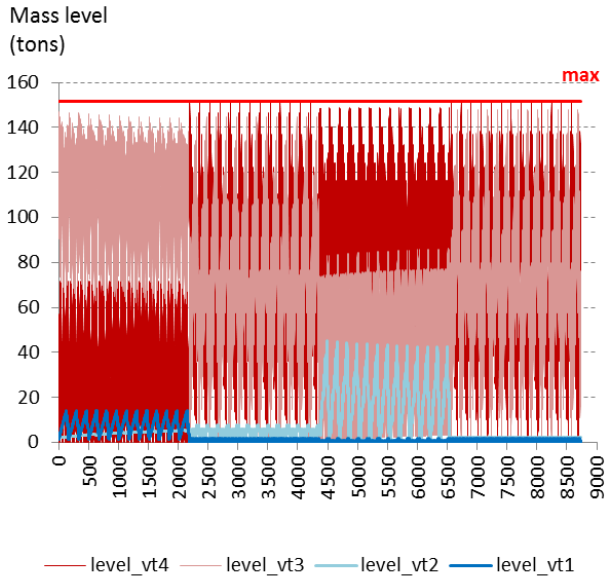

Fig. 85: Evolution mass levels virtual tanks

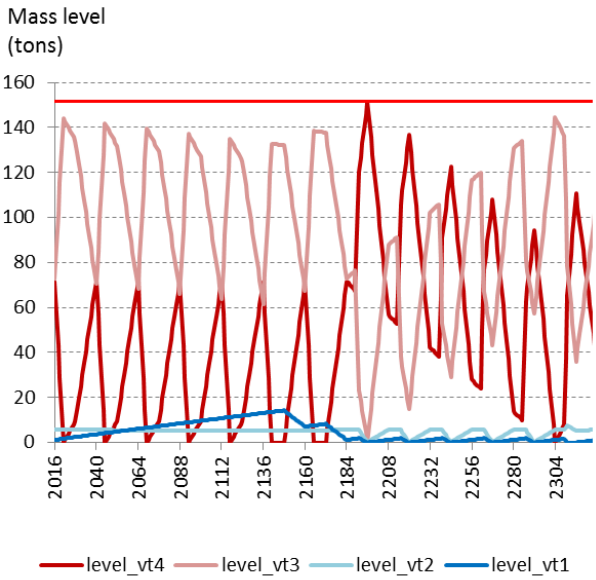

Fig. 86: Evolution mass levels virtual tanks – detail

The reason why the list of key virtual tank temperature levels can be derived from the source temperatures of the process and utility streams is explained and illustrated below for case study 1, disregarding the practical upper temperature limit of 95°C:

Consider a time slice in which the boiler is not operated and no waste heat (hP1) is available. As a consequence, the heat required by cP1 and cP2 must be provided by discharging the thermal storage. The hot stream from vt4 to vt3 with shifted temperature range 125 °C - 35 °C can transfer

heat to the cold streams cP1 and cP2 with shifted temperature ranges 35 °C - 65 °C and 35 °C - 55 °C. However, if tank vt3 would have a temperature of 30 °C instead of 40 °C, the source temperatures of cP1 and cP2 are too high and an additional cold stream (e.g. CW) is required to absorb the heat from the storage in the shifted temperature range 35 °C - 25 °C. If not, the storage hot stream from vt4 to vt3 cannot deliver heat to cP1 and cP2. As a consequence, the storage is less flexible.

Analogously, if tank vt3 would have a temperature of 50 °C instead of 40 °C, the hot stream from vt4 to vt3 is not covering the maximum temperature range that could be used to deliver heat to cP1 and cP2 and therefore the needed mass flow to deliver the heat required by cP1 and cP2 will be higher. This will lead to a higher storage capacity requirement and related capital costs.

Consider a time slice where waste heat is available (hP1) over a shifted temperature range from 135 °C to 85 °C. The cold stream from vt3 to vt4 with shifted source and target temperatures from 45 °C to 135 °C can be heated up by the waste heat. However, if tank vt4 would have a temperature of 140 °C instead of 130 °C, the source temperature of hP1 is too low and an additional hot stream covering the shifted temperature range 135 °C - 145 °C is required. If not, the storage cold stream from vt3 to vt4 cannot be heated up and consequently, the storage cannot be charged by that stream.

The reasoning for hot and cold streams between any other pair of subsequent virtual tanks is analogous. In conclusion, the optimal temperature discretisation for thermal storage can be derived from the source temperatures of the process and utility streams.

5.2. Case study 2

This example is based on the case study described by Becker *et al.* [62], in which heat recovery is optimised for a drying process in the paper industry. Firstly, a simplified version of the original problem is set up, using the technology models introduced in Section 4.3. Subsequently, the problem is extended to demonstrate the features of Syn-E-Sys (Fig. 15).

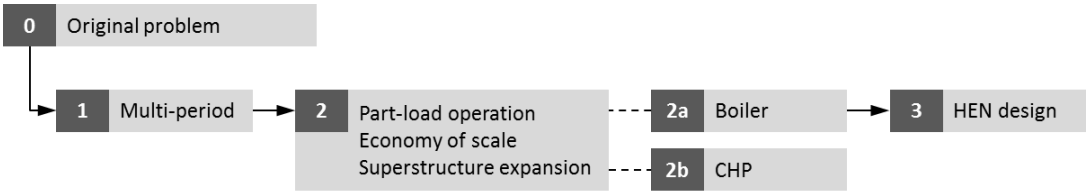

Fig. 87: Scheme for extensions of original problem

5.2.1. Original problem: Energy integration with heat exchange restrictions

The process consists of a pulping unit, in which the pulp is preheated, and a drying unit, where the pulp is dried by means of heated paper mill rolls and hot air (Fig. 94). To generate steam for heating up the paper mill rolls, and to produce hot air for evacuating water vapour from the pulp, the hot flue gasses of a boiler are used. No direct heat exchange is allowed between the pulping, the drying, and the boiler units. Consequently, these units are modelled as different subsystems ($Sub1$, $Sub2$, $Sub3$), connected by a heat transfer system (Hts) in which a cooling water unit (CW) is available. Process stream data are given in Table 14, while Table 15 specifies stream data, efficiencies and specific costs for utilities. By assumption, the capacity ranges of both boiler and cooling water are unlimited and both utilities operate at their nominal efficiencies at every part-load. For the cooling water unit, an electricity consumption of 2% of its cooling load is assumed.

	Process	TsP_P (°C)	TtP_P (°C)	$\Delta Tmin_P$ (°C)	$\dot{Q}P_P$ (kW)
$Sub1$	ph_c1	20	50	4	11262
	ph_h1	50	30	4	7297
$Sub2$	st_c1	105	105	1	6057
	st_h3	105	105	1	892
	st_h2	105	95	4	112
	air_c1	20	150	1	664
	air_h1	100	30	1	5278

Table 14: Process stream data derived from [62]

	Utility	TsU_U (°C)	TtU_U (°C)	$\Delta Tmin_U$ (°C)	ηnom_U	cF_U (€/kWh)
$Sub3$	Boiler	1000	120	1	0.9	0.0392
Hts	CW	7	20	4	50	0
	Buying electricity		0.0620	(€/kWh)		
	Selling electricity		0.0496	(€/kWh)		

Table 15: Utility stream data (excl. heat networks) and specific fuel and electricity costs

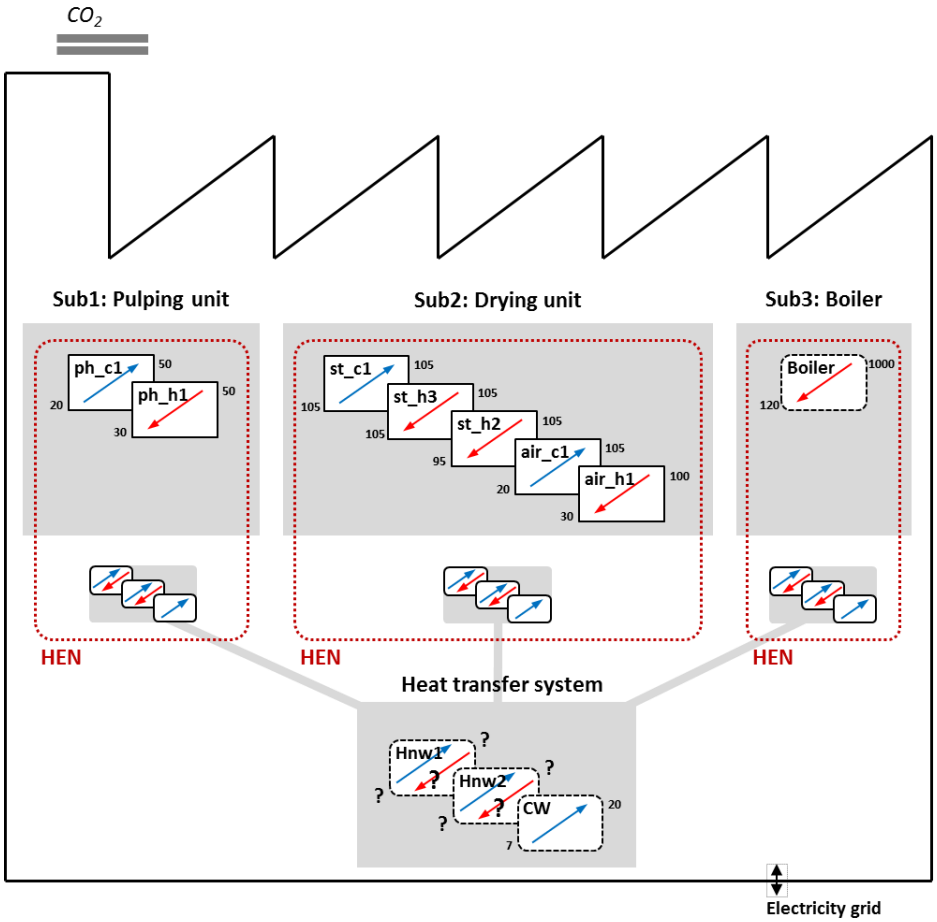

Fig. 88: Schematic representation of energy system in case study 2

The energy system is optimised in different situations to illustrate the role of heat networks. Investment costs are not taken into account. In *situation a*, the energy system is optimised without heat exchange restrictions. In *situation b*, these restrictions are included by locating the process streams in their respective subsystems, while the boiler is located in the heat transfer system to enable feasible system operation. The optimised utility heat loads are presented in Table 16 and the energy penalty resulting from the heat exchange restrictions is visualised in Fig. 89.

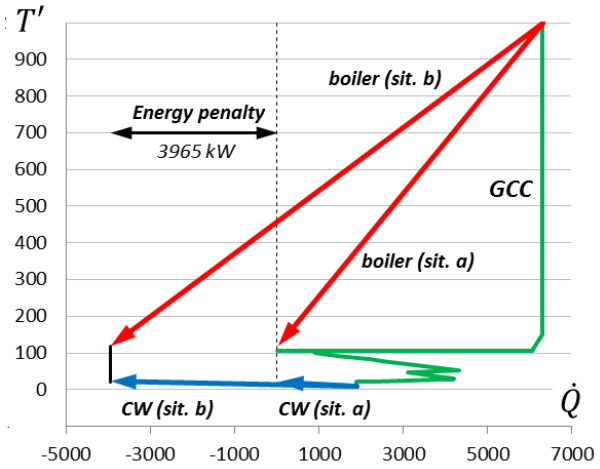

Fig. 89: Energy penalty between situations (sit.) a and b

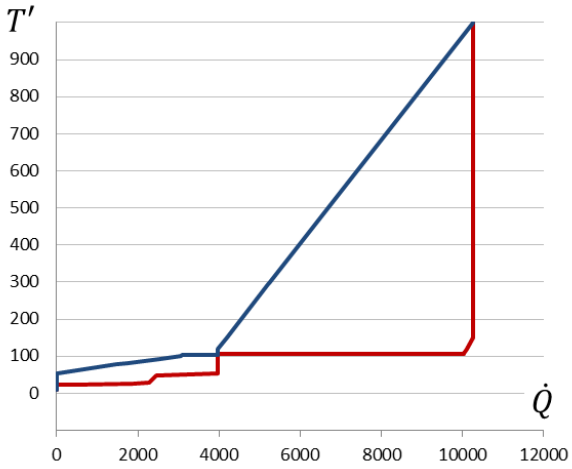

Fig. 90: Heat transfer unit envelope in situations c, d, e

To enable identification of appropriate temperature ranges for heat networks, the heat transfer unit envelope is generated, taking into account the heat exchange restrictions (see Section 4.4.6). To completely avoid the energy penalty, heat networks should be integrated in such a way that their optimised hot and cold composite curves are embedded in the envelope (Fig. 90). For this purpose, a hot water loop (Hnw1) between 25 °C and 80 °C is installed in the lower envelope part, assuming a $\Delta Tmin$ of 4 °C. For the heat network in the upper part of the envelope (Hnw2), different temperature ranges are considered to illustrate the effect on the energy penalty (*situations c, d, e*). As a simplification, it is assumed that the electricity consumption of a heat network equals 2% of the transported heat load.

In *situation c*, a thermal oil loop between 110 °C and 295 °C is installed with a $\Delta Tmin$ of 4 °C. In this case, the optimised hot and cold stream of the heat network will be completely embedded in the envelope, avoiding the energy penalty. In *situation d*, however, the lower temperature of the loop is increased to 165 °C. Since the thermal load of the heat network's hot and cold stream is equal to the heat load of the upper part of the envelope, these streams are pushed out of the envelope. To ensure that sufficient heat at appropriate temperature levels is available to heat up to the network's cold stream, a higher boiler load is required. As a consequence, the energy penalty is not completely avoided and equals 347 kW. In *situation e*, a steam network is installed at 295 °C with a $\Delta Tmin$ of 1 °C. Analogous to *situation d*, the energy penalty is not entirely avoided and is equal to 1573 kW.

The optimised heat loads of boiler, cooling water and heat networks, the energy penalty and system costs are listed for all situations in Table 16. The parameters characterising Hnw2 in each situation, the optimised thermal streams and the envelope are visualised in Appendix B.1.

The results obtained here slightly differ from those presented by Becker *et al.* [62], and the main reason lies in the applied boiler technology model. Becker *et al.* [62] use an elaborated boiler model that consists of an isothermal hot stream related to radiative heat transfer, and a hot stream between radiation temperature and stack temperature representing convective heat transfer [70]. Moreover, the flue gasses in the stack are used to preheat the incoming air, thus increasing the boilers heat output for the same fuel use rate. In Syn-E-Sys, however, the boiler is represented by means of the generic technology model, which consists of one single hot stream and does not include air preheating. As a result, we obtain higher thermal loads for the boiler and the cooling water. In addition, the shape of the transfer unit envelope is slightly different in both approaches, since the air preheating in the elaborated boiler model creates an additional cold stream.

Situation	***a***	***b***	***c***	***d***	***e***
Loads (kW)	QU_U				
Boiler	6292	10257	6292	6639	7865
CW	1888	5853	1888	2235	3461
Hnw1	-	-	3965	3965	3965
Hnw2	-	-	6292	6292	6292
Energy penalty (kW)	-	3965	0	347	1573
Costs (k€/y)					
Fuel	2401	3914	2401	2533	3001
Electricity	21	64	132	136	149
Total	2421	3977	2533	2669	3150

Table 16: Optimised utility heat loads, energy penalty and costs

5.2.2. Multi-period

In order to illustrate the effects of changes in process operating conditions over the year on the system's configuration and operation, *situation c* is extended to multi-period. Therefore, the year is divided into 4 arbitrary time slices containing respectively 4380, 1752, 1752 and 876 hours. In each of these time slices the process heat loads and temperatures take different values. In time slice S4, the source temperatures of process streams air_c1 and ph_c1 are increased from 20 °C to 30 °C and the target temperatures of ph_h1 and air_h1 from 30 °C to 40 °C, for example to represent increased environmental temperatures. The process heat loads in time slice S2 are derived from the original values in S1 by multiplying all cold stream loads with a factor 1.25 and all hot stream loads with a factor 0.75, and vice versa for the heat loads in time slice S3. In time slice S4, all process heat loads in the pulping unit are multiplied with 1.25 and all process heat loads in the drying unit with 0.75. All other data keep their original values over all time slices. The multi-period process stream parameters are summarised in Appendix B.2.

After running the optimisation model, a different heat transfer unit envelope is obtained for each time slice. To avoid the energy penalty, heat networks must span the envelope and be completely embedded in it in each time slice, as depicted in Fig. 91. Therefore, the heat network temperatures need to adopt appropriate values in each time slice. The lower temperature of Hnw1 needs to be increased from 25 °C to 60° C in time slice S3 and to 36°C in slice S4. The optimised heat loads and related system costs are listed in Table 17.

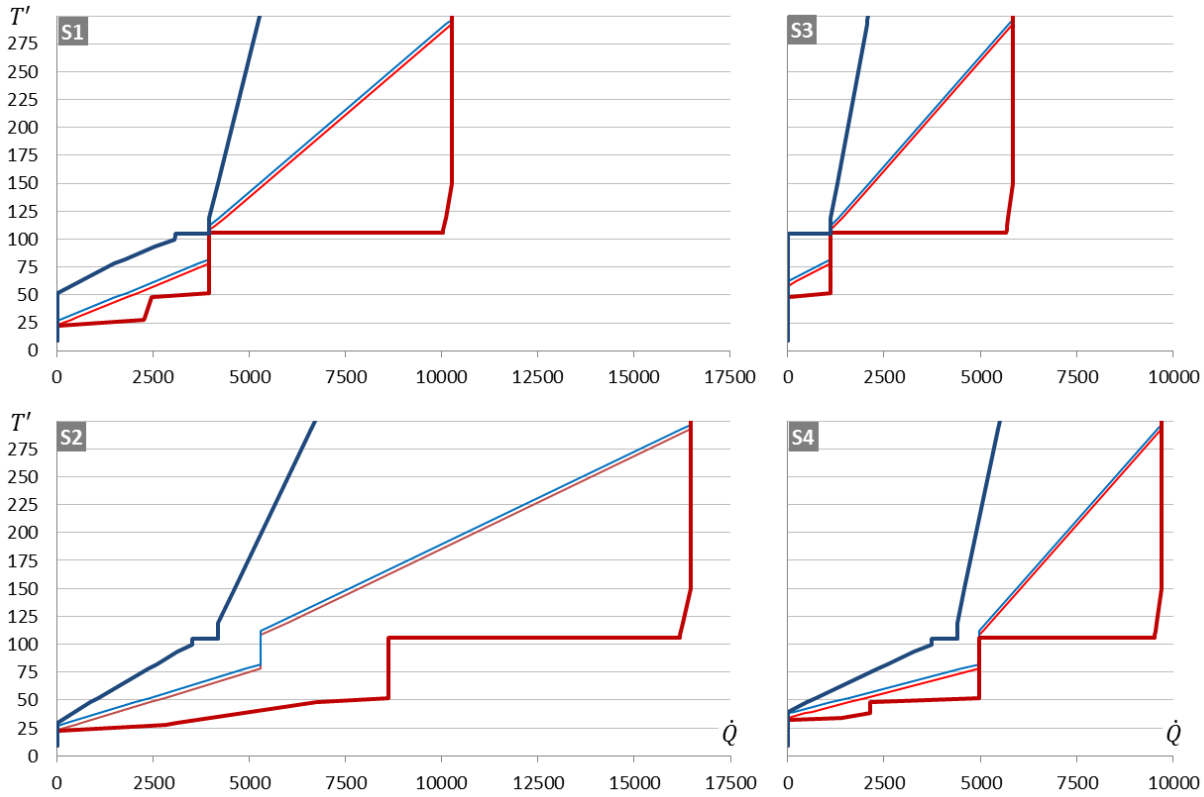

Fig. 91: Multi-period envelope curves and embedded heat networks in time slices S1-S4

	$\dot{Q}U_{U,S}$			
	S1	***S2***	***S3***	***S4***
Loads (kW)				
Boiler	6292	12294	4719	5286
CW	1888	0	8205	0
Hnw1	3965	5631	1126	4957
Hnw2	6292	10838	4719	4734
Costs (k€/y)				
Fuel	2700			
Electricity	143			
Total	2843			

Table 17: Optimised utility heat loads and costs - multi-period

For a chosen transport fluid, fluid speed and temperature difference, the pipe diameter of a heat network is a function of the heat load. The investment cost of a heat network does not only depend on the pipe diameter, and thus the heat load, but also on the pipe length. Since distance is not included in the formulation of the energy system model, pipe length and related costs are not taken into account in the cost trade-off. This could be circumvented by a priori estimating the pipe length and using a heat load-related specific investment cost calculated for that pipe length.

5.2.3. Part-load behaviour and investment cost boiler

In a next step, the part-load behaviour of the boiler and economy of scale effects on its capital costs are taken into account. For this purpose, the part-load curve of the generic technology model is tuned by specifying the values in its reference points R, in the same way as done for Case study 1. Similarly, the reference points Rc in the investment cost curve are specified. The investment cost of the boiler is annualised assuming a technology lifetime of 5 years and a discount ratio of 5%.

Optimisation results for the envelope and the heat networks are identical to the previous calculation without part-load and investment cost for the boiler. Fuel and electricity costs are also equal to previously calculated values, but investment costs are added to the total system cost (see Table 18). Note that heat network investment costs are not included. Because of the maximum limit on boiler unit capacity, the automated superstructure expansion procedure (see Section 4.5) is activated and a second boiler unit is added to the superstructure. The set points for part-load operation and investment are indicated on the curves for normalised part-load and specific investment cost in Appendix B.3.

	$\dot{Q}nom_U$	$\dot{Q}U_{U,S}$			
		S1	***S2***	***S3***	***S4***
Loads (kW)					
Boiler Ins1	6292	6292	6292	0	0
Boiler Ins2	6002	0	6002	4719	5286
CW	8205	1888	0	8205	0
Hnw1	5631	3965	5631	1126	4957
Hnw2	10838	6292	10838	4719	4734
Costs (k€/y)					
Investment	62				
Fuel	2702				
Electricity	143				
Total	2908				

Table 18: Optimised utility heat loads and costs - multi-period + boiler part-load and economy of scale

5.2.4. Part-load behaviour and investment cost CHP

To demonstrate one of the specific technology models, the boiler is replaced with a CHP. Thermal and electrical part-load operation and investment cost subject to economy of scale are approximated by piecewise linearisation (see Appendix B.4). An overall nominal efficiency of 0.9 is assumed consisting of an electrical and a thermal nominal efficiency of respectively 0.36 and 0.54. The capacity of the CHP is determined by its thermal nominal load, ranging from 0.5 MW to 10 MW. Furthermore, the CHP generates a hot stream that needs to be cooled from 450 °C down to 120 °C. Moreover, an overall electricity demand is added to the problem (S1: 10000 kW, S2: 2000 kW, S3: 5000 kW, S4: 7000 kW)

After optimisation, slightly different envelopes are obtained than in Subsection 5.2.3, but the heat networks are still completely embedded within the envelope and consequently the energy penalty is avoided. The automated superstructure expansion procedure selects 3 CHP units in the optimal solution, which are all running at full load when activated. Results are listed in Table 19 and the set points for part-load and investment are indicated in Appendix B.4.

	$\dot{Q}nom_U$	$\dot{Q}U_{U,S}$				$P\_el_{E,S}$			
		S1	***S2***	***S3***	***S4***	***S1***	***S2***	***S3***	***S4***
Loads (kW)									
CHP Ins1	6292	6292	6292	0	0	4195	4195	0	0
CHP Ins2	5286	0	5286	5286	5286	0	3524	3524	3524
CHP Ins3	716	0	716	0	0	0	477	0	0
CW	8772	1888	0	8772	0				
Hnw1	4405	3965	4405	881	4405				
Hnw2	12065	6292	12065	4965	5286				
Costs (k€/y)									
Investment		602							
Fuel		4615							
Electricity	import	2034							
Electricity	export	-510							
Total		6741							

Table 19: Optimised utility heat loads and costs - multi-period + CHP part-load and economy of scale

5.2.5. Heat exchanger network design

Stage 2 of Syn-E-Sys deals with the heat exchanger network design. This is demonstrated on the exemplary energy system with boiler (see subsection 5.2.3). The parameters characterising the heat exchanger costs in the objective function of the HEN optimisation problem are taken from [98]: $cfix = 0$, $acoeff = 6300$, $exp = 0.65$. For all heat exchangers, the overall heat transfer coefficient is set equal to 0.05 kW/m²K. The annualisation factor for heat exchanger costs is the same as for the utilities and based on an equipment lifetime of 5 years and a discount ratio of 5%. By default, the number of stages is equal to the maximum of the number of cold streams and the number of hot streams. Since the 2 boiler instances and the two heat networks generate 4 utility hot streams and the process itself contains 4 hot streams, the number of stages is set to 8.

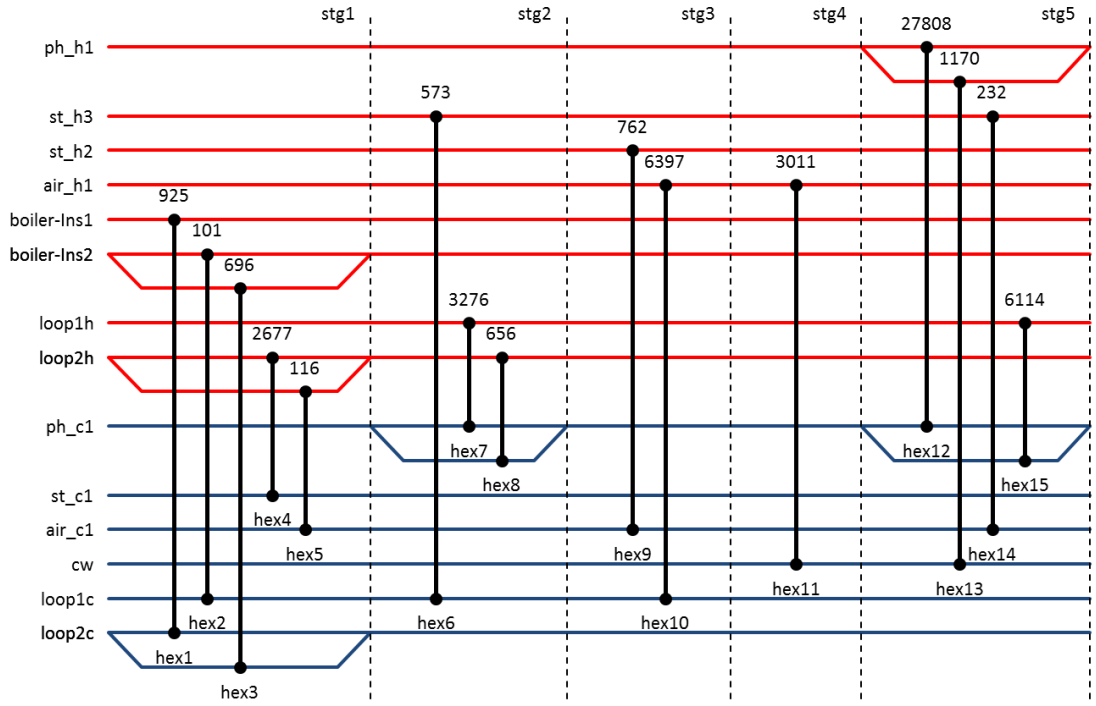

Fig. 92: Optimised HEN configuration in multi-period superstructure with 5 stages and heat exchanger areas (m²)

To investigate the effect of the number of stages on the optimised HEN configuration and corresponding costs, the number of stages is gradually reduced. The HEN configuration with the lowest annualised investment cost of 3550 k€ is obtained in a superstructure containing 5 stages and is shown in Fig. 92. The heat exchanger areas and the transferred heat loads per time slice are listed in Appendix B.5.

6. Summary and conclusions

In the third part of this work, an energy model is proposed that offers a holistic approach to cost-optimal synthesis of low carbon energy systems on business park scale. A two-staged approach forms the backbone of the model. In a first stage, heat recovery within the system is maximised and simultaneously, the synthesis and integration of the energy supply and storage system is optimised to fulfil remaining energy requirements at minimum total annualised costs. Subsequently, a HEN is generated that enables the required heat exchanges, while related investment costs are minimised.

For this purpose, a multi-period heat cascade model with heat exchange restrictions is combined with a superstructure containing generic submodels for thermal and electrical energy conversion technologies and storage. The technology model features part-load operation and investment cost subject to economy of scale, whereas the storage model is customised for intra-yearly storage subject to conversion losses and hourly energy losses. In addition, a more complex model for sensible heat storage consisting of a stack of virtual tanks is integrated and adapted. Furthermore, an automated superstructure expansion procedure is incorporated. The resulting model corresponds to the first stage of *Syn-E-Sys*. After calculation, the optimised thermal streams in the utility system, together with the known thermal process streams, are sent to the second stage of the model. In this stage, the HEN is optimised, using a multi-period HEN design model.

Two shortcomings inherent to the heat cascade formulation are discovered during model development and discussed. The first problem is referred to as phantom heat and can be avoided by embedding the heat network in the heat transfer unit envelope. As a second issue, the heat cascade formulation does not prevent that a thermal storage releases its heat to a cooling technology.

A user-defined division of the year into time slices, allows to take into account predefined variations in temperature levels, energy demands or in the availability of renewable energy resources. Due to the generic formulation, a variety of energy conversion and storage technologies can be modelled. The advantage of adding extra technology units is automatically investigated by the superstructure expansion procedure. Moreover, the effect of storage losses over time on the evolution of the storage level is taken into account without increasing the number of time segments to be analysed. The effects of a carbon emission cap on the optimal energy system configuration can be explored. If the different companies in a business park cannot directly exchange heat, the model allows us to perform energy integration in each company separately, while simultaneously optimising heat exchange between different companies via heat networks and joint energy production via common utilities. Finally, the model automatically generates an optimal heat exchanger network for multi-period operation. As demonstrated by the two case studies, *Syn-E-Sys* offers a tool for the development of low carbon energy systems integrating heat recovery, heat networks, energy storage and renewable energy.

Fig. 93 and Fig. 94 schematically represent an energy system model on business park scale and its thermal and electrical components.

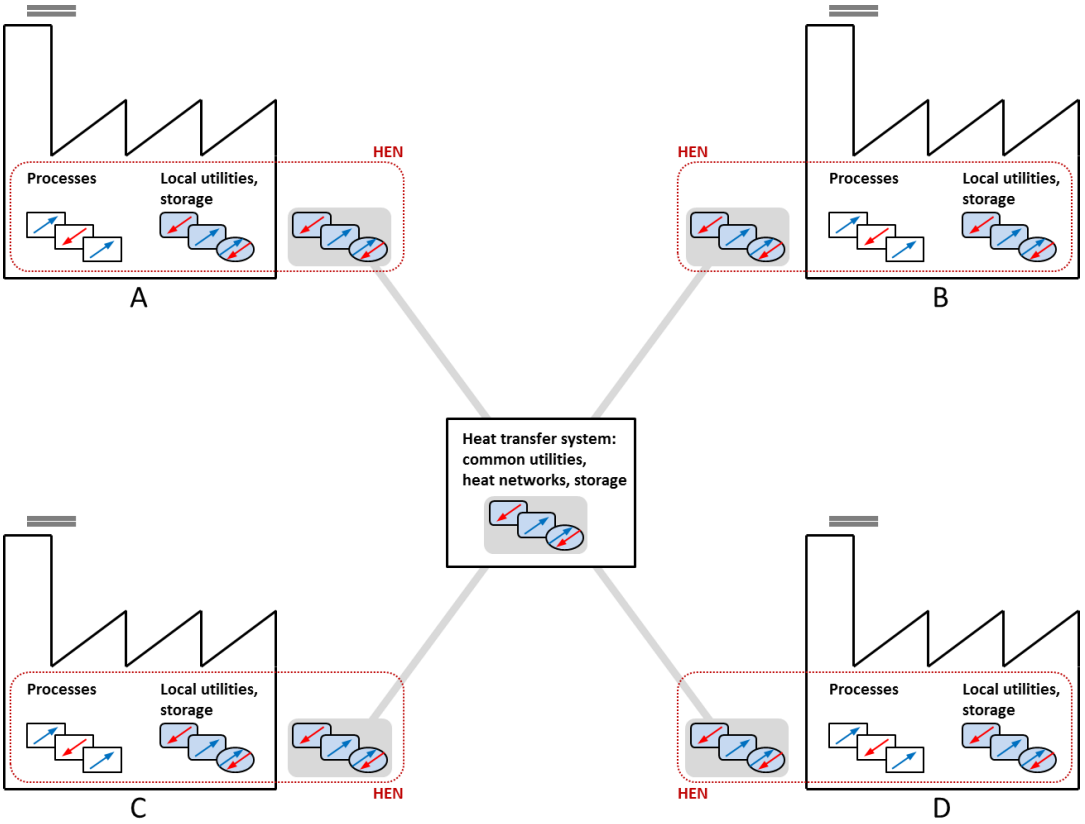

Fig. 93: Schematic representation of energy system model on business park scale –Thermal part

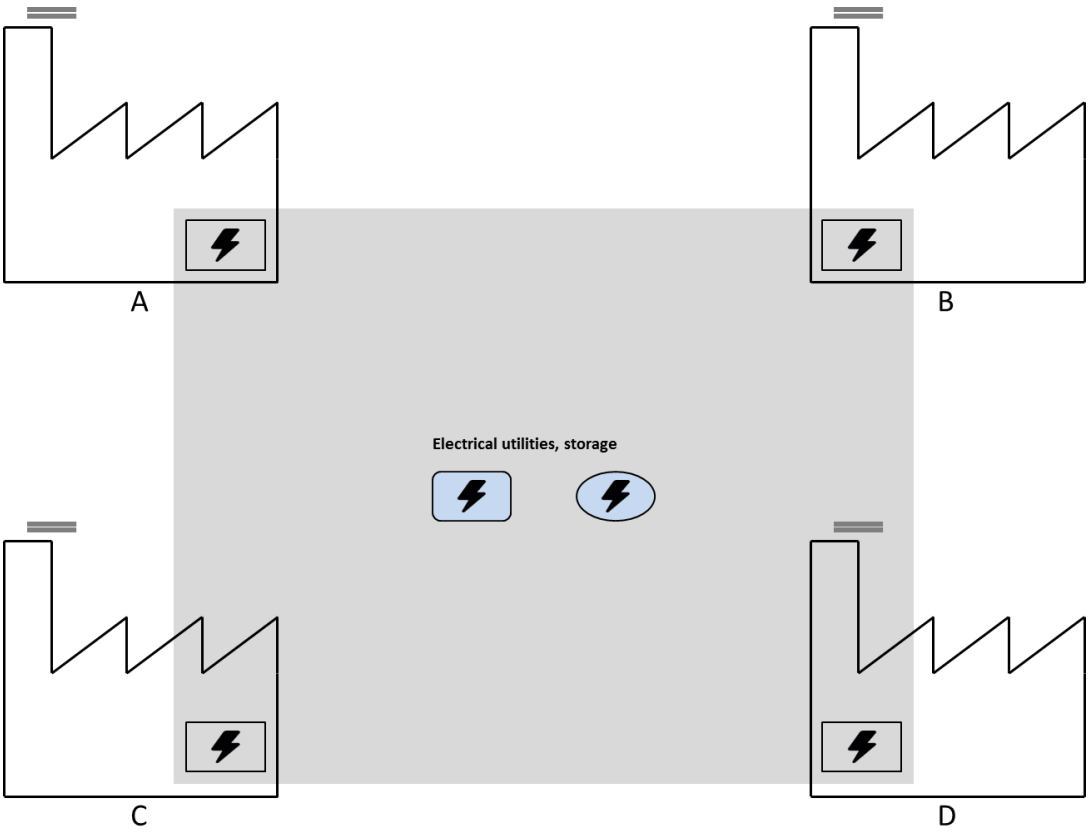

Fig. 94: Schematic representation of energy system model on business park scale –Electrical part

Syn-E-Sys facilitates the optimal design of low carbon energy systems on business park scale. The model can be applied for grass-root design, but could be adapted for retrofit design. Hence, Syn-E-Sys facilitates decision-making for investments in energy infrastructure corresponding to the integration of low carbon energy measures into the energy system. In this way the energy engineer commissioned by the investor (individual company, joint corporation of companies, energy service company) is able to identify the most cost-effective energy system design. Alternatively, energy system analysts commissioned by climate and energy policy makers can calculate the effect of decreasing carbon emission caps on investment costs and take appropriate action to promote low carbon investments. By introducing a thermodynamically correct representation of heat in a superstructure-based optimisation model, the model developed in this work delivers a significant contribution to close the gap between the large scale models used by energy system analysts and industrial site scale models used by energy or process engineers.

7. Future Perspectives

In this chapter, future perspectives are discussed regarding the theoretical formulation on the one hand and the practical application of the model on the other hand.

7.1. Model formulation

This section first explains a number of theoretical limitations imposed by the nature of the model. Next, straightforward extensions to the model formulation are proposed and finally, aspects that require further research and development are discussed.

7.1.1. Theoretical limitations

A number of theoretical limitations are inherent to the nature and formulation of the model: Firstly, the model starts from perfect foresight, which implies that the parameters characterising energy demand and supply are known a priori for the whole year. In reality, however, these parameters can be subject to unpredictable variations. More specifically, the yearly profiles of thermal and electrical energy demands, variations in temperature levels of thermal energy demands and utilities, fluctuations in electricity prices, and the variations in availability of wind and solar energy over the year need to be specified as input.

Secondly, the year is divided into empirically defined time slices, each representing steady state conditions within the energy system. The effects related to transition from one state to the next are not taken into account.

As a third point, the heat cascade formulation in stage 1 does not decide which thermal streams in the energy system need to be connected to establish the required heat exchanges. This is only done in stage 2. Consequently, the spatial layout and corresponding pipe length of a heat network selected by the optimisation cannot directly be calculated in stage 1. As a result, the dependency of a heat network's investment cost on pipe length cannot be included in the objective function. Therefore, the specific investment cost of a heat network is expressed relative to its nominal heat load or capacity (€/kW). This value needs to reflect the influence of both internal pipe diameter and pipe

length on the investment costs of a heat network. The specific investment cost of a heat network in €/kW can be determined by a priori estimating the pipe length and subsequently expressing the investment cost as a piecewise linear function of the capacity. After a *Syn-E-Sys* run, this value can be refined based on the heat network pipe length in the optimised system. This procedure can be iterated.

As a fourth point of attention, the set of input parameters characterising the utility and storage system must allow a feasible solution. This can be ensured either by a superstructure customised for the specific problem or by a sufficiently large an versatile superstructure. Moreover, when the model is applied to case studies with a high level of complexity, verification and interpretation of the results and gaining insight into the system's behaviour can be a cumbersome task.

7.1.2. Straightforward model extensions

The objective function can be easily extended to include CO_2 taxes and one-off installation charges for utility and storage units. Moreover, constraints can be added to ensure a minimum share of renewable technologies in the total annual electricity or heat generation. To allow for long term investment planning, the model can be extended to a multi-year time horizon.

The electrical and (dual reservoir) thermal storage models can be extended to keep charge and discharge rates below a specified limit in every time slice, or to enable different conversion efficiencies for charge and discharge. In the current formulation, the storage level is free to fluctuate between an upper and lower limit, while only the levels at start and end of the year are forced to be equal. However, constraints can be added to manipulate the operation of storage units (exclusively daily, weekly or inter-seasonal storage).

Thermal process and utility streams could be represented in more detail by piecewise linear temperature-heat curves. As an example, the cold and hot stream in respectively the evaporator and the condenser of a heat pump consist of a horizontal segment corresponding to latent heat and inclined segments related to sensible heat. Such piecewise linear streams could be incorporated in stage 1 of *Syn-E-Sys* by customising the calculation of heat loads per temperature interval (see 4.4.2.2) for thermal processes and utilities. In stage 2, the HEN superstructure could be adapted to include piecewise linear streams as proposed by Ponce-Ortega *et al.* [95].

Welsch *et al.* [48] introduced prioritising of energy demands and demand shifting into their model. A similar approach could be implemented in stage 1 of Syn-E-Sys.

7.2. Further research and development

7.2.1. Optimisation

Decreasing CO_2 emissions and reducing system costs are equally important, but conflicting targets in the design of low carbon energy systems. *Syn-E-Sys* optimises the energy system to achieve minimum total annualised costs, subject to a carbon emission limit. By performing the optimisation for a range of carbon emission limits, the influence of both targets on the optimal system configuration can be analysed. However, multi-objective optimisation (MOO) and the resulting Pareto-curve is a more

efficient approach to analyse the trade-off between multiple targets. Reformulating the model to incorporate MOO can be the subject of further research.

Syn-E-Sys comprises two stages and is in fact sequential. A simultaneous model could be obtained by merging a multi-period version of the HEN superstructure proposed by Ponce-Ortega *et al.* [81] or by Na *et al.* [82] with the utility and storage models proposed in this work. In this case, the thermal energy balances of the heat cascade model need to be removed. Investigating the feasibility of such a model and limiting its complexity is a major challenge for future research. The advantage of a simultaneous model is that phantom heat could be blocked by forbidding heat exchangers between the hot and cold streams of a heat network. Moreover, the pipe length of a heat network could be integrated in the optimisation, since the connections between a heat network and other streams (parallel or in series) are optimised in the superstructure.

7.2.2. System

In reality, the utility and storage system needs to be able to deal with sudden extreme values in energy demands. Therefore, the formulation in stage 1 needs to be extended with additional constraints representing extreme conditions of short duration. In this work, electrical energy is modelled as a commodity. Further research should point out if a more detailed representation of electrical energy (taking into account different voltage levels) is required.

7.2.3. Storage

For modelling of sensible heat storage subject to hourly losses, it is assumed in this work that the temperature level of the bottom reservoir or tank in both the dual reservoir model as in the virtual tank model is set at environmental temperature. In this way no heat loss occurs from the bottom tank to the environment. However, a higher bottom tank temperature might allow a more optimal integration of the storage's hot and cold streams of in the heat cascade. Further study is required to determine whether the proposed storage models can be modified to accept a bottom tank temperature higher than environmental temperature.

It is the author's understanding that even in the situation where the bottom tank temperature is above environmental temperature, no heat losses have to be assigned to the bottom tank. The reason is that the temperature range of the storage, specified by the analyst, represents steady state conditions. In other words, the chosen bottom tank temperature already accounts for the effects of heat loss. However, in the dual reservoir model, the expression for hourly storage efficiency ηh of the hot reservoir (Eq. 7) needs to be reformulated as indicated below (Eq. 7*). The heat loss is driven by the temperature difference $(Tup - Tenv)$, but it is modelled as a mass flow from the hot reservoir at temperature Tup to the cold reservoir at temperature Tlo:

Eq. 7* $$\eta h = 1 - 3600 \cdot \frac{4 \cdot k}{\rho \cdot D \cdot cp} \cdot \frac{(Tup - Tenv)}{(Tup - Tlo)}$$

Due to the analogy between the dual reservoir model and the virtual tank model (see 4.6.7.2), the hourly storage efficiency from each virtual tank is now calculated with Eq. 7*. As a result, the calculation of the time discount factors needs to be reconfigured using a separate hourly storage

efficiency per virtual tank. This is proposed as further research. Furthermore, the abilities of the storage models to accurately represent various types of energy storage technologies should be analysed in more detail.

7.2.4. Time structure

The proposed hierarchical time structure is empirically specified. Throughout the year, the same subdivision of weeks into daytypes, daytypes into days, days into daily time brackets, and daily time brackets into hours is followed (see 4.6.3). This significantly facilitates the assembly of the natural time sequence and the identification of the positions in time of possibly critical storage levels, needed to calculate the evolution of the storage level over the year. On the other hand, cluster algorithms allow to represent yearly profiles of energy demand and supply parameters more accurately using typical days (see 4.2.2). However, the allocation of typical days to the sequential days of the year is unstructured: The occurrence of a certain typical day can be dispersed over the year [100]. A hybrid form between the proposed hierarchical time structure and typical day clustering could be the subject of further research.

Such hybrid approach could be achieved by using a clustering algorithm in which each typical day can only represent a single group of sequential days. Subsequently, an analogous algorithm could cluster the hours of each typical day into sequential groups (‘typical day parts’) each containing a set of sequential hours. This approach could be connected to the proposed hierarchical time structure as follows: Each group of days represented by a typical day is represented in the time structure by a season. This season contains only 1 fictive week, subdivided in only 1 daytype. The number of days in that daytype is equal to the number of days belonging to the typical day. Furthermore, ‘typical day parts’ are represented in the time structure by daily time brackets. Moreover, the time structure could be altered to allow for a separate subdivision of the day in daily time brackets per daytype (= week = season). But in that case, the calculation of critical storage levels and time discount factors needs to be modified. In conclusion, the combination of a modified cluster algorithm and the manipulation of the time superstructure could lead to a hybrid form of time representation.

7.2.5. Utilities

Syn-E-Sys employs a generic electrical and thermal technology model. More complex technologies are modelled by an artificial interconnection of two instances of the generic technology models. However, a separate advanced model per technology could improve the accuracy of the overall model, albeit at the expense of increasing its complexity.

7.2.6. Heat networks

When the optimised heat network streams are not embedded in the equivalent heat transfer unit envelope, phantom heat may corrupt the calculation of utility requirements (see YYY). Equivalence between heat networks and envelope can only be guaranteed under certain conditions. Therefore, it should be further investigated whether the heat cascade formulation can be modified to effectively block phantom heat.

7.2.7. HEN

In the sequential energy integration approach, the connections between hot and cold streams are optimised in the second step, referred to as the Heat Load Distribution (HLD) problem. Pouransari *et al.* [87] adapted the HLD to take into account the geographical distance between the different streams in each match. They introduced weighting factors in the objective function to penalise connections with greater distances, since these will implicate higher piping costs. The two-staged approach of *Syn-E-Sys*, however, does not include the HLD step and connections between streams are only determined during the HEN design in stage 2. Further research is needed to find a way to account for the distance between the streams connected by each heat exchanger during the optimisation of the HEN.

The hot and cold stream segments between subsequent tanks of the virtual tank storage model do not represent physically real streams. However, they are treated as separate physical streams in the HEN superstructure. Further research is necessary to decide how these streams should be dealt with in the HEN design.

7.2.8. Sensitivity

Case studies with Syn-E-Sys should be extended with sensitivity analysis, to investigate the effect of parameter uncertainty on the optimal system configuration [112]. Robust optimisation must lead a system design that is less sensitive to parameter uncertainty.

7.2.9. Near-optimal solutions

The single optimal solution might not be practically optimal. To assist the system design engineer in finding a practical optimal solution, integer-cut constraints can be applied to find a series of near-optimal, structurally different, but equally-good solutions [115]. This approach could be applied in stage 1 on the utility system and storage configuration, as well as in stage 2 on the selection of heat exchangers (MIN_NHEX problem)

7.3. Model application and practical challenges

In this work, a generic case study has been set up and a case study from literature has been selected with the aim to demonstrate all specific model features. These small scale examples allow for straightforward verification and interpretation of the results. However, Syn-E-Sys is developed to handle energy systems on business park scale. Consequently, future research should focus on full scale applications.

To model a full scale business park energy system, data for all relevant energy demands (related to building use or industrial processes) need to be provided, and a database of available energy conversion and storage units needs to composed. The acquisition of energy demand data depends on whether the energy system needs to be designed for a newly planned business park or for an existing business park.

In the case of an existing business park, energy demand data can be acquired through extensive energy monitoring over a sufficiently long timespan (e.g. 1 year) in every company involved. Although this may be organisationally and financially challenging, energy monitoring leads to detection of energy inefficiencies on company level. Consequently, energy measures to reduce energy costs can already be taken during the monitoring phase as demonstrated in practise in the ACE project [9].

In case of a newly planned business park, the energy profiles (energy service demands related to building use and production) of the companies that will settle on the park need to be estimated a priori, based on data from identical existing companies. However, such estimations might be subject to a high degree of uncertainty.

Starting from the energy demand data and the utility and storage system database, the energy system design can be optimised using *Syn-E-Sys*. However, the optimal configuration might include connections between components of the energy system that are practically infeasible. As an example, a company might be opposed to direct heat exchange with other companies because of operational or strategic reasons, prevailing energy legislation might prohibit the rollout of a local heat network or smart grid, spatial planning legislation might prohibit the installation of large wind turbines (e.g. due to an adjacent residential area), etc. It is therefore important to include as much practical constraints as possible into the modelling phase.

The optimised energy system can only be realised when a heat exchanger network is installed to physically enable the required heat exchanges between hot and cold streams in all time slices. Such a heat exchanger network involves significant costs related to the pipes that transport thermal streams and the heat exchanger units that enable the actual heat transfers between them. In some cases, this network may be too complex or too expensive to be realised. Moreover, a control system is required to regulate the bypasses around each heat exchanger, which might form a practical challenge.

In case of a newly planned business park, there is a time-related mismatch between the modelling and the actual realisation of the energy system. While the energy system design is performed as if all companies would settle simultaneously, in reality, companies might settle on the park over a time span of several years. Consequently, the energy system is build up gradually. These intermediary steps could be taken into account, by extending the model to a multi-year time horizon. The “Low carbon business park manual” [3] provides an extensive description of the different development phases of a business park.

In conclusion, future work should primarily focus on the application of *Syn-E-Sys* on business park scale case studies, starting with low carbon energy system design on existing business parks. Energy monitoring should enhance the availability of energy data on company level for possible case studies. To enable theoretical solutions in practise, an adequate legal context should be created and companies should be encouraged to exploit energy synergies in terms of heat exchange, collective renewable energy production and collective energy infrastructure.

Appendices

A. Case study 1

A.1. Hierarchical time structure

The year is divided in 32 empirically defined time slices according to a hierarchical time structure composed of three levels; season, daytype and daily time bracket. In this structure, the year consists of four seasons ls (winter, spring, summer, autumn), each containing 13 weeks. Every week comprises two daytypes ld (weekday and weekend day) containing respectively 5 and 2 days. Each day is subdivided into 4 daily time brackets lh (morning, midday, afternoon, night), containing 5, 2, 5 and 12 hours respectively. Table 20 displays the sets and parameters composing the hierarchical time structure, whereas Table 21 lists the conversion factors that link the time slices to this structure.

	wks_ls_{ls}			$days\_ld_{ld}$			hrs_lh_{lh}	
winter	$ls1$	13	***weekday***	$ld1$	5	***morning***	$lh1$	5
spring	$ls2$	13	***weekend***	$ld2$	2	***midday***	$lh2$	2
summer	$ls3$	13				***afternoon***	$lh3$	5
autumn	$ls4$	13				***night***	$lh4$	12

Table 20: Sets and parameters in time structure

	$conv\_S_{S.ls}$ ***ls***				$conv\_S_{S.ld}$ ***ld***		$conv\_S_{S.lh}$ ***lh***			
S	*ls1*	*ls2*	*ls3*	*ls4*	*ld1*	*ld2*	*lh1*	*lh2*	*lh3*	*lh4*
ls1ld1lh1	**1**	0	0	0	**1**	0	**1**	0	0	0
ls1ld1lh2	**1**	0	0	0	**1**	0	0	**1**	0	0
ls1ld1lh3	**1**	0	0	0	**1**	0	0	0	**1**	0
ls1ld1lh4	**1**	0	0	0	**1**	0	0	0	0	**1**
ls1ld2lh1	**1**	0	0	0	0	**1**	**1**	0	0	0
ls1ld2lh2	**1**	0	0	0	0	**1**	0	**1**	0	0
ls1ld2lh3	**1**	0	0	0	0	**1**	0	0	**1**	0
ls1ld2lh4	**1**	0	0	0	0	**1**	0	0	0	**1**
ls2ld1lh1	0	**1**	0	0	**1**	0	**1**	0	0	0
ls2ld1lh2	0	**1**	0	0	**1**	0	0	**1**	0	0
ls2ld1lh3	0	**1**	0	0	**1**	0	0	0	**1**	0
ls2ld1lh4	0	**1**	0	0	**1**	0	0	0	0	**1**
ls2ld2lh1	0	**1**	0	0	0	**1**	**1**	0	0	0
ls2ld2lh2	0	**1**	0	0	0	**1**	0	**1**	0	0
ls2ld2lh3	0	**1**	0	0	0	**1**	0	0	**1**	0
ls2ld2lh4	0	**1**	0	0	0	**1**	0	0	0	**1**
ls3ld1lh1	0	0	**1**	0	**1**	0	**1**	0	0	0
ls3ld1lh2	0	0	**1**	0	**1**	0	0	**1**	0	0
ls3ld1lh3	0	0	**1**	0	**1**	0	0	0	**1**	0
ls3ld1lh4	0	0	**1**	0	**1**	0	0	0	0	**1**
ls3ld2lh1	0	0	**1**	0	0	**1**	**1**	0	0	0
ls3ld2lh2	0	0	**1**	0	0	1	0	**1**	0	0
ls3ld2lh3	0	0	**1**	0	0	1	0	0	**1**	0
ls3ld2lh4	0	0	**1**	0	0	1	0	0	0	**1**
ls4ld1lh1	0	0	0	**1**	**1**	0	**1**	0	0	0
ls4ld1lh2	0	0	0	**1**	**1**	0	0	**1**	0	0
ls4ld1lh3	0	0	0	**1**	**1**	0	0	0	**1**	0
ls4ld1lh4	0	0	0	**1**	**1**	0	0	0	0	**1**
ls4ld2lh1	0	0	0	**1**	0	**1**	**1**	0	0	0
ls4ld2lh2	0	0	0	**1**	0	**1**	0	**1**	0	0
ls4ld2lh3	0	0	0	**1**	0	**1**	0	0	**1**	0
ls4ld2lh4	0	0	0	**1**	0	**1**	0	0	0	**1**

Table 21: Conversion parameters to assign time slices to seasons, daytypes and daily time brackets

A.2. Time profiles of energy demand and supply

Thermal process loads, the electricity demand and the relative distribution over the year of renewable energy production vary over the year. These variations are represented by assigning different parameter values to each time slice (Table 22, Fig. 95-Fig. 100).

		$ld1$				$ld2$			
		$lh1$	$lh2$	$lh3$	$lh4$	$lh1$	$lh2$	$lh3$	$lh4$
$\dot{Q}P_{hP1}$	$ls1$	250	250	250	0	250	250	250	0
(kW)	$ls2$	1250	2500	1250	0	1250	2500	1250	0
	$ls3$	2500	5000	2500	0	2500	5000	2500	0
	$ls4$	1250	2500	1250	0	1250	2500	1250	0
$\dot{Q}P_{cP1}$	$ls1$	2000	1000	1000	500	2000	1000	1000	500
(kW)	$ls2$	1000	500	500	200	1000	500	500	200
	$ls3$	0	0	0	0	0	0	0	0
	$ls4$	1000	500	500	200	1000	500	500	200
$\dot{Q}P_{cP2}$	$ls1$	300	300	300	300	150	150	150	150
(kW)	$ls2$	300	300	300	300	150	150	150	150
	$ls3$	300	300	300	300	150	150	150	150
	$ls4$	300	300	300	300	150	150	150	150
dem_el	$ls1$	1200	1200	1200	360	360	360	360	360
(kW)	$ls2$	960	720	960	240	240	240	240	240
	$ls3$	720	720	720	120	120	120	120	120
	$ls4$	960	720	960	240	240	240	240	240
$fEa\_el_{PV,S}$	$ls1$	3.71	2.35	1.40	0.00	1.48	0.94	0.56	0.00
(%)	$ls2$	10.53	5.72	6.84	0.65	4.21	2.29	2.73	0.26
	$ls3$	11.73	5.75	7.28	1.57	4.69	2.30	2.91	0.63
	$ls4$	6.81	3.78	3.19	0.13	2.72	1.51	1.28	0.05
$fEa\_el_{WT,S}$	$ls1$	4.33	1.71	4.53	11.10	1.73	0.68	1.81	4.44
(%)	$ls2$	2.82	1.25	3.37	7.88	1.13	0.50	1.35	3.15
	$ls3$	3.15	1.42	3.28	7.19	1.26	0.57	1.31	2.88
	$ls4$	3.90	1.51	3.77	10.21	1.56	0.60	1.51	4.08

Table 22: Energy demand profiles and relative energy yield per time slice for PV and WT – Example2

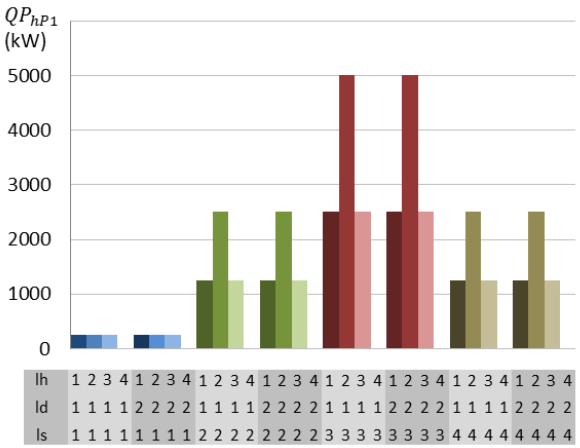

Fig. 95: Cooling load process hP1 per time slice

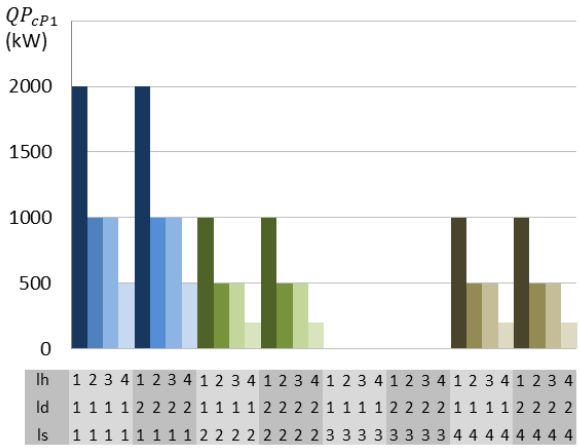

Fig. 96: Heating load process cP1 per time slice

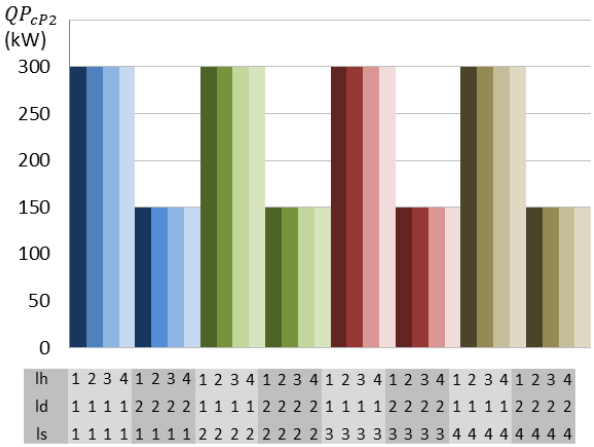

Fig. 97: Heating load process cP2 per time slice

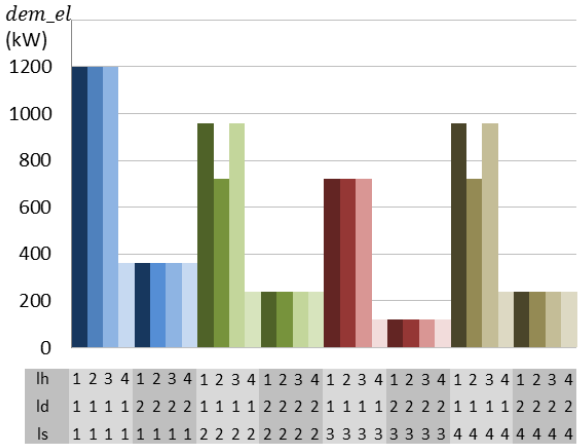

Fig. 98: Electricity demand per time slice

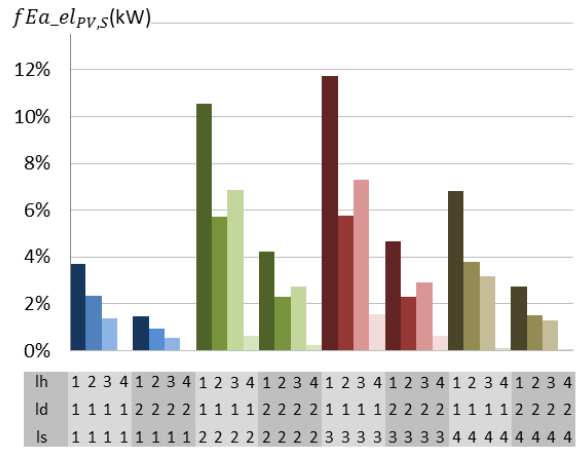

Fig. 99: Fraction of annual energy yield PV per time slice

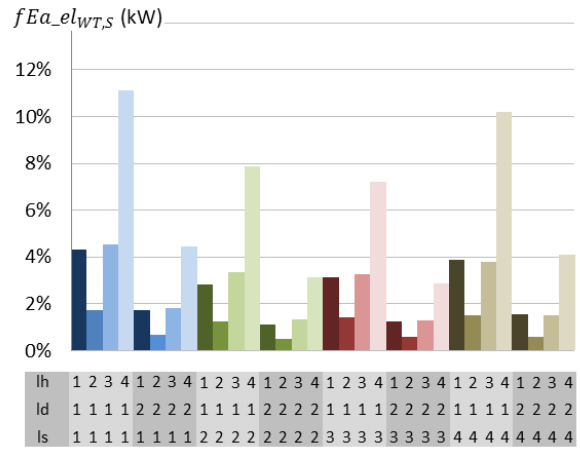

Fig. 100: Fraction of annual energy yield WT per time slice

A.3. Part-load operation boiler

The non-linear equations (Eqs. a, b) characterising efficiency and investment cost of the boiler are adopted from Voll [75], Appendix A.

Eq. a $$\eta rel = \frac{C_1 + C_2 \cdot \dot{Q}rel + C_3 \cdot \dot{Q}rel^2 + C_4 \cdot \dot{Q}rel^3}{C_5 + C_6 \cdot \dot{Q}rel + C_7 \cdot \dot{Q}rel^2 + C_8 \cdot \dot{Q}rel^3}$$

Eq. b $$Inv = Inv_B \cdot \left(\dot{Q}nom/\dot{Q}B\right)^M \Leftrightarrow cI = \frac{Inv}{\dot{Q}nom} = \frac{Inv_B \cdot \left(\dot{Q}nomrel \cdot \dot{Q}nommax\right)^{M-1}}{\dot{Q}B^M}$$

values of constants $C_1 - C_8$, $Inv_B, \dot{Q}B, M$ taken from [75], $\dot{Q}nommax = 10MW$, $\dot{Q}nommin = 0.1MW$

The generic technology model (See Section 4.3) is calibrated by fitting the reference points for part-load operation (R) and investment costs (Rc) as close as possible to these non-linear curves, as shown by the squares in Fig. 101 and Fig. 102. Available boiler sizes range from $\dot{Q}nommin$ = 0.1 MW to $\dot{Q}nommax$ = 10 MW.

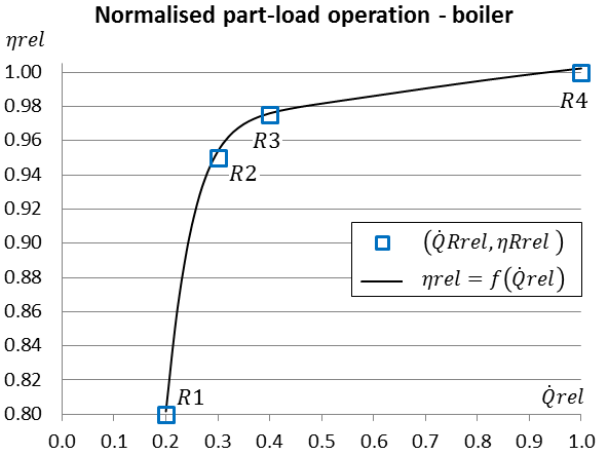

	$R1$	$R2$	$R3$	$R4$
$\dot{Q}Rrel$	0.200	0.300	0.400	1
$\eta Rrel$	0.800	0.950	0.975	1

Fig. 101: Boiler: non-linear part-load curve and calibrated reference points *R* for piecewise linearisation

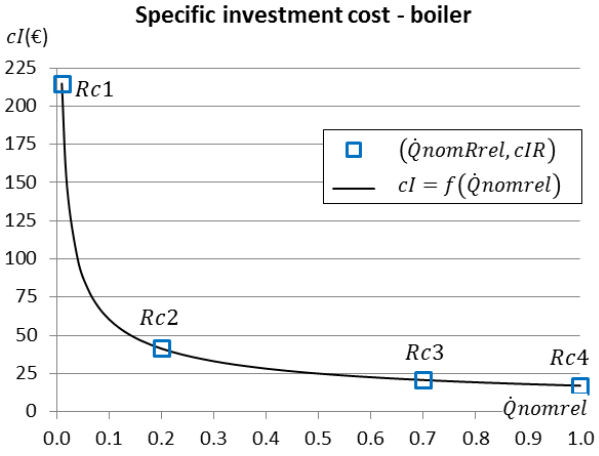

	$Rc1$	$Rc2$	$Rc3$	$Rc4$
$\dot{Q}nomRrel$	0.010	0.200	0.700	1
cIR	214.8	41.40	20.80	17.10

Fig. 102: Boiler: non-linear investment cost curve and calibrated reference points *Rc* for piecewise linearisation

A.4. Input data

Process	TsP_P (°C)	TtP_P (°C)	$\Delta Tmin_P$ (°C)
hP1	140	90	10
cP1	30	60	10
cP2	30	50	10

Table 23: Properties of process streams

Utility	TsU_U (°C)	TtU_U (°C)	$\Delta Tmin_U$ (°C)	ηnom_U (-)	cF_U (€/kWh)	$iUCO2_U$ (kg CO_2/kWh)
Boiler	1000	120	10	0.9	0.0392	0.23
CW	7	20	10	100	0	0

Utility	$Ea1\_el_E$ (kWh/kW)	$cIR\_el_{E,Rc}$ (€/kW)	cOM_el_E (€/kWh)
PV	930	1800	0.030
WT	2215	1325	0.025
Buying electricity		0.0620	(€/kWh)
Selling electricity		0.0496	(€/kWh)

Table 24: Properties of utilities

Storage	Tlo_{Sto_th} (°C)	Tup_{Sto_th} (°C)	$\Delta Tmin_{Sto\_th}$ (°C)
Sto_th	40	70	10
Storage	$\eta conv_{Sto}$ (-)	ηh_{Sto} (-)	cI_{Sto} (€/kWh)
Sto_th	1	0.999312	10
Sto_el	0.768	1	2

Table 25: Properties of storage units

A.5. Results: Optimised system operation

The optimised thermal and electrical utility loads and storage charge and discharge loads are tabulated in Table 26 and graphically represented in Fig. 103 and Fig. 104. The hot and cold side of the thermal energy balances in each time slice are presented in Table 27 and visualised in Fig. 105 and Fig. 106. The supply and the demand side of the electrical energy balances are presented in Table 28 and visualised in Fig. 107 and Fig. 108.

	Thermal utilities		*Thermal storages*		*Electrical utilities*		*Electrical storages*	
	Boiler	***CW***	***Sto_th1***		***PV***	***WT***	***Sto_el1***	
(kW)	$\dot{Q}U_S$	$\dot{Q}U_S$	$\dot{Q}Stoc_S$	$\dot{Q}Stoh_S$	P_el_S	P_el_S	$PSto\_in\_S_S$	$PSto\_out\_S_S$
S	Ins1	Ins1	in	out	Ins1	Ins1	in	out
ls1ld1lh1	1135	0	0	915	63	590	0	494
ls1ld1lh2	1135	0	85	0	99	583	0	518
ls1ld1lh3	1135	0	85	0	24	617	0	0
ls1ld1lh4	1135	0	335	0	0	630	270	0
ls1ld2lh1	985	0	0	915	62	590	292	0
ls1ld2lh2	900	0	0	0	99	579	318	0
ls1ld2lh3	900	0	0	0	24	617	280	0
ls1ld2lh4	1034	0	384	0	0	630	270	0
ls2ld1lh1	0	0	0	50	177	384	0	210
ls2ld1lh2	0	0	1700	0	241	426	0	53
ls2ld1lh3	0	48	402	0	115	459	0	386
ls2ld1lh4	0	0	0	500	5	448	212	0
ls2ld2lh1	0	0	100	0	177	385	322	0
ls2ld2lh2	0	0	1850	0	241	426	427	0
ls2ld2lh3	0	0	600	0	115	460	335	0
ls2ld2lh4	0	52	0	402	5	447	211	0
ls3ld1lh1	0	2186	14	0	198	429	0	115
ls3ld1lh2	0	2186	2514	0	242	484	0	16
ls3ld1lh3	0	2186	14	0	123	447	0	172
ls3ld1lh4	0	184	0	484	11	408	0	0
ls3ld2lh1	0	2186	164	0	198	429	485	0
ls3ld2lh2	0	2186	2664	0	242	486	586	0
ls3ld2lh3	0	2186	164	0	123	446	427	0
ls3ld2lh4	0	271	0	421	11	409	40	0
ls4ld1lh1	0	0	0	50	115	532	0	314
ls4ld1lh2	0	0	1700	0	159	515	0	46
ls4ld1lh3	0	48	402	0	54	514	0	393
ls4ld1lh4	0	0	0	500	1	580	309	0
ls4ld2lh1	0	0	100	0	115	532	406	0
ls4ld2lh2	0	0	1850	0	159	511	0	0
ls4ld2lh3	0	126	474	0	54	515	0	0
ls4ld2lh4	0	0	0	350	1	579	340	0

Table 26: Optimal operation thermal and electrical utilities and storages

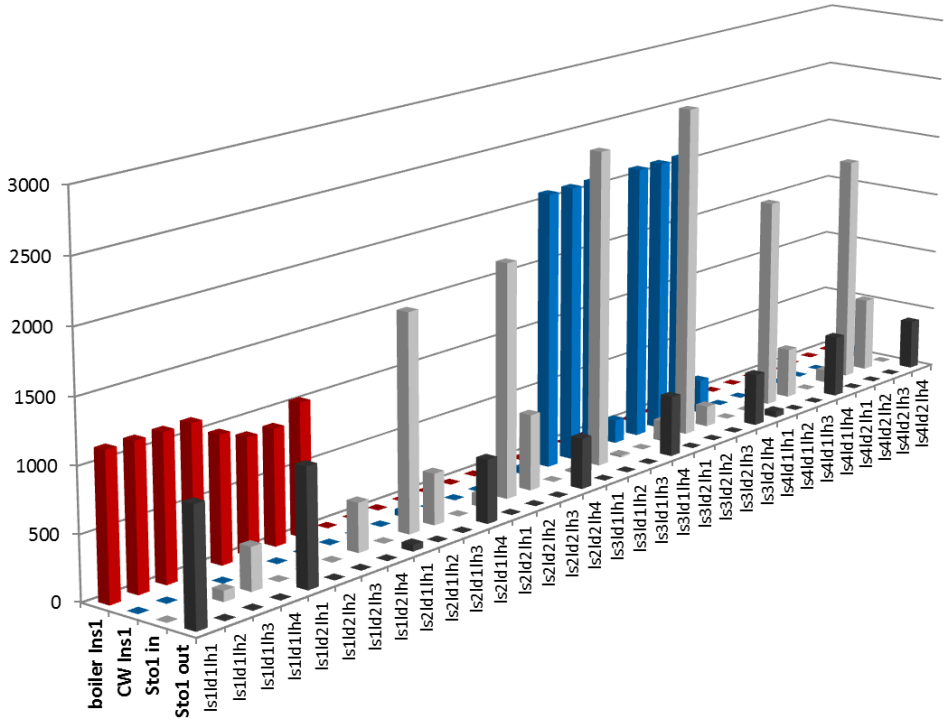

Fig. 103: Optimal operation thermal utilities and storages (kW)

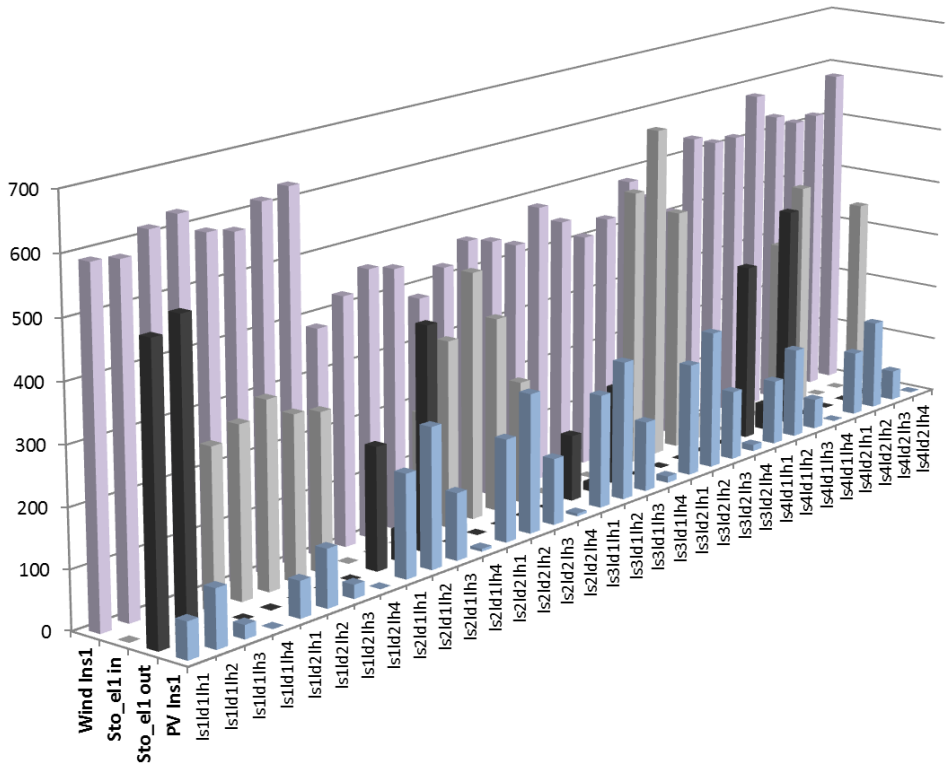

Fig. 104: Optimal operation electrical utilities and storages (kW)

	Thermal energy balance - hot side				*Thermal energy balance - cold side*				[=0]
(kW)	Q_hp	Q_hu	Q_hsto	Q_in	Q_cp	Q_cu	Q_csto	Q_out	bal
ls1ld1lh1	250	1135	915	0	-2300	0	0	0	0
ls1ld1lh2	250	1135	0	0	-1300	0	-85	0	0
ls1ld1lh3	250	1135	0	0	-1300	0	-85	0	0
ls1ld1lh4	0	1135	0	0	-800	0	-335	0	0
ls1ld2lh1	250	985	915	0	-2150	0	0	0	0
ls1ld2lh2	250	900	0	0	-1150	0	0	0	0
ls1ld2lh3	250	900	0	0	-1150	0	0	0	0
ls1ld2lh4	0	1034	0	0	-650	0	-384	0	0
ls2ld1lh1	1250	0	50	0	-1300	0	0	0	0
ls2ld1lh2	2500	0	0	0	-800	0	-1700	0	0
ls2ld1lh3	1250	0	0	0	-800	-48	-402	0	0
ls2ld1lh4	0	0	500	0	-500	0	0	0	0
ls2ld2lh1	1250	0	0	0	-1150	0	-100	0	0
ls2ld2lh2	2500	0	0	0	-650	0	-1850	0	0
ls2ld2lh3	1250	0	0	0	-650	0	-600	0	0
ls2ld2lh4	0	0	402	0	-350	-52	0	0	0
ls3ld1lh1	2500	0	0	0	-300	-2186	-14	0	0
ls3ld1lh2	5000	0	0	0	-300	-2186	-2514	0	0
ls3ld1lh3	2500	0	0	0	-300	-2186	-14	0	0
ls3ld1lh4	0	0	484	0	-300	-184	0	0	0
ls3ld2lh1	2500	0	0	0	-150	-2186	-164	0	0
ls3ld2lh2	5000	0	0	0	-150	-2186	-2664	0	0
ls3ld2lh3	2500	0	0	0	-150	-2186	-164	0	0
ls3ld2lh4	0	0	421	0	-150	-271	0	0	0
ls4ld1lh1	1250	0	50	0	-1300	0	0	0	0
ls4ld1lh2	2500	0	0	0	-800	0	-1700	0	0
ls4ld1lh3	1250	0	0	0	-800	-48	-402	0	0
ls4ld1lh4	0	0	500	0	-500	0	0	0	0
ls4ld2lh1	1250	0	0	0	-1150	0	-100	0	0
ls4ld2lh2	2500	0	0	0	-650	0	-1850	0	0
ls4ld2lh3	1250	0	0	0	-650	-126	-474	0	0
ls4ld2lh4	0	0	350	0	-350	0	0	0	0

Table 27: Thermal energy balances

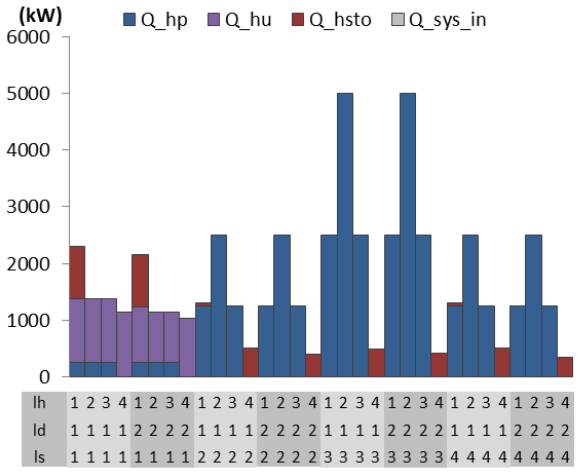

Indexes Q: hp: hot processes, hu: hot utilities, hsto: hot streams storage sys_in: from heat transfer system

Fig. 105: Thermal energy balance – hot side

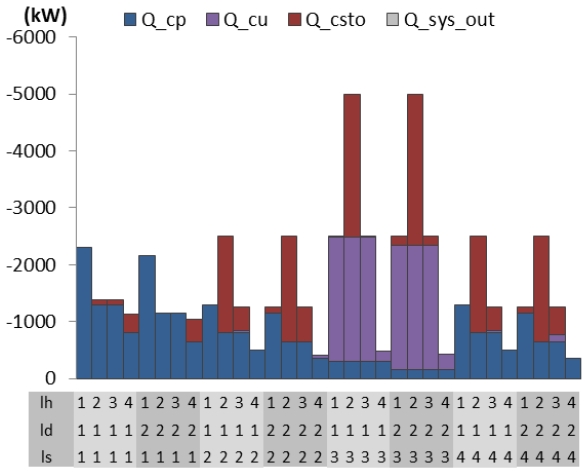

Indexes Q: cp: cold processes, cu: cold utilities, csto: cold streams storage, sys_out: to heat transfer system

Fig. 106: Thermal energy balance – cold side

	Electricity balance - supply side				*Electricity balance - demand side*				
(kW)	Gen	Imp	Sto_out	total	Dem	Use	Exp	Sto_in	total
ls1ld1lh1	653	53	494	1200	1200	0	0	0	1200
ls1ld1lh2	682	0	518	1200	1200	0	0	0	1200
ls1ld1lh3	641	559	0	1200	1200	0	0	0	1200
ls1ld1lh4	630	0	0	630	360	0	0	270	630
ls1ld2lh1	652	0	0	652	360	0	0	292	652
ls1ld2lh2	678	0	0	678	360	0	0	318	678
ls1ld2lh3	640	0	0	640	360	0	0	280	640
ls1ld2lh4	630	0	0	630	360	0	0	270	630
ls2ld1lh1	562	188	210	960	960	0	0	0	960
ls2ld1lh2	667	0	53	720	720	0	0	0	720
ls2ld1lh3	575	0	386	960	960	0	0	0	960
ls2ld1lh4	452	0	0	452	240	0	0	212	452
ls2ld2lh1	562	0	0	562	240	0	0	322	562
ls2ld2lh2	667	0	0	667	240	0	0	427	667
ls2ld2lh3	575	0	0	575	240	0	0	335	575
ls2ld2lh4	452	0	0	452	240	1	0	211	452
ls3ld1lh1	627	0	115	742	720	22	0	0	742
ls3ld1lh2	726	0	16	742	720	22	0	0	742
ls3ld1lh3	570	0	172	742	720	22	0	0	742
ls3ld1lh4	419	0	0	419	120	2	298	0	419
ls3ld2lh1	627	0	0	627	120	22	0	485	627
ls3ld2lh2	728	0	0	728	120	22	0	586	728
ls3ld2lh3	569	0	0	569	120	22	0	427	569
ls3ld2lh4	420	0	0	420	120	3	258	40	420
ls4ld1lh1	646	0	314	960	960	0	0	0	960
ls4ld1lh2	674	0	46	720	720	0	0	0	720
ls4ld1lh3	568	0	393	960	960	0	0	0	960
ls4ld1lh4	581	0	0	581	240	0	32	309	581
ls4ld2lh1	646	0	0	646	240	0	0	406	646
ls4ld2lh2	670	0	0	670	240	0	430	0	670
ls4ld2lh3	568	0	0	568	240	1	327	0	568
ls4ld2lh4	580	0	0	580	240	0	0	340	580

Table 28: Electrical energy balances

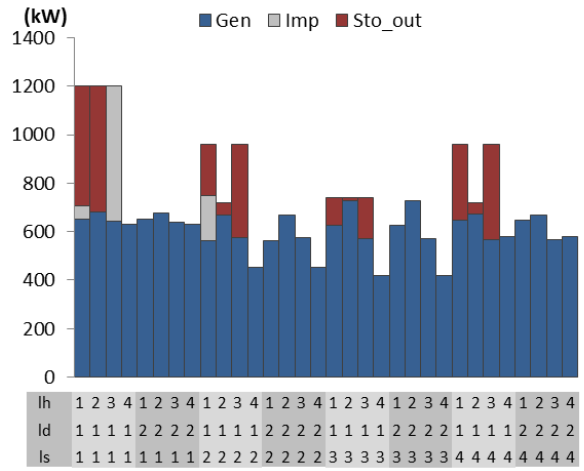

Fig. 107: Electrical energy balance – supply side

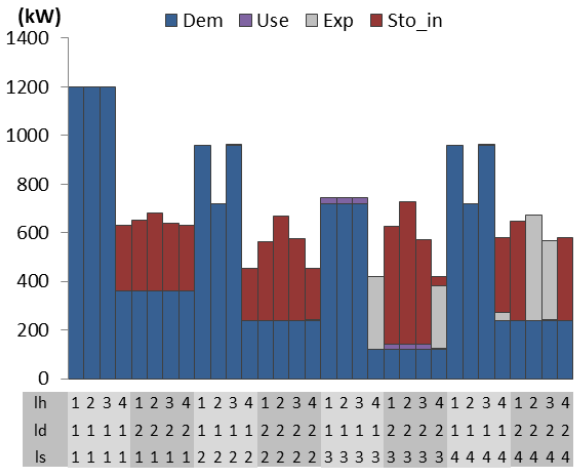

Fig. 108: Electrical energy balance – demand side

A.6. Results: Storage level evolution

The evolution of the thermal storage level over the year is visualised in Fig. 109 and Fig. 110 zooms in on the transition between the first and the second season.

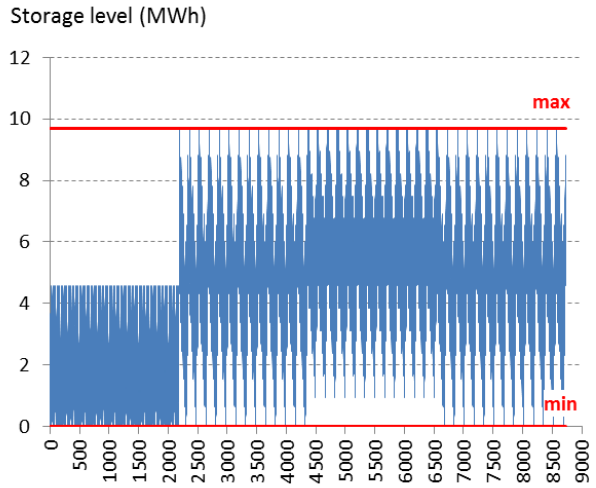

Fig. 109: Evolution thermal storage level

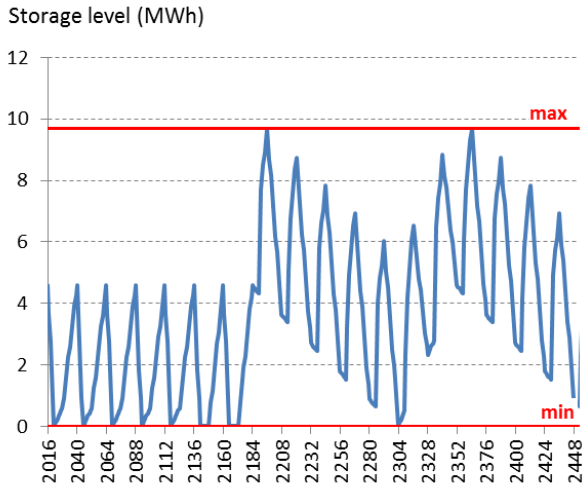

Fig. 110: Evolution thermal storage level – detail

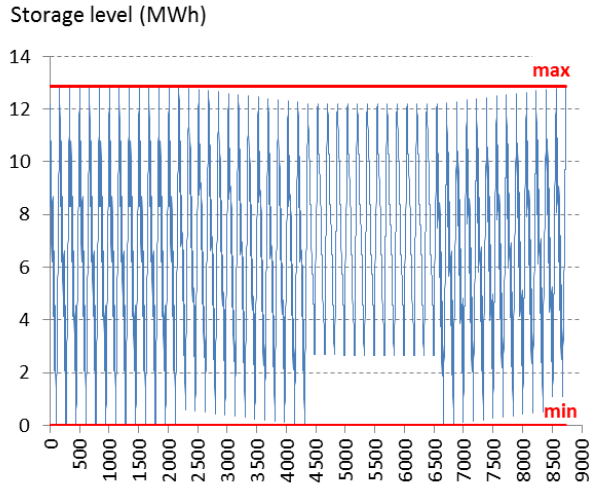

Fig. 111: Evolution electrical storage level

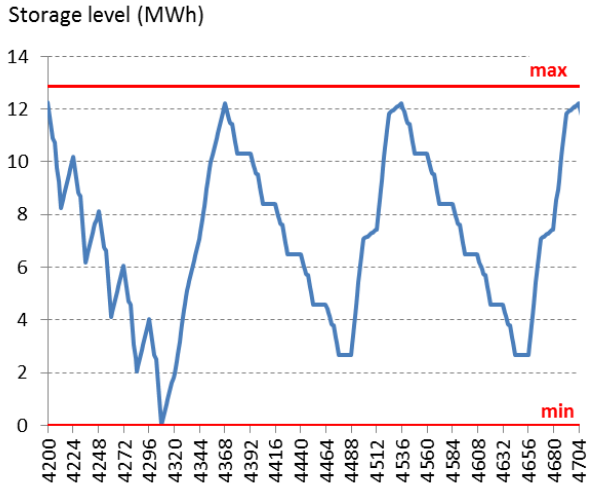

Fig. 112: Evolution electrical storage level – detail

A.7. Results: Heat exchanger network

qhc_s (kW)	*hex1*	*hex2*	*hex3*	*hex4*	*hex5*	*hex6*	*hex7*	*hex8*	*hex9*	*hex10*
ls1ld1lh1	250	1135			615	300				
ls1ld1lh2		1000	250	85						50
ls1ld1lh3		1000	250	85						50
ls1ld1lh4		500		335						300
ls1ld2lh1	250	985			765	150				
ls1ld2lh2	100	900	150							
ls1ld2lh3	250	750								150
ls1ld2lh4		500		384						150
ls2ld1lh1	1000		250			50				
ls2ld1lh2	500		300						1700	
ls2ld1lh3	500		300					48	402	
ls2ld1lh4					200	300				
ls2ld2lh1	1000		150						100	
ls2ld2lh2	500		150						1850	
ls2ld2lh3	500		150						600	
ls2ld2lh4					200	150	52			
ls3ld1lh1			300					2186	14	
ls3ld1lh2			300					2186	2514	
ls3ld1lh3			300					2186	14	
ls3ld1lh4						300	184			
ls3ld2lh1			150					2186	164	
ls3ld2lh2			150					2186	2664	
ls3ld2lh3			150					2186	164	
ls3ld2lh4						150	271			
ls4ld1lh1	1000		250			50				
ls4ld1lh2	500		300						1700	
ls4ld1lh3	500		300					48	402	
ls4ld1lh4					200	300				
ls4ld2lh1	1000		150						100	
ls4ld2lh2	500		150						1850	
ls4ld2lh3	500		150					126	474	
ls4ld2lh4					200	150				
	hex1	*hex2*	*hex3*	*hex4*	*hex5*	*hex6*	*hex7*	*hex8*	*hex9*	*hex10*
$\max_s qhc_s$	1000	1135	300	384	765	300	271	2186	2664	300

Table 29: Exchanged heat loads per time slice and maximum of exchanged heat loads

B. Case study 2

B.1. Effect of temperature range Hnw2 on utility requirements

The parameters characterising the technology model for heat network Hnw2 in *situations c, d and e* are presented in Table 30. This technology model consists of two interconnected instances of the generic thermal utility model. Fig. 113, Fig. 114 and Fig. 115 illustrate the effect of different temperature ranges for Hnw2 (*situations c, d, e*) on the utility requirements (boiler and CW).

	Utility	TsU_U (°C)	TtU_U (°C)	$\Delta Tmin_U$ (°C)	ηnom_U
Situations c, d, e	Hnw1h	80	25	4	50
	Hnw1c	25	80	4	0
Situation c	Hnw2h	295	110	4	50
	Hnw2c	110	295	4	
Situation d	Hnw2h	295	165	4	50
	Hnw2c	165	295	4	
Situation e	Hnw2h	295	295	1	50
	Hnw2c	295	295	1	

Table 30: Stream data heat networks in situations c, d and e

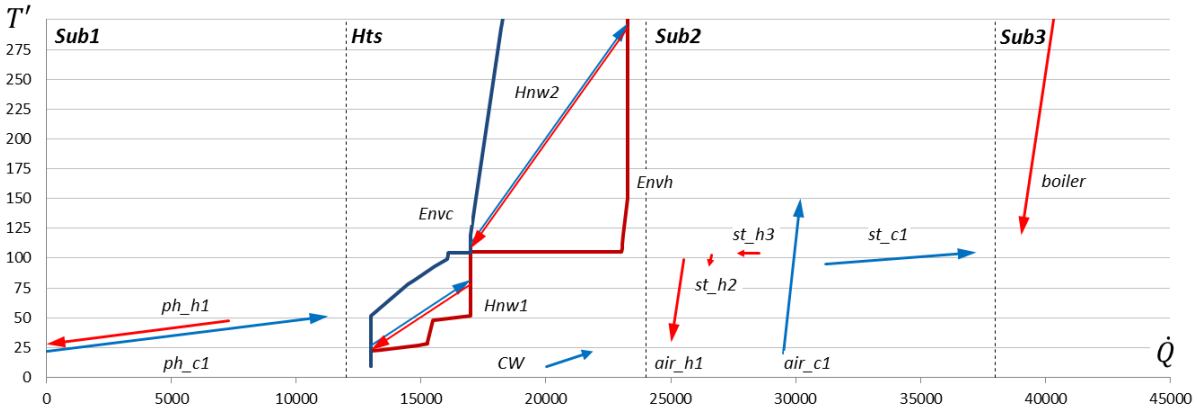

Fig. 113: Thermal streams and heat transfer unit envelope in situation c

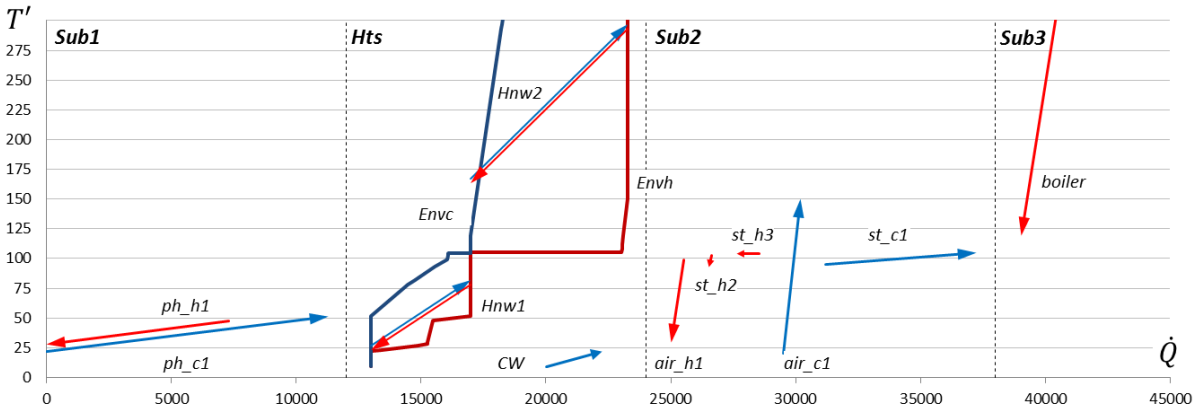

Fig. 114: Thermal streams and heat transfer unit envelope in situation d

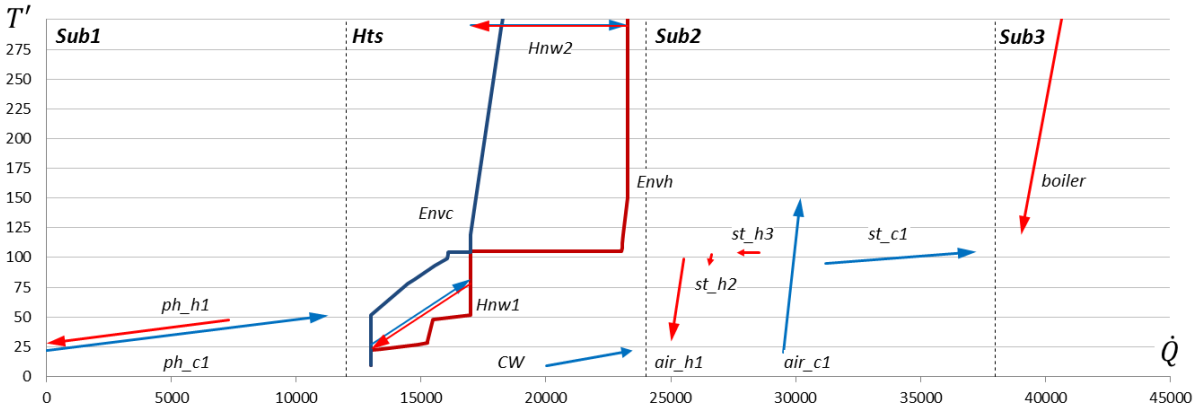

Fig. 115: Thermal streams and heat transfer unit envelope in situation e

B.2. Multi-period operation

Multi-period process stream data (source and target temperatures, heating and cooling loads) are listed in Table 31: Multi-period process stream data for problem 1. The heat network temperatures ensuring that the corresponding hot and cold composite curves are embedded in the heat transfer unit envelope are shown in Table 32.

		S1, S2, S3		***S4***		***S1***	***S2***	***S3***	***S4***
	Process	TsP_P (°C)	TtP_P (°C)	TsP_P (°C)	TtP_P (°C)	$\dot{Q}P_P$ (kW)			
$Sub1$	ph_c1	20	50	**30**	50	11262	14078	8447	14078
	ph_h1	50	30	50	**40**	7297	5473	9121	9121
$Sub2$	st_c1	105	105	105	105	6057	7571	4543	4543
	st_h3	105	105	105	105	892	669	1115	669
	st_h2	105	95	105	95	112	84	140	84
	air_c1	20	150	**30**	150	664	830	498	498
	air_h1	100	30	100	**40**	5278	3959	6598	3959

Table 31: Multi-period process stream data for problem 1

	S1, S2		***S3***		***S4***	
(°C)	TsU_U	TtU_U	TsU_U	TtU_U	TsU_U	TtU_U
Hnw1h	80	25	80	**60**	80	**36**
Hnw1c	25	80	**60**	80	**36**	80
Hnw2h	295	110	295	110	295	110
Hnw2c	110	295	110	295	110	295

Table 32: Source and target temperatures of heat networks embedded in envelope in each time slice

B.3. Part-load operation Boiler

The non-linear curves for part-load operation and investment cost of the boiler are approximated by piecewise linearisation as explained in Appendix A.3. Fig. 116 and Fig. 117 show the optimised operation and investment points for the selected boiler instances.

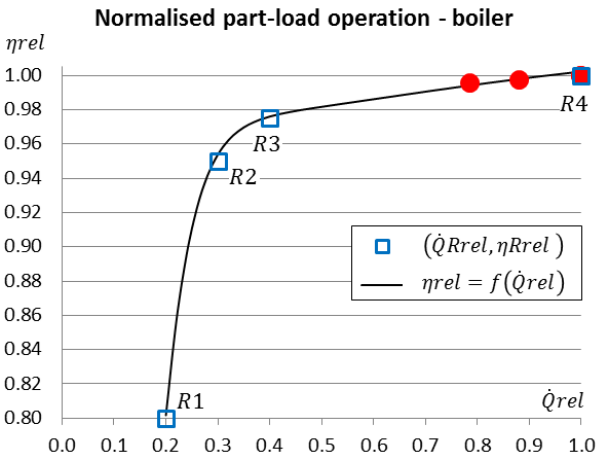

	R1	R2	R3	R4
$\dot{Q}Rrel$	0.200	0.300	0.400	1
$\eta Rrel$	0.800	0.950	0.975	1

Fig. 116: Boiler: non-linear part-load curve and calibrated reference points *R* for piecewise linearisation (bullets: optimised operation points of boiler instances)

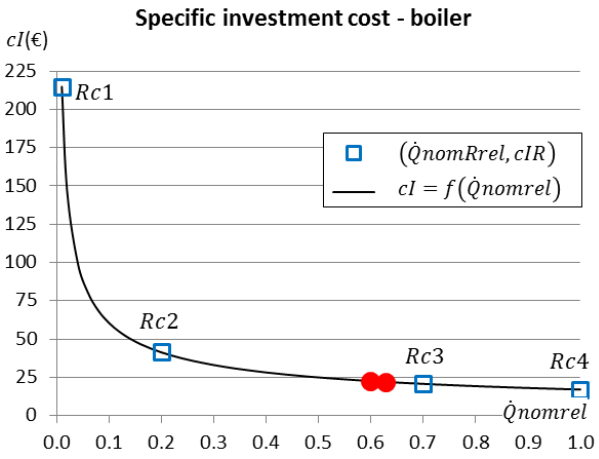

	Rc1	Rc2	Rc3	Rc4
$\dot{Q}nomRrel$	0.010	0.200	0.700	1
cIR	214.8	41.40	20.80	17.10

Fig. 117: Boiler: non-linear investment cost curve and calibrated reference points *Rc* for piecewise linearisation (bullets: optimised investment points of boiler instances)

B.4. Part-load operation CHP

The non-linear equations (Eqs. c, d) characterising efficiency and investment cost of the CHP are adopted from Voll [75], Appendix A.

Eq. c $$\eta rel = C_1 + C_2 \cdot \dot{Q}rel + C_3 \cdot \dot{Q}rel^2$$

values of constants $C_1 - C_3$ taken from [75]

Eq. d $$Inv = Inv_B \cdot \left(\dot{Q}nom/\dot{Q}B\right)^M \Leftrightarrow cI = \frac{Inv}{\dot{Q}nom} = \frac{Inv_B \cdot \left(\dot{Q}nomrel \cdot \dot{Q}nommax\right)^{M-1}}{\dot{Q}B^M}$$

values of constants $Inv_B, \dot{Q}B, M$ taken from [75], $\dot{Q}nommax = 10\ MW$

The generic technology model is calibrated by fitting the reference points for part-load operation (R) and investment costs (Rc) as close as possible to these non-linear curves, as shown by the squares in Fig. 118 and Fig. 119. The thermal as well as the electrical part of the CHP are modelled with the same relative part-load curve (Fig. 118), with a minimum threshold of 50% of the nominal load. Furthermore, the capacity of the CHP is determined by its thermal nominal load, ranging from $\dot{Q}nommin$ = 0.5 MW to $\dot{Q}nommax$ = 10 MW. The optimised operation and investment points for the selected CHP instances are indicated in Fig. 118 and Fig. 119.

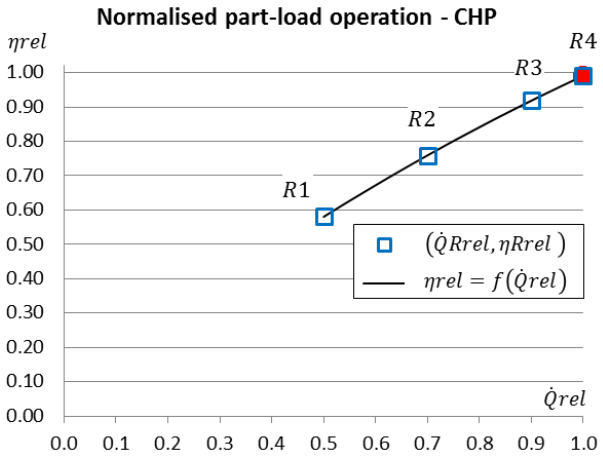

	$R1$	$R2$	$R3$	$R4$
$\dot{Q}Rrel$	0.500	0.700	0.900	1.00
$\eta Rrel$	0.581	0.759	0.919	0.991

Fig. 118: CHP: non-linear part-load curve and calibrated reference points *R* for piecewise linearisation (bullets: optimised operation points of CHP instances)

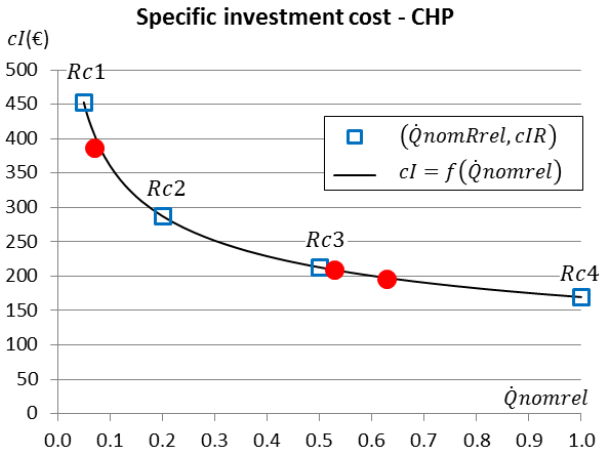

	$Rc1$	$Rc2$	$Rc3$	$Rc4$
$\dot{Q}nomRrel$	0.05	0.20	0.50	1.00
cIR	452.8	287.6	213.0	169.8

Fig. 119: CHP: non-linear investment cost curve and calibrated reference points *Rc* for piecewise linearisation (bullets: optimised investment points of CHP instances)

B.5. Results: Heat exchanger network

	Ahc (m²)	qhc (kW) ***S1***	***S2***	***S3***	***S4***
hex1	925	6292	6292		
hex2	101		1456		552
hex3	696		4546	4719	4734
hex4	2677	6057	7571	4543	4543
hex5	116	235	294	176	191
hex6	573	575	217	933	446
hex7	3276	879	3202	668	2833
hex8	656		2974		
hex9	762	112	84	140	84
hex10	6397	3390	3959	193	3959
hex11	3011	1888		6405	
hex12	27808	7297	5473	7321	9121
hex13	1170			1800	
hex14	232	317	452	182	223
hex15	6114	3086	2429	458	2124

Table 33: Heat exchanger areas and exchanged heat loads per time slice

References

[1] IPCC. Climate Change 2014: Synthesis Report. Eds. Core Writing Team, Pachauri RK, Meyer LA, Contribution of Working Groups I, II and III to the Fifth Assessment Report of the Intergovernmental Panel on Climate Change, ed, Geneva, Switzerland: IPCC, 2014.
[2] IEA. CO2 Emissions from Fuel Combustion Highlights - 2014 Edition. Paris, France, 2014.
[3] Timmerman J, Deckmyn C, Vandevelde L, Van Eetvelde G. Low carbon business park manual: A guide for developing and managing energy efficient and low carbon businesses and business parks. Ghent, Belgium, 2014.
[4] IPCC. Summary for Policymakers. Eds. Stocker TF, Qin D, Plattner G-K, Tignor M, Allen SK, Boschung J, et al., Climate Change 2013: The Physical Science Basis Contribution of Working Group I to the Fifth Assessment Report of the Intergovernmental Panel on Climate Change, ed, Cambridge, United Kingdom and New York, NY, USA.: Cambridge University Press 2013.
[5] EEA. Observed trends in total global concentration of the Kyoto gases. 2015. www.eea.europa.eu/data-and-maps/indicators/atmospheric-greenhouse-gas-concentrations-4/assessment. accessed 09-09.
[6] MIT. Featured Stories. Cambridge, USA2013. oceans.mit.edu/featured-stories/5-questions-mits-ron-prinn-400-ppm-threshold. accessed 06-10.
[7] IEA. CO2 Emissions from Fuel Combustion Highlights - 2012 Edition. Paris, France, 2012.
[8] EC. 2014. ec.europa.eu. accessed 01-01-2014.
[9] Mukerjee M. A Mechanism of Hot Air A popular carbon-off set scheme may do little to cut emissions. Sci Am. 2009;300(6):18-+.
[10] Lysen EH. The Trias Energica: Solar Energy Strategies for Developing Countries. In: NOVEM, editor. Eurosun Conference. Freiburg1996.
[11] Maes T. Reductie van CO2-emissies op bedrijventerreinen in Vlaanderen door energiemanagement en energieplanning: Ghent University, 2011.
[12] Roberts BH. The application of industrial ecology principles and planning guidelines for the development of eco-industrial parks: an Australian case study. Journal of Cleaner Production. 2004;12(8-10):997-1010.
[13] Van Eetvelde G, Deridder K, Segers S, Maes T, Crivits M. Sustainability scanning of eco-industrial parks. European Roundtable on Sustainable Consumption and Production, 11th, Proceedings. Basel, Switzerland.
[14] Kalundborg Symbiosis. 2014. www.symbiosis.dk. accessed 01-01-2014.
[15] Sokka L, Pakarinen S, Melanen M. Industrial symbiosis contributing to more sustainable energy use – an example from the forest industry in Kymenlaakso, Finland. Journal of Cleaner Production. 2011;19(4):285-93.
[16] Gibbs D, Deutz P. Reflections on implementing industrial ecology through eco-industrial park development. Journal of Cleaner Production. 2007;15(17):1683-95.
[17] Konz W, van den Thillart C. Industriële symbiose op bedrijventerreinen. Eindhoven: Technische Universiteit Eindhoven, 2002.
[18] Linhoff M. Introduction to Pinch Technology. Northwich, Cheshire, 1998.
[19] Dhole VR, Linnhoff B. Total site targets for fuel, co-generation, emissions, and cooling. Comput Chem Eng. 1993;17, Supplement 1(0):S101-S9.
[20] Hackl R, Harvey S, Andersson E. Total Site Analysis (TSA) Stenungsund. Göteborg, Sweden: Chalmers University of Technology, Department of Energy and Environment, Division of Heat and Power Technology, 2010.
[21] van Gastel T. Geen buren maar wel samen energie inkopen : Agrogas: de eerste 'virtuele cluster'. Vakblad voor de bloemisterij. 2002;57(26):48-9.
[22] Vansteenbrugge J, Gabay S, Timmerman J, Van Eetvelde G. Energy clustering in greenhouse horticulture - submitted. Sustainable Energy Technologies and Assessments. 2014.

[23] Marino A, Bertoldi P, Rezessy S, Boza-Kiss B. Energy service companies market in Europe - Status report 2010. Ispra, Italy: European Commission - Joint Research Centre - Institute for Energy, 2010.
[24] Frederiksen S, Werner S. District heating and cooling. Lund, Sweden: Studentlitteratur AB, 2013.
[25] Vandoorn TL, Vasquez JC, De Kooning J, Guerrero JM, Vandevelde L. Microgrids Hierarchical Control and an Overview of the Control and Reserve Management Strategies. IEEE Industrial Electronics Magazine,. 2013;7(4):42-55.
[26] Zwaenepoel B, Vansteenbrugge J, Vandoorn T, Van Eetvelde G, Vandevelde L. Ancillary services for the electrical grid by waste heat. Applied Thermal Engineering. 2014;70(2):1156-61.
[27] Vandoorn T, Vandevelde L, Van Eetvelde G, Meersman B, Zwaenepoel B. Slimme Microgrids en Virtual Power Plants, bouwstenen van het net van de toekomst. Elektrotechnisch ingenieur. 2012;140:18-21.
[28] Van Eetvelde G, De Zutter B, Deridder K, De Rouck V, Devos D. Groeiboeken Duurzame BedrijvenTerreinen - juridisch, economisch, ruimtelijk en technisch bekeken. Ghent, Belgium, 2005.
[29] Maes T, Van Eetvelde G, De Ras E, Block C, Pisman A, Verhofstede B, et al. Energy management on industrial parks in Flanders. Renewable and Sustainable Energy Reviews. 2011;15(4):1988-2005.
[30] Timmerman J, Vandevelde L, Van Eetvelde G. Towards low carbon business park energy systems: Classification of techno-economic energy models. Energy. 2014;75(0):68-80.
[31] van Beeck N. A new decision support method for local energy planning in developing countries. Tilburg, the Netherlands: Tilburg University, 2003.
[32] Nakata T, Silva D, Rodionov M. Application of energy system models for designing a low-carbon society. Prog Energ Combust. 2011;37(4):462-502.
[33] Connolly D, Lund H, Mathiesen BV, Leahy M. A review of computer tools for analysing the integration of renewable energy into various energy systems. Applied Energy. 2010;87(4):1059-82.
[34] Grubb M, Edmonds J, Tenbrink P, Morrison M. The costs of limiting fossil-fuel CO2 emissions - a survey and analysis. Annu Rev Energ Env. 1993;18:397-478.
[35] Loulou R, Goldstein G, Noble K. Documentation for the MARKAL Family of Models. Energy Technology Systems Analysis Programme, 2004.
[36] Loulou R, Remne U, Kanudia A, Lehtila A, Goldstein G. Documentation for the TIMES Model. Energy Technology Systems Analysis Programme, 2005.
[37] Drouet L, Thénié J. An Energy-Technology-Environment Model to Assess Urban Sustainable Development Policies: Reference Manual - Version 2.1. Chêne-Bougeries, Switzerland: ORDECSYS, 2009.
[38] Howells M, Rogner H, Strachan N, Heaps C, Huntington H, Kypreos S, et al. OSeMOSYS: The Open Source Energy Modeling System An introduction to its ethos, structure and development. Energy Policy. 2011;39(10):5850-70.
[39] Rosenthal RE. GAMS - A User's Guide. Washington, USA: GAMS Development Corporation, 2012.
[40] Makhorin A. GLPK (GNU Linear Programming Kit). Moscow, Russia: Department for Applied Informatics, Moscow Aviation Institute2012. www.gnu.org/software/glpk. accessed 29/04/2014.
[41] Kannan R, Strachan N, Pye S, Anandarajah G, Balta-Ozkan N. UK MARKAL Model Documentation. London, United Kingdom: UK Energy Research Centre, 2007.
[42] Kannan R. The development and application of a temporal MARKAL energy system model using flexible time slicing. Applied Energy. 2011;88(6):2261-72.
[43] Cosmi C, Macchiato M, Mangiamele L, Marmo G, Pietrapertosa F, Salvia M. Environmental and economic effects of renewable energy sources use on a local case study. Energy Policy. 2003;31(5):443-57.
[44] Kannan R, Turton H. Documentation on the Development of the Swiss TIMES Electricity Model (STEM-E). London, United Kingdom: Paul Scherrer Institut, 2011.
[45] Kannan R, Turton H. A Long-Term Electricity Dispatch Model with the TIMES Framework. Environmental Modeling and Assessment. 2012:1-19.
[46] Devogelaer D, Duerinck J, Gusbin D, Marenne Y, Nijs W, Orsini M, et al. Towards 100% renewable energy in Belgium by 2050. Belgium: FPB, ICEDD, VITO, 2012.

[47] Comodi G, Cioccolanti L, Gargiulo M. Municipal scale scenario: Analysis of an Italian seaside town with MarkAL-TIMES. Energy Policy. 2012;41(0):303-15.
[48] Welsch M, Howells M, Bazilian M, DeCarolis JF, Hermann S, Rogner HH. Modelling elements of Smart Grids – Enhancing the OSeMOSYS (Open Source Energy Modelling System) code. Energy. 2012;46(1):337-50.
[49] Zachary DS, Drouet L, Leopold U, Aleluia Reis L. Trade-offs between energy cost and health impact in a regional coupled energy–air quality model: the LEAQ model. Environmental Research Letters. 2011;6(2):024021.
[50] Voll P, Klaffke C, Hennen M, Bardow A. Automated superstructure-based synthesis and optimization of distributed energy supply systems. Energy. 2013;50(0):374-88.
[51] Lund H. EnergyPLAN Advanced Energy Systems Analysis Computer Model Documentation Version 10.0. Aalborg, Denmark: Aalborg University, 2012.
[52] Connolly D. A User's Guide to EnergyPLAN. Limerick, Ireland: University of Limerick, 2010.
[53] Homer Energy LLC. Homer. Boulder, USA2013. homerenergy.com. accessed 20/02/2013.
[54] Lambert T, Gilman P, Lilienthall P. Micropower system modelling with HOMER. In: Farret FA, Simões MG, editors. Integration of Alternative Sources of Energy. Hoboken, New Jersey, USA: John Wiley & Sons Inc., 2006. p. 408.
[55] RETScreen. Clean Energy Project Analysis: RETScreen Engineering & Cases. Varennes, Canada: Natural Resources Canada, 2005.
[56] RETScreen. Combined Heat & Power (Cogeneration). Varennes, Canada: Natural Resources Canada, 2005.
[57] Schweiger H. Guide for Einstein Thermal Energy Audits. Barcelona, Spain, Berlin, Germany: energyXperts.NET, 2011.
[58] Schweiger H, Danov S, Vannoni C, Facci E, Ries J, Bertrand A, et al. EINSTEIN Software Tool Technical Manual. Barcelona, Spain, Berlin, Germany, 2012.
[59] Palazzi F. Osmose User Manual. Lausanne, Switzerland: Industrial Energy Systems Laboratory, Swiss Federal Institute of Technology Lausanne, 2010.
[60] Fazlollahi S, Maréchal F. Multi-objective, multi-period optimization of biomass conversion technologies using evolutionary algorithms and mixed integer linear programming (MILP). Applied Thermal Engineering. 2013;50(2):1504-13.
[61] Maréchal F, Kalitventzeff B. Targeting the integration of multi-period utility systems for site scale process integration. Applied Thermal Engineering. 2003;23(14):1763-84.
[62] Becker H, Maréchal F. Energy integration of industrial sites with heat exchange restrictions. Computers and Chemical Engineering. 2012;37(0):104-18.
[63] Nemet A, Klemeš JJ, Varbanov P, Aktins MJ, Walmsley M. Total Site methodology as a tool for planning and strategic decisions. Chemical Engineering Transactions. 2012;29:115-20.
[64] Weber C, Maréchal F, Favrat D. Design and optimization of district energy systems. Computer Aided Chemical Engineering. 2007;24(0):1127-32.
[65] Gerber L. Integration of Life Cycle Assessment in the conceptual design of renewable energy conversion systems. Lausanne, Switserland: Swiss Federal Institute of Technology Lausanne, 2012.
[66] Heaps C, Long-range Energy Alternatives Planning (LEAP) system, Somerville, MA, USA, 2012. www.energycommunity.org.
[67] Babonneau F, Haurie A, Tarel GJ, Thénié J. Assessing the future of renewable and smart grid technologies in regional energy systems. Swiss journal of economics and statistics. 2012;Vol. 148.2012(2):p. 229-73.
[68] Klemeš J, Dhole VR, Raissi K, Perry SJ, Puigjaner L. Targeting and design methodology for reduction of fuel, power and CO2 on total sites. Applied Thermal Engineering. 1997;17(8–10):993-1003.
[69] Yokoyama R, Hasegawa Y, Ito K. A MILP decomposition approach to large scale optimization in structural design of energy supply systems. Energy Conversion and Management. 2002;43(6):771-90.
[70] Maréchal F, Kalitventzeff B. Process integration: Selection of the optimal utility system. Comput Chem Eng. 1998;22, Supplement 1(0):S149-S56.

[71] Verheyen W, Zhang N. Design of flexible heat exchanger network for multi-period operation. Chem Eng Sci. 2006;61(23):7730-53.
[72] GAMS Development Corporation, General Algebraic Modeling System (GAMS) Release 24.2.3 Washington, DC, USA, 2014.
[73] Østergaard PA. Reviewing optimisation criteria for energy systems analyses of renewable energy integration. Energy. 2009;34(9):1236-45.
[74] Fazlollahi S, Mandel P, Becker G, Maréchal F. Methods for multi-objective investment and operating optimization of complex energy systems. Energy. 2012;45(1):12-22.
[75] Voll P. Automated optimization-based synthesis of distributed energy supply systems. Aachen: RWTH Aachen, 2013.
[76] Drud AS. CONOPT: A System for Large Scale Nonlinear Optimization, Reference Manual for CONOPT Subroutine Library. Bagsvaerd, Denmark ARKI Consulting and Development A/S, 1996.
[77] Land AH, Doig AG. An automatic method for solving discrete programming problems. Econometrica. 1960;28:497–520.
[78] Viswanathan J, Grossmann IE. A combined penalty function and outer-approximation method for MINLP optimization. Comput Chem Eng. 1990;14(7):769-82.
[79] Vanderbei RJ. Linear programming: Foundations and Extensions. 2nd ed, 2001.
[80] Aaltola J. Simultaneous synthesis of flexible heat exchanger networks [Dissertation/Thesis]. Helsinki Helsinki University of Technology 2003.
[81] Ponce-Ortega JM, Serna-Gonzalez M, Jimenez-Gutierrez A. Synthesis of Heat Exchanger Networks with Optimal Placement of Multiple Utilities. Ind Eng Chem Res. 2010;49(6):2849-56.
[82] Na J, Jung J, Park C, Han C. Simultaneous synthesis of a heat exchanger network with multiple utilities using utility substages. Comput Chem Eng. 2015;79(0):70-9.
[83] Gundersen T, Naess L. The synthesis of cost optimal heat exchanger networks: An industrial review of the state of the art. Comput Chem Eng. 1988;12(6):503-30.
[84] Yee TF, Grossmann IE. Simultaneous optimization models for heat integration. II. Heat exchanger network synthesis. Comput Chem Eng. 1990;14(10):1165-84.
[85] Papoulias SA, Grossmann IE. A structural optimization approach in process synthesis—II: Heat recovery networks. Comput Chem Eng. 1983;7(6):707-21.
[86] Maréchal F, Kalitventzeff B. Synep1 : A methodology for energy integration and optimal heat exchanger network synthesis. Comput Chem Eng. 1989;13(4–5):603-10.
[87] Pouransari N, Maréchal F. Heat exchanger network design of large-scale industrial site with layout inspired constraints. Comput Chem Eng. 2014;71(0):426-45.
[88] Floudas CA, Ciric AR, Grossmann IE. Automatic synthesis of optimum heat exchanger network configurations. Aiche J. 1986;32(2):276-90.
[89] Linnhoff B, Hindmarsh E. The Pinch Design Method for Heat-Exchanger Networks. Chem Eng Sci. 1983;38(5):745-63.
[90] Pouransari N, Maréchal F. Heat recovery networks synthesis of large-scale industrial sites: Heat load distribution problem with virtual process subsystems. Energy Conversion and Management. 2015;89(0):985-1000.
[91] Floudas CA, Ciric AR. Strategies for overcoming uncertainties in heat exchanger network synthesis. Comput Chem Eng. 1989;13(10):1133-52.
[92] Floudas CA, Grossmann IE. Synthesis of flexible heat exchanger networks for multiperiod operation. Comput Chem Eng. 1986;10(2):153-68.
[93] Floudas CA, Grossmann IE. Automatic generation of multiperiod heat exchanger network configurations. Comput Chem Eng. 1987;11(2):123-42.
[94] Ciric AR, Floudas CA. Heat exchanger network synthesis without decomposition. Comput Chem Eng. 1991;15(6):385-96.
[95] Ponce-Ortega JM, Jimenez-Gutierrez A, Grossmann IE. Optimal synthesis of heat exchanger networks involving isothermal process streams. Comput Chem Eng. 2008;32(8):1918-42.
[96] Chen JJJ. Comments on improvements on a replacement for the logarithmic mean. Chem Eng Sci. 1987;42(10):2488-9.

[97] Paterson WR. A replacement for the logarithmic mean. Chem Eng Sci. 1984;39(11):1635-6.
[98] Becker HC. Methodology and thermo-economic optimization for integration of industrial heat pumps. Lausanne: EPFL École Polytechnique Fédérale de Lausanne, 2012.
[99] Domínguez-Muñoz F, Cejudo-López JM, Carrillo-Andrés A, Gallardo-Salazar M. Selection of typical demand days for CHP optimization. Energ Buildings. 2011;43(11):3036-43.
[100] Fazlollahi S, Bungener SL, Becker G, Maréchal F. Multi-Objectives, Multi-Period Optimization of district energy systems: I-Selection of typical operating periods. Comput Chem Eng. 2012.
[101] CANMET. Pinch analysis: for the efficient use of energy, water and hydrogen. Natural Resources Canada, 2003.
[102] Kemp IC. Pinch Analysis and Process Integration - A User Guide on Process Integration for the Efficient Use of Energy. 2nd ed. Oxford: Butterworth-Heinemann, 2006.
[103] Linnhoff B, Ahmad S. Cost optimum heat exchanger networks—1. Minimum energy and capital using simple models for capital cost. Comput Chem Eng. 1990;14(7):729-50.
[104] Gundersen T, Grossmann IE. Improved optimization strategies for automated heat exchanger network synthesis through physical insights. Comput Chem Eng. 1990;14(9):925-44.
[105] Smith R. Chemical process: design and integration: John Wiley & Sons, 2005.
[106] Dhole VR, Linnhoff B. Total Site Targets for Fuel, Cogeneration, Emissions, and Cooling. Comput Chem Eng. 1993;17:S101-S9.
[107] Gil A, Medrano M, Martorell I, Lázaro A, Dolado P, Zalba B, et al. State of the art on high temperature thermal energy storage for power generation. Part 1—Concepts, materials and modellization. Renewable and Sustainable Energy Reviews. 2010;14(1):31-55.
[108] Mira-Hernandez C, Flueckiger SM, Garimella SV. Comparative Analysis of Single- and Dual-Media Thermocline Tanks for Thermal Energy Storage in Concentrating Solar Power Plants. J Sol Energy Eng Trans-ASME. 2015;137(3):10.
[109] Welsch M. Enhancing the Treatment of Systems Integration in Long-term Energy Models. Stockholm: KTH Royal Institute of Technology, 2013.
[110] Fazlollahi S, Becker G, Maréchal F. Multi-objectives, multi-period optimization of district energy systems: II—Daily thermal storage. Comput Chem Eng. 2014;71(0):648-62.
[111] Pfeiffer B. Identification of optimal Heat Supply Concepts for the Ski Resort of Verbier by Means of MILP and Heat Integration. Lausanne: Ecole Polytechnique Federale de Lausanne, 2014.
[112] Rager J. Urban Energy System Design from the Heat Perspective using mathematical Programming including thermal Storage. Lausanne, Switserland: EPFL École Polytechnique Fédérale de Lausanne, 2015.
[113] Aaltola J. Simultaneous synthesis of flexible heat exchanger network. Applied Thermal Engineering. 2002;22(8):907-18.
[114] Luo X, Wang J, Dooner M, Clarke J. Overview of current development in electrical energy storage technologies and the application potential in power system operation. Applied Energy. 2015;137:511-36.
[115] Voll P, Hennen M, Klaffke C, Lampe M, Bardow A. Exploring the near-optimal solution space for the synthesis of distributed energy supply systems. Chemical Engineering Transactions. 2013;35(1):277-82.